DOCTOR OF PHILOSOPHY

Molecular studies using the Aspergillu nidulans a-COP homologue

Milward, Kelly

Award date:
2001

Awarding institution:
University of Wales, Bangor

Molecular studies using the *Aspergillus nidulans* α-COP homologue

Presented for the degree of Doctor of Philosophy

June 2001

Kelly Milward
University of Wales
Bangor

Table of Contents

Appendices

Acknowledgements

I would like to thank my supervisor Dr. Susan Assinder for all her support, help and proof reading of this thesis.

A huge thanks go to all the members of G41 past and present, especially Shell who put up (and still puts up) with all my questions, Debbie for all her support and endless media making and Dr. Sue Whittaker for passing on this project to me. I would also like to thank all the other people within the department who have helped me over the last four years, especially to Beth and Rheinallt for help and generally making me smile when things get me down. I would also like to thank Andy, who recently started his PhD in G41, its been a pleasure and hope you've been 'loving it, loving it, loving it', good luck with your work.

Finally I would like to thank the people who have supported me throughout my degree and my PhD. To Dad, Sally, James, Alex and Tom, I love all very much and really can't even begin to tell you how much your support has meant to me, I've got here at last! To my partner Matt, well fatboy I love you so much and I couldn't have got through the last four years without your love, support and beefing. A big hug to Danna, Lucy, Helen, Mefty, Carli, and Jamie, thank you for keeping me sane and to Billy big, big thanks for my mapping program, it saved me so much time!

Last but not least, I would like to thank Patrick Hickey and Nick Read from the Institute of Cell Biology, Edinburgh for all their help with the confocal work. Also, John Doonan, Helen Fox and Chris Pitts at the John Innes Centre, Norwich, for help and support on numerous visits.

Abstract

The *sod*^{VI}*C* gene from *A. nidulans* encodes a homologue of yeast, bovine and human α-COP, which functions as part of the protein coat complex COPI involved in vesicle production in the protein secretory pathway.

Phenotypic characterisation of the temperature sensitive *sod*^{VI}*C1* mutation showed that at 37°C a stable disomic for chromosome VI was produced. This was confirmed genetically and the duplication of chromosome VI is proposed to act as a 'gene dosage' effect at the semi-restrictive temperature. Preliminary studies show that the *sod*^{VI}*C1* mutation may have an effect on secretion of certain classes of proteins from the hyphal tip.

Genetic characterisation of the *sod*^{VI}*C* gene showed that the cloned gene was indeed the *bona fide sod*^{VI}*C* gene and not a multicopy suppressor of the *sod*^{VI}*C1* mutation. The *sod*^{VI}*C* gene was also shown to be an essential gene and the *sod*^{VI}*C1* mutation identified as affecting the putative promoter region of the *sod*^{VI}*C* gene. It is proposed that the *sod*^{VI}*C1* mutation in some way causes a down regulation of the transcription of the *sod*^{VI}*C* gene, which is supported by the gene dosage effect seen at 37°C.

The endomembrane system of *A. nidulans* was studied using GFP-tagged constructs. The endoplasmic reticulum of *A. nidulans* was studied in a mutant background using an ER-localising GFP. It may be expected that the function of COPI in the recycling of ER resident proteins from the Golgi to the ER is impaired by a mutation in the α-COP subunit, and therefore, would produce visible changes within ER morphology. However, this was not observed suggesting that the role of COPI within the secretory system is far more diverse, and the effect of the *sod*^{VI}*C1* mutation comes into play well before any visible changes in ER morphology occur. GFP-tagging of the *sod*^{VI}*C* gene showed localisation to putative Golgi equivalents within *A. nidulans*.

Chapter One

Introduction

1.1 The Protein Secretory Pathway

1.1.1 Overview

The protein secretory pathway functions in the processing, sorting and delivery of newly synthesised proteins to organelles within the endomembrane system (Golgi, vacuoles, lysosomes etc), and to the plasma membrane for secretion into the extracellular matrix. In eukaryotes the key organelles of the secretory pathway are the Endoplasmic reticulum (ER) and the Golgi apparatus. Secretion has been extensively studied in mammalian and yeast cells, and these act as model systems for this pathway.

At the basic level secretion consists of the synthesis and insertion of a nascent polypeptide into the lumen of the ER, within which folding and initial modification of the peptide occurs. The newly synthesised protein then passes into the Golgi body where it is further modified and sorted for secretion to specific compartments. Figure 1.1 shows an overview of transport through the secretory system. The next sections of this review discuss each stage in more detail.

A large amount of protein transport through the secretory system occurs via vesicle transport. The forward transport of proteins from the ER to the Golgi is known as anterograde transport. The Golgi apparatus also contains a mechanism to allow the recycling of ER resident proteins mis-incorporated into anterograde vesicles. This reverse movement of proteins is known as retrograde transport. A number of different classes of vesicle exist in the secretory pathway, which are defined by the type of coat-protein used to form the vesicle.

1.1.2 Coat Protein (COP) –II

COPII coated vesicles function in the anterograde transport of secretory cargo from the ER to the Golgi apparatus. Once sorted from the background of proteins in the ER, cargo proteins destined for the Golgi are concentrated at sites on the ER for incorporation into vesicles. Eukaryotic cells typically produce vesicles 50-80nm in diameter (111, 12). During the formation of a vesicle, a limited set of coat proteins carries out a programmed set of sequential interactions. These lead to budding from parent membranes, uncoating and fusion with a target membrane (81). Vesicles budding from the ER are covered with the protein coat complex COPII. The proteins that constitute the COPII coat protein were originally identified in *Saccharomyces cerevisiae*, but have since been shown to have mammalian (81) and plant homologues (3). COPII coat complexes were identified by the isolation of a number of temperature-sensitive *S. cerevisiae* mutants, which showed blockages in protein transport (70). These mutants led to the identification of the core-coat complex, which consists of a 400kDa Sec23p/Sec24p complex (70, 71, 12) and a 700 kDa Sec13p/Sec31p complex (120, 129, 12). These protein coat complexes are recruited to donor membranes by the activation of the small GTPase Sar1p (14, 12). The protein Sec23p is a cytosolically orientated membrane protein (70) and acts as the GTPase-activating protein (GAP) for Sar1p (170, 12). A fifth protein, Sec12p, acts as the guanine nucleotide exchange factor (GEF) (99, 14, 32, 12) for Sar1p and is required for vesicle budding (12). Attachment of COPII coat proteins to the ER membrane results in the recruitment of cargo proteins to that site (Section 1.1.3). The method of vesicle formation in not known but is thought to occur by deformation of the lipid bilayer by COPII (81). Hydrolysis of GTP leading to the release of Sar1p-GDP is

thought to lead to uncoating after formation of the vesicle and before targeting to the target membrane (81).

1.1.3 COPI (Coatomer)

The COPI protein coat shows much greater biochemical diversity than seen with COPII coat protein, and the exact nature and direction of transport by COPI-coated vesicles is still under much debate. In mammalian cells, COPI has possible roles in the anterograde transport of proteins from pre-Golgi complexes to the main Golgi body, the anterograde/retrograde transport of cargo proteins/Golgi enzymes through individual Golgi cisternae, and in the stabilisation of ER exit sites and Golgi complexes (Section 1.1.4). However, it is agreed that the main role of COPI is in the recycling of resident ER proteins lost from the ER to the Golgi body by mis-incorporation into COPII-coated vesicles.

COPI (coatomer) consists of a heptameric protein complex, which in addition to its membrane associated form is present as a soluble form in the cytosol (163), (166). The main components have been characterised, and the seven subunits are classified as α, β, β', γ, δ, ε, and ζ –COP in mammalian cells. Homologues from *S. cerevisiae* (Ret1p, Sec26p, Sec27p, Sec21p, Ret2p, Sec28p, and Ret3p) (166) and from plants (3, 116) have been identified. The β, δ, ε, and ζ –COP subunits of COPI also show a limited homology to subunits of the AP complexes of clathrin coats (Section 1.1.4) (7).

With the exception of ε-COP, all of the coatomer subunits have been shown to be essential in *S. cerevisiae*. ε-COP is thought to act in some way to stabilise the coatomer subunits (41). Yeast mutants having impaired proteasome functions have been shown to rescue cells lacking ε-COP (80). Impairment of proteasome function presumably impairs degradation of coatomer, which in ε-COP deleted cells is

unstable. Once assembled coatomer is a stable complex with a half-life in mammalian cells of 28 hours and no exchange of subunits occurs once coatomer has been formed (41).

COPI-coat recruitment requires the association of the GTPase ARF1 (ADP-ribosylation factor 1) in its active form to the donor membrane (39, 81). The recruitment of the GTPase to the donor membrane is analogous to the recruitment of Sar1p in the formation of COPII-coated vesicles. Targeting of ARF1 to donor membranes requires specific association with an appropriate GTP-exchange factor (GEF). The GEF, ARF1GEF, seems to be responsible for the actions of coatomer in the COPI pathway (47, 81). ARF1 differs from Sar1p in that upon activation it inserts into the donor membrane. A myristoylated group on the protein becomes exposed upon exchange of GDP for GTP by ARF1 and is inserted into the lipid bilayer (81). The COPI complex is then recruited *'en-masse'* to the donor membrane, deformation of the membrane occurs by polymerisation of the coat protein to form a vesicle, which is then released into the cytosol. Hydrolysis of GTP by ARF1 causes the myristoylated group on ARF1 to become hidden, resulting in loss of anchoring to the membrane and COPI de-coating from the vesicle (81).

The main role of coatomer in the recycling of ER-resident proteins relies on the ability of the cell to recognise and sort these proteins. The cell identifies ER-resident proteins by their possession of short carboxyl-terminal sequences. Type I ER-membrane proteins contain the KKXX signal, while ER-lumenal proteins possess the KDEL signal (114, 145, 90). These signal sequences are recognised by receptors in the pre-Golgi and *cis*-Golgi compartments and are tagged for recruitment into COPI vesicles. An example of a KDEL-receptor is the multi-spanning membrane receptor Erd2 (113, 4). The Erd2 receptor recognises the KDEL-motif on certain soluble

proteins (4) and binds them for retrieval. The Erd2 receptor has also been shown to interact with coatomer via recruitment of the GTPase-activating protein (GAP) required for ARF1 activity (4).

The α, γ, δ, and ζ-COP subunits of coatomer have all been shown to be required for retrieval of KKXX-tagged proteins (84, 31, 41). Recruitment of coatomer by Erd2 receptors mediates incorporation of the KDEL-protein-receptor complex into COPI vesicles. The subsequent binding of KKXX-motifs by coatomer leads to the enrichment of these retrograde vesicles with ER-destined cargo. The Erd2 receptor, KKXX-, and KDEL motifs have been shown to localise to the ER, pre-Golgi and *cis*-Golgi compartments (92, 90).

Retrograde transport, although thought to be the main function of COPI-coat protein, in mammalian cells it has been shown to occur via the production of tubules from the Golgi, which track towards and fuse with the ER (86). This suggests that COPI is not the only form of retrograde transport, leaving the door open for different roles of COPI within the cell. COPI coat proteins have also been shown to recycle very quickly on and off membranes, showing that not all coatomer interactions lead to vesicle budding (86). This suggests that COPI may have numerous roles within the cell, maybe in the stabilisation of membranes and intermediate compartments. (section 1.1.5).

1.1.4 Other Coat-proteins

A third coat protein found within the secretory pathway is clathrin. Clathrin acts in a similar way to COPI and COPII-coat proteins, in that it accumulates on donor membranes and forms a scaffolding enabling deformation of the membrane and vesicle production (126). Clathrin has been localised to the plasma membrane, where it selectively accumulates plasma membrane receptors into clathrin-coated pits and

vesicles, and to the *trans*-Golgi membrane where it is thought to act in the transfer of selective proteins to endosomes, vacuoles and other destinations (136, 104). Adaptor proteins function within the cell, linking clathrin protein to the membrane. Two different adaptor proteins have been classified for clathrin (126, 104). Adaptor protein-1 (AP-1) is found associated with the *trans*-Golgi network, and AP-2 with the plasma membrane

AP-1 and -2 are heterotetrameric complexes, which are composed of two large subunits (β1- and δ-adaptin for AP-1, β2- and α-adaptin for AP-2) a medium sized subunit (μ1 or μ2), and a small subunit (σ1 or σ2) (104). Adaptor protein complexes sort cargo to be included in clathrin budding membranes by the binding of specific sorting signals on the cytoplasmic tails of certain membrane proteins (126). A large number of proteins (81) have been shown to be required for the formation of clathrin coated vesicles and pits. AP-1 has been shown to require activation by binding of ARF1GTPase (as in COPI) to the donor membrane, but AP-2 binding appears not to require this GTPase. A second GTPase, dynamin, has been shown to be required for pinching off of the AP-1 clathrin-coats on the plasma membrane, and a dynamin homologue is likely to serve the same role for AP-2 clathrin-coats budding from the *trans*-Golgi network (126).

The most recently classified AP protein AP-3 is found associated with the perinuclear area containing the *trans*-Golgi and other endocytic compartments. AP-3 is required in yeast for delivery of alkaline phosphatase from the *trans*-Golgi to the vacuole (104). The AP-3 adaptor proteins have been classified and consist of β- and δ-adaptin (the large subunits), μ3 (medium sized subunit), and σ3 (the small subunit) (104). However, the AP-3 adaptor protein binds to the protein coat complex

Vps41/39p, instead of clathrin. Like AP-1, AP-3 requires priming of the donor membrane by ARF1 GTPase before recruitment can occur (41).

1.1.5 The Endoplasmic reticulum (ER)

The ER is the largest membrane system in eukaryotes, consisting of highly invaginated tubules and flattened cisternae. Some of the ER membrane is connected to ribosomes and is known as the rough-ER, while ribosome-free regions are known as the smooth-ER. The rough-ER is responsible for the production of proteins, while the smooth-ER is thought to be involved in lipid biosynthesis (86). A large number of tubules and vesicles connect the ER to the nuclear envelope and the Golgi body. In plant cells the ER also extends through plasmodesmata into neighbouring cells (37). As well as being a key organelle in the secretory system the ER also has a role in detoxification of substrates by UDP-glucuronyl transferases, the preparation of antigens, the synthesis of lipids (63), and it is also the main dynamic Ca^{2+} storage compartment in the cell (96).

Targeting of proteins to the ER

Soluble proteins are recognised and targeted to the ER via a region known as the signal sequence. This sequence is located at the N-terminus of the nascent peptide and consists of a continuous short stretch of hydrophobic residues, flanked by one or more basic residues to the N-terminal side of the hydrophobic core (159, 144). Integral membrane proteins are targeted to the ER either by a cleavable signal sequence or by a signal anchor domain that becomes stably integrated into the lipid bilayer (72, 144).

When mRNA is translated by a ribosome the signal sequence at the N-terminus is recognised by the signal-recognition-particle (SRP). SRP directs the

nascent protein and accompanying ribosome to translocation machinery located on the ER. Identification of translocation complexes on the ER occurs by recognition of the SRP-nascent protein complex by an SRP-receptor protein (66, 157). Translocation of the nascent protein into the lumen of the ER occurs by specialised machinery known as a 'translocon'. The translocon consists of an aqueous channel, which translocates proteins across the ER membrane by receptor-mediated events (66). The translocon is made up of a heterotrimeric complex of membrane proteins known as Sec61p in eukaryotes (121), and is located exclusively in rough-ER regions (13, 15). The nascent protein-containing ribosome is thought to interact directly with the translocon, feeding the nascent protein into the lumen of the ER. In most cases the signal sequence from the nascent protein is cleaved by signal peptidase during translocation (144). Interestingly, mutants identified as being defective in the translocation of several secretory precursors showed little or no effect on the insertion of integral membrane proteins into the ER, suggesting that mechanisms for targeting membrane proteins may differ from those reported for secretory proteins (144).

Inside the lumen of the ER

Once inside the lumen of the ER, proteins destined for secretion to the plasma membrane and other cellular destinations branching from the secretory pathway undergo a number of co- and post-translational modification (121). Some of these modifications are almost universal and include cleavage of the N-terminal signal peptide, formation of disulphide bonds, and the glycosylation of Asn residues in the sequence Asn-X-Thr (Ser)..., while others are specific to different classes of proteins, such as the hydroxylation of Pro and Lys residues in procollagens (121).

Correct folding of proteins destined for secretion is one of the main roles of the ER, and the ER contains a large number of proteins in order to achieve this. The

first group, known as molecular chaperones, are present as soluble proteins within the lumen of the ER or as membrane-bound proteins facing the lumen of the ER (63). Molecular chaperones associate with nascent peptide chains or with the polypeptide after its release from the ribosome, in order to control and facilitate proper folding and assembly of the newly synthesised protein (63). Molecular chaperones found within the ER include BiP, calnexin and calreticulin (86). A second group of ER resident proteins comprises folding enzymes, which assist in the folding of newly synthesised proteins e.g. protein disulphide isomerase (PDI) (48), and peptidyly-prolyl *cis-trans* isomerase (63, 121).

The ER also acts as a filtering system for mis-folded proteins, either retaining them in the ER for degradation, or re-exporting them to the cytosol in a Sec61p-dependent manner for degradation in proteasomes (167, 63). Hong *et al.* (74) showed that a mutant hybrid protein engineered to be thermodynamically unstable was targeted to the vacuole for degradation, rather than being retained in the ER, suggesting a role for the ER in sorting of mis-folded protein. Retention of mis-folded proteins within the ER may allow further interactions of the protein with PDI and molecular chaperones in an attempt to correct mis-folding. Interactions have been shown between a non-cysteine containing mis-folded secretory protein and PDI implicating this enzyme in interactions with all mis-folded proteins (167).

Getting out of the ER

The next step for proteins destined to pass into the later stages of the secretory pathway, is the passage from the ER to the pre-Golgi/Golgi apparatus. Transportation of proteins from the ER involves the incorporation of cargo proteins into vesicles, which bud from the ER and are transported to the Golgi body. Before incorporation of cargo proteins into vesicles a number of hurdles must be overcome.

Both the ER lumen and the ER membrane are densely packed with proteins, some of which are incompletely folded or unassembled components of multi-subunit complexes (69). Correctly folded proteins must be sorted from this background by a range of accessory proteins. The first group of accessory proteins known as 'outfitters' (69), are made up of permanent ER resident proteins that either establish or maintain the secretory-competent conformation of the protein. These include folding catalysts and chaperones. An example of this type of protein is Shr3p, a non-essential ER-resident protein that is specifically required for the delivery of amino acid permease to the plasma membrane, acting to maintain the correct folding of the protein. In yeast the gene *CHS7* has been shown to be required for the activity of chitin synthase III (CSIII). *CHS7* regulates CSIII activity by controlling Chs3p export from the ER (147) in a similar way to Shr3p.

A second group of proteins, known as 'escorts' (69), function in much the same way as 'outfitters' but accompany the secretory protein to the Golgi apparatus e.g. the receptor-associated protein RAP. RAP is a soluble ER protein that binds to and stabilises newly synthesised low-density lipoprotein (LDL) receptor proteins. In the absence of RAP, LDL-receptors bind prematurely to ligand and are retained in the ER and targeted for degradation (69).

The final task for the ER is the accumulation of cargo proteins into COPII vesicles for transport to the pre-Golgi and Golgi compartments (102, 37). Exit of proteins from the ER occurs at specific sites on the membrane. Tagging of COPII components (125, 143, 86) has shown the localisation of COPII to distinct ER exits sites. These sites have been shown to correlate to sites where GFP-tagged vesicular stomatitis virus glycoprotein (VSVG) in infected cells first accumulates on exit from the ER (86). ER exit sites show very little movement within the ER and are long-

lived, which is consistent with their acting as fixed domains for recruitment and concentration of secretory cargo (143, 86).

Original work on transport of cargo proteins from the ER suggested a role for COPI in anterograde trafficking. In mammalian cells targeting of antibodies against subunits of the COPI complex was shown to block transport of proteins. Cell incubations at 15°C, which allows exit of proteins from the ER but prevents entry into the Golgi, has shown COPI co-localising with cargo proteins (e.g. VSVG in infected cells) to specialised tubular structures of the ER. Also treatment of mammalian cells with Brefeldin A (BFA) (section 5.1) has shown formation of pre-Golgi complexes 'de-novo' by membrane association of COPI (63).

Some of these observations may be explained by a role for COPI in the maintenance of the ER/Golgi structure. Cooling of cells has been reported to affect vesicle transport, predominantly that of COPII-coated vesicles (18, 86). Formation of ER tubules by COPI coat proteins may be an attempt by the secretory pathway to overcome this blockage. The treatment of cells with BFA has a more adverse effect on the secretory pathway than cooling. In mammalian cells BFA has been shown to cause the breakdown and re-absorption of the Golgi apparatus into the ER due to blockage of binding of COPI by interaction with the GTPase ARF1 (134). Re-generation of pre-Golgi and Golgi compartments from the ER by COPI upon removal of BFA may further support its role in the maintenance of the secretory pathway.

Studies in yeast with COPI mutants have shown that COPI is not required for anterograde transport of most cargo proteins through the secretory pathway. Instead it is suggested that ER-Golgi trafficking of some cargo proteins may require COPI for retrieval of limiting factors (such as vesicle receptors) required for packing of cargo into COPII anterograde vesicles (49). In mammalian cells COPI has clearly been

shown to be essential for trafficking through the early secretory pathway (83), and a role for COPI in the generation and maintenance of ER exit sites and pre-Golgi complexes has been defined (83).

This raises the question of why is COPI not essential for exit from the yeast ER? An explanation of this may be due to the nature of the Golgi apparatus within *S. cerevisiae*. Under normal conditions the Golgi bodies within this yeast exist as individual non-stacked cisternae dispersed throughout the cytoplasm. Recent work on *S. cerevisiae* and the yeast *Pichia pastoris*, which contains stacked cisternae, has highlighted differences in ER exit sites between these two organisms. *P. pastoris* possesses clearly defined tER sites within the ER as seen in mammalian cells. However, *S. cerevisiae* appears to form ER-buds from non-discrete sites throughout the ER (127). ER exit sites may therefore be a pre-requisite of stacked Golgi cisternae. Maintenance of ER exit sites by COPI may indicate why this coat protein is required for transport in the early secretory pathway in mammalian cells.

Accumulation of COPII and cargo proteins at ER exit sites suggests a role for receptor proteins, which interact with cargo proteins and coat-subunits leading to cargo enrichment of anterograde vesicles. ERGIC53 protein, a member of the lectin family, is abundant in vesicles produced from the ER. This protein is thought to bind mannose residues in some glycoproteins, possibly serving as a receptor for secretory proteins. Most ER-resident lumenal proteins are not glycosylated and therefore not selected for inclusion into transport vesicles by ERGIC53 (45). As well as the production of vesicles from the ER the Sec23p/Sec24p complex is thought to be one of the components responsible for cargo recognition by binding of receptors. One group of proteins identified as interacting with this complex are the p24 family of proteins. These proteins have also been found to interact with components of the

COPI (coatomer) complex (section 1.1.3) (45). The p24 proteins are proposed to act as cargo adaptors allowing sorting and incorporation of cargo molecules into transport vesicles (81). However, recent work in *S. cerevisiae* (141) has shown that yeast p24 proteins (Emp24p, Erv25p, and Erp1p-Erp6p) are not essential for vesicle transport. It is suggested (141) that p24 proteins act as 'quality control factors' to restrict the entry of unwanted proteins into COPII vesicles. The role of receptors in cargo-enrichment will become clearer as more putative receptor proteins are identified.

The final crucial stage in the life of a vesicle is the correct targeting, docking and fusion of it with the appropriate target membrane. Rothman *et al.* (40) proposed that a soluble NSF (NEM-sensitive fusion protein) attachment protein (SNAP) on vesicle membranes (v-SNAREs) bind to SNAP receptors on target membranes (t-SNAREs), thus allowing recognition of vesicles and targeting of cargo to the correct compartments. If individual SNAREs were required for each targeting event, then a large number of proteins from this family would have to exist. However, work in *S. cerevisiae* has shown that an individual t-SNARE defining a target membrane can interact with a number of different v-SNAREs on different vesicles. Similar results have been obtained showing that v-SNAREs are also capable of docking with a number of different t-SNAREs (55). This raises many questions as to how SNAREs are differentiated from each other, and how a vesicle would know in which direction transport is being directed. As with many other parts of the secretory pathway SNARE-mediated targeting of vesicles may require a number of yet undefined proteins to mediate these events.

SNAREs identified for ER-Golgi transport include the protein Ykt6p (95), which is highly conserved from yeast to humans and the mammalian Sly1p protein (115). Interestingly, two proteins (Sec34p and Sec35p) (155) have been shown to be

essential for the docking of ER-derived vesicles with the Golgi apparatus. These proteins are proposed to be tethering proteins, which act to hold the vesicle to the Golgi membrane prior to SNARE-mediated docking and fusion, further increasing the level of complexity of vesicle docking and fusion. One of the important questions raised for the production of vesicles is whether SNAREs and their associated tethering proteins are recruited prior to formation of the vesicle, or whether vesicles can form without these proteins and subsequently fuse with other vesicles containing cargo and SNAREs directed to the same compartments. This has been compared to the difference between an elevator and an escalator, with vesicles either being produced constitutively upon binding of coat proteins, or only forming when the correct cargo and selection molecules have been incorporated (126). Two ER-Golgi v-SNAREs (Bet1p and Bos1p) have been shown to interact with the COPII coat, suggesting that incorporation of these SNAREs into vesicles may be a requirement for vesicle budding (102).

1.1.6 The Golgi

The Golgi body was first identified in spinal neurons by the Italian biologist Camillo Golgi in the 1900's. In mammalian cells the Golgi apparatus consists of stacks of flattened sac-like cisternae. Smaller membranous tubules, sacs and vesicles are found surrounding these cisternae. The Golgi apparatus functions in the chemical modification and sorting of two types of newly synthesised proteins, those destined for secretion by the cell (e.g. hormones, blood plasma proteins and exoenzymes), and those proteins that function in the various compartments within the cell (e.g. vacuoles, lysosomes and proteasomes) (43). The Golgi apparatus is also intimately associated with the cytoskeleton. In mammalian cells, the Golgi body is centred at the microtubule organising centre and is actively maintained there by associations with

microtubules and microtubule motors. A scaffold of actin and actin binding proteins also surrounds the Golgi; these filaments may also facilitate spatial control of membrane traffic (33).

The Golgi body modifies proteins using glycosyltransferase enzymes, which function in distinct cisternae within the Golgi body. Modification by these enzymes consists of the addition of complex sugar chains to the proteins delivered from the ER. These sugar chains are found on most secreted and transmembrane proteins within the cell. Golgi cisternae can be divided into three distinct regions based on the order of sugar addition to glycoproteins (60, 9). These compartments are known as *cis*, *medial*, and *trans*. Recently a novel compartment known variously as the pre-Golgi compartment, vesicular tubular clusters (VTCs) or ER-Golgi Intermediate compartment (ERGIC) (65, 132, 12) has been identified. This complex has been visualised in mammalian cells and putative ERGIC equivalents have been observed transiently in *S. cerevisiae* upon reforming of Golgi equivalents (98). However, no intermediate compartment has yet been identified in plant cells (19). COPII buds derived from the ER fuse with the VTCs and cause cargo enrichment at these sites. Meanwhile COPI vesicles are seen to bud from this compartment, recycling proteins back to the ER (94). Retrograde transport of ER-resident proteins also occurs from individual cisternae within the Golgi stack (section 1.1.3).

Transport through the Golgi apparatus

Although biochemically defined, the exact mechanism of anterograde movement of proteins through the Golgi apparatus is still much debated. Two models for transport in this organelle have been proposed, and are known as the 'cisternal maturation' model and the 'static cisternae' model (12). In the static cisternae model, distinct Golgi compartments exist, each of which contains the required

glycosyltransferase enzymes for that stage of glycoprotein modification. These cisternal elements are stable in nature and transport of cargo proteins through the cisternae occurs by vesicle transport. The vesicle coat protein COPI has been proposed to act in this anterograde trafficking event. Evidence for this model comes from a number of sources; two distinct populations of COPI vesicles have been shown to exist (*in vitro*), one containing retrograde (KDEL receptor) cargo and the other containing anterograde (pro-insulin) cargo (106, 162, 105). COPI vesicles carrying anterograde cargos have been shown to fuse with Golgi membranes *in vitro* (110), (162). The fact that Golgi cisternae show such marked division of Golgi-resident enzymes would suggest that they form discrete, stable elements and proteins are delivered to these for modification (162).

In the cisternal maturation theory, the newly synthesised proteins are retained in individual cisternae. These cisternae then progress through the Golgi apparatus, with the addition of new ER/ERGIC-derived cisternae to the *cis*-face of the Golgi and the loss of mature cisternae by fission/vesicle budding at the *trans*-face. In this model it is the Golgi-resident enzymes that are shuttled between cisternae mediated by retrograde COPI vesicles, ensuring that early-acting enzymes are contained within *cis*-cisternae, and late-acting enzymes within *trans*-cisternae. Evidence for this type of transport includes, COPI vesicle produced from the Golgi apparatus that contain resident Golgi enzymes (91, 162), yeast COPI mutants that show defects in retrograde and not anterograde transport (49), and VTC complexes that have been shown to form *cis*-Golgi compartments by homotypic fusion of COPII derived vesicles and tubules (119, 112, 162, 86).

Increasing evidence suggests that transport of proteins through the Golgi apparatus is actually a combination of both models. One of the first suggestions for

include interaction with the COPI GTPase ARF1, this subunit has been shown to be capable of producing significant changes in membrane phospholipid composition and also stimulates the assembly of spectrin, actin, and other cytosolic proteins onto Golgi membranes (33). This suggests a role for ARF1 in membrane sorting, budding and docking processes at the Golgi complex.

A number of SNARE complexes have been identified in vesicles budding from the Golgi apparatus. The action of SNAREs at the Golgi complex must be able to discriminate those vesicles directed to the ER and those vesicles destined for docking and fusion with the other cytosolic compartments. A yeast t-SNARE, Ufe1p, a member of the syntaxin family of t-SNAREs has been identified and is thought to be responsible for the retrograde docking of vesicles at the ER. The v-SNARE Vti1p identified in yeast has been shown to be required for the anterograde transport of vesicles through the Golgi cisternae, and is thought to interact with the *cis*-Golgi t-SNARE Sed5p (85). The forward and retrograde transport of proteins via SNARE complexes are closely coupled, with v-SNAREs for both transport directions being present within different Golgi-derived vesicles. Overlap between v-SNAREs resulting in novel interactions between SNARE complexes, could result in the targeting of vesicles for transport in a particular direction (85).

Out of the Golgi apparatus

Exit of proteins from the Golgi apparatus occurs at the *trans* Golgi network (TGN). Large amounts of newly synthesised proteins are destined for secretion to the plasma membrane, where proteins may be integrated into the lipid bilayer, the cell wall, or be secreted into the extracellular matrix by the cell. Carriers involved in transport from the TGN consist of large, pleiomorphic tubular structures and small

cisternal maturation came from the transport of algal scales through Golgi cisternae (158). Scales are large glycoprotein complexes formed by some algal cells, which are too large to enter into vesicles and are proposed to be transported by cisternal progression. Transport of large aggregates such as pro-collagen was found to take a few hours, which contrasts dramatically with the average time of 10-20 minutes for transport of other proteins through the Golgi cisternae (158). These type of data suggest that slower cisternal progression of some proteins may occur at the same time as faster anterograde vesicle trafficking of other proteins (105).

Sorting at the Golgi complex

Vesicles budding from the Golgi apparatus, whether anterograde or retrograde, are subject to the same requirements as COPII vesicles: namely the incorporation of cargo molecules, exclusion of non-cargo proteins, and the directing of the vesicle to the correct compartments by v- and t-SNAREs. The method of cargo selection in the Golgi apparatus is probably even less well defined than for the ER. Coatomer has been shown to interact with ER-resident proteins and ER-receptor proteins such as Erd2 (section 1.1.3). COPI coatomer vesicles have also been shown to be rich in a protein called p23. This protein is a member of the p24 protein family shown to be present in COPI and COPII vesicles. In COPI vesicles p23 may act to mediate polymerisation of COPI subunits (123). As was mentioned earlier p24 proteins contain sorting determinants in their transmembrane domains, which may serve to exclude (141)/ include (45) proteins from COPI vesicles. The binding of COPI subunits by p23 leads to polymerisation and possible cargo enrichment of the COPI vesicles. A recent study suggests that transmembrane cargo proteins, cargo receptor proteins such as the p24 family and a Rho family GTPase (Cdc42), which organises actin formation, compete for binding sites on COPI subunits (52, 33). This may

vesicles (86). Proteins at the TGN are sorted into distinct regions where they are concentrated; the membrane then deforms to produce tubule structures incorporating the cargo molecules (86). These post-Golgi carriers (PGC) are then transported to the plasma membrane where they are localised to specific regions for docking and fusion.

Genetic and biochemical studies in budding yeast and mammalian cells have resulted in the identification of protein subunits known as the 'exocyst' complex. The exocyst complex consists of the proteins Sec3/5/6/8/10/15/exo70 and is also known as the Sec6/8 complex. This complex is thought to be an important component of the machinery that mediates exocytosis (76). In yeast cells the Sec6/8 complex is recruited to sites of rapid growth (e.g. the budding site of mother and daughter cells) and serves to regulate the delivery of vesicles to their designated exocytic sites (76). In fungi the vesicle supply centre, also known as the Spitzenkörper, may serve a similar function to the 'exocyst' in mammalian and yeast cells.

The docking and fusion of vesicles and tubules to the plasma membrane is also reliant on the same SNARE apparatus as for earlier parts of the pathway. The overlapping function of v- and t-SNAREs seen within the early pathway is also reflected at the later stages. SNARE complexes between a number of different v-SNAREs present in other parts of the pathway are again thought to provide novel targeting complexes. In yeast the protein Sec1p has been shown to bind *in vitro* to specific SNARE complexes thought to be involved in plasma membrane trafficking (25). The same group showed that a Sec1p-GFP fusion localised to exocytic sites within the cell, and proposed that Sec1p acts after assembly of SNARE complexes, promoting high-fidelity vesicle docking and fusion. Sec1p may act as a component of the 'exocyst' complex targeting vesicles to actively growing sites within the cell.

Evidence also exists for a novel sub-apical sorting centre within the cell (154). This compartment is derived from the endosome and is found in mammalian and yeast cells exhibiting polarized secretion. It is thought to be involved in the transcytosis and recycling of proteins and lipids (154), acting to sort and subsequently target molecules derived from, and destined for, either the apical or basolateral plasma membrane domains. The sub-apical compartment implicates another level of complexity existing in cells with highly polarised secretion.

1.2 Filamentous Fungi

Protein secretion in filamentous fungi has been a field studied increasingly over the past decade. Fungi have been used for a long time in the production of proteins for the food and paper industry, with the vast majority being made up of homologous glycoprotein products. Some of the most commonly used fungi include species of *Aspergillus* (e.g. *A. nidulans, A. awamori, A. niger,* and *A. oryzae*) and *Trichoderma* (e.g. *T. reesei*). Examples of industrially useful fungal enzymes include, α- and β-Galactosidase, β-Glucoronidase, Glucoamylase, α- and β-amylase, cellulases, lipases, and proteases (68). Over the past few years increasing interest in the use of fungal host strains to produce heterologous proteins and glycoproteins has come about with the potential of production for the pharmacological industry. This has led to a quest for the better understanding of factors that affect protein transport in fungi. Better knowledge of this pathway will aid in the engineering of strains and vectors for use in heterologous protein production, the aim being to produce industrially significant levels of these proteins.

Heterologous protein production

Filamentous fungi are good candidates for heterologous protein production for a number of reasons (68, 6, 57):

(1) Production of homologous proteins from fungi over a number of years means that this system already has the skills, and technology in place for the production of heterologous proteins.

(2) Fungi have been used for the production of proteins for the food and food-processing industries for a number of years, and have been given a GRAS (Generally Regarded As Safe) status. The objectives of protein production in heterologous hosts are to achieve high yields of authentic target protein in a safe strain.

(3) The transformation of filamentous fungi leads to the genomic integration of transforming DNA, resulting in the production of stable transformants. Plasmids can also be integrated into a number of loci within the genome.

(4) Although not all of the species of fungi used in the fermentation industry are well studied, the filamentous fungus *A. nidulans* has been the focus of much genetic and molecular study, and is capable of serving as a good model system for other filamentous fungi.

Filamentous fungi are capable of secreting high levels of homologous proteins (10-20g/litre of culture medium). Levels of heterologous protein production are much lower in comparison with only a few mg of protein produced per litre (57). Some heterologous proteins have been expressed with much better results e.g. *Rhizomucar miehei* aspartic proteinase has been produced in *A. oryzae* at levels of up to 3g/litre in controlled fermentation (28, 57). Because enzymes are often used to replace relatively inexpensive chemical processes, yields from these fungi must be very high (in multiple grams/litre) for them to be industrially relevant (169). Methods for improving heterologous protein production in filamentous fungi requires an

understanding of events at both the transcriptional and post-transcriptional level as well as an understanding of the secretory pathway as a whole.

One of the limiting factors of transcription for heterologous proteins is in the type of promoter used. Work has focused around the use of highly expressed protein promoters such as the glucoamylase gene (*glaA*) promoter from *A. niger*. This enzyme is expressed at high levels within *A. niger*, and fusion of heterologous proteins to its promoter region in theory could enhance the amounts of heterologous protein produced. Work in *A. niger* using the *glaA* gene promoter fused to chymosin showed that the amount of prochymosin mRNA was comparable to that of glucoamylase mRNA in a w.t. strain, but that the level of protein produced by the transformant was much lower (6). This suggested that other post-transcriptional events were affecting the amount of protein being produced. Post-transcriptional events that may affect production of the protein include codon usage, stability of the mRNA molecule, correct folding of the protein, translocation through the secretory pathway and degradation of the heterologous protein by host proteases.

Studies on the production of heterologous proteins in *A. awamori* have shown, unsurprisingly, that the transcription and secretion of fungal enzymes by a host strain (e.g. 1,4-β-endoxylanase, glucoamylase, and lipase) occurs at much higher levels than for non-fungal proteins (e.g. plant α-galactosidase (*aglA*), and human Interleukin 6 (*hIL-6*) (56). In this study, levels of mRNA of the fungal genes reflected levels of protein produced by the host strain, whereas the level of hIL-6 mRNA was much higher than the amount of protein produced. In the case of the *aglA* gene no full-length mRNA transcripts were obtained from the original gene, but neutral changes in codon usage within the gene resulted in the production of full-length transcripts (56).

The fusion of a heterologous protein to another highly expressed protein has been shown to increase the amount of heterologous protein produced by a host strain. Proteins used as fusion proteins include the highly secreted glucoamylase protein from *A. niger* (6, 57, 58) and the cellulobiohydrolase protein from *T. reesei* (58). The secreted protein is fused to the N-terminus of the heterologous protein through a linkage group separating the two proteins into distinct domains (6). This type of protein production requires the cleavage of the desired protein from the secretory 'helper' protein. This can occur either endogenously via the action of host strain proteases, or by the inclusion of cleavage sites within the linking region (6). An example of the latter is the Kex-2 cleavage sequence (140). In yeast the Kex-2 maturation site (Lys-Arg) is cleaved by the Kex-2 endoprotease (109), whilst in filamentous fungi cleavage occurs by host Kex-2-like proteases. A Kex-2-like cleavage site is found in the pro-region of the glucoamylase gene from *A. niger* (140). Production of proteins using glucoamylase gene fusions can increase the yield of heterologous proteins by 5-1000 fold (57). Secretion of hen egg white lysozyme (HEWL) fused to the first 498 upstream residues of the glucoamylase protein, increased levels of HEWL secretion by 10-20 fold that of unfused HEWL (6).

Many factors, including the site of genomic integration and plasmid copy number affects the production of significant amounts of heterologous proteins. A detailed discussion of them is beyond the scope of this literature review, but has recently been reviewed in Archer 2000 (5).

The secretory system in filamentous fungi

Although not greatly studied at the molecular and genetic level, some idea of the secretory pathway in filamentous fungi can be gleaned from cytological studies carried out on fungi. The structure of the secretory pathway in filamentous fungi is

analogous to that seen in the yeast *S. cerevisiae* (Fig. 1.2). Fungi contain a large network of ER membranes, which span the whole hypha (Fig. 1.2(A) and Fig. 5.2(A)). Like *S. cerevisiae* filamentous fungi contain Golgi equivalents (dyctyosomes) (Fig. 1.2(B)), in yeast these are thought to comprise individual *cis-*, *medial-* and *trans-*cisternae based on localisation of early and late acting Golgi-enzymes (127). Results produced in this thesis indicate that this may also be the case for filamentous fungi (section 5.4.6). Filamentous fungi also contain a specialized structure known as the vesicle supply centre or Spitzenkörper (88). This organelle is located just below the apex of the growing hyphal tip and is thought to supply vesicles to the actively growing tip. This novel organelle is probably a reflection of the rapid polarised growth exhibited by fungal hyphae. Smaller 'satellite' Spitzenkörpers have been seen to form and move towards the main Spitzenkörper body. These satellite Spitzenkörper may halt for a few seconds before fusing with the main Spitzenkörper body and visibly deform the hyphal wall at these points (89). Satellite Spitzenkörper may play a role in hyphal branch formation as well as in the directional growth of the hyphal tip. The highly polarised growth exhibited by filamentous fungi is likely to be a highly regulated system. Recent work has proposed that this polarised hyphal growth is generated by the maintenance of the equilibrium between endocytic and exocytic pathways (The 'Triple E' hypothesis)(122). This suggests that these two distinct pathways may be closely coupled, allowing regulation of anterograde and retrograde trafficking within fungal cells.

1.3 *Aspergillus nidulans* as a model genetic organism

A. nidulans is probably the most studied filamentous fungus, and although not a native high-secretor, this organism acts as a good model system for the study of other more highly secreting fungi such as *A. niger*. *A. nidulans* is a saprophytic

fungus, which was first isolated from soil and belongs to the subdivision *Ascomycotina* or *Deuteromycotina*. Along with *N. crassa* and *S. cerevisiae* it has been extensively studied as a model system for genetic analysis. *A. nidulans* is haploid, having a genome size of $2.5x10^7$ bases, which is separated into eight chromosomes. All eight chromosomes form genetically defined linkage groups containing hundreds of mapped genes affecting diverse developmental and metabolic characteristics (30).

Life cycle of *A. nidulans*

A. nidulans grows predominately by asexual growth (Fig. 1.3 (A)). However, it is also capable of undergoing sexual (Fig. 1.3 (B)) and parasexual (Fig. 1.3 (C)) cycles enabling the crossing of different strains and the production of diploids respectively. The asexual cycle is the standard means by which the fungus is cultured in the laboratory. An asexual spore (conidia) from *A. nidulans* will germinate when provided with a suitable environment containing water and nutrients. Germination of conidia occurs over 4-8 hours and a mature colony with a radius of approx. 3 inches is produced within 48 hours of incubation at the standard growth temperature of 37°C (93). The mature colony consists of a network of filamentous hyphae, which are coenocytic, having cytoplasmic compartments containing several nuclei separated by septa. These hyphae produce aerial branches, which differentiate to form terminal structures known as conidiophores; these contain chains of asexual uninucleate spores produced by mitotic division. When propagated onto fresh medium these spores will grow to form new asexual colonies. Spores from wild-type (w.t.) strains of *A. nidulans* normally contain a green spore pigment. A number of mutations in the spore colour genes have resulted in the production of mutants containing different spore pigments. This is one of the most useful features of *A. nidulans*; a spore colour

mutation contained in a nucleus from a single conidium is directly expressed by that conidium. Observation of conidial pigment of a colony can indicate whether it is heterokaryotic, whether the parent nuclei are well distributed and whether diploid formation has occurred (93).

During the parasexual cycle, hyphae from two strains growing adjacent to each other fuse to form heterokaryotic mycelium containing nuclei from both parents (Fig. 1.3 (C)). These heterokaryotic strains can be cultured by the transfer of small portions of mycelium onto fresh MM lacking the nutritional requirements for both parents. Growth of the mycelium can only occur by the maintenance of the two parent nuclei within the common cytoplasm, each parent nuclei complementing the auxotrophic requirements of the other. The fusion of parent nuclei within the heterokaryon leads to the production of a heterozygous diploid (93). *A. nidulans* diploids are relatively stable and can be sub-cultured by transfer of conidia or small pieces of mycelium onto fresh medium. Spontaneous haploidisation of diploids is rare but can be induced by growth on certain chemicals like benomyl (Benlate fungicide) (64) and chloral hydrate (137). The parasexual cycle can be used to localise new mutations to a chromosome by studying the segregation of whole chromosomes during haploidisation of a diploid. Master strains bearing markers on all chromosomes have been constructed for this purpose (29).

The sexual cycle (Fig. 1.3 (B)) of *A. nidulans* allows the crossing of two individual strains. *A. nidulans* is a homothallic fungus and so does not require strains of different mating types. Sexual crossing occurs when mycelium from two different strains are mixed together on a plate and allowed to form heterokaryons. Plates are then sealed to limit oxygen supply and after 10 days incubation at 37°C fruiting bodies known as cleistothecia are seen within the mycelium. Hybrid cleistotheca can

be identified by growing samples of ascospores and observing the spore colours of the resulting colonies. The sexual cycle can be used to map loci and to look for complementation in diploids/heterokaryons (93).

A. nidulans transformation system

A. nidulans has a well-established transformation system, which relies on the production of mycelial protoplasts (10, 146, 46). Protoplasts act essentially as bacterial cells, although they are far more sensitive to osmotic stress and require the inclusion of osmotic stabilisers (e.g. mannitol, sorbitol, sodium chloride, or magnesium sulphate) (46). Transformation of *A. nidulans* is usually by integration of the transforming DNA into the genome. If substantial homology exists between cloned sequences and chromosome, integration will occur predominantly at the site of homology. Integration of non-homologous DNA can be achieved by the complementation of the *pyrG89* auxotrophic mutation by the non-homologous $pyr4^{+}$ gene of *N. crassa*.

Autonomously replicating sequences (ARS) have been identified for *A. nidulans*. The ARS sequence ANS1 was found to enhance the frequency of transformation of *A. nidulans* by 50-100 fold (11). A second ARS, AMA1 has also been identified. Unlike ANS1, which acts as a transformation enhancer, AMA1 acts as a plasmid replicator in *A. nidulans* and can increase the frequency of transformation up to 2000 fold (1).

Other useful tools

A. nidulans is a valuable system for cytological studies, with the use of the fluorescent dye, DAPI (4'6-diamidino-2-phenylindole), which stains nucleic acid allowing the visualisation of nuclei (34). This serves as an important tool for the study of nuclear positioning and monitoring of the cell division cycle within this organism.

The advent of green fluorescent protein (GFP) in *A. nidulans* allows the tagging and visualisation of proteins of interest (for detailed discussion see section 5.1). *A. nidulans* also benefits from an inducible system based on the *alcA* promoter (section 5.1) allowing the under- and over-expression of genes.

1.4 The *sod^{VI}C* gene from *A. nidulans*

The *sod^{VI}C* gene is located on chromosome VI and was first identified in a screen for chromosome mis-segregation mutants (150). The *sod^{VI}C1* mutation is a temperature-sensitive (ts) mutation that causes a characteristic loss of growth at the restrictive temperature of 42°C. Spores undergo swelling and usually a single round of nuclear division, after which, growth ceases. Only a very small percentage of the germinating spores manage to produce a germ tube, and those that do only produce a very small protuberance and never develop into true germlings. The reason the *sod^{VI}C1* mutation was identified as a possible chromosome mis-segregation mutant was due to its phenotype at the semi-restrictive temperature of 37°C. At this temperature the *sod^{VI}C1* mutant strain forms a disomic colony, possessing an extra copy of chromosome VI. However, the *sod^{VI}C1* mutant differs from most chromosome segregation mutants in that the disomic colony is stable and is maintained throughout growth at 37°C hence the name *sod*, which stands for Stabilisation of Disomy.

The *sod^{VI}C* gene was cloned by complementation with a chromosome VI specific cosmid library (section 3.1). The cloned complementary fragment was sequenced and a Blast homology search carried out. This showed the *sod^{VI}C* gene to be homologous to the α-COP subunit of the coat protein complex COPI (section 3.1). This is the first coat protein to be cloned from *A. nidulans* and gives a unique opportunity to study its role in the secretory pathway of this organism.

1.5 Aims of this study

There are three main aims in this study.

1) To further characterise the phenotype of the *sod*^{VI}*C1* mutation (Chapter 3).

At the start of this study initial work had been carried out to look at the growth of the temperature sensitive *sod*^{VI}*C1* mutant strain. This chapter aimed to further characterise the novel *sod*^{VI}*C1* phenotype seen upon incubation at 37°C. At this temperature a *sod*^{VI}*C1* mutant undergoes a spontaneous duplication of chromosome VI. In this chapter the duplication event was characterised cytologically and genetically. The second part of this chapter aimed to look at any possible secretory phenotype, which may be expected from a mutation in a key protein involved in the secretory pathway.

2) The molecular characterisation of the *sod*^{VI}*C1* mutation (Chapter 4).

In this chapter work was carried out to confirm that the cloned gene was indeed the true *sod*^{VI}*C* gene and not a multicopy suppressor. A gene knockout experiment was carried out to confirm that the *sod*^{VI}*C1* mutation is a loss-of-function mutation, and that the *sod*^{VI}*C* gene is essential in *A. nidulans*. The final work in this chapter aimed to clone and identify the nature of the *sod*^{VI}*C1* mutation to try and understand the effect it has on the α-COP protein.

3) To study the endomembrane system of *A. nidulans* (Chapter 5).

The first work in this chapter aims to look at the effect of the *sod*^{VI}*C1* mutation on the ER of *A. nidulans*. This work uses the versatile reporter protein GFP to study the morphology of the ER in the *sod*^{VI}*C1* mutant at the restrictive temperature of 42°C. The second work presented here is a study of the over-expression of the *sod*^{VI}*C* gene in a w.t. *sod*$^{VI}C^{+}$ strain, using the *A. nidulans alcA* promoter. This promoter is

commonly used in *A. nidulans* expression studies and is also the main promoter used in *A. nidulans* GFP-constructs. The final work in this chapter looks at the localisation of the *sod*^{VT}*C* protein by tagging with GFP and expression from the w.t. *sod*^{VT}*C* promoter, allowing the study of possible organelles that take part in COPI vesicle production.

Figure 1.1: Overview of the protein secretory pathway in mammalian cells.

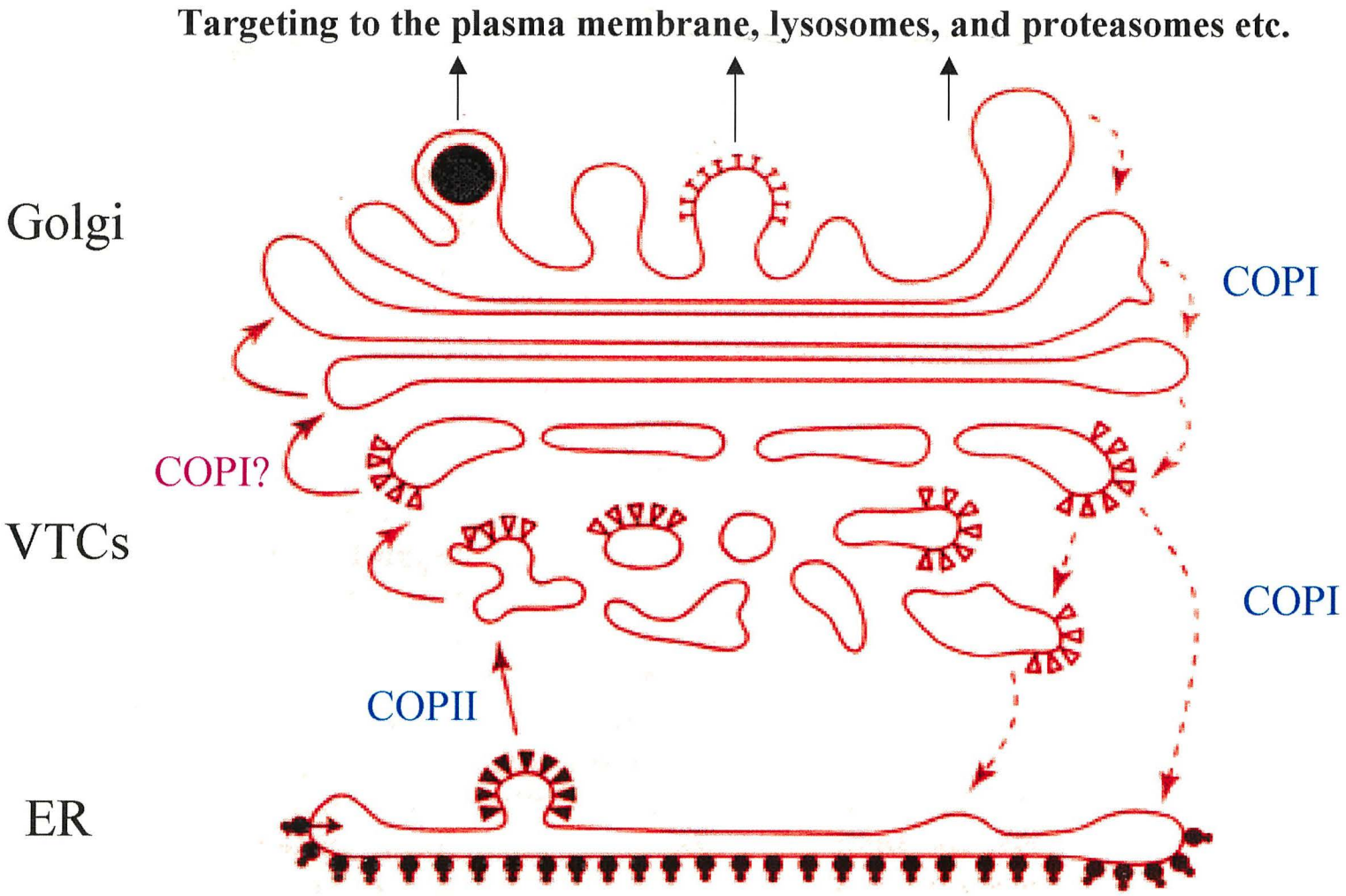

Figure 1.3: The secretory pathway of filamentous fungi. (A) The ER. (B) Golgi equivalents and Spitzenkörper.

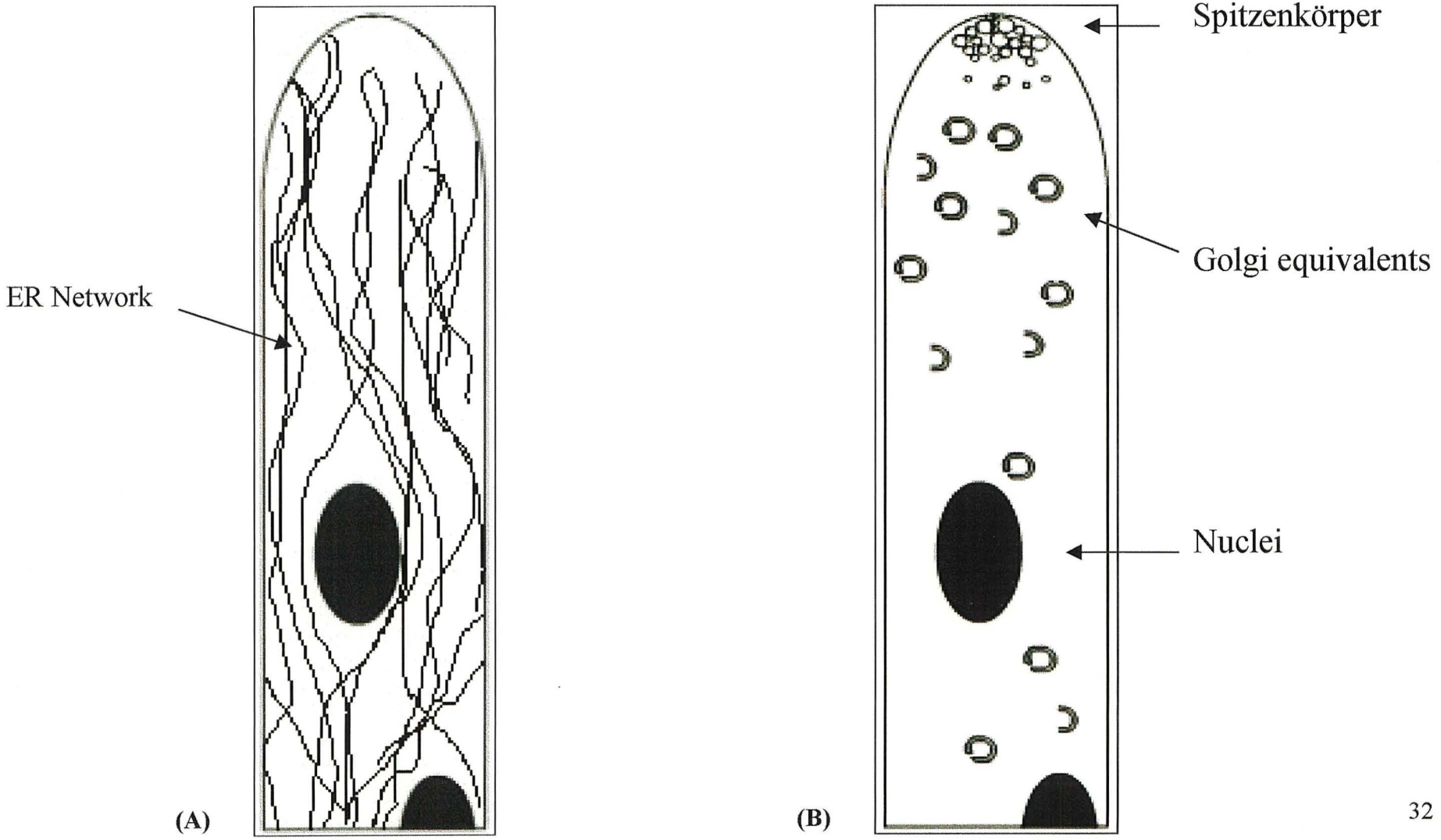

Figure 1.3: The *Aspergillus nidulans* life cycle (93). (A) Asexual cycle. (B) Sexual Cycle. (C) Parasexual cycle.

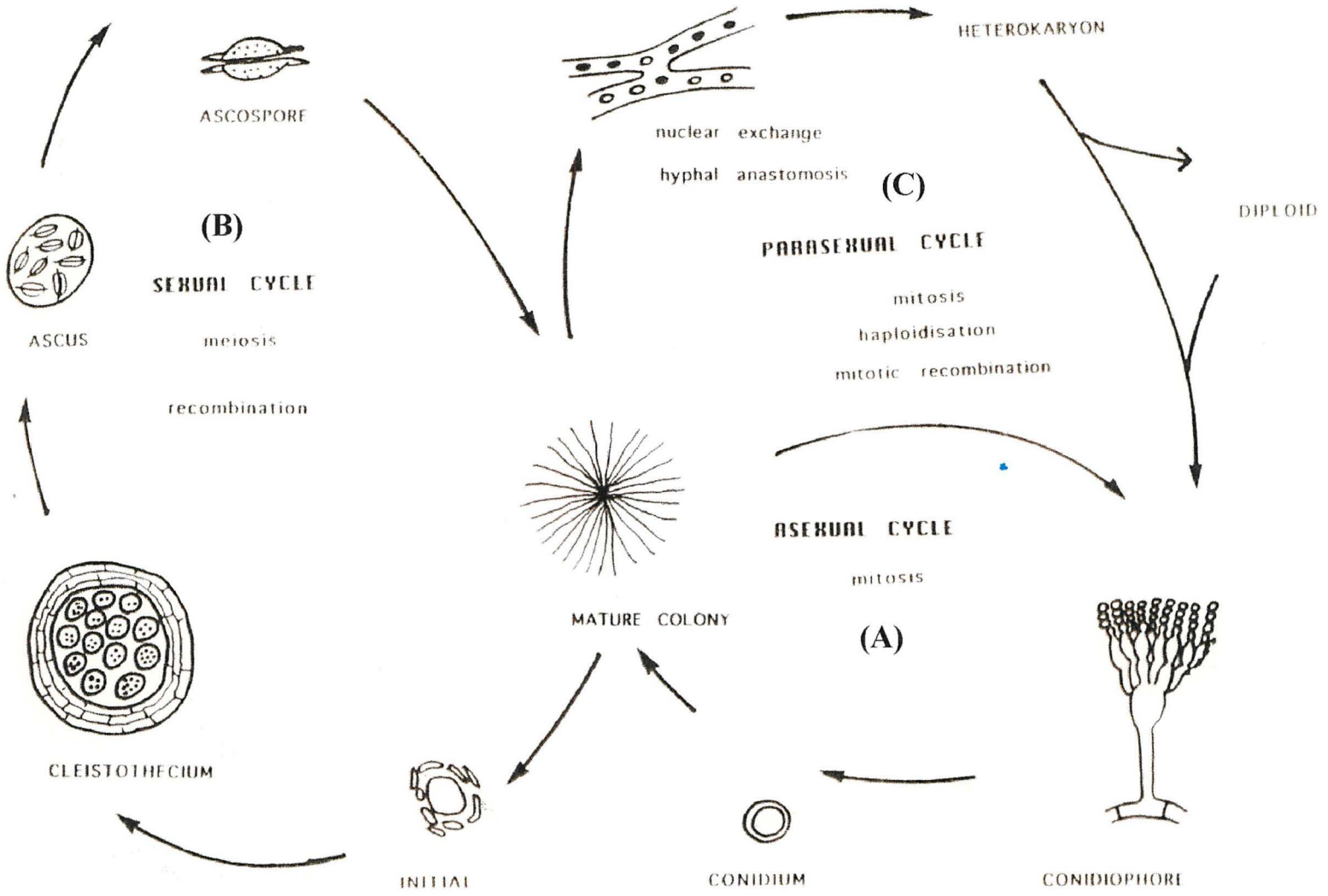

Chapter Two

Materials and Methods

2.1 Vectors and Strains used

2.1.1 Vectors

Table 2.1: List of plasmids used and their characteristics. *

Vector	Marker		Comments	Reference
	Escherichia coli	*A nidulans*		
pDHG25	amp^R	$argB^+$	Autonomously replicating vector containing AMA1 sequence. Generates high frequencies of low stability transformants.	(50)
pAB	amp^R	$pyr4^+$	Autonomously replicating vector containing AMA1 sequence. Generates high frequencies of low stability transformants.	Gift of J.H.Doonan.
pAL3X	amp^R	$pyr4^+$	Vector derived from pUC18 (156) containing the *alcA* promoter sequence providing an inducible vector system.	Gift of J.H.Doonan.
pBluescript	amp^R lacZ		Autonomously replicating *E.coli* vector containing the *lacZ* gene for blue/white screening.	Strategene. La Jolla. CA USA.
Topo 2.1	amp^R lacZ kan^R		Vector allowing the cloning of blunt-ended PCR products, contains *lacZ* for blue/white screening.	Invitrogen.
pRG3	amp^R lacZ	$pyr4^+$	Vector derived from pUC18 (156) containing the *lacZ* gene for blue/white screening.	(161)
pUC18	amp^R		Autonomously replicating *E.coli* vector containing the *lacZ* gene for blue/white screening.	(156)

* amp^R, kan^R confer resistance to ampicillin and kanamycin respectively, $argB^+$, $pyr4^+$ (*N. crassa*) complement the *argB2* and *pyrG89* mutations respectively.

2.1.2 Bacterial strains

Plasmids and constructs made using the above vectors were propagated in *Escherichia coli* XL1-Blue MRA (P2) strain (24), which has the genotype: *ΔmcrA 183, Δ(mcrCB-hsdSMR-mrr) 173, endA1, supE44, thi-1, gyrA96, relA1, lac*^{c} P2 lysogen. Exceptions were clones constructed in Topo 2.1®, which were first transformed into super competent cells of *E.coli* provided in the Topo2.1® Cloning Kit (Invitrogen®), with subsequent culture of selected clones being carried out in XL1-Blue. See Appendix 2 for key to abbreviations.

2.1.2 Aspergillus nidulans strains

Table 2.2: Genotypes of *A.nidulans* used in the study. A semi-colon separates markers on different linkage groups. 'A' prefix denotes a fungal genetics stocks centre (FGSC) strain, 'L' prefix denotes a Lancaster strain, 'B' prefix denotes a Bangor strain and 'G' prefix denotes a Glasgow strain. For recombinants isolated from sexual crosses during the course of study, parental strains are given, separated by *. See Appendix 3 for key to gene abbreviations.

Strain	Genotype	Notes
A188	*riboA1; wA3*	
L2	*pabaA1 yA2*	
L489	*wA3; sod^{VI}C1*	Original *sod^{VI}C1* mutant. (150)
L248	*adE20; pyroA4; chA1*	
L710	*adE20; argB2*	
GR5	*pyrG89; wA3; pyroA4*	
G66	*yA2; tsB5; lacA1 sbA3*	
G611	*biA1; nicC10; (glc$^-$)*	
B118	*adE20; wA3; argB2; sod^{VI}C1*	L154*L710
B120	*pyrG89 yA2; sod^{VI}C1*	L2*L489
B337	*pabaA1 yA2; sod^{VI}C1*	L489*L2
B339	*pabaA1 yA2; pyroA4; sod^{VI}C1*	L248*B337
B340	*pabaA1 yA2; pyroA4*	L248*B337
B706	*wA3; nicC10 sod^{VI}C1*	B118*G611
B707	*riboA1; wA3; lacA1 sbA3*	A188*G66
B708	*riboA1, yA2; lacA1 sbA3 sod^{VI}C1*	B120*B707
B709	*wA3; nicC10 sod^{VI}C1* *riboA1 yA2; lacA1 sbA3 sod^{VI}C1*	Multiply-marked chromosome VI diploid

2.2 Media

2.2.1 Media used for culture of *E. coli*

All media was autoclaved at 15 psi for 15 minutes.

LB (Luria-Bertani)-medium

10g	Tryptone
5g	Yeast Extract
5g	Sodium Chloride

Made up to 1 litre with distilled water. Glycerol was included at a final concentration of 10%(v/v) for strain storage. 10g agar was added for L-broth plates. Ampicillin was added to a final concentration of 70 μg/ml to cooled molten agar.

Sensitivity Test Agar

20g STA media (Lab M media)

Made up to 500 ml with distilled water and autoclaved. To cooled medium ampicillin was added to a final concentration of 70μg/ml.

STAAmp IPTG\X-Gal plates

STA Amp plates were made as above, and then overlaid with 5ml of top agar.

Top Agar

2g	Yeast Extract
1.25g	Sodium Chloride
2.5g	Agar

Made up to 250ml with distilled water and autoclaved. To the cooled media ampicillin was added to a final concentration of 70μg/ml. To this 15 mg of Isopropyl-β-D-thiogalactosidase (IPTG) dissolved in 500μl SDW and 20mg of 5-Bromo-4-Chloro-3indolyl β-D-galactopyranoside (X-Gal) dissolved in 500μl dimethylformamide was added. All chemicals were obtained from Sigma®.

2.2.2 Media used in the culture of *A. nidulans*

Complete medium (CM)

30g	Malt Extract
10g	D-glucose
5g	Yeast Extract
1ml	CM supplement (see below)
100µl	Vitamin Solution (see below)
100µl	0.1M Copper Sulphate

Made up to 1 litre with distilled water and autoclaved. Plates additionally contained 1% agar. Most strains grew on CM but strains carrying *argB2* required arginine (0.42mg/ml) (CMA medium), and strains carrying *pyrG89* required additional supplementation with uracil and uridine (1% each) (CMUU medium). Other supplements and amounts added are shown in Table 3. Sodium deoxycholate was added to CM at 0.01% (=CMSD) to restrict colony size (8).

Complete medium supplement (CMS)

7.5g	Adenine
5.0g	L-methionine
3.65g	Lysine monohydrochloride
0.5g	Riboflavin

Made up to 1 litre with distilled water.

Vitamin Solution

1.5g	Thiamine
50ml	0.05% Biotin
20g	Choline

2.5g	Nicotinic acid
0.8g	4-Aminobenzoic acid
10g	Pyridoxine
2.5g	Riboflavin

Made up to 1 litre with distilled water.

Yeast extract medium (YAG)

10g	Yeast extract
20g	D-Glucose

Made up to 1 litre with distilled water. Supplements were added for different auxotrophic strains as to MM. 1% (w/v) agar was added when required for plates.

Malt extract medium MAG

10g	Malt extract
20g	D-Glucose

Made up to 1 litre with distilled water. Supplements were added for different auxotrophic strains as to MM. 1% (w/v) agar was added when required for plates.

Minimal medium (MM)

5g	D-glucose
50ml	*Aspergillus* salt solution (see below)
1ml	Hunter's trace elements (see below)

Adjusted to pH 6.5 and 5g agar added. Made up to 1 litre with distilled water. For media requiring lactose or sorbitol, glucose was omitted and the other sugars added at a concentration of 5g/litre.

Aspergillus salt solution

120g	Sodium nitrate
10.4g	Potassium chloride
10.4g	Magnesium sulphate heptahydrate
30.4g	Potassium dihydrogen phosphate

Made up to 1 litre with distilled water.

Hunter's trace elements solution

1.1g	Ammonium molybdate
11g	Boric acid
1.6g	Cobalt chloride hexahydrate
1.6g	Copper sulphate hexahydrate
50g	Ethylenediamine tetra acetic acid (EDTA)
5g	Ferrous sulphate heptahydrate
5g	Manganese chloride
22g	Zinc sulphate

Made up to 1 litre with distilled water, heated to boiling, cooled to 60°C and adjusted to pH 6.5 to 6.8 with 1M potassium hydroxide. Stored for two weeks before use.

Fermentation media

100g	Maltose
20g	Malt extract
1g	Peptone

Before autoclaving, 4-Morpholinethan-sulphonic acid (MES) was added to a final concentration of 50mM. 100ml aliquots of the fermentation medium were transferred into 250ml flasks, which were then autoclaved.

Ethanol, Glycerol and Threonine media

1ml	Hunter's trace elements (see above)
10ml	1M Ammonium Sulphate (replace sodium nitrate)
25ml	Modified salt solution (as *Aspergillus* salt solution minus sodium nitrate)

Adjusted to pH 6.5 and 5g agar added. Made up to 1 litre with distilled water. Glycerol or threonine was added at a concentration of 1% (v/v)/(w/v) prior to autoclaving. For ethanol plates, 1% (v/v) ethanol was added just before pouring and plates were incubated in a damp chamber.

Medium supplements

Table 2.3: Supplements added to *A. nidulans* media

Supplement	Stock (%)	**Final concentration (mg/ml)**
Adenine	0.86	0.17
Arginine	4.2	0.42
Biotin	1.0	0.025
D-Methionine	0.5	0.05
Nicotinic acid	0.5	0.05
4-Aminobenzoate	0.17	0.0085
Pyridoxine	1.0	0.10
Riboflavin	0.05	0.0025
Uridine	Added solid	6mg/ml
Uracil	Added solid	6mg/ml

2.3 Solutions and Buffers

2.3.1 Solutions for Agarose Electrophoresis

Ethidium bromide (EtBr)

Made as 10mg/ml stock and stored at 4°C. EtBr was included in gels to a final concentration of 0.25µg/ml.

Gel loading buffer (5X Stock)

0.25% (w/v)	Bromophenol blue
40% (w/v)	Sucrose

Dissolved in distilled water. 3µl of loading buffer was added to samples (20µl volume) before loading onto gel.

5x TBE gel running buffer

54g	Tris
27.5g	Boric acid
4.65g	EDTA

pH adjusted to 8.0 and made up to 1 litre with distilled water. Stock was diluted 5-fold before use.

TE buffer for storing DNA in solution

0.74g EDTA

0.2ml 1M Tris. HCl pH 7.5

Made up to 200ml with distilled water.

2.3.2 Lysis buffer for bacterial STET preps (73)

8g Sucrose

5ml Triton X100

5ml 1M Tris pH 8

Made up to 100ml with distilled water.

2.3.3 Solutions used in transformation of *A. nidulans*

Transformation solution I

52.8g Ammonium sulphate

10.51g Citric acid

pH 6.0 with potassium hydroxide, made up to 500ml with distilled water and autoclaved.

Transformation solution II

5g Yeast extract

10g Sucrose

1.23g Magnesium sulphate

Made up to 500ml distilled water and autoclaved.

Transformation solution III

26.4g Ammonium sulphate

5g Sucrose

5.25g Citric acid

pH 6.0 with potassium hydroxide, made up to 500ml and autoclaved.

Transformation solution IV

25g Polyethylene glycol 6000

10ml 1M Calcium chloride

4.47g Potassium chloride

10ml 1M Tris-HCl pH7.5

Made up to 100ml with distilled water, filter sterilised and stored at -20°C in aliquots.

Transformation solution V

4.47g Potassium chloride

10ml 1M Calcium chloride

19.52g MES

pH 6.0 with potassium hydroxide, made up to 100ml and stored at 4°C.

Lytic mix

20ml Solution I

20ml Solution II

2.5µl/ml β-Glucoronidase (141U/µl (Sigma®))

0.4g Glucanex (or 0.1g Novozyme)

0.16g Bovine Serum Albumin (BSA)

Filter sterilised and used immediately.

2.3.4 Solutions used for preparation of XL1-Blue competent cells

Solution I

50ml 1M Magnesium chloride

Made up to 500ml with sterile distilled water.

Solution II

50ml 1M Calcium chloride

Made up to 500ml with sterile distilled water.

Solution III

50ml 1M Calcium chloride

70ml Glycerol

Made up to 500ml with sterile distilled water.

2.3.5 Solutions used in Southern Blotting

De-purination Solution

25ml Concentrated HCl

Made up to 1 litre with distilled water.

Denaturation Solution

20g Sodium Hydroxide

87.7g Sodium Chloride

Made up to 1 litre with distilled water.

Neutralisation Solution

121.4g Tris

175.3g Sodium Chloride

Made up to 1 litre with distilled water, pH 7.5 with NaOH.

20xSSC Solution

88.2g Sodium Citrate

175.3g Sodium Chloride

Made up to 1 litre with distilled water.

50xDenhardts reagent

5g Ficoll 400

5g Polyvinyl pyrrolidine

5g Bovine Serum Albumin

Made up to 500ml with distilled water. Solution is filter sterilised, aliquoted and stored at -20°C).

Pre-Hybridisation Solution

5 x SSC

5 x Denhardts Solution

0.5%(v/v) SDS

0.1mg/ml denatured Salmon sperm DNA

Made up to 100ml with distilled water

Hybridisation Solution

5 x SSC

5 x Denhardts reagent

0.1%(v/v) SDS

0.1mg/ml denatured Salmon sperm DNA

Made up to 20ml with distilled water.

2.4 *Aspergillus nidulans* techniques

2.4.1 Culture techniques

Techniques were originally from Pontecorvo *et al.* (117). *A. nidulans* is easily propagated by transferring conidia using a sterile glass needle. Single spore colonies were made by spreading serial dilutions of a suspension of spores on CMSD.

Velvet replication was used for screening large numbers of colonies. A plate was inverted onto damp sterile velvet, which replicates the spores onto the velvet. The velvet was then used to transfer the spores to a fresh plate containing various supplements (for checking the genotype of a strain) or subjected to different conditions (for selection purposes).

For most strains 37°C was the general incubation temperature for growth of *A. nidulans*. For temperature-sensitive strains (ts^-), 30°C was the permissive, 37°C the semi-restrictive and 42°C the restrictive temperature.

2.4.2 Sexual crosses–ascospore propagation and analysis

Conidia from the two parental strains to be crossed (of different colours and auxotrophic requirements) were mixed on the centre of a thick MM plate using a sterile loop. The agar was chopped up and spores of the two strains were buried in order to increase the surface area for better strain mixing. A drop of liquid complete medium (LCM) was added to the agar surface to ensure a little initial growth of these two strains. After one to two days incubation, the plate was sealed to create partially anaerobic conditions and thus encourage formation of cleistothecia. Mature cleistothecia were observed after incubation for a further ten to fourteen days. Crosses involving ts^- strains were carried out at 30°C whilst those containing no ts-markers were incubated at 37°C.

Mature cleistothecia could be seen as black balls covered by yellow Hulle cells. These cells were removed by rolling 10 cleistothecia from each cross on the surface of a 3% agar plate and the cleistothecia burst to release ascospores. To test for hybridity, a sample of ascospores from each cleistothecium was first stab-inoculated onto CM plates, while the burst cleistothecia were kept at 4°C. Hybrid cleistothecia were distinguished by the growth of different spore colours. More ascospores from a hybrid cleistothecium were then plated onto CMSD plates by dipping a sterile needle into a cleaned and burst cleistothecium under a dissecting microscope. The needle was then transferred to the centre of a fresh plate in which had been placed a drop of sterile 0.02% tween 80 or sterile distilled water to disperse the spores and aid in spreading on plate. The suspension was spread using a sterile rod.

From each cross, a random sample of 100 meiotic progeny was inoculated onto glass master plates of CM (supplemented if appropriate) following a 26-pin pattern. The master plates were then replicated onto MM with or without supplements in order to determine the genotypes of the progeny.

2.4.3 Heterokaryon formation

In order to create a diploid a heterokaryon must first be established. Two parental strains, each with different spore colours and auxotrophies, were inoculated into a test-tube containing 5ml LCM, with added appropriate supplements. The test tube was incubated overnight at 30°C. The mycelial mat that formed on the surface of the media, was removed, washed in SDW and teased out in small pieces on a MM plate. After incubation at 30°C for two to three days, a heterokaryon was observed as a fan-shaped growth from the inoculum, which contained both parental spore colours. This indicated that the hyphae contained both types of nuclei, which complemented each

other's auxotrophic mutations. Heterokaryons were sub-cultured by transferring small ($1mm^2$) pieces of mycelia onto MM plates.

2.4.4 Diploid formation

The different nuclei in a heterokaryon occasionally fuse to form a diploid nucleus. Spores produced by a heterokaryon are usually haploid of one or other parental auxotrophic type and therefore will not grow on MM. However, a diploid spore will grow on MM if all of the auxotrophic markers are heterozygous and are complemented. The diploids could be selected (seen as prototrophic green colonies) if spores from the heterokaryon were spread on MM (117).

2.4.5 Haploidisation analysis

The "Benlate Test" (149) was used to distinguish haploids from diploids when constructing diploid strains and when analysing breakdown of disomic and trisomic strains.

2.4.6 Transformation of *A. nidulans*

All solutions are described in Section 2.3.3. The procedure was adapted from Ballance *et al.*, (10) and Osmani *et al* (108). Conidial suspensions of an arginine-requiring or uridine/uracil-requiring transformation host strain were inoculated respectively onto cellophane circles of CMA or CMUU and incubated until a mycelial mat had formed (usually overnight). Cellophanes were then transferred to fresh petri dishes containing 20ml of lytic mix; cellophanes were then incubated with shaking at 37°C for 1-2 hours. The cellophanes were filtered through a sterile nylon mesh membrane to remove mycelial debris and the filtrate transferred into a sterile Beckman JA20 centrifuge tube. Harvesting was by centrifugation at 4000g for 5 minutes. Pellets were

washed twice with cold solution III and suspended in a variable volume (up to 1ml) of solution V depending on the size of the pellet obtained.

Aliquots of DNA (up to 12µl) were placed in microfuge tubes and kept on ice. To each tube, 100µl protoplasts were added, followed by 50µl of solution IV and then left to incubate for 20 minutes on ice. After this time, 1ml of solution IV was added and the mixture left for a further 20 minutes at room temperature.

For selection of transformants, the reaction mixes were plated on appropriately supplemented MM containing 0.6M KCl as osmotic stabiliser, but lacking arginine or uridine/uracil depending on the host strain used. If a clone complementing a ts^- mutation was being sought, the plates would either be kept at the restrictive temperature (in this case 42°C) for about four days or velvet replicated to 42°C after growth at 30°C. A set of plates was routinely incubated at 30°C as a control. For determining the viability of the protoplast suspension, diluted samples of untransformed protoplasts were plated on medium containing KCl and all supplements (including arginine and uridine/uracil). For assessing the efficiency of protoplasting, dilutions of the protoplasts were plated on fully supplemented medium lacking KCl. A no DNA control was included in the transformation by treating a tube containing an equivalent transformation volume of TE buffer as for tubes containing DNA being transformed. Two x 100µl of this tube was plated onto MM KCl media lacking either arginine or uridine/uracil.

2.4.7 4', 6-diamidino-2-phenylindole (DAPI) staining and fluorescence microscopy

Spore suspensions (10^5 spores/ml) of the strains were made in 0.8% NaCl and 20µl pipetted onto a round coverslip placed in a petri dish. Approximately 80µl LCM was added to the spore suspension and the Petri dish was placed in a damp chamber at the

appropriate temperature. The fixative (8% formaldehyde, 5% DMSO, 0.1% phosphate buffer pH 7.0) was allowed to soak the spores for 30 to 45 minutes before removal by washing thrice with SDW. The coverslips were air-dried, stained with 0.5μg/ml DAPI and mounted on slides. Slides were sealed with nail varnish and viewed under a Nikon fluorescence microscope at x1000 magnification. Photographs were taken using a Nikon digital cameral or using T-max 400 black and white film.

Details of filters used for microscopy:

DAPI microscopy	UV-1A (Nikon) EX = 365/10nm DM = 400nm BA = 400nm
GFP microscopy:	GFP(R) –LP HQ.FITC-LP (Nikon) EX = 460-500nm DM = 505nm BA = 400nm

For visualisation of GFP expressing transformants slides were prepared as above using the appropriate inducing media in place of LCM. After incubation the coverslips were inverted onto fresh microscope slides and visualised without fixation.

2.4.8 Confocal Microscopy

Confocal microscopy was carried out using a Bio-Rad MRC 600 confocal laser-scanning microscope fitted with a 25mW argon laser. This was connected to a Nikon Diaphot TMD inverted microscope with epifluorescence microscope equipment (all supplied by Bio-Rad Microscience, Hemel Hempstead UK).

A. nidulans cultures were grown on plates of MM containing 2% glucose, MM glycerol or MM media supplemented with yeast extract 10g/litre plus additional supplements if required by the strain. Sections from the leading edge of the colony

were cut with a scalpel and inverted onto a coverslip with a few drops of liquid MM. The sections were then allowed to recover for an hour in a damp chamber before visualisation using standard confocal techniques.

2.5 General molecular techniques

2.5.1 Preparation of genomic DNA

Mycelium was harvested by filtration through sterile muslin and squeezed between filter paper to remove as much liquid as possible. Mycelium was ground in liquid nitrogen using a pestle and mortar and approximately 40mg ground mycelium was then transferred to a sterile 1.5ml Eppendorf tube on ice. DNA extractions were carried out using the Promega® Wizard DNA kit following manufacturer's instructions. The DNA was eluted into 100µl elution buffer and stored at 4°C.

2.5.2 Agarose gel electrophoresis

In order to visualise DNA, samples were run on 0.7% agarose gels in 1 x TBE buffer (Section 2.3.1) containing 2.5µg/ml EtBr. Samples were loaded in 1x loading buffer with DNA markers such as λ*Hin*dIII (purchased from Promega®) for comparison, 100ml gels were run at 60 to 80mA for 3 to 4 hours or 20mA overnight. The gels were visualised on an UV-transilluminator (254nm) and photographed.

2.5.3 Isolation of genomic DNA fragments from agarose

Fragments of the DNA were isolated from the agarose gel using the Geneclean® Spin (BIO 101 Protocol) Method. A gel slice of DNA (about 300mg) was melted into GC Spin Glassmilk for 5 minute at 55°C. The solution was loaded onto a Spin filter and centrifuged for 1 min at 11,000g. The filter was then washed twice in GC Spin NewWash and dried by centrifugation of the empty filter for 1 min at 11,000g. The

DNA was eluted in 20µl of GC Spin Elution solution and used in ligation experiments.

2.5.4 Ethanol precipitation of DNA

DNA was concentrated by precipitation with absolute ethanol. A one-tenth volume of 3M sodium acetate (pH 5.2) was added to the DNA pellet, followed by two to three volumes of cold 100% ethanol. The mixture was placed at either -20°C overnight or at -70°C for about 45 minutes. The precipitated pellet was collected after centrifugation at 11,000g for 30 minutes at 4°C. The supernatant was discarded and one volume of cold 70% ethanol was added to wash the pellet. After spinning at 11,000g for 10 minutes, the ethanol was poured off and the pellet air-dried. The dry pellet was re-suspended in an appropriate amount of TE buffer (Section 2.3.2).

2.5.5 Complete digestion of genomic and plasmid DNA

After estimation of DNA concentration the appropriate amount of DNA was pipetted into a sterile 1.5ml Eppendorf tube. 1unit/µg DNA of the appropriate restriction enzyme(s) (Promega®) was added along with 2µl of the appropriate 10Xrestriction enzyme buffer. The volume was made up to 20µl with sterile distilled water. The tube was incubated at 37°C for most enzymes (25°C for *Sma*I) for 1 hour. The samples were then run on a 100ml 0.7% agarose gel for further analysis.

2.5.6 Ligation of insert DNA

Appropriate amounts of insert DNA and plasmid DNA were digested with the required restriction enzymes as in section 2.5.5. The digests were run on a 0.7% agarose gel (section 2.5.2), photographed and the appropriate DNA fragments extracted as in section 2.5.3. Between 1 and 5µg of band-extracted insert DNA was

added to a 1.5ml Eppendorf tube along with 0.5-1μg of band-extracted plasmid DNA, 2μl of 10Xligation buffer and 1μl of DNA T4 ligase (3U/μl) (both supplied by Promega®) and the volume made up to 20μl with sterile distilled water. The ligation reaction was incubated overnight at 4°C before transformation into XL1-Blue competent cells (section 2.5.8).

2.5.7 Preparation of E. coli competent cells

3ml L-Broth tubes were inoculated with a single colony of *E. coli* XL1-Blue and incubated overnight at 37°C with shaking. The following day 50ml of L-Broth was inoculated with 1ml of the overnight culture and incubated at 37°C with shaking. After 1½ hour the optical density (OD) of the cells at 600nm was taken and monitored thereafter until an OD between 0.5 and 0.6 achieved. The cells were harvested at 4°C by centrifugation at 4,000g for 5 minutes and re-suspended in solution I (Section 2.3.4) to give a total volume of 12ml. The cells were again centrifuged at 4,000g for 5 minutes and re-suspended in a total volume of 12.5ml of solution II then incubated on ice for 20 minutes. After incubation the cells were harvested as before and re-suspended in 2.5ml solution III. Cells were then aliquoted into 1.5ml Eppendorf tubes and stored at -70°C until needed.

2.5.8 E.coli transformation

Between 5 and 10μl of ligation reaction (section 2.5.6) was added to a sterile Eppendorf tube on ice. To this was added 100μl of *E.coli* XL1-Blue competent cells (section 2.5.7) and the reaction was incubated on ice for 30 minutes. After incubation 400μl of L-Broth (section 2.2.1) was added and the tube incubated at 37°C for 1 hour. After incubation, 50, 100 and 250μl of the transformation reaction were spread onto

STA Amp plates (section 2.2.1). For vectors allowing blue/white colony selection, the reaction was plated onto STA Amp plates containing IPTG\X-Gal (section 2.2.1). The plates were incubated overnight at 37°C and desired colonies were inoculated onto fresh STA Amp plates.

2.5.9 Analysis of bacterial transformants

Crude plasmid (73) preps were used to analyse the colonies obtained from transformation of XL1-Blue cells. Tubes containing 5ml L-Broth plus ampicillin (70μg/ml) were inoculated with single transformant colonies. These tubes were grown up overnight with shaking at 37°C. The next day 3ml of the cells were harvested by centrifugation at 13,000g for 1 minute. The excess media was removed by pipetting and the cells re-suspended in 500μl lysis buffer (section 2.3.2). The tubes were placed in a boiling water bath for 1 minute and then spun at 13,000g for 10 minutes. The protein pellet was removed and discarded using a sterile pipette tip. 600μl of room temperature isopropanol was added and the tubes inverted several times to mix. The tubes were spun at 13,000g for 2 minutes and the supernatant discarded. 500μl of 70% ethanol was added to the pellet and the tubes spun again for 2 minutes. The ethanol was removed by aspiration using a sterile pipette, and the pellet air-dried for 15-20 minutes. The pellet was re-suspended in 50μl TE buffer. 5μl of DNA was used in restriction enzyme digests to analyse the plasmid and insert.

2.5.10 Mini-prep preparation of Plasmid DNA

A Qiagen® mini-prep kit was used to extract plasmid DNA. All solutions were supplied with the kit unless stated otherwise (16).

A 200ml conical flask containing 100ml of L-broth plus ampicillin (70 μg/ml) was inoculated with a single colony of *E. coli* containing the plasmid of interest. The flask was incubated overnight with shaking at 37°C. The culture was transferred into a JA-14 centrifuge bottle and the cells harvested by centrifugation at 4,000g for 15 minutes at 4°C. The excess media was removed and the pellet re-suspended in 4ml of buffer P1 and the cells transferred to a sterile JA-20 tube. Four ml of buffer P2 was added to the re-suspended cells and mixed by inverting the tube 5 times. This reaction was incubated at room temperature for 5 minutes. The proteins were precipitated from solution by the addition of 4ml chilled P3 buffer and the tubes were again mixed by inversion and centrifuged at 18,000g for 30 minutes at 4°C. The supernatant was removed to a fresh JA-20 tube and centrifuged at 18,000g for 10 minutes at 4°C. The supernatant was again removed and added to a Qiagen mini-prep column that had been equilibriated with 4ml QBT buffer. The supernatant was allowed to enter the column by gravity. The column was washed twice with 10ml QC wash buffer and the DNA eluted into a fresh JA-20 tube by the addition of 4ml QF buffer. 0.7 volumes of ice-cold isopropanol was added and the DNA pelleted by centrifugation for 30 minutes at 18,000g at 4°C. The Isopropanol was removed and the pellet washed by the addition of 0.3 volumes of room temperature 70% ethanol and centrifugation at 18,000g for 15 minutes. The excess ethanol was removed and the pellet air-dried for 15-20 minutes before re-suspending in 500μl TE buffer. The amount of DNA was

quantified by running 1µl of DNA on a 0.7% agarose gel along with known concentrations of MW markers (section 2.5.2).

2.5.11 PCR Amplification of DNA

All solutions and enzymes were obtained from Promega® unless stated otherwise. 1µl of template DNA (100ng) was added to a 0.5 ml Eppendorf tube along with 5µl dNTPs (final concentration 50mM), 5µl 10xbuffer (Supplied with *Pfu* polymerase), 1µl forward primer (stock=100mM), 1µl reverse primer (stock=100mM) (primers obtained from MWG-Biotech) and 0.5µl *Pfu* polymerase (3U/µl). The reaction volume was made up to 50µl with sterile distilled water. Tubes were kept on ice during addition of PCR components. The tubes were transferred to a Techne Progene® PCR machine and run on the following standard PCR program (any changes in this program are listed in the relevant chapters):

Program 1	94°C 1 min 52°C 1 min 72°C 1 min/1000bp product 30 Cycles
Linked to Program 2	Final extension 72°C 10 minutes, one cycle 4°C hold

Twenty µl of PCR product was then run on either a 0.7% or 1% gel (depending on product size) as in section 2.5.2.

2.5.12 Addition of 3' A-Overhangs to PCR products produced using *Pfu* polymerase.

Direct cloning of DNA amplified by *Pfu* polymerase into TOPO®2.1 cloning vector produces low cloning efficiencies. This is because the proofreading ability of the *Pfu* polymerase removes the 3' A-overhangs necessary for TA Cloning®. These overhangs must be added to the PCR product before proceeding with cloning.

After amplification with *Pfu* polymerase, the whole reaction was run on an agarose gel (section 2.5.2) and the PCR product band extracted (section 2.5.3). One unit of *Taq* polymerase was then added to the band extracted DNA along with 1µl of dATP (final concentration 50mM). The tube was then incubated for 10-15 minutes at 72°C and then the reaction used in the TOPO® Cloning reaction.

2.5.13 The TOPO® Cloning Reaction

In a 0.5ml Eppendorf tube the following reaction was set up:

1µl PCR product

1µl Salt Solution (provided in kit)

1µl TOPO® vector

3µl Sterile distilled water.

The tube was then incubated for 5 minutes at room temperature and then placed on ice. 2µl of cloning reaction was then added to a vial of TOP10 One Shot cells (provided in kit) and the vial then incubated on ice for 30 minutes. The cells were then heat shocked by transferring the vial to a water bath at 42°C for 30 seconds and then immediately placed back on ice. To the reaction 250µl of LB medium was then added and the tube incubated at 37°C with shaking for 1 hour. Fifty and 100µl aliquots of the transformation were spread onto fresh STAAmp IPTG/X-Gal plates, which were

incubated overnight at 37°C. The following day up to 10 white colonies were picked and screened for inserts using standard techniques (Section 2.5.9).

2.5.14 Southern Blotting

Digested genomic DNA was run on an agarose gel and photographed as in section 2.5.2. All solutions used for Southern blotting are detailed in section 2.3.5). The gel was washed with agitation for 2x15 minutes in depurination solution and then in distilled water to remove the acid. The gel was washed a second time in denaturation solution with agitation for 2x15 minutes and finally for 30 minutes in neutralisation solution. The blot was then stacked as shown in Fig.1.1 and left overnight. The following day the membrane was air dried for 15 minutes and dried for 2 hours at 80°C.

Figure 1.1: Diagram to show stacking of the Southern blot.

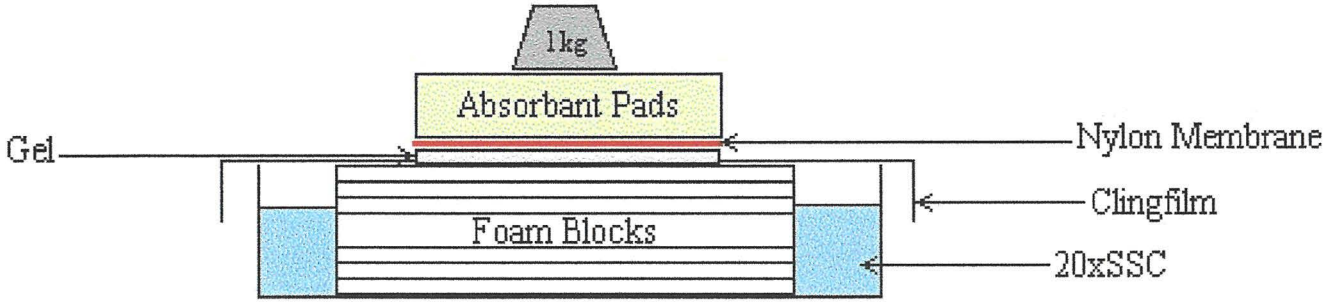

Nylon membranes used for Southern blotting were positively charged (Boehringer Mannheim).

2.5.15 Probing and Detection of Blot

The radioisotope ^{32}P was used to label probes. All solutions for labelling of the probe were supplied in the Appligene Nona primer kit except where stated. One hundred ng of probe was denatured by boiling for 10 minutes and chilling on ice for 5 minutes. To the denatured probe were added 4µl Nona primer mix, 1µl dATP, 1µl dTTP and 1µl dGTP (50mM final concentration). In the radiation lab 5µl ^{32}P dCTP (Anachem®) and 1µl Klenow enzyme (5U/µl) added. The tube was incubated for 30 minutes at 37°C. After incubation 60µl Adsorp and 2µl DNAprep resin were added and the solution was vortexed and incubated at room temperature for 2 minutes. The solution was spun at 10,000g for 2 minutes and the supernatant discarded. The pellet was washed in 100µl wash buffer and spun at 10,000g for 2 minutes. This wash was repeated again, with the supernatant being discarded each time. 100µl of elute solution was added to the pellet and the tube vortexed vigorously to resuspend the pellet. The tube was incubated for 10 minutes at 60°C then spun at 10,000g and the supernatant retained. The elution step was repeated for a second time.

Pre-Hybridisation

For a large blot (200ml agarose gel) 100 ml of pre-hybridisation solution is required. The blot was pre-hybridised for 2-5 hours at 55°C in hybridisation bottles.

Hybridisation

For a large blot 20 ml of hybridisation solution is required. The pre-hybridisation solution was removed and the hybridisation solution added. After addition the labelled probe was added (150µl for a large (200ml agarose gel) blot and 50µl for a small (50/100ml agarose gel) blot). The blot was then hybridised at 55°C overnight.

Washing and exposure of blots

After hybridisation the blot was washed with the following solutions:

2 x SSC/0.1% SDS 2 x 10 minutes at room temperature. (2x100ml)

1 x SSC/0.1% SDS 15 minutes at 55°C (1x 200ml)

0.1%SSC/0.1% SDS 15 minutes at 55°C (1x 200ml) (This wash was used only if background of the blot was very high).

After washing the blot was sealed in clingfilm and placed in a film cassette. In the dark room a Kodak® blue film was placed on top of the blot. The blot was stored at -50°C overnight and then the film was exposed. If bands were faint another piece of film was placed in the cassette, which was left for varying amounts of time (from 24hours to 2 weeks) until bands were visible.

Exposure of film

The film was developed for 3 minutes in developer solution, washed in distilled water then fixed for 1 minute in fixer solution. All solutions were obtained from Sigma®.

Chapter Three

Phenotypic Characterisation of the *sod^{VI}C1* Mutation

3.1 Introduction

The *sod^{VI}C1* strain L489 was isolated by Upshall *et al.* (150) in a screen for mutants defective in chromosome segregation resulting in the production of strains carrying extra copies of chromosomes (aneuploidy). At the permissive temperature of 30°C a *sod^{VI}C1* strain grows as wild-type (w.t.). However, at the restrictive temperature of 42°C the *sod^{VI}C1* mutation is lethal, with spores being unable to progress through germination. The phenotype of L489 seen on plates has been correlated at the microscopic level by germinating spores overnight, staining with DAPI and studied using UV microscopy. L489 spores germinated at the permissive temperature of 30°C grow as w.t. producing germ tubes > 12μM long with more than 8 nuclei per germling. At the restrictive temperature of 42°C the w.t. strain grows as at 30°C, however spores from the *sod^{VI}C1* strain L489 incubated at restrictive temperature rarely contained more than 2 nuclei. Measurements of the Chromosome Mitotic Index (CMI) of the *sod^{VI}C1* strain at 42°C were similar to that of the *sod^{VI}C^{+}* control strain, suggesting that the *sod^{VI}C1* mutation does not cause an arrest at a particular point in the cell cycle. Germination of the *sod^{VI}C1* spores was severely disrupted, although all spores swelled only 10% of them produced even a slight protuberance with the rest remaining spherical.

When grown on plates at the sub-restrictive temperature of 37°C, L489 produced a stable aneuploid that was phenotypically suggestive of an n+VI disomic. Käfer *et al.* (79) studied the phenotypes of disomic and trisomic strains for the eight *A. nidulans* chromosomes. Each aneuploid produces characteristic growth phenotypes

depending on which chromosome has been duplicated. The characteristic growths of the aneuploids enable the phenotypic designation of the *sod*^{VI}*C1* aneuploid as carrying an extra copy of chromosome VI. The *sod*^{VI}*C1* strain is unusual in that it forms a stable n+VI disomic, aneuploids normally breakdown to give euploid sectors at the semi-restrictive temperature. The stability of the *sod*^{VI}*C1* aneuploid was predicted to be the result of a gene dosage effect, whereby a strain containing 2 copies of the *sod*^{VI}*C1* mutation is more viable at the semi-restrictive temperature.

When the disomic *sod*^{VI}*C1* strain is downshifted to the permissive temperature of 30°C the strain simply loses the extra copy of chromosome VI producing presumed haploid (n) sectors. Likewise, if a colony grown at permissive temperature is up-shifted to 37°C it will duplicate a copy of chromosome VI and the colony will produce presumed disomic (n+VI) sectors.

The duplication of chromosome VI has only been confirmed phenotypically, and not genetically and no cytological studies have been carried out on the disomics. To study the duplication at the genetic level the segregation for markers on chromosome VI must be studied. This can only be done using a heterozygous diploid strain, as a haploid strain will only contain homologous copies of chromosome VI

Work presented in this chapter aims to show genetically that the duplication of chromosome VI occurs at 37°C and to further characterise the cytological phenotype of *sod*^{VI}*C1* strains grown at this temperature.

The *sod*^{VI}*C* gene was cloned by complementation using a chromosome VI specific cosmid library by Dr. S. Whittaker (23). Transformations were carried out with this library and a single cosmid W28G06 was found to fully complement the *sod*^{VI}*C1* mutation, as did its 9kb *Pst*I-*Hin*dIII sub-clone. This and the complementing region from the *PstI-Hin*dIII clone were sequenced on both strands by standard

procedures. On analysis the sequencing results showed the presence of a single open reading frame (ORF) of 3615bp (Appendix 5), which was predicted to encode a protein of 1205aa (Appendix 6) with an estimated size of 135kDa. The resulting sequence was used to screen DNA databases using the BLAST algorithm (2).

Homology searches showed that the predicted $Sod^{VI}C$ protein encodes a homologue of the yeast (51, 84), human (27), and bovine (42) α-COP proteins. The highest degree of homology was found to be with yeast α-COP, the highest homology (78%) was found at the N-terminus region of the protein. The lowest homology (43%) was found with the C-terminus this region is thought to be involved in organism specific functions.

The results from the cloning and sequencing of the *sod*^{VI}*C* gene show that it is involved in the early secretory pathway, but no work has been carried out to date to show whether the *sod*^{VI}*C1* mutant has a secretory phenotype. In common with all filamentous fungi *A. nidulans* forms elongated hyphae by the laying down of new cell wall material at the hyphal tip. This type of polarised growth is highly dependent on the delivery of newly synthesised cell wall precursors to the tip and so is tightly coupled to the secretory pathway. As well as requiring new cell wall material the fungus also needs to secrete enzymes (e.g. amylase) from the hyphal tip in order to break down complex polysaccharides present in the media to provide smaller units for metabolism.

The α-COP protein encoded by the *sod*^{VI}*C* gene is one of the seven subunits that form the protein coat complex coatomer. The main role of this complex has been shown in a number of studies (section 1.1.2) to be involved in the recycling (retrograde transport) of resident membrane and lumenal ER proteins from the Golgi back to the ER. In mammalian cells coatomer has also been implicated in the forward

(anterograde) transport of proteins between sequential Golgi cisternae (section 1.1.6). The arrangement of Golgi cisternae differ in fungi in that individual cisternae are spread through the cytoplasm, not located in the characteristic stacked structures seen in mammalian cells. Effects on this pathway due to the *sod*^{VI}*C1* mutation may lead to significant decreases in protein transport through the individual cisternae. Any effects on this process caused by the *sod*^{VI}*C1* mutation could lead to a loss of integrity of the endomembrane system. Since the ER and Golgi body are key organelles in the secretory pathway, any effect on their function may have a knock-on effect on the later stages of the pathway, causing a decrease in the amount of secretory vesicles being delivered to the hyphal tip. The effects of the *sod*^{VI}*C1* mutation on the ER and Golgi apparatus could be reflected by a decrease in the amount of enzymes secreted into the media and/or a build-up intracellularly of enzymes that are normally secreted.

In the third part of this work attempts were made to study the secretory phenotype of the *sod*^{VI}*C1* mutation, specifically the delivery of enzymes to the growing hyphal tip. A simple growth assay was used where by growth rates of both a *sod*^{VI}*C1* and a control strain were compared on different carbon and nitrogen sources. Plates in which the normal carbon and nitrogen sources of glucose and sodium nitrate were substituted with complex nutrients such as starch, albumin and casein, were used to grow test strains. These complex nutrients require the secretion of amylase (for utilisation of starch) and protease enzymes (for the utilisation of albumin and casein) in order to breakdown them down into smaller units suitable for endocytosis and metabolism. A decrease in the secretion of these enzymes at the hyphal tip would lead to a lower growth rate in the strain due to the limiting effect of nutrient availability

Results

3.2 Analysis of Disomic and Trisomic Strains

3.2.1 Construction of Chromosome VI-Marked Strains

In order to generate the strains required for the chromosome VI-marked diploid, sexual crosses (section 2.4.2) were carried out as in Fig.3.1. The chromosome VI-marked strain G66 was outcrossed with A188, recombinants from this cross were genotyped and the recombinant B707 was chosen, purified, and retested. This recombinant was then used in a second cross with the *sod*^{VI}*C1* strain B120 to generate B708. To generate the second marked strain the *sod*^{VI}*C1* strain B118 was crossed with strain G611, which contains the chromosome VI marker *nicC10*. Recombinants from this cross were again genotyped and a single recombinant B706 was chosen, purified and the genotype retested. The two recombinants B706 and B708 were then used to generate the diploid strain B709 as in section 2.4.4; the diploid was purified and the 'benlate test' carried out (section 2.4.5) to confirm diploid formation.

Figure 3.1: Generation of chromosome VI-marked strains for analysis of *sod*^{VI}*C1* disomics and trisomics.

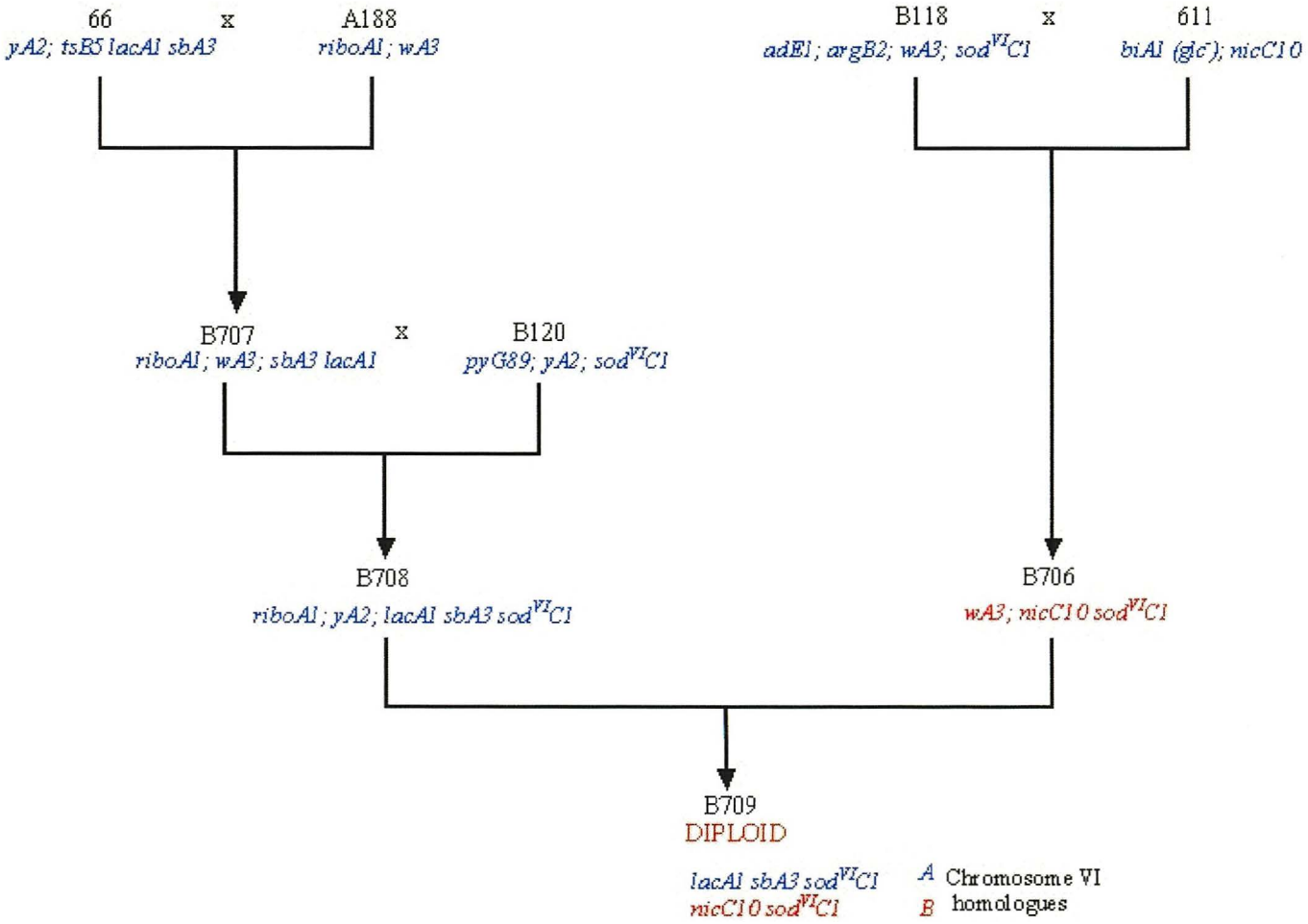

3.2.2 Analysis of Stable Trisomics

A stable presumed trisomic was formed by incubation of the diploid B709 at the semi-restrictive temperature of 37°C. The strain was maintained at this temperature through three propagations by sampling of spores from the periphery of the colony. This was carried out to ensure that a stable trisomic colony had been formed. The stable trisomic was used to inoculate fresh CM plates in duplicate; these plates were incubated at 37°C until the culture had grown to a diameter of about 2 inches. The culture was downshifted to the permissive temperature of 30°C for three to four days until sectors could be seen emerging from the central colony. Under this temperature regime the diploids grew in a manner analogous to that of the haploids illustrated in Fig. 3.2. Upon downshift to the permissive temperature, the central (presumed aneuploid) colony broke down to give presume euploid sectors (Fig. 3.3). The two different chromosome VI homologues allowed the segregation of the chromosome VI homologues upon downshift to be followed. Spore samples were taken from the edge of the sectors from both inoculations of the diploid with a sterile needle and streaked onto fresh CM plates. These samples were genotyped and their ploidies determined using the benlate test (section 2.4.5); tables 3.1 (A) and (B) show the results for the duplicate presumed trisomics tested.

The plates containing the sectoring presumed trisomic colonies were also velvet replica plated (section 2.4.1) onto MM plates with or without the required supplements to test the genotype of all the colony sectors (Fig. 3.4).

Figure 3.2: Sectoring seen with *sod*^{VI}*C1* strain B120 when shifted between permissive (30°C) and sub-restrictive (37°C) temperatures.
a) Colony grown at permissive temperature and up-shifted to sub-restrictive temperature.
b) Colony grown at sub-restrictive temperature and down-shifted to permissive temperature.

a)

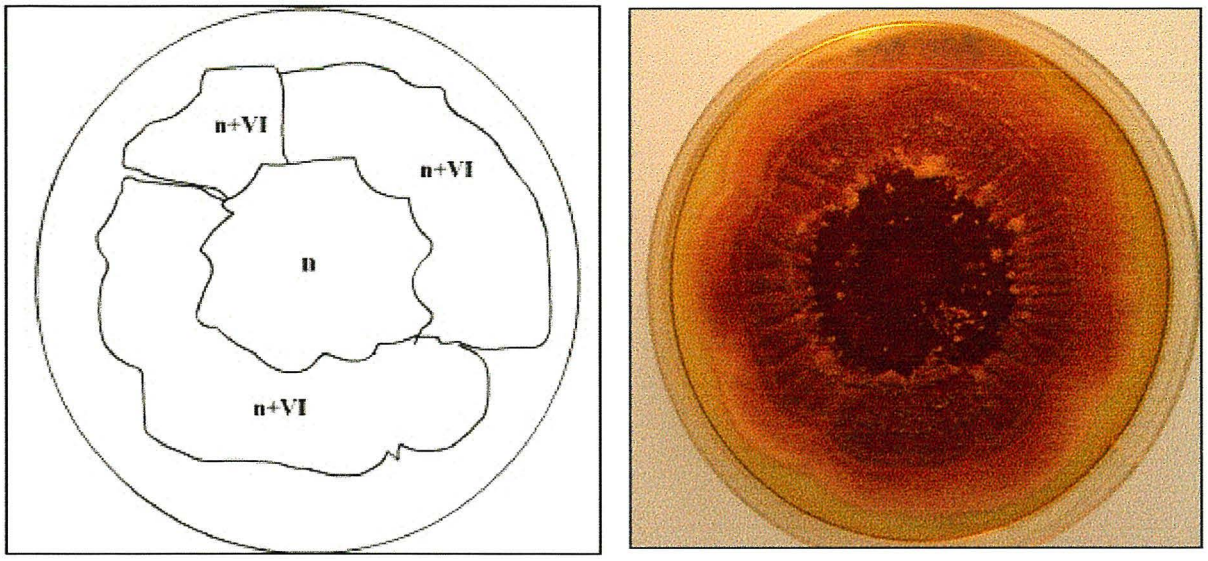

30 → 37°C

b)

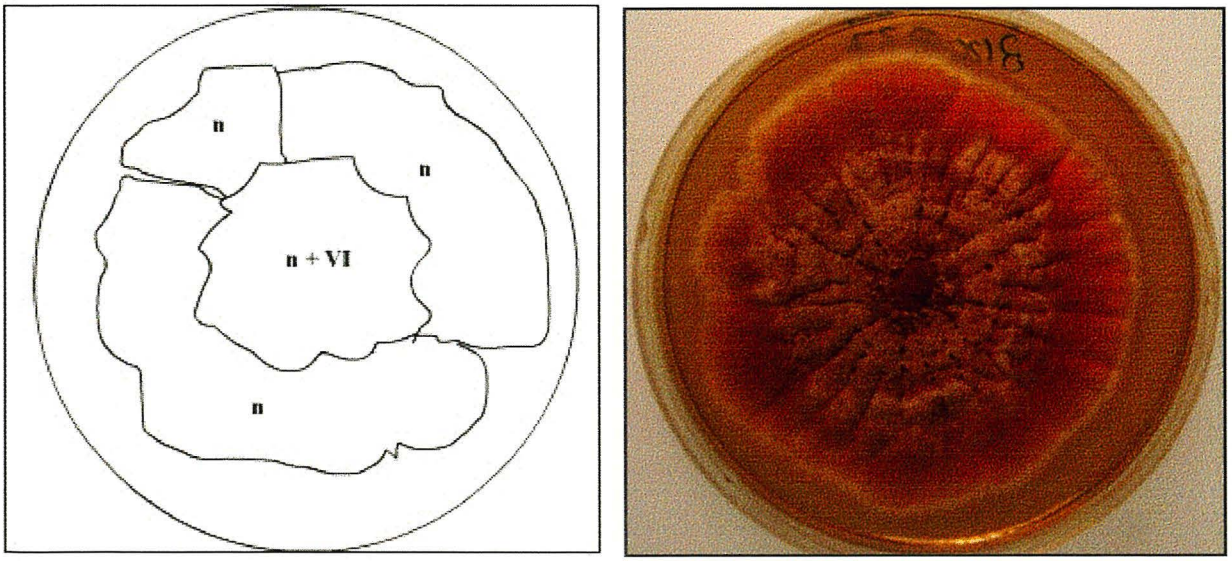

37 → 30°C

Figure 3.3: Mis-segregation of Chromosome VI in the diploid strain B709. Mis-segregation produces diploid (or occasionally haploid) sectors. These are either homozygous for markers on chromosome VI, with the diploid having either two copies of homologue A or two copies of homologue B, or heterozygous for markers on chromosome VI with the diploid having one copy of homologue A and one copy of homologue B. A third of the diploids produced should be homozygous for either homologue and 2/3 of the diploids will be heterozygous.

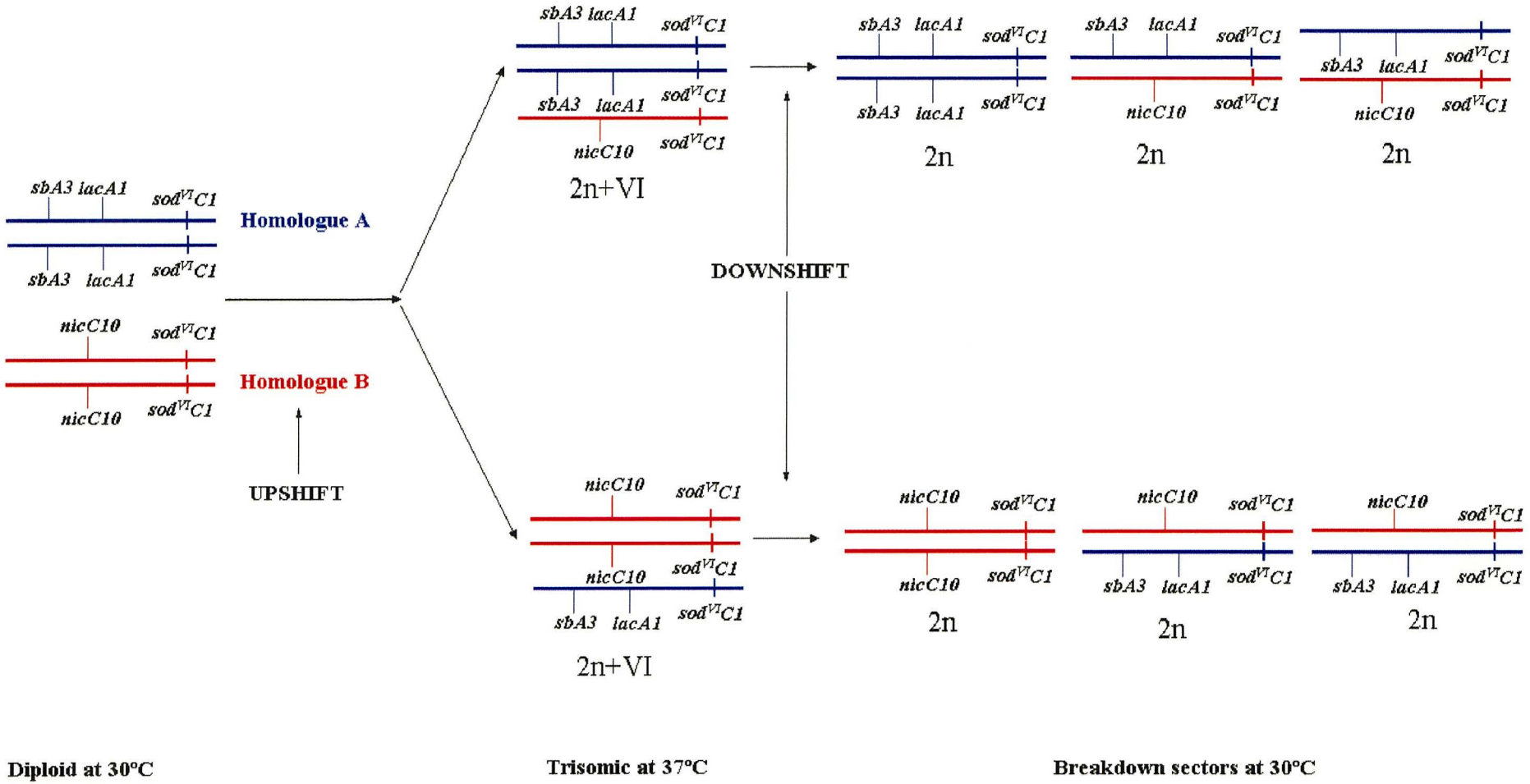

Table 3.1: Tables A and B show the genotypes and ploidies of the sectors recovered from the presumed duplicate trisomics upon downshift to the permissive temperature of 30°C. A '+' indicates w.t phenotype and a '-' indicates a mutant phenotype. N/A = not applicable for that sector.

(A) Trisomic 1

Sector	*ribo A1*	*sbA3*	*micC10*	*lacA1*	*sod^{VI}C1*	*wA3*	*yA2*	Ploidy	Chromosome VI
1	+	-	+	-	-	+	+	**2n**	**Homozygous**
2	+	+	+	+	-	+	+	**2n**	**Heterozygous**
3	+	+	+	+	-	+	+	**2n**	**Heterozygous**
4	+	+	+	+	-	+	+	**2n**	**Heterozygous**
5	+	+	+	+	-	+	+	**2n**	**Heterozygous**
6	+	+	+	+	-	+	+	**2n**	**Heterozygous**
7	+	+	+	+	-	+	+	**2n**	**Heterozygous**
8	+	+	+	+	-	+	+	**2n**	**Heterozygous**
9	+	+	+	+	-	+	+	**2n**	**Heterozygous**
10	+	+	+	+	-	+	+	**2n**	**Heterozygous**
11	-	+	-	+	-	-	+	**n**	**N/A**
12	+	+	+	+	-	+	+	**2n**	**Heterozygous**
13	-	+	-	+	-	+	-	**n**	**N/A**

(B) Trisomic 2

Sector	*riboA1*	*sbA3*	*nicC10*	*lacA1*	*sod^{yT}C1*	*wA3*	*yA2*	Ploidy	Chromosome VI
1	+	+	+	+	-	+	+	**2n**	**Heterozygous**
2	+	+	+	+	-	+	+	**2n**	**Heterozygous**
3	+	-	+	-	-	+	+	**2n**	**Homozygous**
4	+	+	+	+	-	+	+	**2n**	**Heterozygous**
5	+	-	+	-	-	+	+	**2n**	**Homozygous**
6	+	+	+	+	-	+	+	**2n**	**Heterozygous**
7	+	-	+	-	-	+	+	**2n**	**Homozygous**
8	+	+	+	+	-	+	+	**2n**	**Heterozygous**
9	-	+	-	+	-	+	-	**n**	**N/A**
10	+	-	+	-	-	+	+	**2n**	**Homozygous**

The results for the test trisomics show that for the two trisomics tested 15 sectors were heterozygous and 5 homozygous for markers on chromosome VI. The results strongly indicate that chromosome VI is indeed mis-segregated at 37°C. The generation of homozygous chromosome VI sectors can only be produced if this is the case. Homozygosity for other markers such as *riboA1* on chromosome I, which would result in the production of *riboA1* diploid sectors and wA3 on chromosome II, which would result in the formation of white diploid sectors, is not seen showing that no mis-segregation is occurring with these chromosomes. In order to completely show mis-segregation is due to chromosome VI alone, and is not occurring in any of the other chromosomes, a strain that has all 8 chromosomes marked should be tested. The observed ratios are skewed from the expected ratio shown in figure 3.4, however, this is probably due to the small sample of sectors taken.

As can be seen from the data in Fig. 3.5 haploid sectors are also generated when the trisomic breaks down. Haploid sectors are produced at a much lower level than disomic sectors these may occur due to the presence of a small number of disomic spores within the trisomic, which will then revert to haploidy upon downshift, the mis-segregation of chromosome VI upon downshift results in the formation of 2n-1 sectors, which then could sequentially lose a copy of each of the other homologues. Given that the cell is trying to segregate an abnormal number of chromosomes it is difficult to predict what can occur. The sectors were confirmed as being haploid by using the benlate test (section 2.4.5).

Figure 3.4: Velvet replication of trisomic colonies onto genotyping plates clearly shows the production of heterozygous and homozygous sectors.
▲ = Sector of recessive spore colour shown by benlate test to be haploid. ↗ = Sector homozygous for homologue A. ↗ = Sector homozygous for homologue B. ↗ = Heterozygous sector.

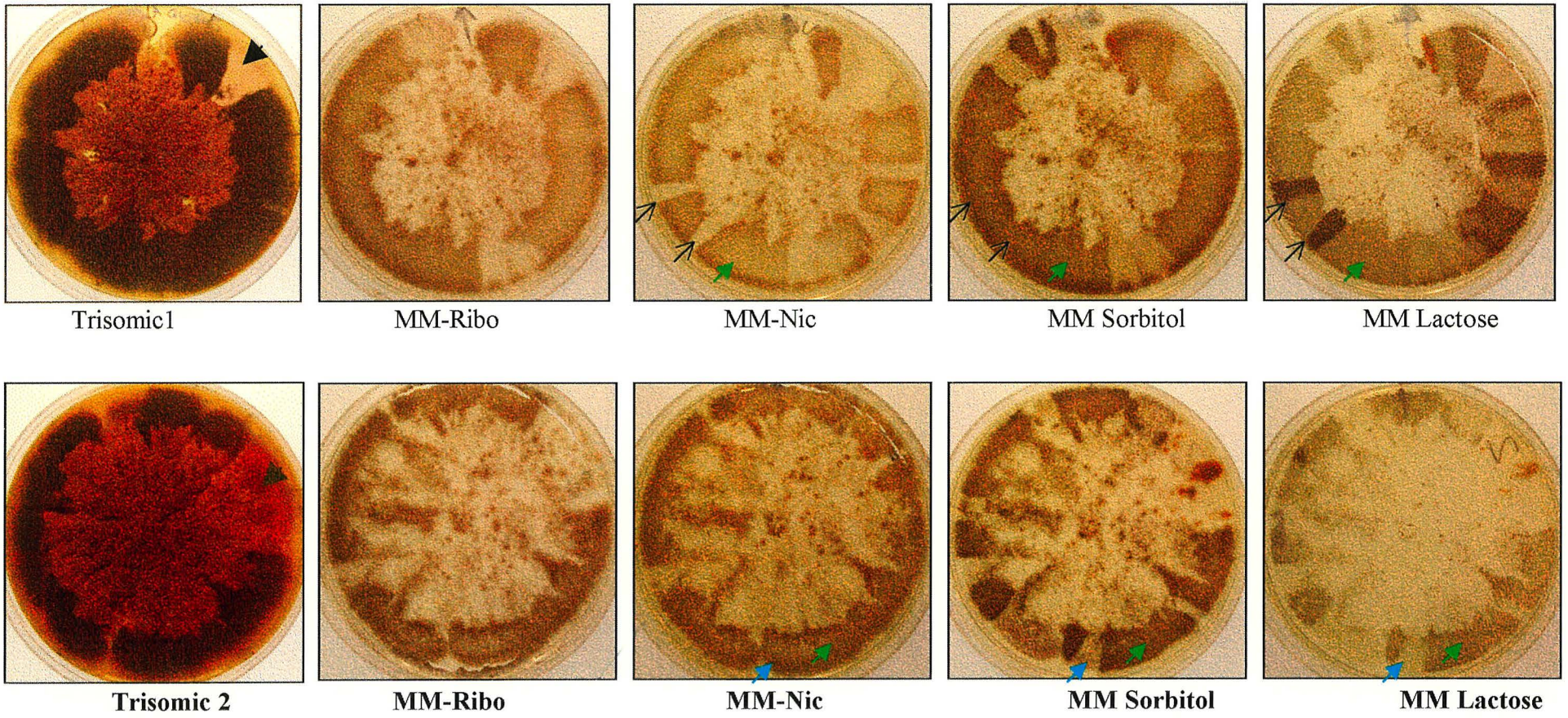

3.2.3 Phenotypes of Disomic and Trisomic strains

Spores from a stable B120 disomic and a stable B709 trisomic were stabbed onto fresh CMUU (B120 disomic) and CM (B709 trisomic) plates and incubated at 30, 37 and 42°C. Stable disomic and trisomic strains were generated by incubation of colonies of B120 and B709 at the semi-restrictive temperature of 37°C. The colonies were sub-cultured through three generations at this temperature to ensure a stable disomic or trisomic colony had been formed.

3.2.4 Cytology of Disomic and Trisomic strains

Spore suspensions from the control strain GR5, the *sod*^{VI}*C1* strain B120 and the *sod*^{VI}*C1* diploid B709 were incubated on coverslips overnight at 30°C (Fig 3.5), 37°C (Fig. 3.6) and 42°C (Fig. 3.7) stained with DAPI and examined by fluorescence microscopy (section 2.4.7). The stable B120 disomic and the stable B709 trisomic (produced as in section 3.2.3) were extremely poor sporulators, producing mainly aerial hyphae and only very small amounts of viable spores could be collected from these strains. Spores from the stable disomic and trisomic strain were used to look at the cytology at the restrictive temperature of 42°C (Fig. 3.7). Spores were incubated at 42°C, fixed and stained with DAPI and examined by fluorescence microscopy.

Figure 3.5: DAPI staining of the *sod*$^{VT}C^{+}$ strain GR5 (A), the *sod*$^{VT}C1$ strain B120 (B), and the diploid strain B709 (C), grown at the permissive temperature of 30°C. Bar on figures = 10μM.

(A)

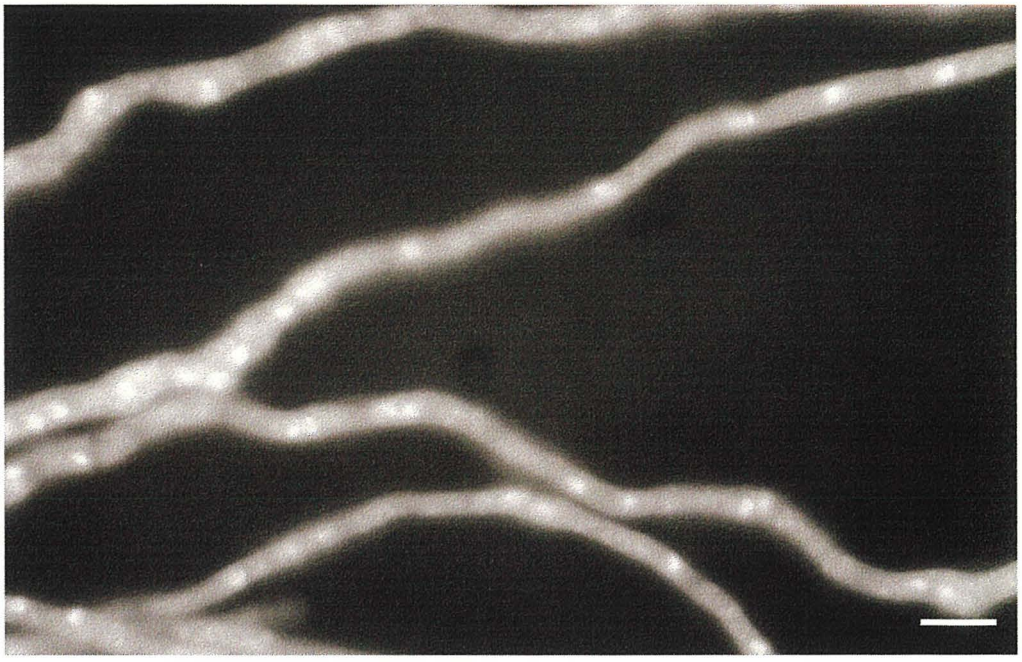

(B)

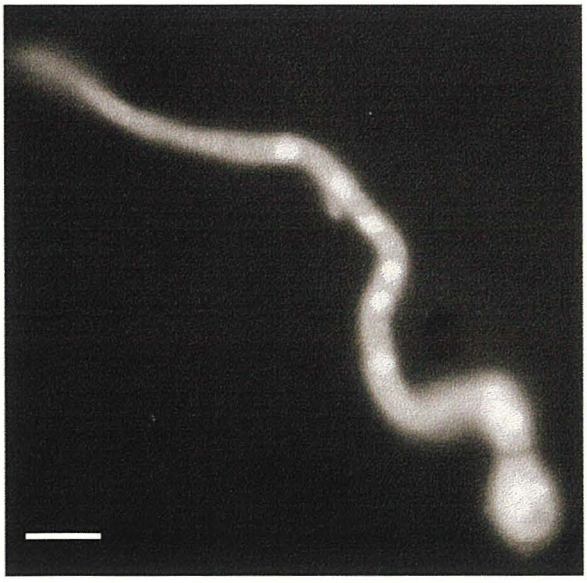

B120 (*sod*$^{VT}C1$)

(C)

B709 (*sod*$^{VT}C1$ diploid)

Figure 3.6: DAPI staining of the *sod*$^{VI}C^{+}$ strain GR5 (A), the *sod*$^{VI}C1$ strain B120 (B) + (C), and the diploid *sod*$^{VI}C1$ strain B709 (D) + (E) grown at the semi-restrictive temperature of 37°C.
Bars on figures = 10μM.

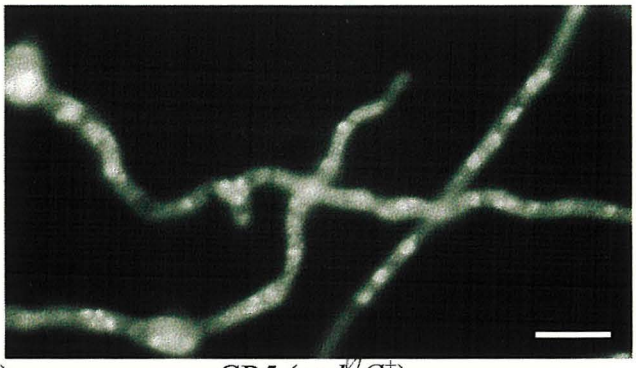

(A) GR5 (*sod*$^{VI}C^{+}$)

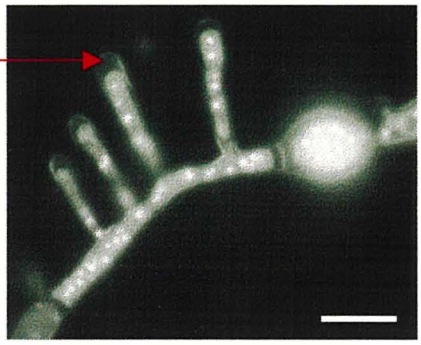

(B) B120 (*sod*$^{VI}C1$) Phenotype A

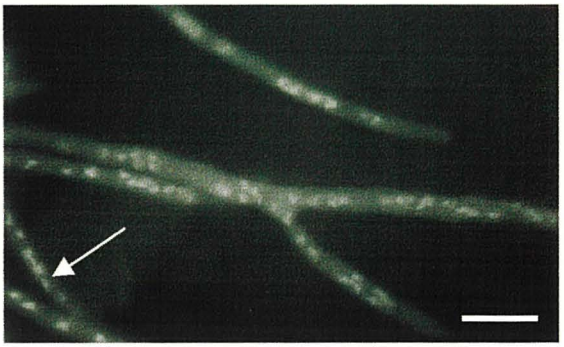

(C) B120 (*sod*$^{VI}C1$) Phenotype B

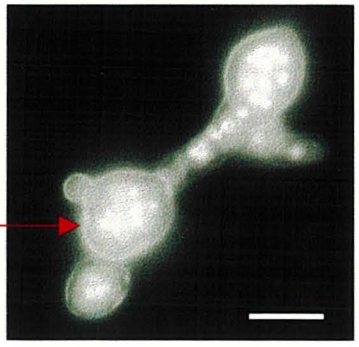

(D) B709 (*sod*$^{VI}C1$) Phenotype A

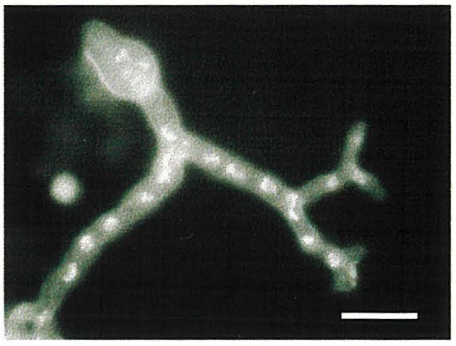

(E) B709 (*sod*$^{VI}C1$) Phenotype B

Figure 3.7: DAPI staining of the *sod*$^{VT}C^{+}$ strain GR5 (A), the *sod*$^{VT}C1$ B120 (B), the diploid B709 (C), the stable B120 disomic (D) + (E), and the stable B709 trisomic (F) + (G), grown at the restrictive temperature of 42°C.

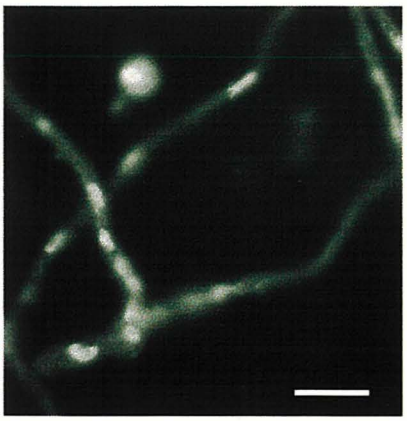

(A) GR5 (*sod*$^{VT}C^{+}$)

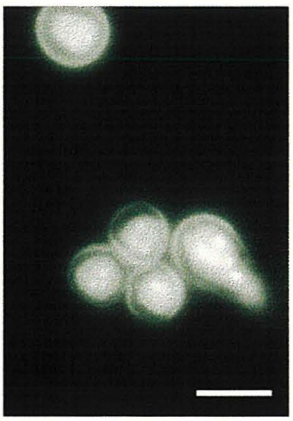

(B) B120 (*sod*$^{VT}C1$)

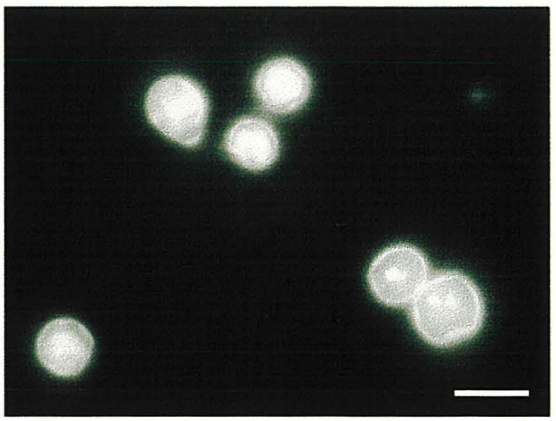

(C) B709 diploid (*sod*$^{VT}C1$)

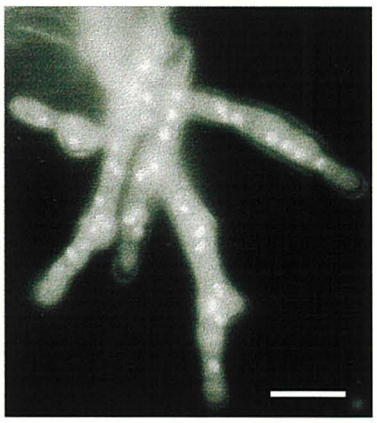

(D) B120 disomic phenotype A

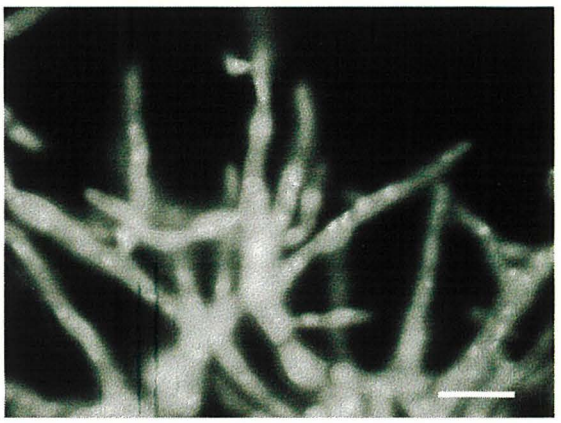

(E) B120 disomic phenotype B

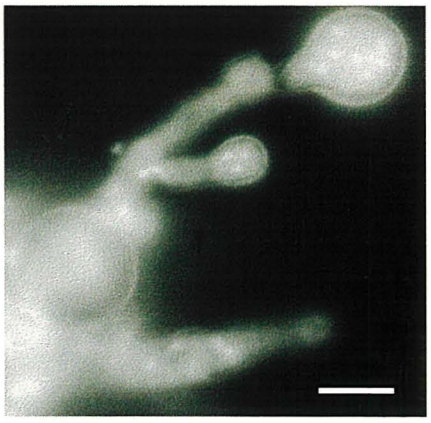

(F) B709 trisomic phenotype A

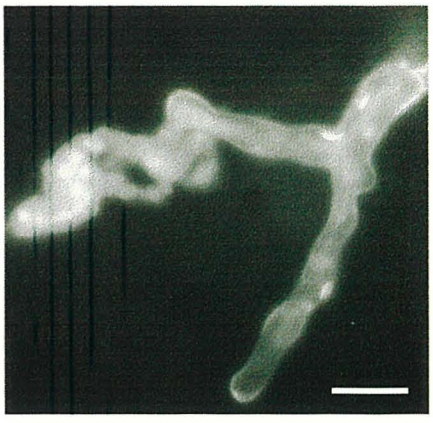

(G) B709 trisomic phenotype B

Upon incubation at the semi-restrictive temperature of 37°C the control strain GR5 (Fig. 3.6 (A)) grew as at 30°C (Fig. 3.5(A)). The haploid *sod*^{VI}*C1* strain B120 showed two phenotypic growth patterns. The first phenotype (Fig. 3.6(B)), produced hyphae with large sack like spore heads packed with nuclei. The germlings emerging from the spore head contained an elevated number of nuclei when compared to w.t. and the hyphae also showed an increase in branching frequency, with the distribution of nuclei within the branches being non-uniform. The second phenotype illustrated in Fig. 3.6(C) had hyphae that were phenotypically much more like w.t., showing lower levels of branching and more elongated hyphae. Most of the hyphae contained elevated numbers of nuclei, but some contained lower levels that showed more regular spacing along the hypha (Indicated by white arrow on Fig. 3.6(C)).

At the semi-restrictive temperature the diploid strain also produced two different phenotypes. The first (Fig. 3.6(D)) was very similar to the first phenotype observed with B120 (Fig. 3.6(B)), with the large sack-like spore heads packed with nuclei and an elevated number of branches. All of these types of hyphae showed irregular distribution of nuclei throughout the germling. The second phenotype (Fig. 3.6(E)) is again very similar to that seen with the B120 strain (Fig. 3.6(D)). The diploid hyphae grew more slowly and had more branches compared to the B120 strain, but contained far fewer nuclei than B120, and also showed relatively normal nuclear spacing. This more normal phenotype may be the result of the slower growth rate of the diploid, allowing more sorting of the nuclear material during the formation of the trisomic. Interestingly both the abnormal B120 and diploid hyphae (Fig. 3.6(B) and Fig.3.6(D)) showed hypersensitivity to fixation at elevated temperatures, resulting in slight plasmolysis of the hyphae (Shown by the red arrows in Fig. 3.6(B)+(D)).

Even fixation for a shorter time span produced this phenotype. This plasmolysis is not seen as much with the more normal hyphae and not at all with the control strain.

At the restrictive temperature of 42°C the w.t. strain GR5 (Fig. 3.7(A)) grew normally producing elongated hyphae as at the permissive temperature, the only difference being that the nuclei were more elongated. This is probably due to the stress on the fungi growing at this high temperature. The haploid B120 strain produced the characteristic *sod*^{VI}*C1* phenotype at restrictive temperature (See Fig. 3.7(B)). The spores were swollen containing between two and four nuclei with some of them producing a small germ tube. When spores from the stable B120 disomic and B709 trisomic plates were incubated at restrictive temperature, germination of the spores occurred (Fig. 3.7(D) + (E) and Fig. 3.7 (F) + (G)). B120 disomic spores incubated at the restrictive temperature of 42°C produced abnormal-looking hyphae, which exhibited much slower growth and contain elevated numbers of nuclei irregularly distributed throughout the hypha. The trisomic spores incubated at this temperature were much more abnormal. Although they germinated the germlings were very swollen and the hyphae had irregularly distributed nuclei, many failing to exit from the spore head. Most of the trisomic hyphae showed extreme sensitivity to fixation, many of them having burst, spilling the cytoplasm from the hypha as in Fig.3.7 (G). Although not as extreme, the disomic germlings at restrictive temperature also showed some plasmolysis. The fact that the stable disomics are able to germinate at the restrictive temperature supports the hypothesis that duplication of chromosome VI acts as a gene dosage response, whereby carrying two partially functional copies of *sod*^{VI}*C1* begins to overcome the block on germination.

The colony morphology of the stable disomic and trisomic strains was also tested on plates at the three temperatures (data not shown). At the permissive

temperature both the stable disomic and trisomic strains broke down in a similar manner to that seen in Fig 3.2 (B) and Fig 3.4, with euploid and diploid sectors being produced. The stable disomic and trisomic are unstable at 30°C and so lose their extra copy of chromosome VI resulting in the production of haploid and diploid sectors. At the semi-restrictive temperature the colonies grew as stable disomic and trisomic colonies, with no production of sectors. Growth at this temperature is much slower than a w.t. strain, presumably due to the extra nuclear material within these strains. At the restrictive temperature of 42°C the disomic and trisomic strains only managed to produce extremely small colonies after 2 days incubation, further incubation (up to 5 days) failed to see a change in colony size. This suggests that the extra copy of chromosome VI allows the *sod*^{VI}*C1* strains to overcome initial blocks in germination, as supported by the cytological data (Fig 3.7 (D), (E), (F), and (G)), but the benefits of the disomic and trisomic states is not sufficient to sustain colony growth with prolonged incubations at this temperature.

3.3 Analysis of the *sod*^{VI}*C1* Secretory Phenotype

3.3.1 Growth Studies on different Carbon Sources

The first growth tests looked at the effect of substituting different carbon sources in place of the normal carbon source of glucose. MM plates were made as in section 2.2.2 substituting glucose with 1% (w/v) of skimmed milk, starch or bovine serum albumin (BSA). Duplicate plates were inoculated with either strain B340 (*sod*^{VI}*C*$^{+}$) or B339 (*sod*^{VI}*C1*). These two strains are isogenic, in that they only differ by having a w.t. copy of *sod*^{VI}*C* (B340) and the mutated *sod*^{VI}*C1* gene (B339). Any differences between these two strains can thus be attributed to the *sod*^{VI}*C1* mutation and not to differences in other genes. One set of inoculated plates was incubated at the

permissive temperature of 30°C and the second set incubated at the semi-restrictive temperature of 37°C. Plates were set up in triplicate for each strain on all carbon sources and at both temperatures. Plates were incubated for 48hours to allow growth to establish and then the radius of the colonies was measured every 24hours for five days. The growth rates (mm/hr) of the strains on the different media at the different temperatures were calculated.

For each strain set, the growth rates on the different media at 37°C were expressed as a percentage of their growths on the same media at 30°C. This means that any differences between growth at 30 and 37°C due to the *sod*^{V7}*C1* mutation itself can be clearly separated from any differences due to the medium upon which the strain is grown. The average growth rates of the three replicates for each strain on each medium were taken, and are plotted in Figure 3.8.

Figure 3.8: Growth studies for the isogenic strains B340 (*sod*$^{VI}C^{+}$) and B339 (*sod*$^{VI}C1$) grown at the semi-restrictive temperature of 37°C. The growth rates shown are expressed as the percentage growth of the strains at 30°C. Error bars show the standard deviation from the mean of three replica experiments carried out for each strain.

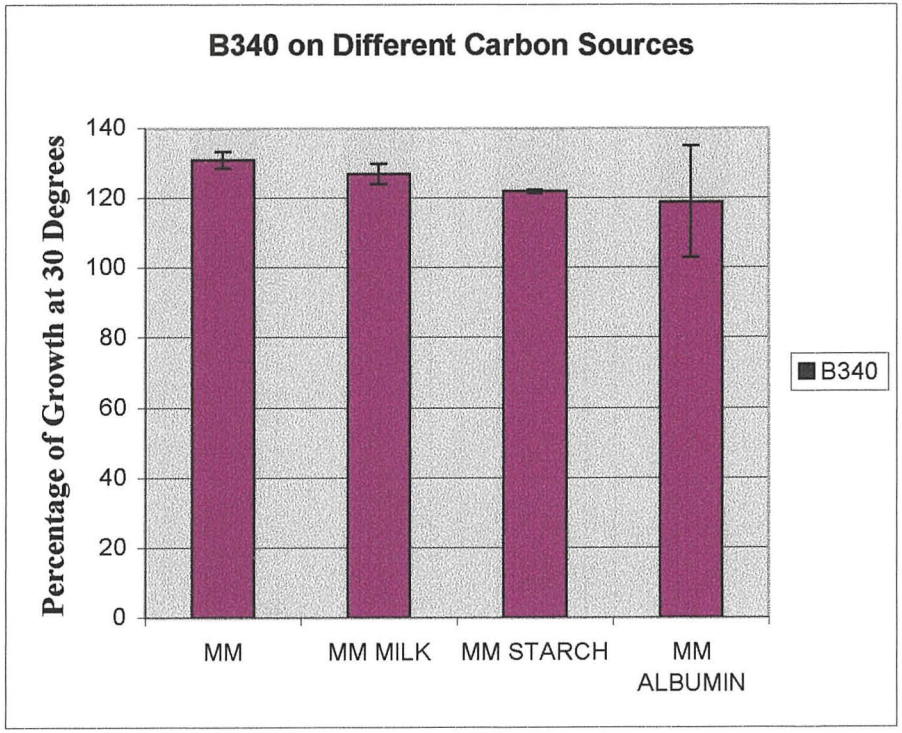

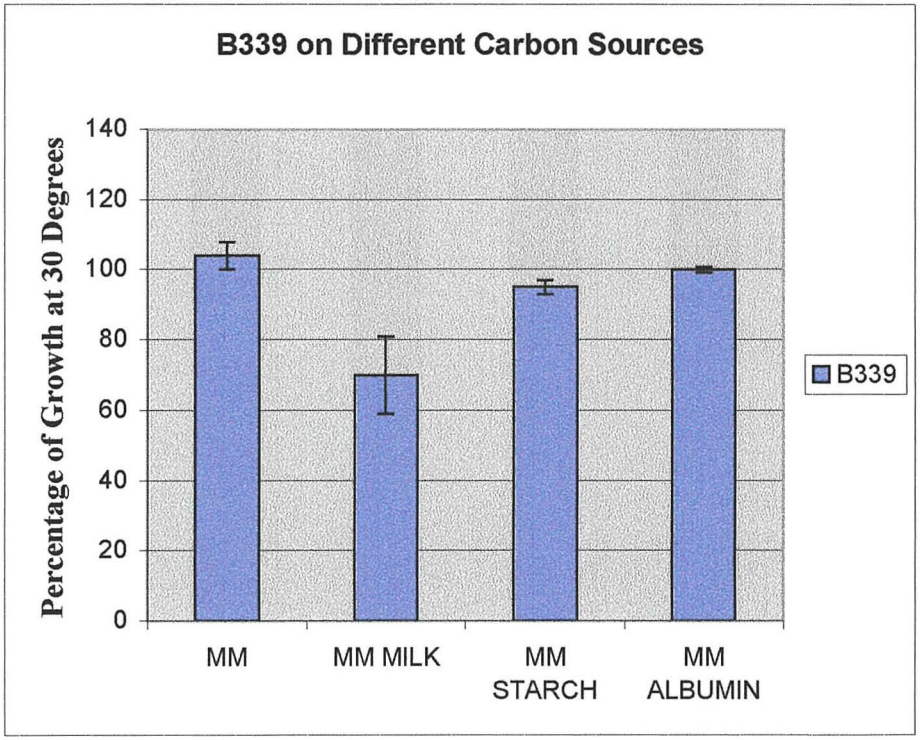

The control strain B340 (*sod*$^{VI}C^{+}$) shows a relatively constant growth rate with all the four carbon sources, being only slightly lower on the poorer carbon sources of starch and albumin. The *sod*$^{VI}C1$ strain B339 on MM glucose media shows a decrease in growth rate when compared to B340. This decrease is due to the effect of the *sod*$^{VI}C1$ mutation. B339 shows fairly constant growth rates on the starch and albumin plates, but on MM Milk B339 shows a significant decrease in growth rate. Strains, temperature and media effects were compared using a general linear model and a significance of 0.00 was obtained for the decrease in growth rate observed. This suggests that the *sod*$^{VI}C1$ mutation has an effect on the utilisation of this compound as a carbon source.

3.4 Discussion

The *sod*^{VI}*C1* mutation was identified in a screen for aneuploids and was found to produce a stable disomic for chromosome VI at the semi-restrictive temperature of 37°C. Chromosome VI was identified as being the chromosome mis-segregated on the basis of the colony morphology of the aneuploid. Disomics for different chromosomes produce characteristic morphologies and are easily identified. In order to confirm this genetically a diploid was produced which contained two different chromosome VI homologues; both were homozygous for *sod*^{VI}*C1,* but heterozygous for different chromosome VI markers. A presumed trisomic was formed by incubation of the diploid at semi-restrictive temperature. This was then allowed to produce diploid sectors by downshifting to the permissive temperature of 30°C. Analysis of these sectors showed that chromosome VI undergoes mis-segregation upon upshift to 37°C, which is supported by the absence of mis-segregation of chromosomes II and I, indicating a specific effect on chromosome VI.

Although the *sod*^{VI}*C1* mutation was isolated in screen for chromosome segregation mutants, the *sod*^{VI}*C* gene product shows that this is clearly not the case. The most likely explanation for the stable disomic produced at 37°C is a gene dosage effect caused by the *sod*^{VI}*C1* mutation, which maps to chromosome VI. The *sod*^{VI}*C* mutation has been shown to map to a putative promoter region just upstream of the start codon. At the semi-restrictive temperature of 37°C, the *sod*^{VI}*C1* mutation may cause a down regulation in the amount of transcript being produced. The doubling up of chromosome VI may help to overcome this block with the production of an aneuploid strain containing two copies of the defective gene. It may seem extreme for an organism to duplicate a whole chromosome, however it is probably the easiest response to a temperature increase. Other methods would require the duplication and

reinsertion of the gene into a suitable position in the genome. When the disomic is downshifted to permissive temperature the strain simply loses the extra copy of chromosome VI producing haploid (n) sectors.

Other examples of a gene dosage effect have been seen in *A. nidulans*, the *adE* gene was shown to undergo spontaneous duplication when *adE* mutants were grown on selective media, although whole chromosome duplications have not been reported to date (100). The $sod^{VI}C1$ mutations effect on the $sod^{VI}C$ gene product is more likely to be causing a gene dosage effect rather than a chromosome mis-segregation event. Mutations that effect chromosome segregation are more likely to give general defects in the sorting of chromosomes, therefore, producing the full range of aneuploids not just the stable n+VI disomic seen in this case (78).

Cytological analysis of the diploid and haploid strains supports the gene-dosage effect hypothesised for the production of the stable n+VI disomic. Spores taken from a stable disomic colony were capable of germination at restrictive temperature. The extra copy of chromosome VI appears to partially overcome the null-phenotype seen at 42°C with the haploid strain. This gene-dosage effect would make sense if the $sod^{VI}C1$ mutation caused a decrease in transcript levels within the cell. Although the extra copy of chromosome VI in the stable disomic and trisomic enables growth at sub-restrictive and restrictive temperature, germination is not 100% normal indicating that the extra copy does not completely overcome the mutation. This is supported by morphological data, which suggests that the extra copy of chromosome VI is only able to sustain growth in the short term, with prolonged incubation at 42°C still being lethal. Apart from the abnormal hyphal and nuclear morphology the hyphae also display sensitivity to fixation at elevated temperatures. This may indicate a problem with cell wall integrity. The effect of the $sod^{VI}C1$

mutation on secretion may be such that new cell walls are not laid down correctly, leading to the production of weaker cell walls that are more sensitive to osmotic changes. A study of living hyphae from the haploid and disomic strains exposed to different osmotic stresses may reveal more conclusive evidence for these.

The third part of this study was to make some initial attempts to characterise the effects of the *sod*^{VI}*C1* mutation on enzyme secretion from the hyphal tip. A study was carried out to look at the ability of the *sod*^{VI}*C1* strain B339 to utilise the complex carbon sources of milk, starch and BSA. In order to successfully use these substrates as carbon and nitrogen sources the fungus must be able to secrete protease and amylase enzymes. Effects of the *sod*^{VI}*C1* mutation on the integrity of the ER and Golgi body may lead to a decrease in the secretion of these enzymes in the mutant strain and therefore a decrease in growth rate due to the amount of substrate available. The isogenic control strain B340 was used to compare the utilisation of these substrates by a w.t. *sod*^{VI}*C* strain. The results indicate that the *sod*^{VI}*C1* mutation causes a slight but significant decrease in growth rate of the B339 strain on MM Milk media. This may be due to a decrease in the amount of protease enzyme being secreted and so casein is not utilised as readily. Although this data suggests an effect of the *sod*^{VI}*C1* mutation on secretion of proteases there are a number of reasons why these results should be regarded with some scepticism. Firstly, no decrease in growth rate was seen on the albumin media, this media also requires the secretion of proteases for utilisation as a carbon source. Secondly, milk medium also contains other nutrients including the milk sugar lactose, which can also be utilised as a carbon source and may be used preferentially to casein as a carbon source.

In light of the limitations of the previous work preliminary attempts were also made using different enzyme assays to look directly at the amounts of a specific

enzyme being secreted. This kind of study is difficult with *A. nidulans* as this fungus is not a high native secretor unlike the fungus *A. niger* commonly used to study hyphal tip secretion. An invertase assay based on the method used by Vainstein *et al.* (151) was used to look at the secretion of invertase into culture medium. However, this method proved unsuccessful with no invertase being detected, although it has been used previously in *A. nidulans.* A second approach to looking at levels of secretion was attempted using the plasmid pGPT (Gift of Genencor International Inc), which encodes the *Mucor michei* aspartyl protease (MMAP). It has been shown MMAP can be expressed in *A. nidulans* under the control of the *Aspergillus awamori* glucoamylase gene promoter (Prof. G. Turner, personal communication). The plasmid expresses the MMAP gene when transformant strains are grown in maltose fermentation media for three days, which can be detected by clotting of casein in plates containing skimmed milk. The pGPT plasmid was transformed into the $sod^{VI}C^{+}$ strain GR5 and the $sod^{VI}C1$ strain B120 and transformants were grown at 30 and 37°C. However, the clotted rings produced by both strains were small (maximum 15mm) and the test did not have the required level of resolution to detect small changes between strains. Unfortunately time restraints prevented optimisation of this approach.

It may also have been useful to look at the intracellular pattern of secretion as well as secretion directly from the hyphal tip. The $sod^{VI}C1$ mutation may cause a build up of enzymes intracellularly that would normally be secreted. A good approach to this kind of study would be to use a GFP-tagged secreted protein. This would allow the monitoring of both the internal and external localisation of the GFP-tagged protein. A number of different secreted proteins would have to be used as effects on the secretory pathway may have specific effects on different enzymes. Work carried

out by Gordon *et al.* in *A. niger* (54) used the *A. niger* glucoamylase gene tagged with GFP to study localisation of the enzyme in the hyphae. They found that glucoamylase localises predominantly to the hyphal tip in *A. niger*. Attempts were made to use this construct in *A. nidulans* but no hyphal tip localisation was noted although some low level GFP fluorescence was detected in the surrounding media. This could be because the *A. niger* glucoamylase protein is not fully functional being poorly expressed from the *A. niger* promoter, or because the localisation of this protein is different in *A. nidulans.* More work using enzymes like this may help to elucidate *sod*^{VI}*C1*'s effect on the secretory pathway.

Chapter Four

Molecular Characterisation of the *sod^{VI}C1* mutation

4.1 Introduction

Initial work carried out on characterisation of the *sod^{VI}C1* mutation had identified a complementing fragment, which had been cloned and sequenced and shown to be the *A. nidulans* α-COP equivalent. However, there were still a number of questions unanswered. Firstly, was the cloned gene the *bona fide sod^{VI}C* gene or a multicopy suppressor of the *sod^{VI}C1* mutation? Secondly, is the *sod^{VI}C1* mutation a loss-of-function mutation and thirdly, where is the *sod^{VI}C1* mutation located?

The *sod^{VI}C* gene was cloned by complementation of the *sod^{VI}C1* mutant phenotype. The use of mutant complementation runs the risk that the cloned gene may be a multicopy suppressor of the mutant phenotype. An extra copy of the *nimE* gene, which encodes the *A. nidulans* cyclinB homologue, partially suppresses a mutation in the *nimT* gene encoding the *A. nidulans* cdc25 homologue (103). Multicopy suppressors have also been used in *A. nidulans* to study proteins that interacted with the NudF protein. This protein is homologous to the human LISI protein and functions in the cytoplasmic dynein/dynactin pathway and is required for distribution of nuclei. Multicopy suppressors of a mutation in the *nudF* gene led to the identification of the protein NUDE encoded by the *nudE* gene (38). Studies of this gene have shown it to be homologous to proteins from *N. crassa* and humans allowing comparisons between different eukaryotic pathways.

In order to distinguish between a multicopy suppressor and the cloning of the *bona fide sod^{VI}C* gene use was made of a two-step gene replacement strategy (103). This strategy exploits the properties of the chemical 5-Fluoroorotic acid (FOA) (17). FOA is a

pyrimidine analogue, which selects against the presence of the *pyr4*$^{+}$ marker from *N. crassa*. Some preliminary work on this study had already been carried out; a 6.4kb *EcoR*I fragment shown to complement the *sod*^{VI}*C1* mutation (165) was cloned into the vector pRG3, (161) to produce the plasmid pSW2 (Fig. 4.2(A)). The vector pRG3 also contains the *pyr4*$^{+}$ marker to allow selection of transformants by complementation of the *pyrG89* mutation from *A. nidulans*. A *sod*^{VI}*C1* was transformed with the plasmid pSW2 and transformants selected by growing on medium lacking uridine and uracil.

A site-specific integration of pSW2 is predicted to result in two copies of the *sod*^{VI}*C* gene flanking the *pyr4*$^{+}$ gene, one copy being derived from the inserted w.t. genomic clone, and the other from the resident mutant *sod*^{VI}*C* gene. Curing of the plasmid from a site-specific transformant by growth on FOA can occur by looping out of the plasmid by homologous recombination between the flanking duplicated sequences (17). This loop-out can result in the loss of the w.t. *EcoR*I fragment contained withini pSW2, or the loss of the corresponding mutant *sod*^{VI}*C* sequence. If the cloned gene is *sod*^{VI}*C*, and the *sod*^{VI}*C1* mutation is located within the *EcoR*I fragment, loop-out of the w.t. copy of the *sod*^{VI}*C* gene will result in the production of ts^{-} strains, whereas the loop-out of the mutant copy of the gene will result in the production of ts^{+} strains. However, if the cloned gene is a multicopy suppressor then all the sectors produced will be ts^{-}.

In the next section of work attempts were made to determine whether the *sod*^{VI}*C1* mutation is a loss-of-function mutation. The *sod*^{VI}*C1* mutation causes a characteristic ts^{-} phenotype, with spores being unable to progress through germination at the restrictive temperature of 42°C. The temperature-sensitive phenotype seen with the *sod*^{VI}*C1* mutation may be due to one of two things. Either *sod*^{VI}*C* is an essential gene and the

sod^{VI}*C1* mutation is a loss-of-function mutation, or the *sod*^{VI}*C1* mutation causes the production of a toxic protein. Production of a toxic protein has been shown with other mutations, for example in the mutant *bimG11* strain. The *bimG* gene encodes the Type 1 protein phosphatase (PP1) of *A. nidulans* (35). The temperature-sensitive *bimG11* mutation results in the mis-splicing of one of the three introns from the *bimG* transcript, resulting in the lethal-phenotype at 42°C. However, when the *bimG* gene is knocked out, no mutant phenotype is detected. This is thought to be due to the *bimG11* mutation causing the production of a toxic truncated protein at 42°C. When deleted the overlapping function of phosphatases within the cell compensates for the loss of BimG (77).

If the *sod*^{VI}*C* gene is essential then a disruption of the gene should result in the null-phenotype seen with the *sod*^{VI}*C1* mutation. Conversely, if the knockout of the *sod*^{VI}*C* gene results in the appearance of the w.t. or different phenotype, it would suggest that the *sod*^{VI}*C1* mutation causes the production of a toxic protein and is not essential.

In order to distinguish between these two possibilities a heterokaryon rescue strategy was used to created and identify a strain in which the gene had been disrupted. This technique was used by Osmani *et al.* (107) and exploits the ability of *A. nidulans* to form stable heterokaryons. A heterokaryon is a strain containing two different types of nuclei within a common cytoplasm. This is formed by the fusion of two adjacent hyphae from different strains. During the transformation of *A. nidulans*, heterokaryotic transformants are often produced spontaneously that contain disrupted and w.t. nuclei within the same hypha. This allows the rescue of potentially essential genes that would normally result in the death of the strain.

The third piece of work in this chapter attempted to identify the position and nature of the *sod*^{VI}*C1* mutation. This was undertaken by using a complementation strategy. A number of smaller sub-clones generated from the 9kb *Pst*I-*Hind*III sub-clone shown to complement the *sod*^{VI}*C1* mutation were transformed as linear fragments into a *sod*^{VI}*C1* strain and transformants incubated at 42°C. The rationale being that transformants able to grow at the restrictive temperature will contain the sub-clone capable of complementing the *sod*^{VI}*C1* mutation. In this way the *sod*^{VI}*C1* mutation could be narrowed down to a smaller fragment for sequencing analysis. The data from the complementation study was used to construct primers form the w.t. sequence; these were then used to amplify the same region from genomic DNA extracted from the *sod*^{VI}*C1* strain B120. This region was then sequenced and the data compared to the published w.t. sequence.

4.2 Two-step Gene Replacement

4.2.1 Transformation and Selection of pSW2 Site-specific Integrants

The pRG3 vector used to construct the plasmid pSW2 also contains the *pyr4*$^{+}$ gene from *N. crassa*, which complements the *A. nidulans pyrG89* mutation. Strains carrying this mutation are unable to grow on normal media (CM) and require the addition of uridine and uracil (CMUU). This marker acts as a useful tool allowing the selection of transformants containing the plasmid of interest. *A. nidulans* transformation hosts were constructed that contained the *sod*^{VI}*C1* mutation in conjunction with the *pyrG89* mutation.

The *sod*^{VI}*C1* strain (B120) was transformed with the plasmid pSW2 (section 2.4.6) and transformants were selected by plating onto media lacking uridine and uracil. The transformants were screened for production of ts^{-} and ts^{+} colonies by stabbing onto CMUU plates containing 1 mg/ml FOA and incubation at 30°C for 2-3 days. Growth on media containing FOA selects for the looping out of the pRG3 plasmid (curing), producing sectors that grow out from the main colony that have lost the *pyr4*$^{+}$ marker. These FOA-resistant sectors were tested for temperature sensitivity by inoculation onto CMUU plates that were incubated at 30°C for 2-3 days. The plates were then velvet replica plated onto CMUU media and incubated at 42°C. Two of the transformants (pSW2-7 and pSW2-8) produced both ts^{-} and ts^{+} sectors and were therefore proposed to be site-specific transformants (Fig. 4.1).

Figure 4.1: a) Four pSW2 transformants grown at 30°C for three days showing the production of FOA resistant sectors. b) Replica plating on CMUU plates incubated at 42°C; pSW2-7 and 8 show the production of ts^+ and ts^- sectors.

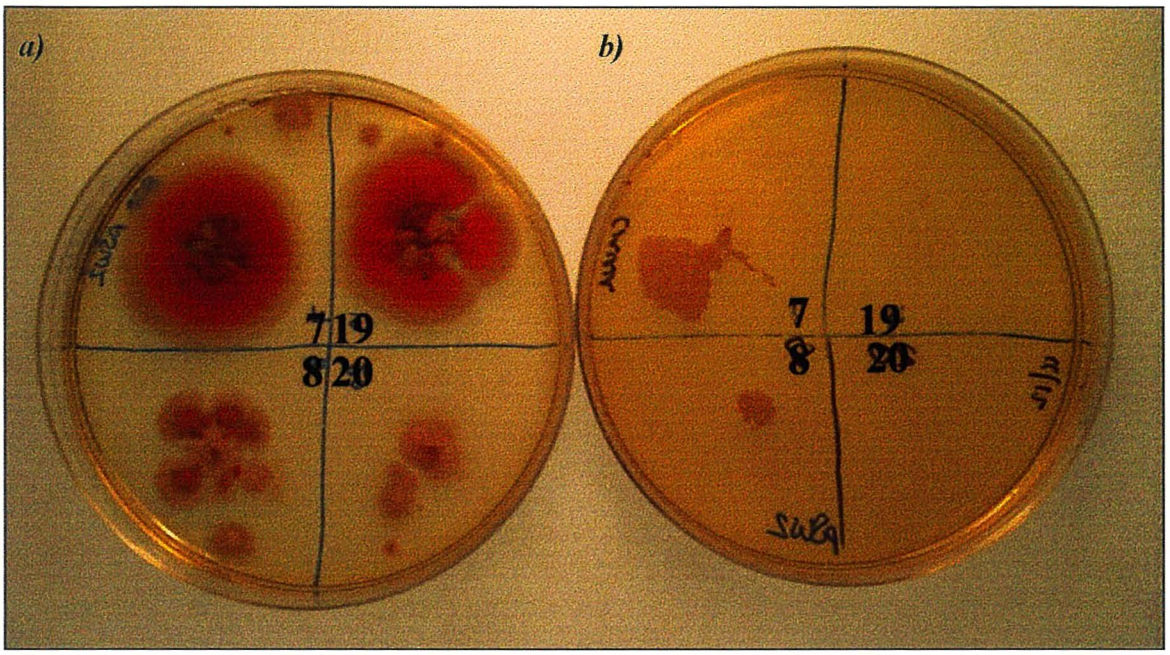

4.2.2 Confirmation of Site-specific Integration by Southern Blotting

Although the production of ts^+ and ts^- colonies is an indication of a site-specific integration it was necessary to confirm this by Southern blotting. Spores from pSW2-7 and 8 were used to inoculate 100ml of liquid CM media in 250ml-bevelled flasks. The flasks were incubated overnight with shaking at 30°C; the mycelia were then harvested by filtration and ground under liquid nitrogen. Genomic DNA was then extracted according to section 2.5.1 and run on a 0.7% agarose gel (section 2.5.2) to quantify and check its quality. Approximately 3µg of DNA from each of the genomic DNA preparations was digested with the restriction enzymes *Pst*I and *Hin*dIII (section 2.5.5.) The samples were electrophoresed on a 0.7% agarose gel (section 2.5.2) along with a 1kb DNA ladder Promega® (Appendix 4) for 12-16 hours at 10mA (Fig. 4.3(D)). The gel was then blotted as in section 2.5.14. After blotting the gel was hybridised (section 2.5.15) and probed using 100ng of ^{32}P labelled (section 2.5.15) 6.4kb *EcoR*I fragment produced by digestion of the 9.0kb *Pst*I-*Hin*dIII clone.

As the *Pst*I-*Hin*dIII fragment had been previously mapped (Fig. 4.2) the bands produced by a site-specific integration of pSW2 could be predicted. The control strain GR5 with a non-disrupted copy of *sod*^{VI}*C* should produce a single 9kb *Pst*I-*Hin*dIII fragment that hybridises to the probe. Integration of the pSW2 at the *sod*^{VI}*C* locus was predicted to produce two hybridising fragments (Fig. 4.3(C)).

Figure 4.2: Map of *Pst*I-*Hin*dIII clone showing sequenced and restriction mapped regions. Some of the map for the *Pst*I-*Hin*dIII is based on restriction mapping of bands by comparison to known band sizes from a marker. Experimental errors are incurred due to an inability to be able to distinguish small differences between the fragment and the marker band. The size variation of the *Pst*I-*Hin*dIII fragment based on these errors is 8.76kb-9.26kb. Taking the average of the values, the size of the *Pst*I-*Hin*dIII fragment is estimated to be 9kb.

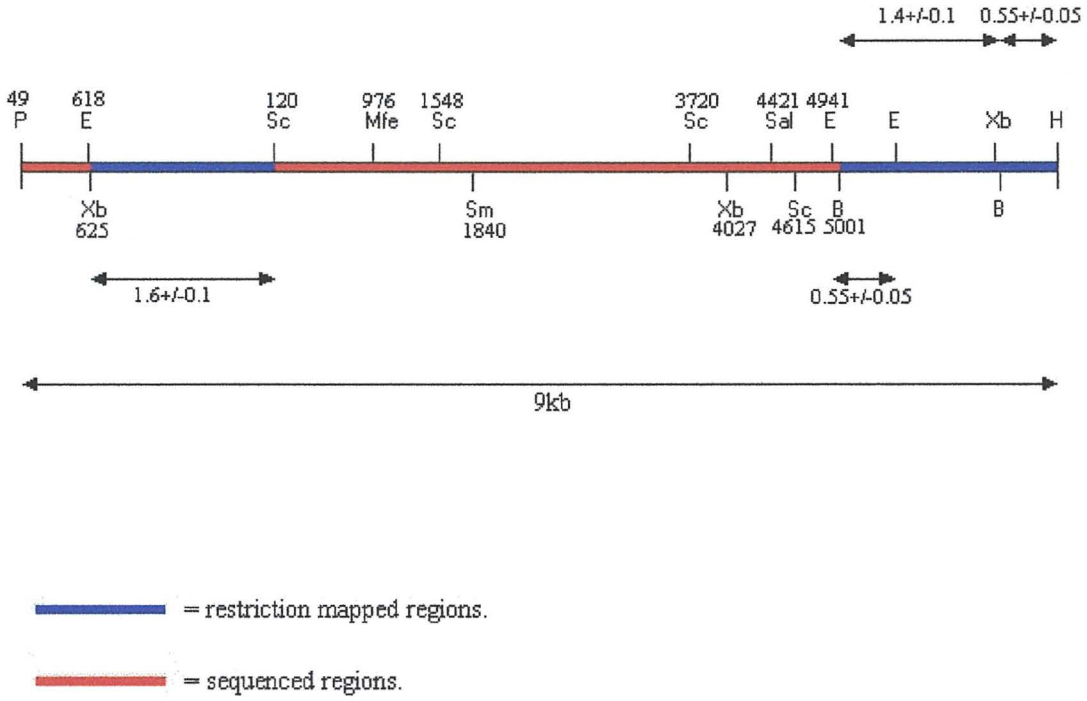

Abbreviations for restriction enzymes

B = *Bam*HI

E = *Eco*RI

H = *Hin*dIII

Mfe = *Mfe*I

P = *Pst*I

Sal = *Sal*I

Sc = *Sac*I

Sm = *Sma*I

Xb = *Xba*I

(A)

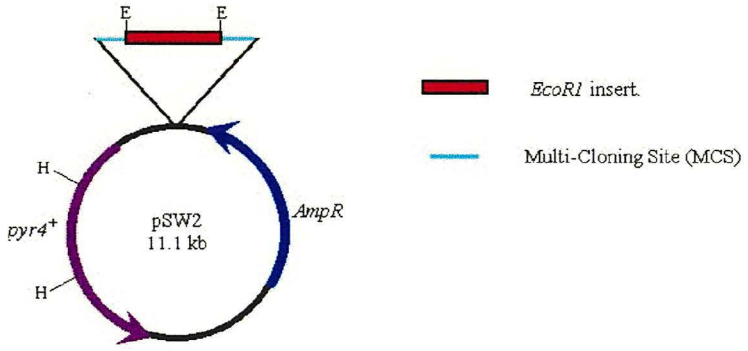
E
E
H
H
pyr4+
pSW2
11.1 kb
AmpR
EcoR1 insert
Multi-Cloning Site (MCS)

(B)

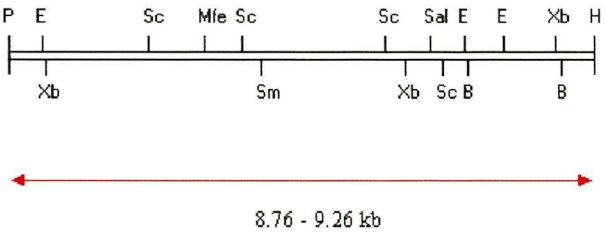
P E Sc Mfe Sc Sc Sal E E Xb H
Xb Sm Xb Sc B B
8.76 - 9.26 kb

(C)

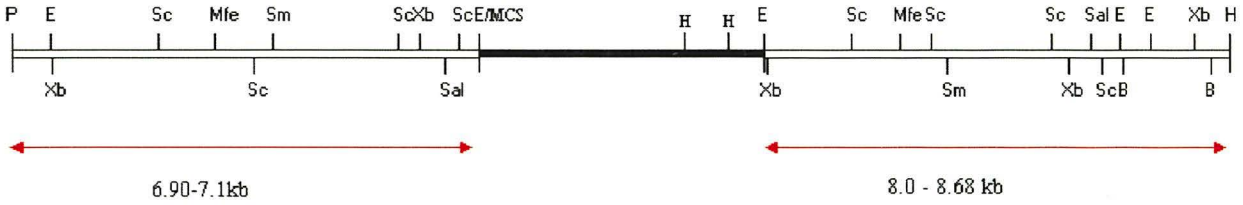
P E Sc Mfe Sm ScXb ScE/MCS H H E Sc Mfe Sc Sc Sal E E Xb H
Xb Sc Sal Xb Sm Xb ScB B
6.90-7.1kb
8.0 - 8.68 kb

(D)

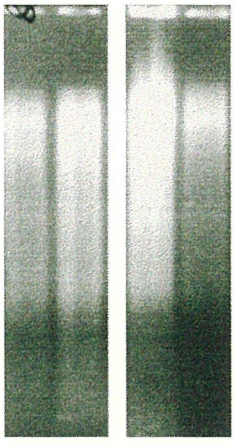
A B C D

(E)

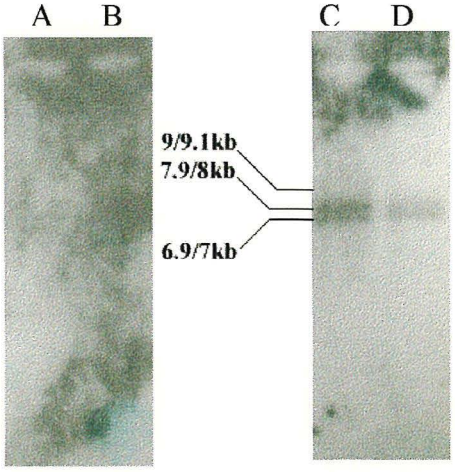
A B C D
9/9.1kb
7.9/8kb
6.9/7kb

On the autoradiograph in Fig. 4.3(E) the tracks containing DNA extracted from the two-pSW2 transformants (pSW2-7 and pSW2-8) (Tracks C + D) lack a 9kb w.t. band expected for a genomic copy of the w.t. *sod*^{VI}*C* gene indicating that integration of the pSW2 has occurred at the *sod*^{VI}*C* gene locus. The w.t. bands in these tracks have been replaced by two bands with approximate sizes of 7.9/8 and 6.9/7kb respectively. These bands are of the expected size for a site-specific integration of pSW2 as shown in Fig. 4.3(C). The tracks containing DNA from the *sod*^{VI}*C*$^{+}$ strain GR5 (Fig. 4.3(E) (A+B)) contain no hybridising band in the region of 9kb as would be expected for this strain. This may be due to the high background seen on the gel or due to poor hybridisation of the probe. GR5 has been shown in a number of Southern blots (Fig. 4.5 (Track 1)) to produce a single 9kb band when hybridised with the 6.4kb *Eco*RI probe. Importantly previous Southern blots using GR5 have not produced the two hybridising bands seen with the two transformants, indicating that these bands are novel to the pSW2 transformants. The position of the 9kb w.t. band on the blots can be estimated (shown on Fig. 4.3(E)(C)) when marked on the blots the position is significantly different from that of the two hybridising bands produced by the transformant strains, eliminating problems with distinguishing it from the smaller bands. A site-specific integration of pSW2 is proposed to have occurred in the two-pSW2 transformants.

4.2.3 Analysis of Site-specific Transformants

In order to look at the percentage of ts^{+} and ts^{-} sectors produced, CMUUFOA plates were stabbed with 100 replicas of each of two pSW2 transformants (pSW2-7 and pSW2-8). The plates were incubated at 30°C for 3 days until sectoring had occurred. One sector from each colony was then picked at random and its growth at 42°C determined. The results obtained for the two transformants were as follows,

pSW2-7 11ts^{+}: 89ts^{-} and pSW2-8 6ts^{+}: 94ts^{-}. Although their overall frequency was relatively low, the production of ts^{+} sectors indicates that the cloned *EcoR*I fragment is indeed the *bona fide sod*^{VI}*C* gene and not a multi-copy suppressor. Site-specific integrations of the pSW2 plasmid can only produce ts^{+} sectors if this is the case. The low frequency of ts^{+} sectors may be a result of the position of the mutation within the *EcoR*I fragment. If the mutation were located at the beginning or end of the *EcoR*I fragment, then recombination at this site would occur at a lower ratio than expected, as the region in which crossovers can occur is much smaller. If the mutation were located centrally within the *EcoR*I fragment than recombination that produced ts^{+} and ts^{-} colonies in more equal amounts would be expected.

4.3 Disruption of the *sod*^{VI}*C* gene

4.3.1 Construction of the Knockout plasmid pSW4

In order to carry out the disruption the plasmid pSW4 was constructed by Dr. S. Whittaker (Fig. 4.5(A)) (165) and is briefly reported here for information. A 1.88kb *Sma*I-*Sac*I sub-clone internal to the *sod*^{VI}*C* gene was ligated into pRG3 (161) digested with *Sma*I and *Sac*I. The plasmid was then transformed into *E. coli* and purified using standard techniques. Plasmid pRG3 (and hence pSW4) contains the selectable marker *pyr4*$^{+}$ allowing the selection of pSW4 transformants on media lacking uridine and uracil (section 4.1). Plasmid pSW4 was introduced into the UU-requiring strain GR5 using the standard transformation procedure (section 2.4.6), and a selection of transformants retained for further analysis at the start of the present body of work.

4.3.2 Identification of Heterokaryotic Transformants

Spores were taken from six pSW4 transformants and streaked onto MM plates with and without UU (Fig. 4.4). The heterokaryotic rescue protocol used by Osmani *et al.* (107) relies on the fact that transformants of *A. nidulans* are often heterokaryotic. A transformant containing a nucleus that has been disrupted site-specifically will survive if it forms a heterokaryon with a non-transformed strain. Furthermore, a non-transformed strain will still contain the *pyrG89* mutation (as it does not contain a copy of pSW4), and so will not be able to grow on MM lacking UU except as a heterokaryon with a transformed strain. In this way each type of strain is "rescued" by the other. Since *A. nidulans* produces uni-nucleate spores heterokaryotic transformants will produce spores containing either a transformed or non-transformed w.t. nuclei. As can be seen from the growth tests (Fig. 4.4) transformants 1, 3 and 4 show very poor growth on MM lacking uridine and uracil but show vigorous growth on MMUU medium. Any growth on MM is derived from spores containing transformed nuclei and so possessing the *pyr4+* marker, which complements the *pyrG89* mutation. The poor growth seen on MM is either due to a site-specific integration of pSW4, indicating that the $sod^{VI}C$ gene is essential. Or, the poor growth could be a result of a non-site specific integration into another essential gene.

Transformants 6 and 8 show vigorous growth on both MM and MMUU this is either due to a site-specific integration of pSW4 indicating that the $sod^{VI}C$ gene is not essential. Or, they are the result of non-site specific integrations that do no disrupt any other essential gene.

Figure 4.4: a) Spores from the six transformants with pSW4 plated on MM lacking Uridine and Uracil. Tr1, 3 and 4 are proposed to be site-specific integrants. Although they show some growth on this medium it is very poor compared to the other non-site specific heterokaryons. Tr6 and 8 are non-site specific transformants showing vigorous growth on MM. Tr5 exhibits intermediate growth when compared to Tr6 and 8. This is presumed to be a non-site specific transformant but possibly with a nuclear ratio in favour of the non-transformed type.
b) Shows spores from the heterokaryons plated out on MM plus Uridine and Uracil, all strains show growth as predicted.

a)

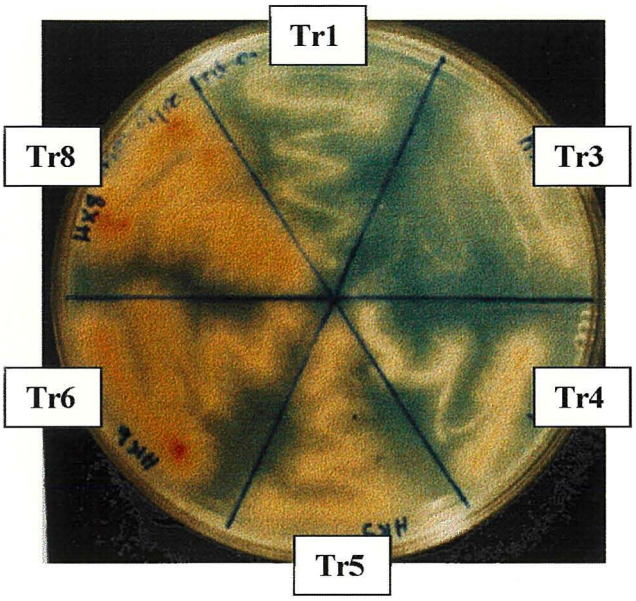

b)

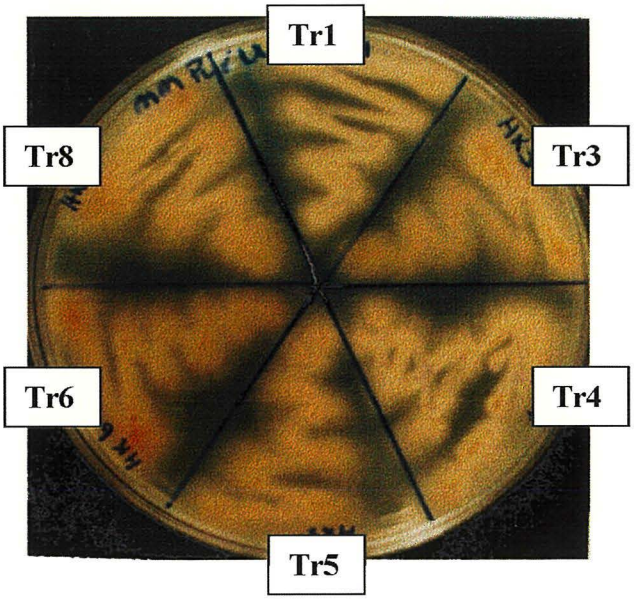

The only way to distinguish between the different growth patterns seen was to carry out a Southern blot to look at the sites of integration of pSW4.

4.3.3 Southern Blotting of Transformants

Mycelial plugs were taken from the three presumed heterokaryotic site-specific transformants (Tr1, 3 and 4) and one proposed non-site specific transformant (Tr8) and placed onto CM plates overlaid with cellophanes. The plates were incubated for 24-48 hrs at 30°C until the cellophanes were covered in a non-sporulating mycelial mat. The mycelia were used to inoculate 250ml conical flasks containing 100ml liquid CM. These flasks were incubated with shaking at 30°C for a further 18 hours. The mycelium were harvested by filtration, blotted dry and frozen in liquid nitrogen and the genomic DNA extracted. A Southern blot was carried out (section 2.5.14 and 2.5.15), using as a probe the 6.4kb *EcoR*I sub-clone produced by digestion of the 9.0kb *Pst*I-*Hin*dIII clone.

As the *Pst*I-*Hin*dIII fragment had been previously mapped (Fig. 4.2) the bands produced by a site-specific integration of pSW4 could be predicted. The control strain GR5 with a non-disrupted copy of $sod^{VI}C$ should produce a single 9.0kb *Pst*I-*Hin*dIII fragment that hybridises to the probe. Integration of the plasmid at the $sod^{VI}C$ locus was predicted to produce two hybridising fragments (Fig. 4.5(D)).

(A)

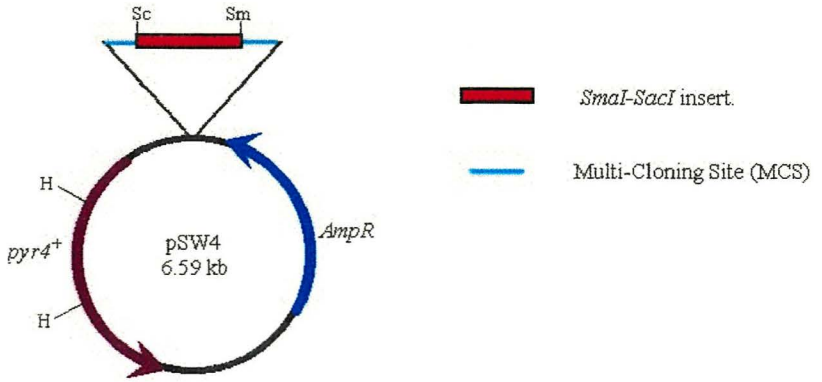
Sc
Sm
H
pyr4+
pSW4
6.59 kb
AmpR
H
SmaI-SacI insert.
Multi-Cloning Site (MCS)

(B)

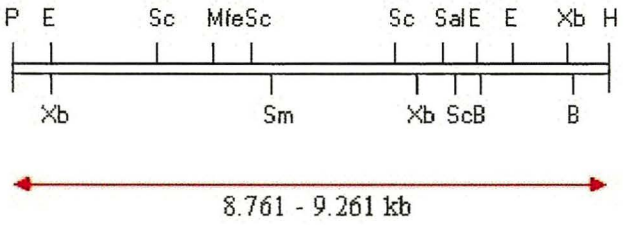
P E Sc MfeSc Sc SalE E Xb H
Xb Sm Xb ScB B
8.761 - 9.261 kb

(C)

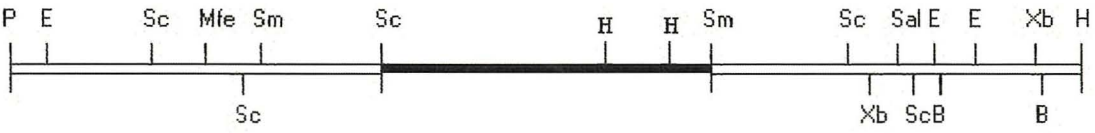
P E Sc Mfe Sm Sc H H Sm Sc SalE E Xb H
Sc Xb ScB B

(D)


5.68 - 5.88 kb
4.961 - 5.261 kb

(E)

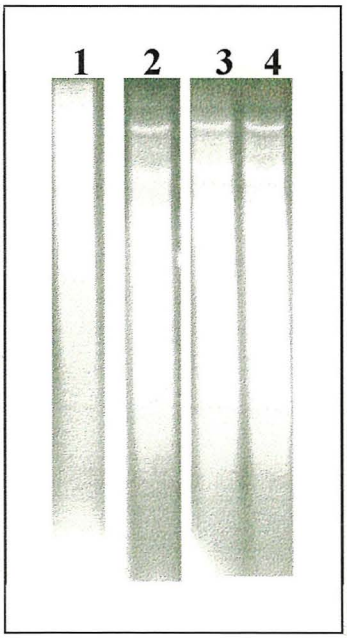
1 2 3 4

(F)

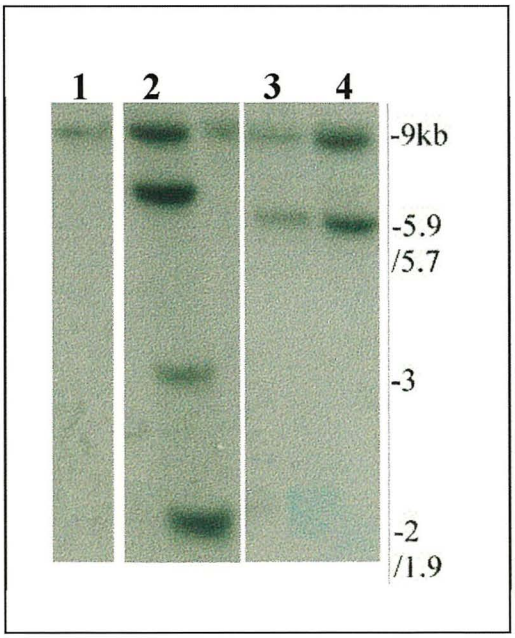
1 2 3 4
-9kb
-5.9
/5.7
-3
-2
/1.9

The autoradiograph in Fig. 4.5(F) shows the expected 9.0kb band for all the strains. The control strain GR5 contains a single non-disrupted copy of *sod*^{VT}*C* and so produces a single band. The other tracks contain DNA from transformant strains containing both transformed and non-transformed nuclei. These non-transformed nuclei contain a w.t. copy of *sod*^{VT}*C* and so all heterokaryons produce the 9.0kb band. It should also be noted that a non-heterokaryotic transformant strain, which contains a non-site specific copy of pSW4 would also produce a w.t. 9kb band along with a number of non-site specific bands. Tracks 2 and 3 contain DNA from the non-site-specific transformant Tr8. This produces a 9.0kb band from the w.t. nucleus plus a number of additional bands derived from the random insertion of the plasmid into the genome. Tracks 4 and 5 contain DNA extracted from Tr1 and Tr4, which were predicted to be site-specific transformants and are expected to produce the w.t. 9.0kb band as well as two bands from the integration. However, the site-specific integrants contained only one band from the disrupted nucleus. This is may be due to the 0.7% agarose gel failing to resolve the two bands. The predicted fragments whose sizes were estimated to be 5.8 and 5.2kb are also based on size estimates for restriction fragments. Sequence data is available only from the *Pst*I site at position 49 to the *EcoR*1 site at position 625 and the *Sac*I site at position 120 to the *BamH*I site at position 5001 (Fig. 4.2). In order to be sure that the heterokaryons were site-specific integrants a PCR-based method was developed to confirm the site of integration.

4.3.4 PCR of DNA from Heterokaryotic Transformants

The PCR reaction was set up as in section 2.5.11 using primers P3uni and P4rev designed using known sequence within the *sod*^{VI}*C* gene (Appendix 7). The PCR was carried out using standard conditions (section 2.5.11). 10µl of each PCR reaction was run out on a 0.7% agarose gel (section 2.5.2.) and photographed on a UV transilluminator using the Kodak® Gel documentation system. The primers P3uni and P4rev were designed to flank the *Sma*I-*Sac*I fragment of *sod*^{VI}*C* that was used to construct the plasmid pSW4 (Fig. 4.6(B)). Genomic DNA extracted from the w.t. GR5 strain, the site-specific transformant Tr1 and the presumed non-site specific transformant Tr8, was used as a template in separate PCR reactions. A PCR carried out on genomic DNA from GR5 with the primers P3for and P4rev resulted in the production of a 1.9kb band (Fig. 4.6 (D)(2)). This was obtained from the amplification of the 1.9kb *Sma*I-*Sac*I fragment flanked by the two primers (Fig. 4.6(B)). A w.t. copy of the *sod*^{VI}*C* gene will always produce this 1.9kb band. The second and third PCR reactions carried out with GR5 used a combination of the primers P3for and P4rev with the M13 standard forward and reverse primers (Appendix 7). The PCR reactions using these primers do not produce any products (Fig. 4.6 (D) (3) + (4)). The M13 primers are located within the pRG3 vector used to construct the plasmid pSW4. As no plasmid is present within the w.t. GR5 strain no PCR product was produced.

PCR amplification using genomic DNA from Tr8 produces the same banding pattern seen with the w.t. GR5 strain. The 1.9kb *Sma*I-*Sac*I PCR product is produced from a w.t. copy of the *sod*^{VI}*C* gene present in this strain (Fig. 4.5 (D) (8)). Again no products were produced with P3for + M13rev and M13uni + P4rev (Fig. 4.5 (D) (9) + (10)). Although Tr8 contains the pSW4 plasmid, products will only be produced with the above primer combinations if pSW4 has been integrated site-specifically at the

sod^{VI}*C* locus (Fig. 4.6(C)). The fact that a product is only produced when P3for and P4rev are used together with genomic DNA from Tr8 confirms that Tr8 contains a non-site specific integration of pSW4.

A PCR carried out with P3for and P4rev on genomic DNA from Tr1 again shows the production of the 1.9kb band from a w.t. copy of the *sod*^{VI}*C* gene (Fig. 4.6 (5)). However, this transformant produces a 1.95kb band with P3for and M13rev and a second 1.95kb band with the primers M13uni and P4rev. These bands are derived from a site-specific integration of pSW4 at the *sod*^{VI}*C* locus. When pSW4 is integrated site-specifically, the M13rev primer site will lie downstream of the P3uni primer site and the M13uni primer site will lie upstream of the P4rev primer site (Fig.4.6(C)). PCR amplifications using P3uni with M13rev and M13uni with P4rev will produce PCR products of 1.95kb. The fact that Tr1 produces PCR products from both a w.t. and disrupted *sod*^{VI}*C* gene confirms that this transformant is a heterokaryon, consisting of non-transformed w.t. and site-specifically transformed nuclei as predicted by the Southern blot.

(A)

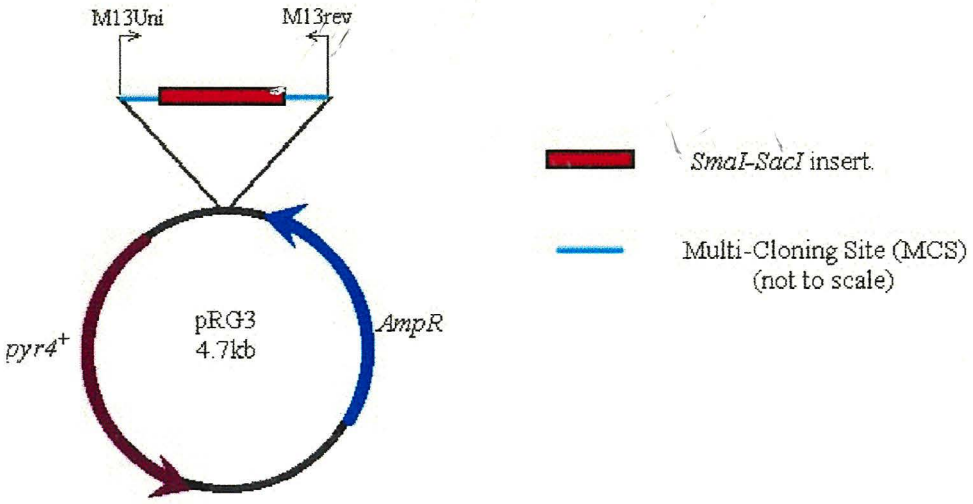
M13Uni
M13rev
pRG3
4.7kb
pyr4+
AmpR
SmaI-SacI insert.
Multi-Cloning Site (MCS)
(not to scale)

(B)

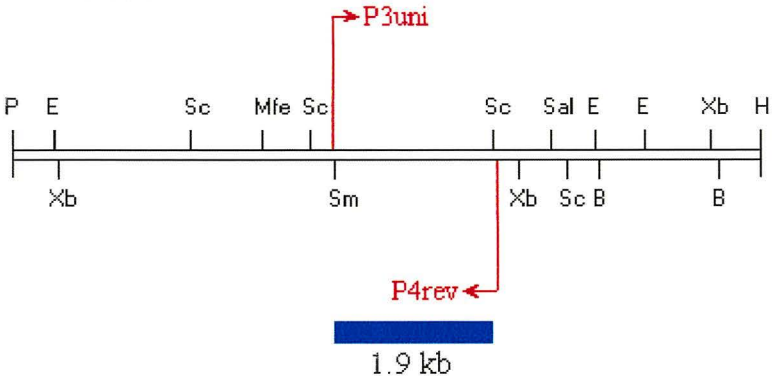
P3uni
P E Sc Mfe Sc Sc Sal E E Xb H
Xb Sm Xb Sc B B
P4rev
1.9 kb

(C)

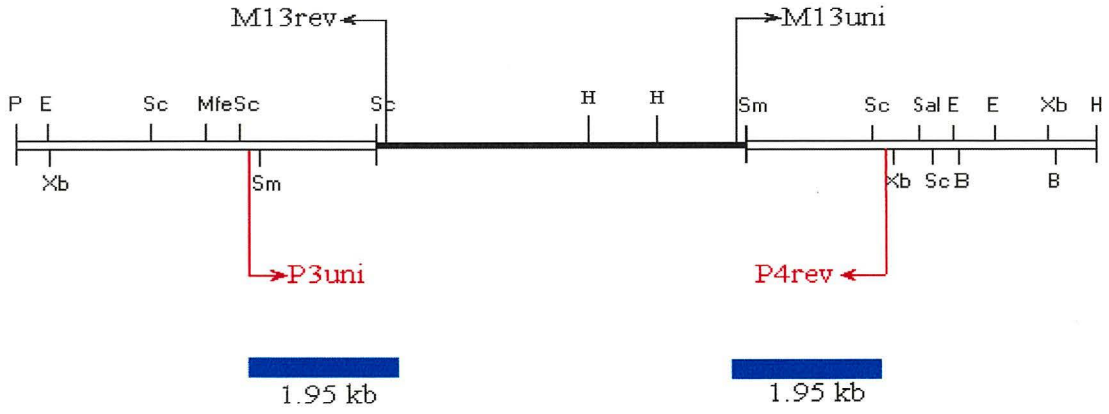
M13rev
M13uni
P E Sc MfeSc Sc H H Sm Sc Sal E E Xb H
Xb Sm Xb Sc B B
P3uni
P4rev
1.95 kb
1.95 kb

(D)

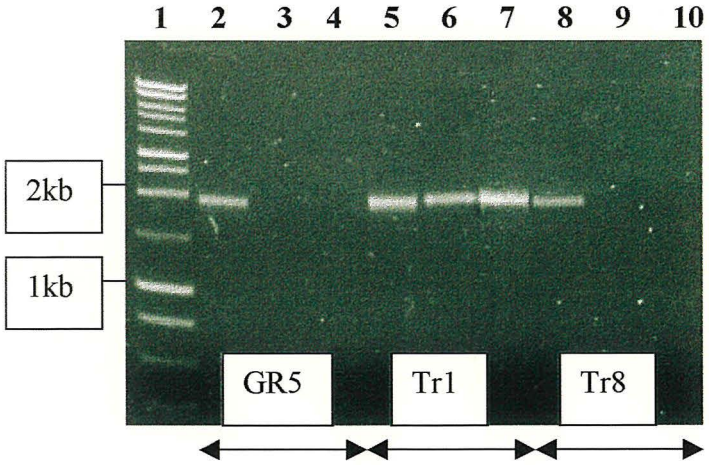
1 2 3 4 5 6 7 8 9 10
2kb
1kb
GR5
Tr1
Tr8

4.4 Complementation of the *sod*^{VI}*C1* Mutation

4.4.1 Construction and Transformation of Sub-clones of the *Pst*I-*Hin*dIII fragment

As restriction mapping of the 9kb *Pst*I-*Hin*dIII fragment had been carried out (Fig. 4.2) a number of restriction sites were chosen and digests carried out to yield a number of smaller sub-clones (Fig. 4.7(B)). Individual digests were set up as in section 2.5.5 using the appropriate enzymes to generate the fragments of interest. The digests were run on a 0.7% agarose gel (section 2.5.2) and the correct sized bands excised and purified (section 2.5.3). The band-extracted fragments were transformed into the *sod*^{VI}*C1* strain B120 along with the co-transforming vector pAB. This vector contains the *pyr4*$^{+}$ gene allowing its selection in the same way as the pRG3 vector used in the first study. The benefit of using a co-transformation is that pAB transformants can be selected for; these transformants are likely to have taken in the linear fragments of DNA at the same time as the co-transforming vector. Transformants were plated out onto MM KCl media lacking uridine and uracil to select for the *pyr4*$^{+}$ marker contained in the pAB plasmid. Transformation plates were incubated at 42°C to select for transformants containing fragments complementing the *sod*^{VI}*C1* mutation.

4.4.2 Complementation Results

A number of transformants were picked for each transformation fragment and streaked onto fresh CM plates to purify. Spores from the different transformants were used to inoculate fresh CM plates in duplicate. One set of plates was incubated at the permissive temperature of 30°C and the second set at the restrictive temperature of 42°C. After 3 days growth the transformants on the plates at 42°C were compared to

those transformants containing the *Pst*I-*Hin*dIII fragment, which contains the full *sod*^{YT}*C* gene, transformants were then scored on their growth (Fig. 4.7(B)). A single transformant containing the DNA from the four complementing fragments (Fig. 4.7(B)) were stabbed on a single plate along with a single transformant containing the non-complementing 2.2kb *Sac*I fragment (Fig. 4.7(B)), the plate was incubated at 42°C for three days and is presented here to confirm complementation (Fig. 4.8). Alignment of the various sub-clones (Fig. 4.7 (B)) and their ability to complement the *sod*^{YT}*C1* mutation (Fig. 4.7(C)) identified a 1.2kb region in which the mutation is presumed to be located (Fig. 4.7 (red box)).

Figure 4.7: (A) Restriction map of the w.t. *Pst*I-*Hin*dIII fragment.
(B) Various sub-clones generated by digestion of the genomic *Pst*I-*Hin*dIII fragment with enzymes shown on fragments.
(C) Complementation of the *sod*^{VT}*C1* phenotype at restrictive temperature by the individual sub-clone, transformed into the *sod*^{VT}*C1* strain B120.
Abbreviations as in Fig. 4.2

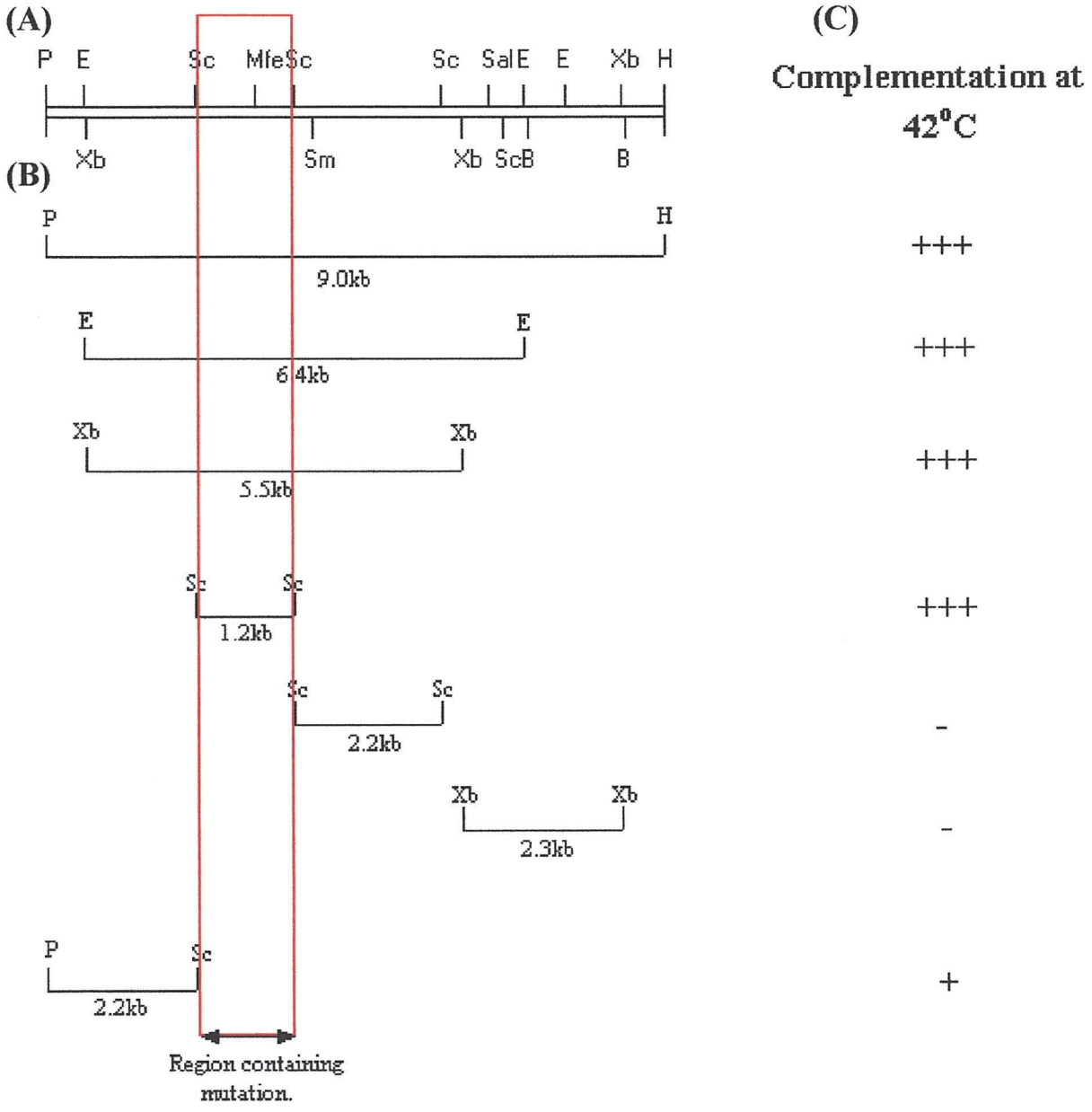

Figure 4.8: CM media plate incubated at 42°C for three days containing complementing and non-complementing DNA fragments (Fig. 4.7(B)).

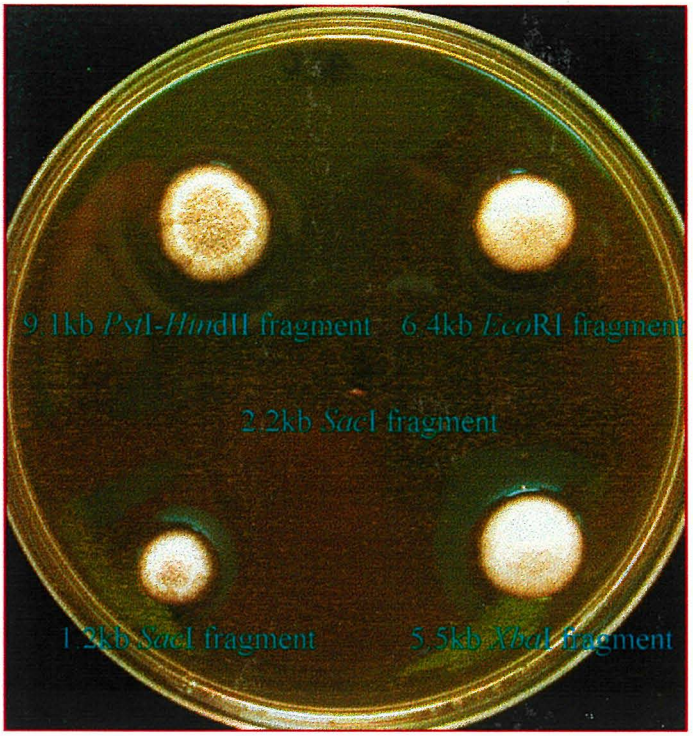

4.4.3 PCR amplification of the 1.2kb *Sac*I fragment from the *sod*^{VI}*C1* strain B120

Previous sequencing carried out on the upstream coding region of the mutant *sod*^{VI}*C* gene revealed no changes when compared to genomic sequence from a *sod*^{VI}*C*$^{+}$ strain. For the mutation to be located within the 1.2kb region it must be contained within non-coding sequence. The primers M1 and M2 (Appendix 7) flanking the non-coding region identified from the complementation studies were designed from w.t. sequence. These were used in a PCR with genomic DNA extracted from the *sod*^{VI}*C1* strain B120 as a template, and a second reaction with genomic DNA extracted from the *sod*^{VI}*C*$^{+}$ strain GR5. The PCR was set up using the same conditions as in section 4.3.4. The expected size of the PCR product is 995bp this was verified by running 10µl of the reaction on a 0.7% agarose gel (section 2.5.2) along side a 1kb DNA ladder (Promega®). Two separate PCR reactions were carried out for the *sod*^{VI}*C1* strain and a single reaction for the *sod*^{VI}*C*$^{+}$ strain for sequence comparison. Each reaction was sent for sequencing to MWG-Biotech® sequencing service.

4.4.4 Sequencing Analysis of 995bp fragment

Sequence comparisons were carried out between the two *sod*^{VI}*C1* product reads and the *sod*^{VI}*C*$^{+}$ product read, these were then compared to the original sequencing carried out on the 9.1kb *Pst*I-*Hin*dIII fragment. Sequence alignments revealed that both of the *sod*^{VI}*C1* products contained an additional thymine (T) residue, which was not present in either of the *sod*^{VI}*C*$^{+}$ sequences (Fig. 4.9).

Figure 4.9: Sequence alignments between the *sod*^{VI}*C1* and *sod*^{VI}*C*$^{+}$ PCR products. (A) *sod*^{VI}*C1* (read 1), (B) *sod*^{VI}*C1* (read 2), (C) *sod*^{VI}*C*$^{+}$ (read 1), and (D) *sod*^{VI}*C*$^{+}$ original *Pst*I-*Hin*dIII sequencing. Red highlighted area shows the additional thymine residue present in both the *sod*^{VI}*C1* sequence reads.

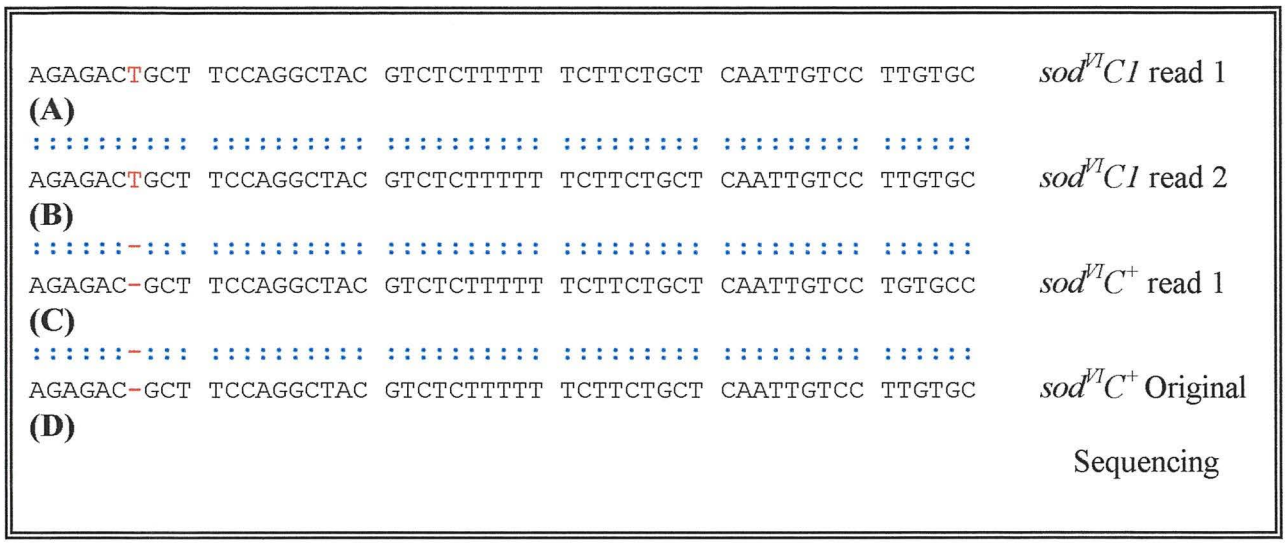

The additional thymine residue is located 146bp before the ATG start codon of the *sod*^{VI}*C* gene. This area may form one of the regulatory areas of the *sod*^{VI}*C* promoter region. The non-coding sequence of the *sod*^{VI}*C* gene was analysed for the possession of well-documented upstream elements such as CCAAT and TATA boxes, the downstream sequence was also analysed for possible polyadenylation sites. The sequences of common CCAAT (consensus CAAT), and TATA (various consensus sequences but commonly TATAAA) sequences from *A. nidulans* were used to search the upstream *sod*^{VI}*C* sequence (62). Analysis revealed a number of possible CCAAT box sequences within the upstream region of the *sod*^{VI}*C* gene (Fig. 4.10 (A)), one of which lay just upstream from the mutation site identified in figure 4.9 (Fig. 4.10 (B)). No putative TATA box motifs were found within the upstream sequence. Comparison of the *sod*^{VI}*C* gene with other regulated *A. nidulans* genes such as *amdS* (62) showed that regulatory sequences are commonly located and may even overlap the CCAAT

binding motif. The putative CCAAT box identified here is located 132bp upstream of possible transcription site (Fig. 4.10(A)). The putative transcription initiation sites identified in the *sod*^{VI}*C* sequence are based on initiation sequences found in a number of *A. nidulans* genes (62). *A. nidulans* CCAAT boxes are typically located from 60-120bp upstream of transcription, but examples of CCAAT boxes up to 200bp upstream have been found (62). Analysis of the downstream non-coding sequence of the *sod*^{VI}*C* gene identified a putative polyadenylation site located 140bp after the stop codon (Fig. 4.10(B)) (62) (164).

Figure 4.10: Sequence analysis of the upstream and downstream non-coding regions in the *sod*^{VT}*C* gene.

(A) Upstream non-coding region Key: Identified CCAAT sequences
Start Codon
* Position of *sod*^{VT}*C1* mutation
Possible *sod*^{VT}*C* CCAAT box
Possible transcription initiation sites

(B) Downstream non-coding region Key: Stop Codon
Putative polyadenylation site

(A)

```
  1 TCTAGAGCGG CCGCCACCGC GGTGGAGCTC AAACTAGGGC TCGCATATTG TGCATCGGTT
 61 ACAAAGGCGG GCTCTCCGGA CGGGGCAGTT CGGACGGGAT TTGTGATAGT AGGCTTTCTT
121 TTCCGGCCCC TCTTTGGACG GATTGATCCT GGATTGTCAT GATCGGAGTT GCAGTACAAC
181 ATTTCCATCG AAGAATCAGG TCCTCCCAGT GTTTGCGCTG TCTTAGCTGC GCTGTTGACA
241 CCTCCGTTTC GGACGTAAGT TCCTCCTCTG GCTCCTCAAT GGCATACGGT TTCACTACCT
301 CACTTTTGAA ACCAATCCCG AATATCAGGA GGTAAGTCCT CAATGTCATA TATTTCTGGT
361 TCGTGAGCTT TAGGGATTTC TCCGTACTGT TGATCTTGGT CGGTTCGAGG AGCAGGCGTC
421 GGGCTGCTTC CGCCCGGATT CTTGTAAGGT TGATACAGAT CCGGGTTTTG GCCGTTTGCT
481 CCCATAGTAC CGAGGCCCCC AATATCCACA ATAAGGGCAA TCGAGTTGTT CGGGCGAGTG
541 CAGTTGCACT GTAGAAGAAA GAGCAAAGTT CAGCTCCTGG TAATGATTAT GGATCGGAGA
601 TATGTCGCAT GGAAATTCCA TAATAGACCA AGTACACACT CAGCTGAGTG CGAGGACCGT
661 CAAACATGGT TTATCATCTC GTGCTTGAAG GCAGGGGGAG ACCAGAGTGG TGGTTACGAT
721 CAACAATGTG AGCGATGTAG CTCTTGACCG CCTTGGGCGC CATTGGCCGG CGCTACTCGC
781 TTATTCAATA AGTCCACGTT ACCGCCATCC AAGGTGTCCT GTCCAGACCC CAGACTGTCA
841 ATAGAGA*CG CTTCCAGGCT ACGTCTCTTT TTTCTTCTGC TCAATTGTCC TTGTGCAGTG
901 GATGAGGTGG TCGCCTTTGT GATTCCTCTG TCTTTAGTGC GCGGAGCTTG CTTCTACTTC
961 TACATGGTGC GGCTTCGGCC AACCCTTCTT CAAGATGCAA TCCTCCCCAA ACATGCTCAC
```

(B)

```
5041 TCTAATCCCC TGACGACGTG TGATGGGTTA TGCTTAAAGA TAGAAAAGTG
5091 GACTTCTATC TTCTTATGGA CTTAATCATG GTCCTAAGGT CTGTTACATA
5141 GATATATGGA TCTGTTGCCT GTCTTCTATA ATTCTTGAGC GTTGTAATTA
5191 AATAGTTTTT CATGCGAATG CAATGCATGT AAGCAAGGAT TGGG
```

4.5 Discussion

The aims of the work in this chapter was to...

1) Confirm the cloning of the *bona fide* *sod*^{VI}*C* gene.

2) To address whether the *sod*^{VI}*C1* mutation is a loss-of-function mutation.

3) To identify the position and nature of the *sod*^{VI}*C1* mutation.

At the point this work began it was important to show that the cloned gene was indeed the *sod*^{VI}*C* gene and not a multi-copy suppressor of the *sod*^{VI}*C1* mutation. In order to do this a strain was produced which contained tandem repeats of the *sod*^{VI}*C* gene flanking the *pyr4*$^{+}$ gene from *N. crassa.* One copy of the *sod*^{VI}*C* gene was derived from a w.t. clone, the other derived from a genomic copy containing the *sod*^{VI}*C1* mutation. Curing of the plasmid from the strain resulted in the production of ts^{+} and ts^{-} strains as expected if the clone gene is indeed *sod*^{VI}*C*. Southern Blotting confirmed the integration of the plasmid at the *sod*^{VI}*C* locus. Confirmation that the cloned gene is indeed *sod*^{VI}*C* allows work to proceed on the identification of the *sod*^{VI}*C1* mutation.

The second section of work carried out was to determine whether *sod*^{VI}*C* is an essential gene. In order to answer this, a heterokaryotic transformant strain was isolated which contained two different nuclei, those containing a disrupted *sod*^{VI}*C* gene and those containing a w.t. copy of *sod*^{VI}*C*. Three transformants were obtained which were hypothesised by their growth responses to be site-specific integrants; Southern blotting and PCR confirmed this. Growth of spores containing disrupted nuclei produced a very fine sickly growth at the permissive temperature of 30°C, however, at the higher temperature of 37°C at which GR5 is normally grown no growth was observed with the site-specific transformant. The growth at 30°C is likely to be due to the partial functionality of the N- and C-terminal portions of the protein.

At the higher temperature of 37°C, these partially functional regions are no longer able to sustain growth, indicating that the *sod*^{VI}*C* gene is essential. Cytology carried out using spores from the site-specific heterokaryon grown on MM at 37°C (data not shown), resulted in the production of the characteristic *sod*^{VI}*C1* null-phenotype. Growth on MM only allows growth of transformed nuclei containing the pSW4 plasmid; in the case of the site-specific transformant Tr1 these nuclei containing the disrupted *sod*^{VI}*C* gene are not viable. It could be argued that the disruption of the *sod*^{VI}*C* gene in this manner still causes the production of a toxic protein, however, this effect would also be apparent at the permissive temperature of 30°C and would be predicted to result the production of the *sod*^{VI}*C1* phenotype at this temperature.

It is not surprising that the *sod*^{VI}*C* gene is essential. The protein α-COP encoded by the gene has a very specific function within the cell. This subunit is one of the seven subunits that go together to make the protein complex coatomer. It is easy to imagine that the loss of the protein would disturb the stoichiometry of the complex. Coatomer is the coat vesicle that is responsible for the recycling of endoplasmic reticulum (ER) resident proteins from the Golgi back to the ER (Retrograde transport). The ER resident proteins are recognised as they contain the dilysine-retrieval motif (KKXX). A screen for yeast mutants defective in KKXX retrieval yielded mutants in α-, γ-, δ-, and ζ-COP (31, 84). The loss of α-COP from the cell would result in a decreased ability of the coatomer subunits to recognise and bind to these ER resident proteins. The yeast α-COP encoding gene has also been shown to be essential, indicating the important role that α-COP plays in the coatomer complex (51). Recently it has been shown in yeast that the terminal 170 residues of the α-COP protein are essential for incorporation of ε-COP into the coatomer complex (41). ε-COP acts as a structural component of coatomer, stabilising coatomer at elevated

temperatures (41) (36). α-COP has also been shown to interact with the β'-COP subunit (42), showing the integral part that α-COP plays in the formation of coatomer.

A number of sub-clones were generated by restriction digestion of the 9.1kb *Pst*I-*Hin*dIII clone. These fragments were transformed into the *sod*^{VI}*C1* strain B120 as linear band-extracted DNA along with the co-transforming plasmid pAB. Transformation plates were incubated at 42°C to select for transformants containing sub-clones capable of complementing the *sod*^{VI}*C1* mutation. Alignment of sequences allowed the identification of a 1.2kb area, in which the *sod*^{VI}*C1* mutation was thought to lie. Sequencing of a portion of this area revealed the addition of a single thymine base in the non-coding DNA region just upstream of the start codon. Analysis of the non-coding region of the *sod*^{VI}*C* led to the identification of a number of putative regulatory sequences, including 11 putative CCAAT boxes, two possible transcription initiation sites, and a 3'-polyadenylation site. One CCAAT box site lies just upstream of the *sod*^{VI}*C1* locus and its location is within the range of other CCAAT box sites identified in *A. nidulans*.

The analysis shows that the *sod*^{VI}*C* gene contains many of the eukaryotic elements found in regulated *A. nidulans* genes. It is therefore proposed that the *sod*^{VI}*C1* mutation affects a putative *A. nidulans* regulatory sequence, causing insufficient amounts of transcript in the *sod*^{VI}*C1* mutant at restrictive temperatures. This finding is supported by the chromosome duplication data (section 3.2) whereby the duplication of chromosome VI is thought to act to overcome the *sod*^{VI}*C1* mutation at the semi-restrictive temperature of 37°C, which would make sense if transcript levels are lower at this temperature. However, at the restrictive temperature of 42°C the duplication of chromosome VI is not able to overcome the effects of the *sod*^{VI}*C1* mutation.

Chapter Five

Using GFP-constructs to Study the Endomembrane System of *Aspergillus nidulans*

5.1 Introduction

The *sod*^{VI}*C* gene encodes a homologue of the mammalian protein α-COP, which forms part of the coat protein complex coatomer (COPI) (See Chapter 1). In mammals COPI functions in the secretory pathway, recruiting endoplasmic reticulum (ER) resident proteins into vesicles for recycling (retrograde transport) back to the Golgi apparatus. COPI has also been implicated in the forward (anterograde) transport of proteins from the ER to the Golgi, and also through the Golgi cisternae. This pathway has been well studied in higher eukaryotes but in filamentous fungi such as *A. nidulans* the pathway has still to be elucidated. Not much work has been carried out on the organisation of the Golgi apparatus in filamentous fungi. Fungi differ from higher eukaryotes in that they possess individual Golgi cisternae instead of stacks and these cisternae show a distinct localisation to the growing hyphal tip (75) (134). The visualisation of the Golgi apparatus within *A. nidulans* is of great interest, this organelle has not been visualised in this fungus to date. So the exact structure and distribution of this organelle is not known. The cloning of the *sod*^{VI}*C* gene, and the isolation of the temperature sensitive (ts) *sod*^{VI}*C1* mutant, provides an opportunity to study the endomembrane system of *A. nidulans* in more detail.

This work in this chapter has been carried out using the versatile reporter Green Fluorescent Protein (GFP). The GFP gene was first isolated by Prasher et al. (118) and is found naturally in the jellyfish *Aequorea victoria.* In the wild, this protein is responsible for the emission of light seen when the jellyfish is mechanically

shocked. When shocked, a second protein Aequorin produces a burst of blue light that excites the GFP fluorophore, which in turn produces a burst of visible light which is the fluorescence seen in the jellyfish (26). Chalfie et al. (26) found that the expression of the GFP cDNA alone in *E. coli* and *Caenorhabditis elegans* was enough to produce fluorescence when excited by U.V. light, indicating that GFP requires no other cofactors to function. GFP has been used extensively as a reporter gene fused to whole or partial protein sequences. Many hundreds of proteins have been GFP-tagged to date, the majority of which show correct function *in vivo.* Among the proteins studied have been a transcription factor (160) and a histone (130), both of which showed normal function *in vivo.* This supports the fact that although GFP is a large protein, it does not seem to perturb the function of the protein to which it is attached. GFP has also been used more recently to study the secretory pathway in a number of different organisms including plants (19) (18, 133) and filamentous fungi (53) (54). See Wouters, F.S *et al.* for a recent review on GFP techniques (168).

Probably the greatest advantage in using GFP as a reporter is that it can be followed in living cells. The GFP-tagged protein can be expressed within a cell, which can then be imaged directly using standard UV microscopy techniques. The position of the tagged protein can be identified, and changes in localisation during growth and development followed using time-lapse photography. This makes GFP a powerful tool when compared to other reporter systems where fixation or other chemical treatments are required, leading to the potential production of artefacts within the cell.

Work on optimisation of GFP for use in *A.nidulans* was carried out by Fernández-Ábalos, et al. (44). It was found that the native GFP did not produce significant amounts of protein when expressed in *A.nidulans*, probably due to a problem in codon usage. Four different GFP genes that contained codons modified for

expression in plants were transformed into a w.t. *A.nidulans* strain. Transformants were then screened for the amounts of GFP protein and fluorescence produced. A clone known as GFP2.5 was found to give optimal fluorescence, and is now used as standard in *A.nidulans* GFP constructs. GFP2.5 contains four codon substitutions: S65T, V163A, I167T, and S175G. These are thought to enhance fluorescence and stability of the fluorophore (44).

The first piece of work described in this chapter uses the plasmid pMCB45, which has been shown to localise the *A. nidulans* optimised GFP (GFP2.5) to the ER. This construct has been shown to localise to the filamentous network of ER membranes that run throughout the cytoplasm and surrounds the nuclei within the hypha (44). The ER is a key organelle of the secretory system and any blockages within this pathway can lead to drastic changes in ER morphology. The pMCB45 plasmid was transformed into both the w.t. *sod*^{VI}*C* strain (GR5) and the *sod*^{VI}*C1* stain B120, in order to determine whether effects on the secretory pathway due to the *sod*^{VI}*C1* mutation lead to visible changes in ER structure within the hypha at restrictive temperatures.

The main work presented in this chapter is the tagging of the *sod*^{VI}*C* gene with GFP, which allowed the localisation of the Sod^{VI}C protein to be visualised in living hyphae. It is important to note that the w.t. copy of the *sod*^{VI}*C* gene has been tagged to allow visualisation of the w.t. function of the protein *in vivo*. A number of decisions have to be made before attempting tagging of any gene. These include how much of the gene is to be tagged (i.e. The whole coding region or just the 5'- or 3' end); the method by which the GFP is to be attached; and which end of the gene will be tagged. Previous work carried out on the complementation of the *sod*^{VI}*C1* mutation (Chapter 4.4) showed that a version of the *sod*^{VI}*C* gene carrying a small truncation at the 3'-end

was still functional, being capable of rescuing the *sod^{VI}C1* phenotype. Based on this result we hypothesised that the attachment of the GFP to the C-terminus would have the least effect on the *in vivo* function of the Sod^{VI}C protein.

It was hoped that it would be possible to study localisation of the Sod^{VI}C::GFP protein by expression of the construct using the native *sod^{VI}C* gene promoter. This would be better as the levels of the GFP-tagged protein expressed would be the same as in a w.t. *sod^{VI}C^{+}* strain. Expression at native levels rules out any effects on the localisation of the *sod^{VI}C::GFP* which may occur if the *sod^{VI}C* gene is over-or under expressed. However, Northern blot analysis of *sod^{VI}C* transcript levels by Dr. S. Whittaker (unpublished) indicated that the *sod^{VI}C* gene is not highly expressed, suggesting that the native level of expression from the *sod^{VI}C* promoter might not be high enough to visualise GFP localisation. Therefore, the *sod^{VI}C::GFP* construct was cloned into the pAL3X expression vector. Constructs made with this vector enable the variable expression of cloned genes, by placing them under the control of the inducible promoter of the *alcA* gene encoding alcohol dehydrogenase I enzyme (ADHI) (Waring *et. al.* 1989). The *alcA* promoter allows the variable expression of a cloned gene by growth on media containing various alcohols and would give a way to express the construct at higher levels to aid visualisation if necessary. The *alcA* promoter has been used in studies to over-express a number of different genes. (161) (139) (97). The levels of induction of the *alcA* promoter have been characterised using Northern and Western blotting, and levels of mRNA and protein from the cloned gene measured when *alcA* transformant strains were grown on different inducing media. Low-level induction of the *alcA* promoter has been shown by growth of transformant strains on MM glycerol and MM fructose media (161) (139), and high levels of

expression have been shown when transformants are grown on MM ethanol and MM threonine media (139) (161).

However, in order to be able to use the strategy of induced over-expression of the *sod^{VI}C::GFP* construct, it was important to establish whether this would cause any adverse effects on the strain. This was explored by monitoring the growth rates and morphologies on different media of strains over-expressing a non GFP-tagged *sod^{VI}C* gene under the control of the *alcA* promoter.

Much has been learnt about endomembrane systems in a variety of different organisms by looking at drugs that interfere with it. Brefeldin A (BFA) is a fungal metabolite first isolated from a strain of *Penicillum decumbens,* which consists of a dihydroxy, α-β unsaturated lactone, first named Decumbin (138) (134). This chemical was originally used as an anti-fungal drug but has since been shown to have a wide range of biological activities, including an inhibitory effect on virus multiplication. It was later shown that BFA blocks retrograde transport in mammalian cells (87) (82) (134). However, the effects of BFA appear to vary from organism to organism (134). Studies have been carried out using BFA in a wide range of organisms to look at the effects on organelle morphology and vesicle transport. Very little work has been carried out on filamentous fungi using this chemical (21, 134), but these preliminary studies suggest that the effects of BFA differ with those seen in mammalian and plant cells. To date no work has been published on the effects of BFA in *A.nidulans*. The pMCB45 and psodGFP19 transformants gave the opportunity to study the effects of BFA on the endomembrane system in *A.nidulans*.

In summary the aims of this chapter were …

1) To look at the effect of the *sod^{VI}C1* mutation on ER morphology at restrictive temperature.

2) To make a preliminary study of the effects of over-expression of the *sod*^{VT}*C* gene.

3) To GFP-tag the w.t. *sod*^{VT}*C* gene and study its localisation in living hyphae.

4) And finally, to carry out a preliminary study on the effects of BFA on endomembrane morphology.

Results

5.2 Visualisation of the Endoplasmic Reticulum of *A. nidulans*

5.2.1 *A. nidulans* ER-GFP plasmid

The plasmid pMCB45 (gift from J.H.Doonan (44)) was used to visualise the ER of *A. nidulans*. This plasmid contains GFP2.5 N-terminally tagged with an ER retention signal (His-Asp-Glu-Leu). The ER retention signal targets the GFP to the endoplasmic reticulum allowing visualisation of this structure. The GFP construct also has the chitinase export signal (ChSP) attached at the N-terminus to aid processing of the transcript (Fig. 5.1). This construct was cloned into the expression vector pAL5 containing the inducible *alcA* promoter, allowing the GFP to be switched on and off by growth on inducing media (glycerol, ethanol, and threonine) or on glucose respectively. The pAL5 vector also contains the His2B terminator sequence. This is required in N-tagged GFP constructs and acts as a terminator of the sequence, aiding in expression of the ER-GFP sequence.

5.2.2 Transformation, Selection and Expression of pMCB45

A $sod^{VI}C^{+}$ (GR5) and a $sod^{VI}C1$ strain (B120) were transformed with the plasmid pMCB45 (section 2.4.6). Both strains contain the *pyrG89* mutation allowing selection of the plasmid. Transformants were selected using the $pyr4^{+}$ marker on pMCB45 by plating on MM lacking UU at the permissive temperature of 30°C. These transformants were then screened for fluorescence on 1% (w/v) Glycerol MM using standard UV microscopy techniques for GFP (section 2.4.7). Three transformants were chosen for each strain (GR5: ER1, ER3, ER5 and B120: ER2, ER4 and ER6).

Temperature shift experiments were carried out in order to look at the effects of the *sod*^{V1}*C1* mutation on ER morphology in the pMCB45 transformants. Spores from the transformants from both strains were patched in duplicate onto 1% Glycerol plates and incubated at 25°C overnight to allow germination. The plates were then up-shifted to 30°C for 1 hour after which time one set of plates from each transformant was up-shifted to 42°C for 1,2,3, or 5 hours. Duplicate plates were left at 30°C for the same time periods as controls.

Figure 5.1: Diagram of the plasmid pMCB45 showing the GFP construct cloned into the expression vector pAL5.

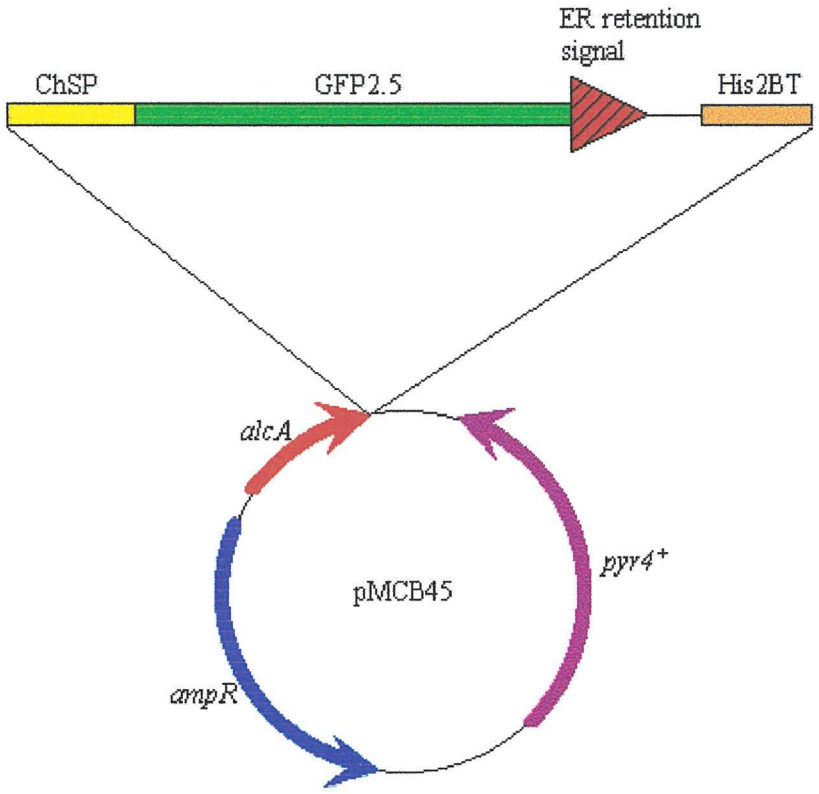

5.2.3 Up-shift experiments ER-1 and ER-2

As all three sets of pMCB45 transformants showed the same results, the data presented in Fig. 5.2 is for one set of transformants ER-1 (*sod*^{VT}*C*$^{+}$) and ER-2 (*sod*^{VT}*C1*). There was no difference seen between the transformants at the permissive temperature of 30°C. At this temperature the *sod*^{VT}*C1* strain behaves as w.t. The *sod*^{VT}*C1* mutation is a temperature-sensitive mutation and the mutant phenotype is only seen at the restrictive temperature of 42°C so no difference would be expected between ER-1 and ER-2 at 30°C. Figure 5.2(A) shows ER-1 and ER-2 incubated at 30°C for 5 hours indicating that there is no change over the course of the experiment at this temperature. Figure 5.2(B) shows the results for the up-shifts carried out with ER-1 and ER-2 at 42°C.

A)

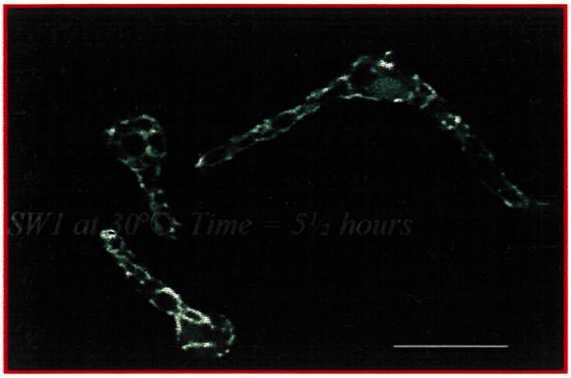

i) **30°C** ER-1. Time = 5 hour

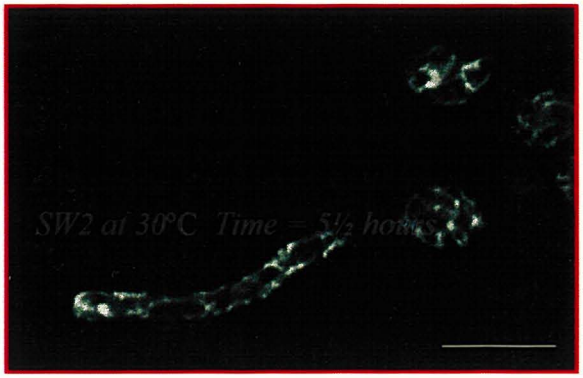

ii) **30°C** ER-2. Time = 5 hour

B)

iii) **42°C** ER-1.Time = **1 hour**

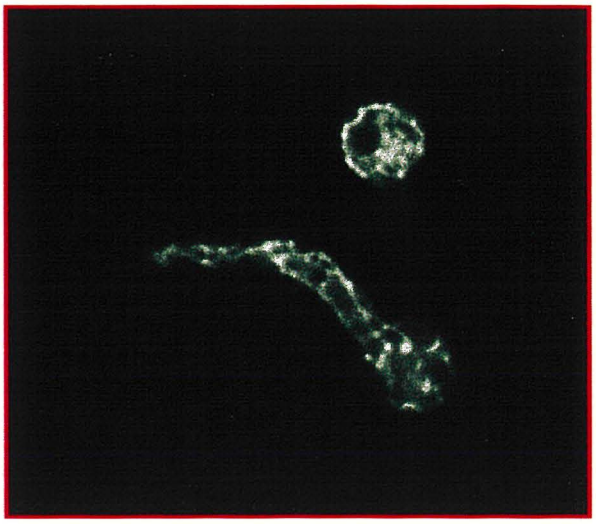

iv) **42°C** ER-2.Time = **1 hour**

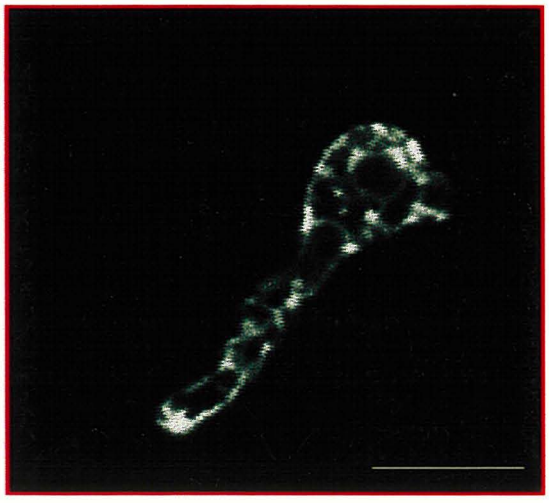

v) **42°C** ER-1. Time = **2 hour**

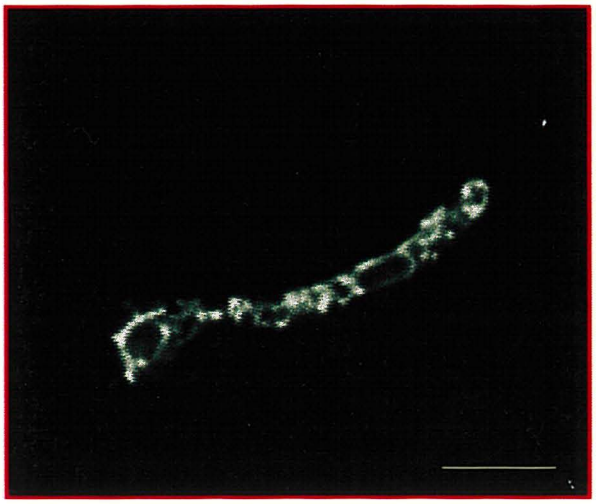

vi) **42°C** ER-2. Time = **2 hour**

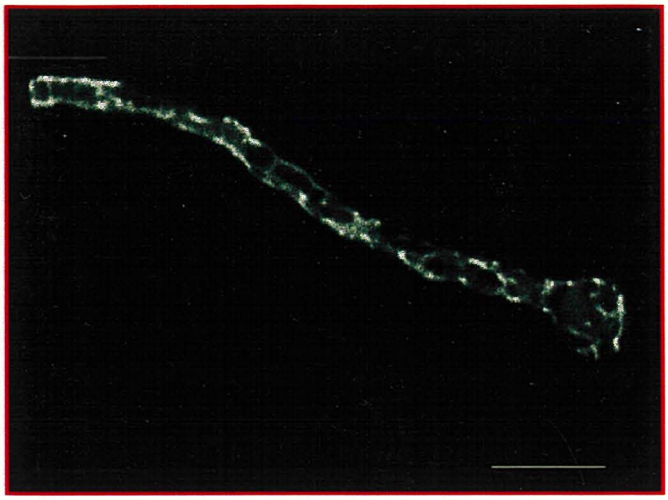

vii) **42°C** ER-1. Time = **3 hour**

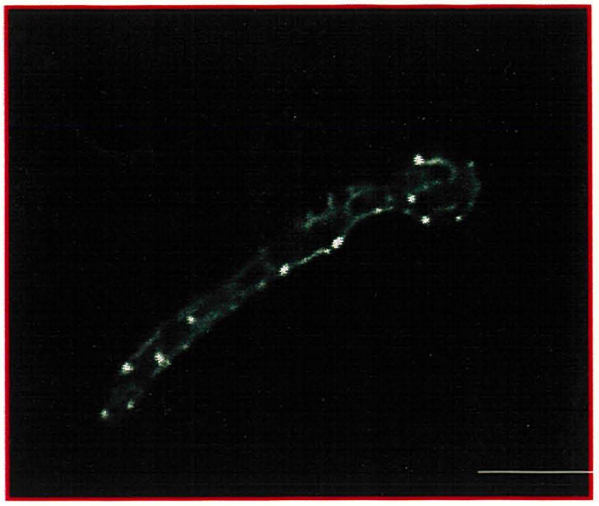

viii) **42°C** ER-2. Time = **3 hour**

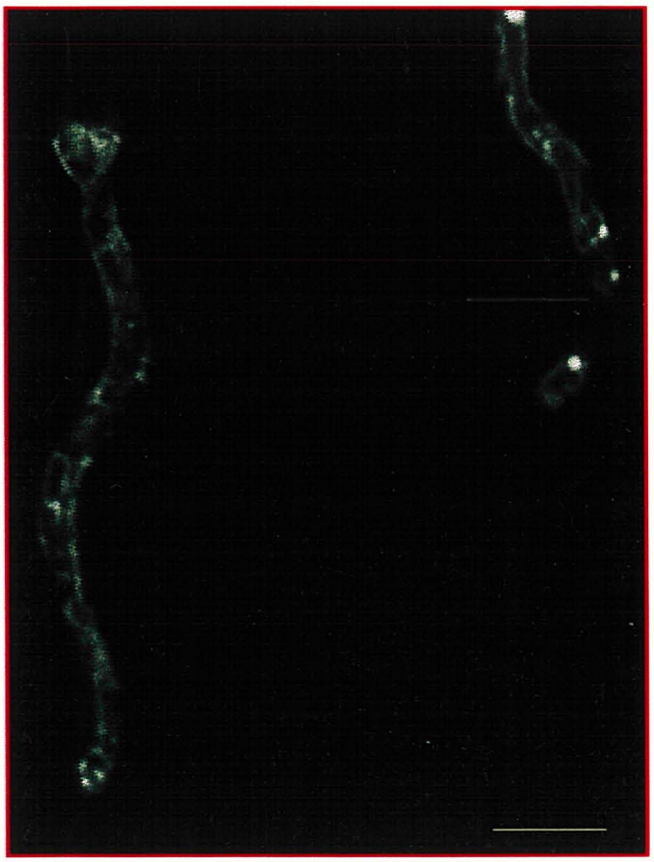

ix) **42°C** ER-1. Time = **5 hour**

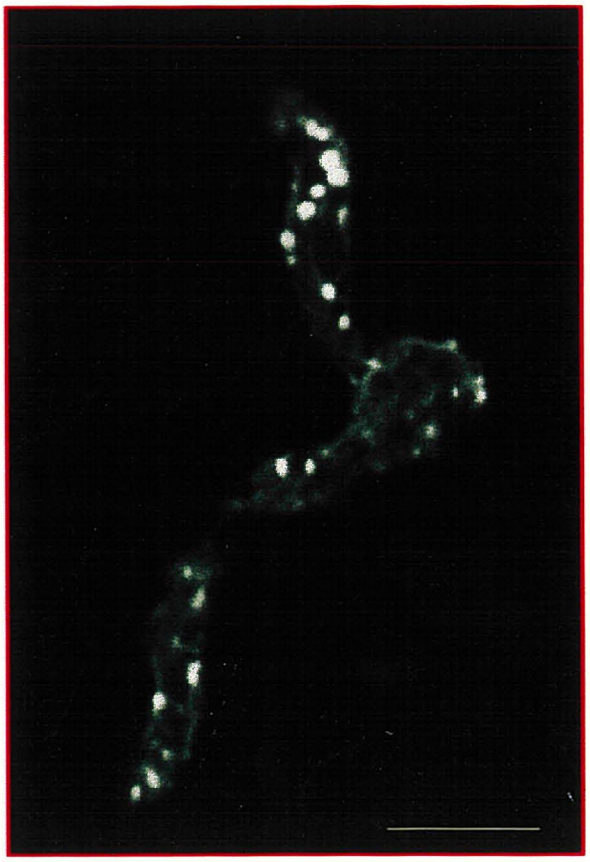

x) **42°C** ER-2. Time = **5 hour**

After incubation at restrictive temperature for three or more hours there was a notable decrease in fluorescence seen in both ER-1 and ER-2. This may due to the instability of the GFP fluorophore at the higher temperature of 42°C. To test this, ER-1 was incubated for five hours at 42°C and compared with ER-1 left at 30°C for the same time period and the decrease in fluorescence was again observed with increasing incubation time (data not shown). These data suggest that the fading seen Figure 5.2 was not associated with the *sod*^{VT}*C1* mutation.

Another phenomenon seen in the up-shift was the appearance of concentrated bright spots of GFP within the ER network after prolonged incubation at restrictive temperature (Fig. 5.2 (viii, ix and x)). These bright spots were observed both in the control strain and in the *sod*^{VT}*C1* transformant, but were more apparent in the mutant strain (Fig. 5.2 (ix) and (x)). Previous work carried out by Dr. S. Whittaker, (165) showed that incubations of the *sod*^{VT}*C1* strain B120 over 4 hours at 42°C resulted in a loss of recovery when down-shifted to permissive temperature. This suggests that the spots seen in the B120 transformants are due to the *sod*^{VT}*C1* mutation causing death of the strain with prolonged incubation at 42°C.

5.3 Effect of Varying Expression of the *sod*^{VI}*C* Gene

5.3.1 Construction of pMX4 expression plasmid

To address whether over-expression of the *sod*^{VI}*C* gene affects viability, the expression plasmid pMX4 was produced (Fig. 5.3). Construction of pMX4 was carried out in three steps; firstly two smaller fragments containing upstream and downstream portions of the *sod*^{VI}*C* gene were produced by digestion of the 9kb *Pst*I-*Hin*dIII clone with the restriction enzymes *Mfe*I and *Xba*I. This yielded a 3.05kb *Mfe*I-*Xba*I fragment containing the upstream portion of the gene including the start codon (ATG), and a 2.3kb *Xba*I fragment containing the downstream portion of the gene including the stop codon (TAA). The digest was run on a 0.7% agarose gel (Section 2.5.2) and the bands of the correct size were excised and purified (Section 2.5.3). In the second step, the 3.05kb *Mfe*I-*Xba*I fragment was ligated into the vector pBluescript, which had been digested with the enzymes *EcoR*1 and *Xba*I. The ligation reaction was then transformed into *E. coli* and a recombinant plasmid purified using standard techniques (designated pM3 (Fig. 5.3(A)). This plasmid was then digested with *XbaI* and the second 2.3kb *XbaI* fragment inserted. Separate recombinant clones were checked by restriction mapping for the correct orientation of the *XbaI* fragment with respect to the upstream sequence already cloned into the vector. The clone pMX2 was chosen as containing the correct insert (Fig. 5.3(B)). The third and final step in the construction of the over expression plasmid was the transfer of the whole *sod*^{VI}*C* gene into the *alcA* vector pAL3X making use of the restriction sites in the MCS of pBluescript. The restriction enzymes *Kpn*I and *Not*I were used to digest out the 5.35kb *sod*^{VI}*C* clone from pBluescript, the digest was run on a 0.7% agarose gel and the correct sized band excised and purified as in section 2.5.3. The 5.35kb *Kpn*I-*Not*I fragment was ligated into *Kpn*I-*Not*I digested pAL3X, which was then

transformed into *E. coli* and purified using standard techniques. A clone pMX4 (Fig. 5.4(A)) was identified as containing the correct insert; a transformation using pMX4 was carried out into the UU-requiring strain GR5 using the standard transformation procedure (section 2.4.6). Transformants were selected on MM KCl medium lacking uridine and uracil to select for the *pyr4*$^{+}$ gene contained within the pAL3X vector.

(A)

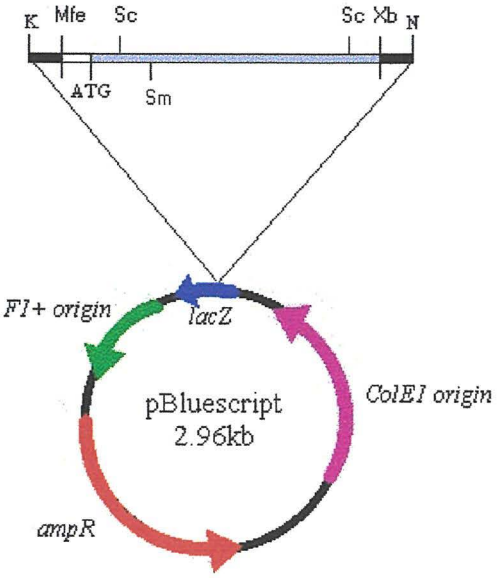

MCS (not to scale).

Coding region of $sod^{VI}C$ gene.

B)

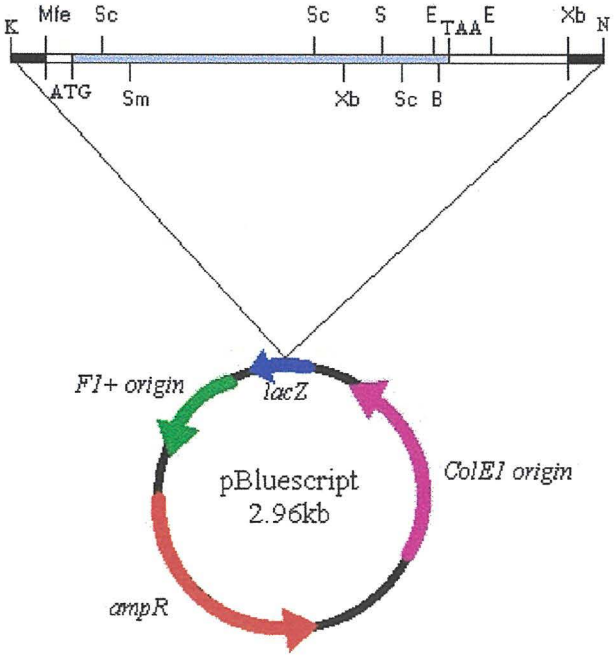

Figure 5.4: Schematic of pMX4 integration. A) Map of pMX4. B) Map of the w.t. *sod*^{VT}*C* locus. C) Site specific integration of the pMX4 plasmid. D) Non-site specific integration of the pMX4 plasmid.
Abbreviations as in Figs. 5.3 and 4.2

A)

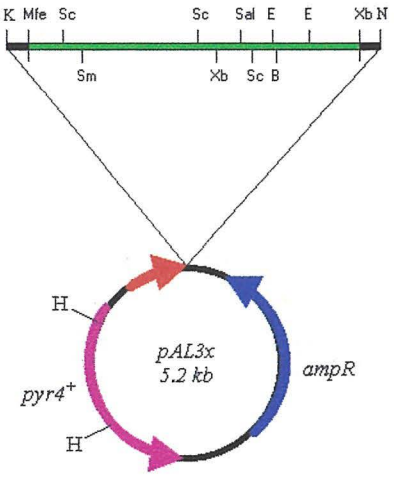

B)

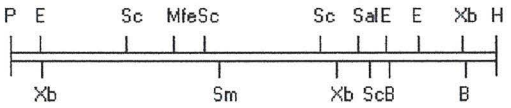

C)

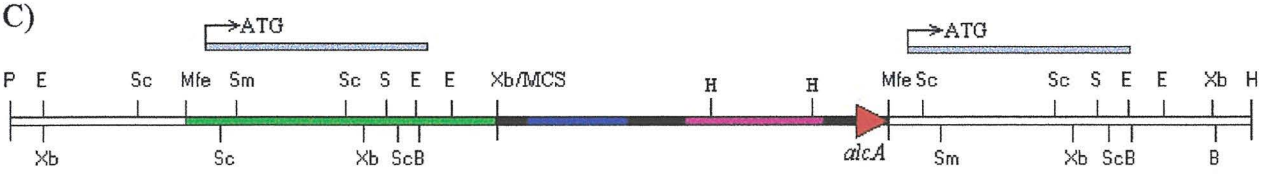

D)

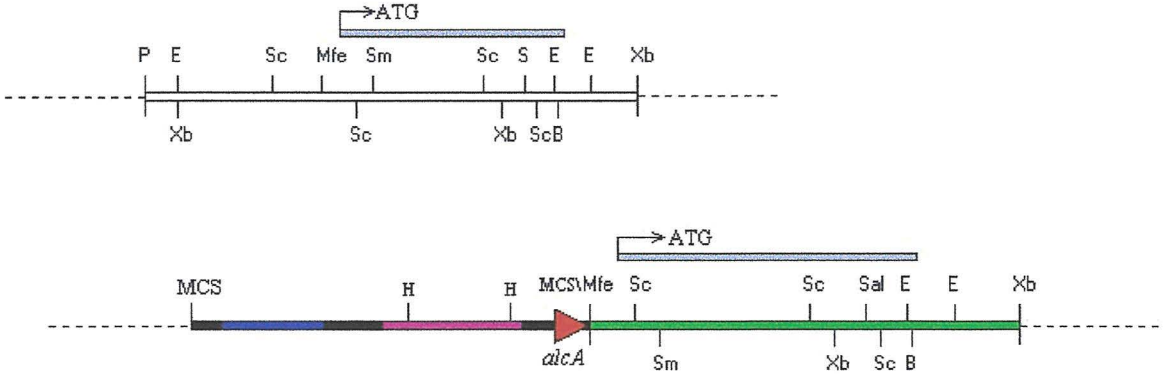

5.3.2 Over-expression Studies on the pMX4 transformants

Spores from pMX4 transformants were purified onto fresh MM glucose plates. Six transformants (MX4-1, 2,3,4,5,6) were chosen at random from the purification plates and used to carry out growth studies on inducing media on containing glycerol or ethanol. Northern and Southern blots were carried out to try to ascertain the copy number and site of integration of the pMX4 transformants, but these were not successful. Work proceeded on the transformants assuming that at least one copy of pMX4 must be present because of the complementation of the *pyrG89* mutation by the *pyr4*$^{+}$ gene. Therefore, although the exact site of integration was not known, some indication of the effects of over-expression could be gained. Both site-specific (Fig. 5.4(C)) and non-site specific (Fig. 5.4(D)) integrations of pMX4 produce a w.t. copy of the *sod*^{VI}*C* gene expressed by the *sod*^{VI}*C* promoter and a second copy of the *sod*^{VI}*C* gene expressed by the *alcA* promoter

The six transformants were stabbed onto separate MM glycerol or MM ethanol plates containing varying percentages of glycerol or ethanol (0.5-2% in 0.5% increments). The inoculated plates were incubated at 30°C and growth studies carried out. All experiments were set up in triplicate and the average growth rates for the strains taken. Figure 5.5 shows the growth rates of the pMX4 transformants on the two inducing media. As all the transformants gave similar growth rates, data for three of the transformants (MX4-1, 2, and 3) are shown as examples.

Figure 5.5: Growth rates of MX4 transformants on inducing media. A) Growth on MM glycerol inducing media. B) Growth on MM ethanol inducing media. Growth rates were calculated by measuring the colony radius over a time period of 5 days, the average growth rate was then calculated for each strain.

A)

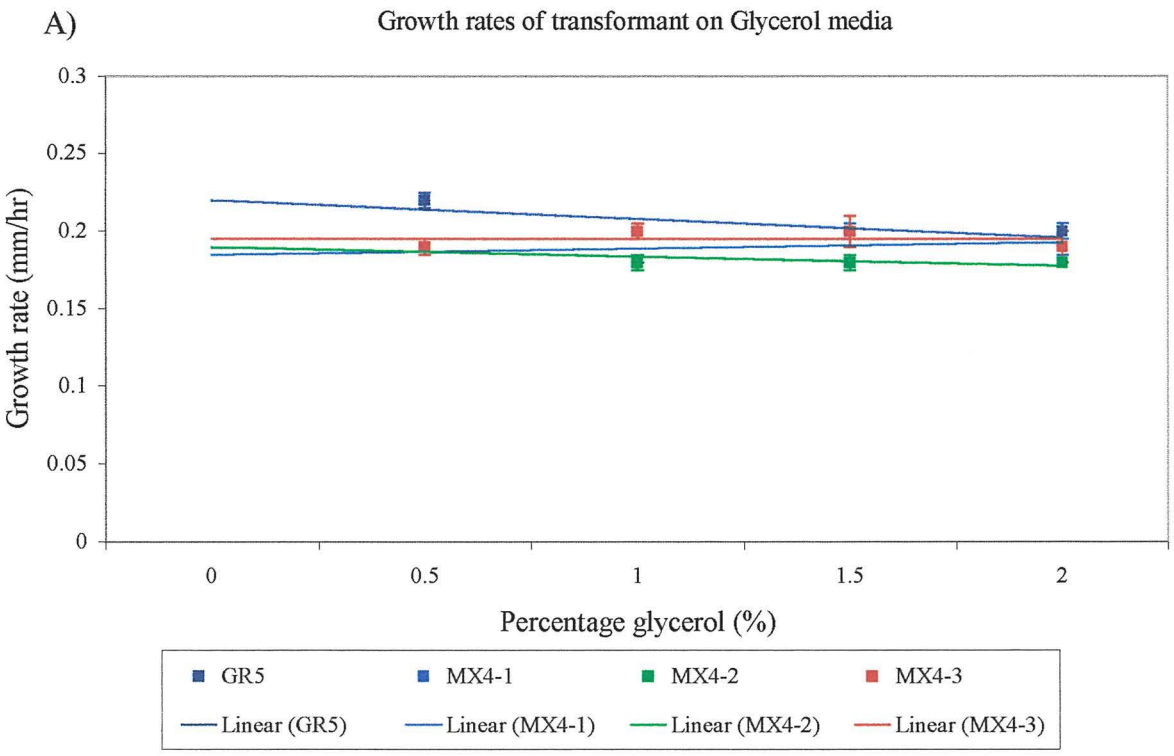

B)

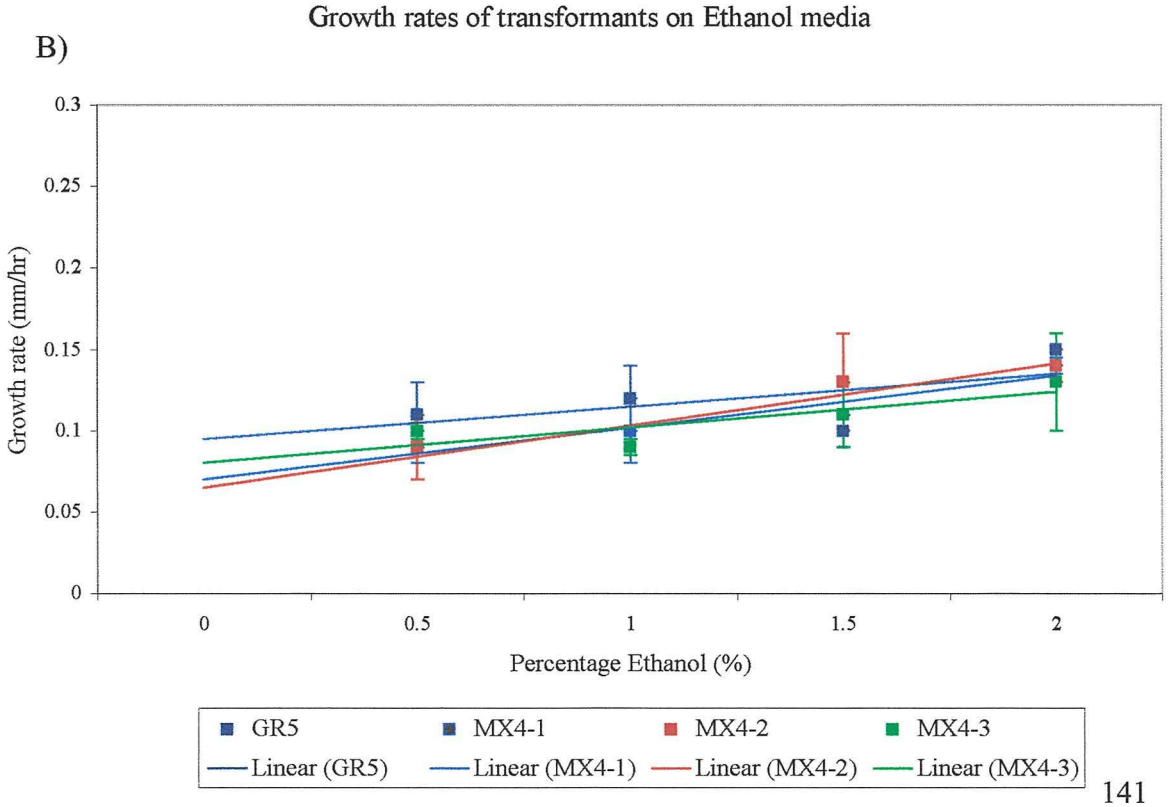

As can be seen from graph 5.5(A) all the MX4 transformants strains showed similar growth rates on increasing percentages of glycerol, the rates in each case being slightly lower than that of GR5. On the higher-inducing ethanol induction plates (Graph 5.5(B)) all of the strains show a much lower growth rate than on glycerol media. This is probably a result of the toxic effect of the ethanol. Previous work carried out showed that above concentrations of 3% ethanol growth was severely inhibited in the control strain, whereas on glycerol at this concentration growth rate was not drastically reduced. All the strains on ethanol media showed an increase in growth rate with increasing ethanol concentration. Ethanol is a poor carbon source and so up to a certain point the more ethanol present in the plates the more growth is achieved. The transformant strains showed a lower growth rate than the control strain GR5, but this was only a decrease of around 0.05mm/hr, which shows that even on the high-inducing ethanol media growth is not severely affected by over-expression of the *sod*^{VI}*C* gene.

As there are no Southern or Northern blots to support the over-expression studies it is difficult to say how much over-expression is occurring. The plasmid pMX4 appeared to be stable within the transformants and growth on MM glycerol and ethanol at higher percentages did not cause looping out of the plasmid, which can be a problem when using the *alcA* promoter. Previous work carried out on over-expression of the *sod*^{VI}*C* gene using a plasmid containing a smaller insert resulted in looping out when over-expressed on high percentage glycerol media (data not shown).

Further work was not carried at out on defining the over-expression in the transformants, since work on the *sod*^{VI}*C::GFP* construct being carried out at the same time showed that expression of the construct from the native *sod*^{VI}*C* promoter was high enough to allow visualisation without the need to use the *alcA* promoter.

5.4 GFP-Tagging of the *sod*^{VI}*C* gene

The GFP-tagging of the *sod*^{VI}*C* gene was carried out in a number of steps to enable tagging of the whole gene. For an overview of the cloning procedure see Figure 5.6.

5.4.1 Cloning of the Upstream Portion of *sod*^{VI}*C* gene into pBluescript

The *sod*^{VI}*C* open reading frame extends just over 4kb, which is too large a product to amplify easily using PCR. In order to reduce the amount of sequence to be amplified, and to limit the opportunities for errors to be introduced by PCR the clone pM3 (section 5.3.1) was used. This clone contains the whole of the upstream portion of the *sod*^{VI}*C* gene; this means that only the downstream portion of the gene needs to be amplified.

5.4.2 PCR of GFP gene, and the Downstream Portion of *sod*^{VI}*C* Gene

All the PCR reactions in this section were carried out using the polymerase enzyme *Pfu* polymerase (Promega®). This enzyme has a proofreading ability, making transcripts produced with this enzyme far less prone to errors than when using conventional polymerases such as *Taq* polymerase (Promega®). For methodological details on PCR reactions using *Pfu* polymerase see section 2.5.11. All PCR products were cloned using the TOPO®2.1 cloning kit (Invitrogen®). This kit relies on the 'A' overhangs produced when carrying out a PCR with *Taq* polymerase. *Pfu* polymerase does not produce these overhangs, but they can be added after gel purification (see section 2.5.3) of the *Pfu* PCR product, by incubation with *Taq* polymerase and dATP (section 2.5.12). The PCR can then be cloned into the TOPO®2.1 vector (section 2.5.13).

The first PCR reaction in the cloning strategy was carried using the primers P1for and P1rev (Appendix 7), which were designed to amplify the downstream

portion of the *sod*^{VI}*C* gene. The template used for this PCR was the 9.0kb genomic *PstI-HindIII* fragment cloned into pUC18; this fragment contains the whole *sod*^{VI}*C* gene. Primer P1for was designed to prime just upstream of the second *Xba*I restriction enzyme site (position 4027) in the *sod*^{VI}*C* gene (Figure 4.2). Primer P1rev was designed to anneal at the C-terminus of the *sod*^{VI}*C* gene introducing an *Nhe*I restriction enzyme site over the *sod*^{VI}*C* stop codon (TAA). The expected product from this PCR was a 1.03kb fragment containing *Xba*I and *Nhe*I sites towards the 5'-and 3'-ends respectively. Ten µl of the PCR reaction was run out on a 0.7% agarose gel and the correct sized band excised and purified (see section 2.5.3). The 'A' tailing reaction using *Taq* polymerase was then carried out on 10µl of purified PCR product, 2µl of this reaction was then cloned into the TOPO2.1 vector (section 2.5.13) and transformed into TOPO2.1 competent cells (Invitrogen®). Varying volumes of the transformation reaction was then plated onto STA plates containing Ampicillin (50µg/ml) and IPTG/X-Gal (section 2.2.1) allowing blue/white selection of transformants. Individual transformants were then isolated and screened using standard methods. The clone (pX-B1) was chosen as containing the correct insert (See Fig 5.7(A)).

The second PCR reaction was carried out to generate the GFP gene with the *Nhe*I restriction site over the START codon. The primers P2for and P2rev (Appendix 7) were used to amplify the sequence. Primer P2for was designed to anneal to the upstream sequence of the GFP gene introducing an *Nhe*I site over the START ATG codon, whilst primer P2rev was designed to anneal over the 3' end of the gene retaining the STOP TAA codon. The downstream primer (P2rev) also introduced a *Not*I restriction site next to the STOP codon providing a novel restriction site for later cloning steps. The PCR reaction was again carried out with *Pfu* polymerase (section

2.5.11), the pMCB45 plasmid containing the *A.nidulans* GFP gene GFP2.5 (section 5.2 was used as a template. Ten µl of the PCR reaction was run out on a 0.7% Agarose gel (section 2.5.2) and the expected 0.75kb product band was purified from the gel (section 2.5.3). The PCR product was then cloned and transformed into Topo®2.1 competent cells and screened in the same way as the first PCR reaction. The clone pGFP1 was chosen as containing the correct insert (Fig. 5.7(B)). The clones pX-B1 and pGFP1 were then sequenced using MWG-Biotech's sequencing service to ensure that the sequences were as w.t. (Appendix 8).

Figure 5.6: Overview of *sod*^{VI}*C::GFP* construction. Abbreviations as in Fig. 5.3 and 4.2

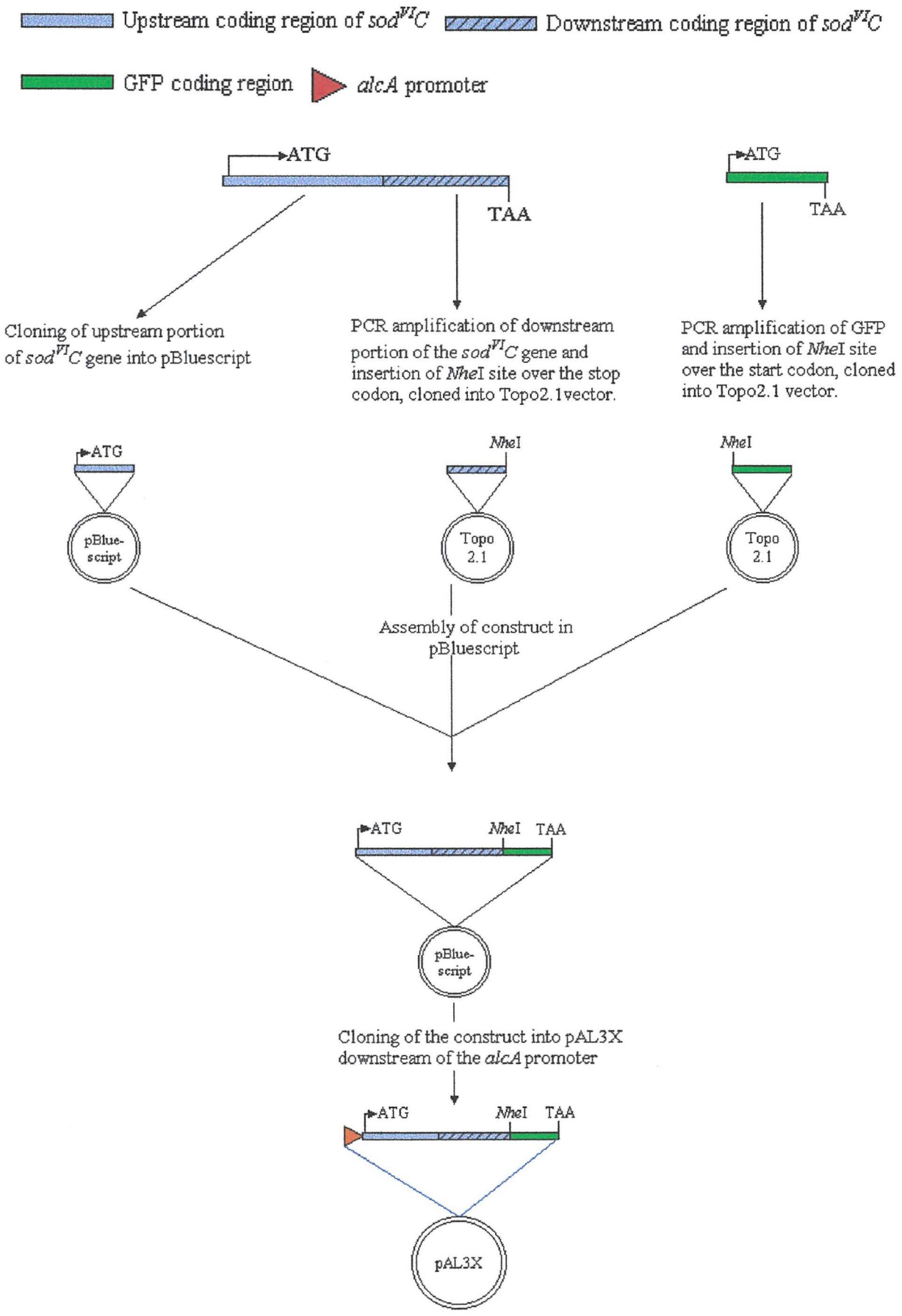

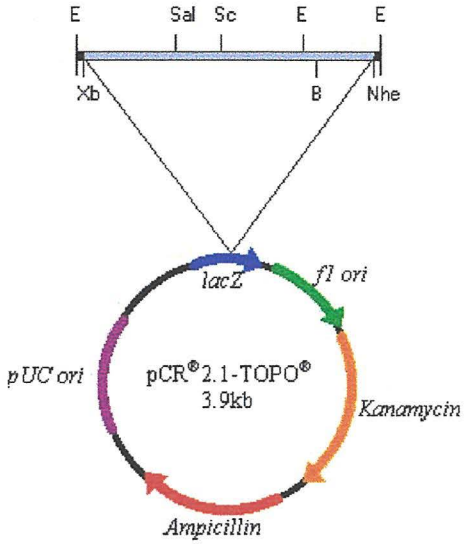

A) pX-B1

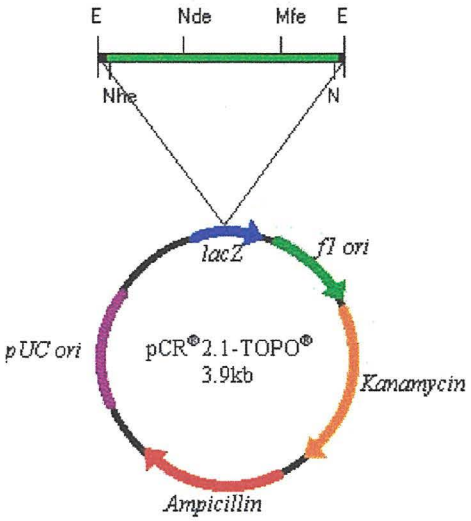

B) pGFP1

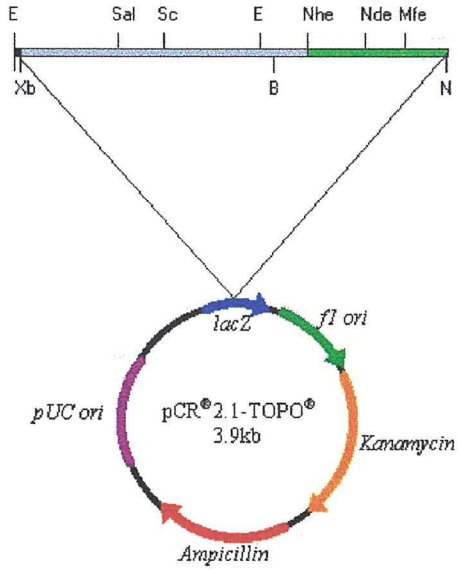

(C) pX-BGFP4

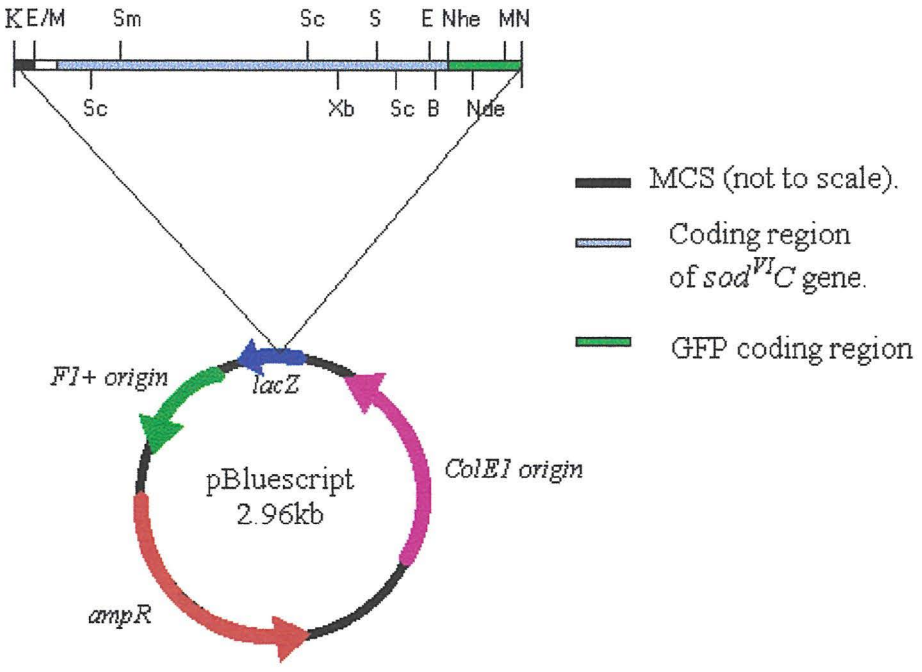

(D) pBlue-sodGFP

5.4.3 Construction of the pSodGFP19 Expression Plasmid

In order to create the *sod*^{VI}*C::GFP* expression vector all of the clones produced in section 5.4.2 needed to be assembled into a single clone. The first step was the attachment of the GFP clone to the 3' end of the fragment in pX-B1. The plasmid pGFP1 was digested with the restriction enzymes *Nhe*I and *Not*I to cut out a 0.72kb *Nhe*I-*Not*I fragment. Following band extraction (section 2.5.3) this fragment was ligated into pX-B1 cut with *Nhe*I and *Not*I, the *Not*I site in pX-B1 is derived from the MCS of TOPO2.1®. This ligation was transformed into *E.coli* and purified using standard techniques. The clone pX-BGFP4 was identified as containing the correct insert (Fig. 5.7(C)). This ligation step attached the GFP gene in frame to the downstream portion of the *sod*^{VI}*C* gene. The plasmid pX-BGFP4 was digested with the restriction enzymes *Xba*I and *Not*I. Following band extraction (section 2.5.3), the 1.75kb *Xba*I-*Not*I fragment was ligated into the plasmid pM3 digested with *Xba*I and *Not*I. The ligation was transformed into *E.coli* and purified using standard techniques. The clone pBlue-sodGFP was identified as having the correct insert (See Fig. 5.7(D)). The final step in the construction of the *sod*^{VI}*C::GFP* was to move the whole construct into the expression vector pAL3X. The plasmid pM3sodGFP was digested with the restriction enzymes *Kpn*I and *Not*I, which cut out the 8.4kb *Sod*^{VI}*C::GFP* construct. Following band extraction (section 2.5.3) the insert was ligated into pAL3X digested with *Kpn*I and *Not*I; this digest allows the cloning of the *Sod*^{VI}*C::GFP* fusion downstream of the *alcA* promoter, in the correct orientation for expression of the gene. The ligation was transformed into *E.coli* and purified using standard techniques. The clone pSodGFP19 was chosen as containing the correct insert (See Fig. 5.8(A)).

5.4.4 Transformation of pSodGFP19 and Selection of Site Specific Transformants

The *sod*^{VI}*C*$^{+}$ strain GR5 was transformed with the plasmid pSodGFP19 (section 2.4.6). Transformants were then screened for fluorescence on MM glucose. If the plasmid-encoded copy of the *sod*^{VI}*C* gene integrates at the *sod*^{VI}*C* locus (i.e. site specifically), recombination between the two homologues will produce two copies of the *sod*^{VI}*C* gene flanking the *pyr4*$^{+}$ marker (See Fig 5.8(C)). One copy of the gene tagged with the GFP reporter will be put under the control of the *sod*^{VI}*C* promoter, and a second homologue lacking a GFP tag will be placed under the control of the *alcA* promoter. This type of integration essentially switches over the promoters for the GFP construct allowing it to be expressed from the *sod*^{VI}*C* promoter at w.t. levels within the hypha. A site specific integration should therefore produce a transformant that expresses the GFP-tagged *sod*^{VI}*C* gene when grown on glucose media.

Spores were spread on fresh MM glucose plates and incubated overnight at 30°C. Coverslips were placed on top of the germinated spores, and the germlings screened for fluorescence using standard UV microscopy techniques. A number of transformants showed varying levels of fluorescence on MM glucose, and the transformant SodGFP-24 was chosen as giving the brightest level.

5.4.5 Confirmation of Site-Specific Integrations by Southern Blotting

Spores from sodGFP-24 were used to inoculate 100ml of liquid CM media in a 250ml-bevelled flask. The flask was incubated overnight with shaking at 30°C, and the mycelium was then harvested by filtration and ground under liquid nitrogen. Genomic DNA was extracted according to section 2.5.1 and run on a 0.7% agarose gel (section 2.5.2) to quantify and check its quality. Approximately 3μg of DNA from genomic DNA preparations was digested with the restriction enzymes *Pst*I and *Hin*dIII (section 2.5.5) The samples were electrophoresed on a 0.7% agarose gel (section 2.5.2) along with a 1kb DNA ladder Promega® (Appendix 4) for 12-16 hours at 10mA (Fig. 5.8(D)). The gel was then blotted as in section 2.5.14. After blotting the gel was hybridised (section 2.5.15) and probed using 100ng of ^{32}P labelled (section 2.5.15) 6.4kb *EcoR*I fragment produced by digestion of the 9.0kb *Pst*I-*Hin*dIII clone.

A site-specific integration of the pSodGFP19 plasmid is predicted to give two hybridising bands (Fig. 5.8(C)) of 7.2 and 5.97kb respectively. Figure 5.8(E)) shows the autoradiograph for the Southern blot carried out on sodGFP-24. As can be seen the control strains give the expected 9kb band derived from the genomic copy of the *sod*^{VT}*C* gene. The sodGFP-24 transformant lacks this 9kb band, showing that one copy of the pSodGFP19 plasmid has been integrated site-specifically as the expression data indicates. However, the sodGFP-24 transformant contains several hybridising bands not predicted from the integration of a single copy of the plasmid. These extra bands are presumably due to additional non-site specific integrations of the pSodGFP19 plasmid into the genome. The sizes of these bands are not predictable as the bands produced are dependent on the site of integration of the plasmid. The expected 5.97kb band predicted from a site-specific integration can be seen on the blot but no 7.2kb band is visible. As was the case for earlier blots this band size was predicted from

both restriction mapping and sequencing of the *Pst*I-*Hin*dIII sub-clone. Restriction mapping within this fragment is subject to errors due to difficulty to size bands with small differences using DNA markers. This could result in the predicted band being slightly larger than expected. A 7.5/8kb band can be seen on the autoradiograph, this may be the actual size of the predicted band. The differences in band sizes will be cleared up when further sequencing is carried out on the upstream portion of the *Pst*I-*Hin*dIII clone. The fact that the sodGFP-24 transformant expresses the *sod*^{VI}*C::GFP* at high levels when grown on glucose media, and that the 9kb band from the w.t. copy of the *sod*^{VI}*C* gene is not present on the autoradiograph confirms that this transformant contains a site-specific copy of pSodGFP19. The other non-site specific copies of this plasmid will only be expressed when transformants are grown on inducing media. In order to rule out any interference of the non-site specific copies when carrying out localisation studies the sodGFP-24 transformant will be grown on MM media containing 2% glucose, which has been shown to completely repress the *alcA* promoter (148). Repression of the *alcA* promoter ensures that only the *sod*^{VI}*C::GFP* gene under the control of the native *sod*^{VI}*C* promoter is expressed. Further work is currently being carried out to look at the number of copies of pSodGFP19 present in sodGFP-24. The presence of extra copies of pSodGFP19 gives the opportunity to carry out over-expression studies of the *sod*^{VI}*C::GFP* in the future.

In order to show that the *sod*^{VI}*C::GFP* fusion protein functions as w.t. the *sod*^{VI}*C1* strain B120 was transformed with the plasmid pSodGFP19 to check for complementation of the *sod*^{VI}*C1* mutation. Due to the site of the mutation within the *sod*^{VI}*C* gene a non-site specific integration of the plasmid expressed from the *alcA* promoter needs to be obtained. With this in mind 100 *sod*^{VI}*C1* transformants were screened for growth on MM Glycerol media at the restrictive temperature of 42°C

(data not shown). Transformants capable of rescuing growth were then screened for fluorescence on 2% glucose and glycerol media. All the transformants capable of restoring growth were found to have optimal expression of the GFP construct on MM Glycerol media, indicating that these transformants contained non-site specific integrations of pSodGFP19 being expressed from the *alcA* promoter. The fact that these integrations are capable of rescuing growth shows that the attachment of the GFP to the *sod*^{V71}*C* gene does not affect its function within the cell. With more time Southern blots would be carried out on the transformants to confirm the sites of integration.

A)

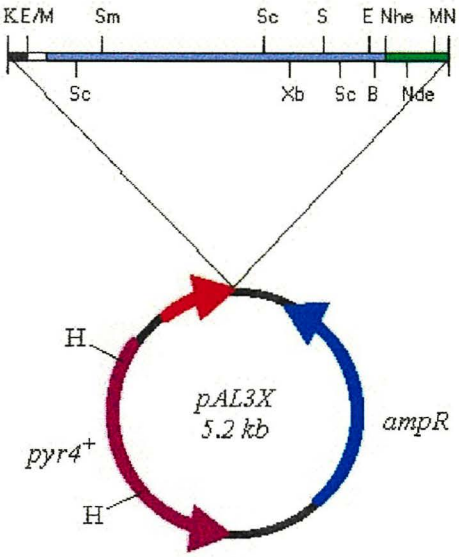
KE/M
Sm
Sc
S
E Nhe
MN
Sc
Xb
Sc B
Nde
H
pAL3X
5.2 kb
ampR
pyr4+
H

B)

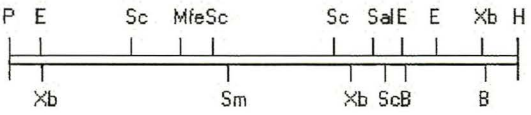
P
E
Sc
MfeSc
Sc
SalE
E
Xb
H
Xb
Sm
Xb
ScB
B

C)

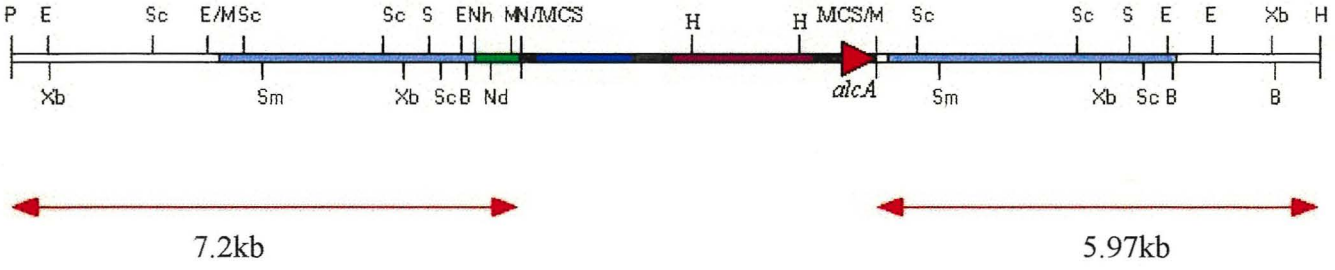
P
E
Sc
E/MSc
Sc
S
ENh
MN/MCS
H
H
MCS/M
Sc
Sc
S
E
E
Xb
H
Xb
Sm
Xb
ScB
Nd
alcA
Sm
Xb
Sc B
B
7.2kb
5.97kb

(D)


1
2
3

(E)

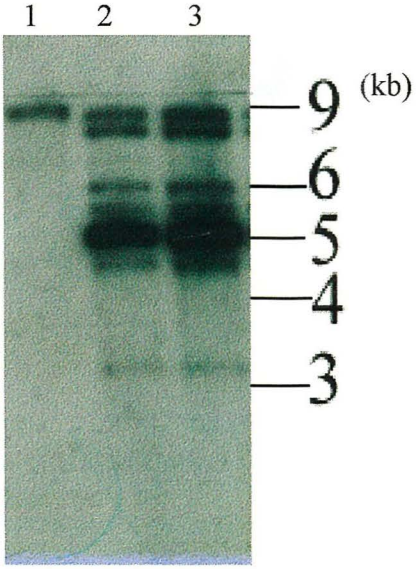
1
2
3
9
6
5
4
3
(kb)

5.4.6 Confocal Microscopy of the sodGFP-24 transformant

Spores from sodGFP-24 were used to inoculate MM media plates containing 2% glucose; the plates were incubated for 24-48 hours and then slides prepared as in section 2.4.8 and observed using standard confocal microscopy techniques.

The Sod^{VI}C::GFP fusion protein showed distinct localisation to the growing hyphal tip (Fig. 5.9(A)) shows a transect of hyphae from the sodGFP-24 transformant. In contrast, Figure 5.9(B) shows a transect along hyphae expressing the pMCB45 plasmid which localises the GFP to the ER, where it lights up a filamentous network throughout the fungi with no distinct regional localisation within the hypha. The localisation seen within the hyphae is due to the targeting of the GFP by the attachment of the *sod^{VI}C* gene. The localisation seen with the Sod^{VI}C::GFP fusion protein has not been seen with any of the other constructs expressed in *A. nidulans*, a soluble GFP transformed into *A. nidulans* (data not shown) produces fluorescence throughout the cytoplasm, and shows no localisation to any of the structures seen with the Sod^{VI}C::GFP fusion protein indicating that the localisation seen is real and not an artefact caused by the GFP protein.

Figure 5.10(A) shows frames from a time-lapse film showing an actively growing hyphal tip alongside an older hypha whose growing tip is further forward (See track 1 of the CD-ROM included in this thesis for movie file). The older hypha shows much less fluorescence than the tip of the adjacent hypha, although localisation in the older hypha is still seen to distinct bodies within the cytoplasm but at a much lower frequency. The growth rates of the strains (average 0.12mm/hr) are comparable to those seen in growth studies on the w.t. strain GR5, which has a growth rate of 0.22mm/hr (data not shown) at 30°C. The slightly lower growth rate of the sodGFP-24 strain is likely to reflect the decrease in temperature due to the slides cooling when

viewed at room temperature. Figure 5.10(B) (Track 2 on CD-ROM) shows stills from a group of hyphae expressing the *sod*^{VI}*C::GFP* on 2% Glucose media. As can be seen the hyphae appear to grow normally with no effect on hyphal morphology.

Figure 5.9: Transects of hyphae expressing psodGFP19 and pMCB45.
(A) Transect taken along hyphae of the transformant sodGFP-24 expressing the pSodGFP19 construct on 2% glucose.
(B) Transect taken along hyphae of the transformant ER-1 expressing the pMCB45 construct on 1% glycerol media expressing the plasmid pMCB45.
Bar = 50μM.

(A)

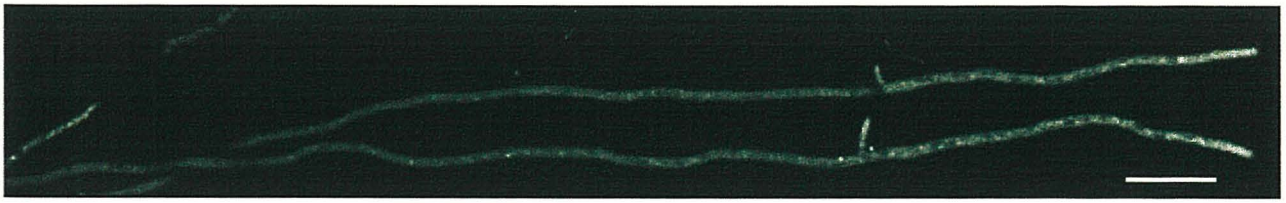

(B)

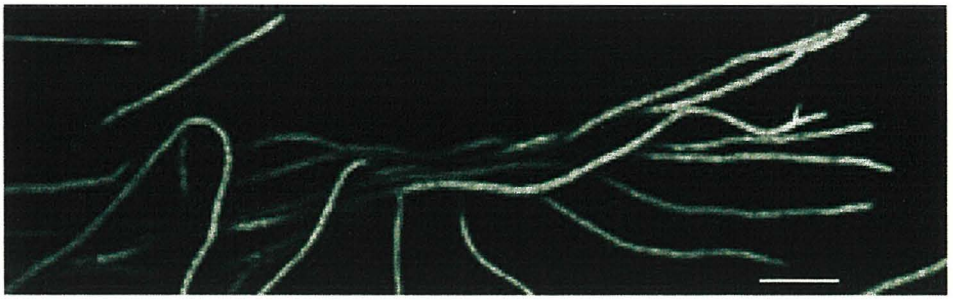

Figure 5.10: Stills taken from time-lapse films showing localisation of *sod*^{VI}*C::GFP* to growing hyphal tips.
(A) Actively growing tip alongside older hypha (Track 1 on CD-ROM)
(B) Growing hyphae from sodGFP-24 showing tip localisation. Growth rate = 0.1 mm/hr. (Track 2 on CD-ROM).
Bar = 10μM.

(A)

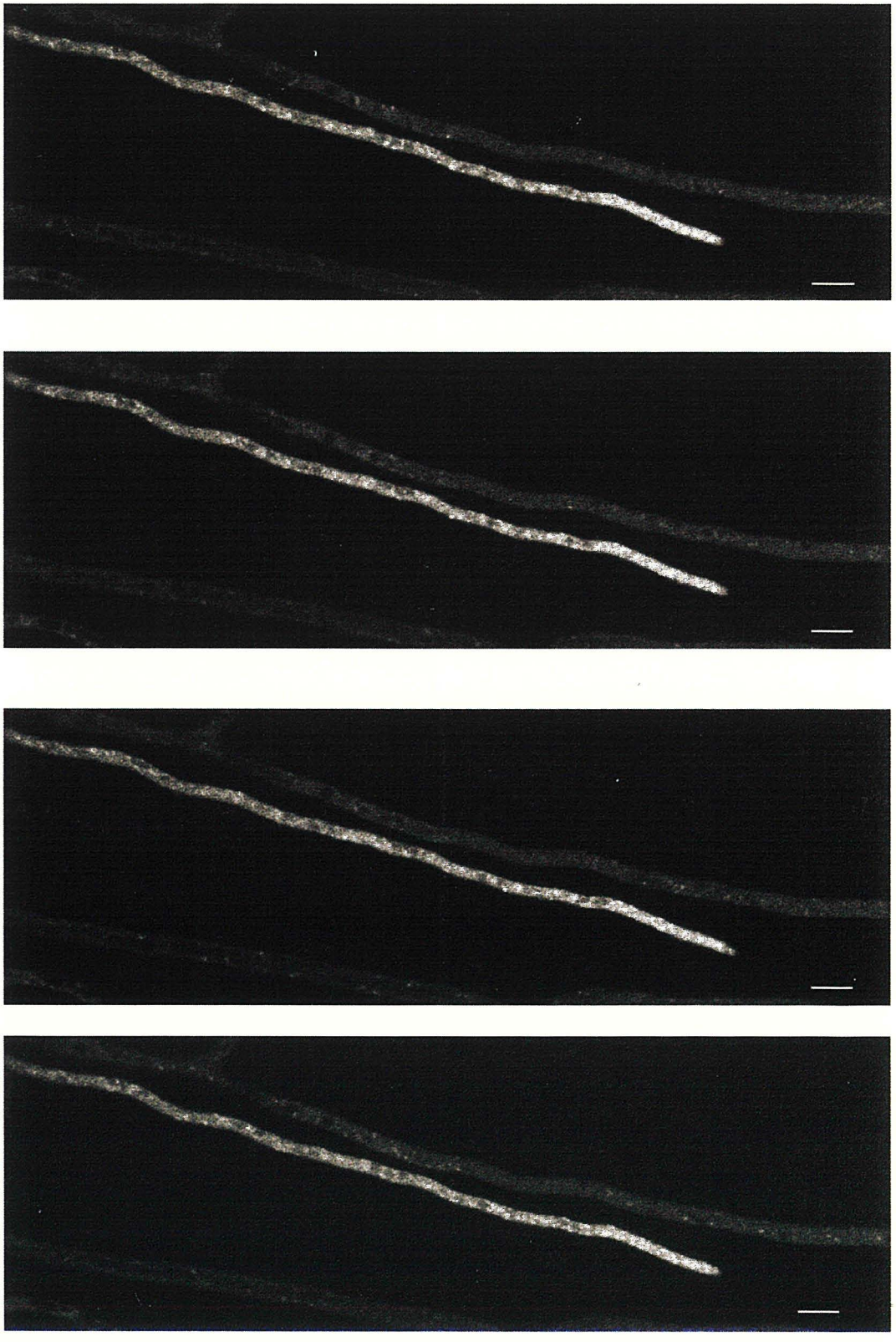

(B)

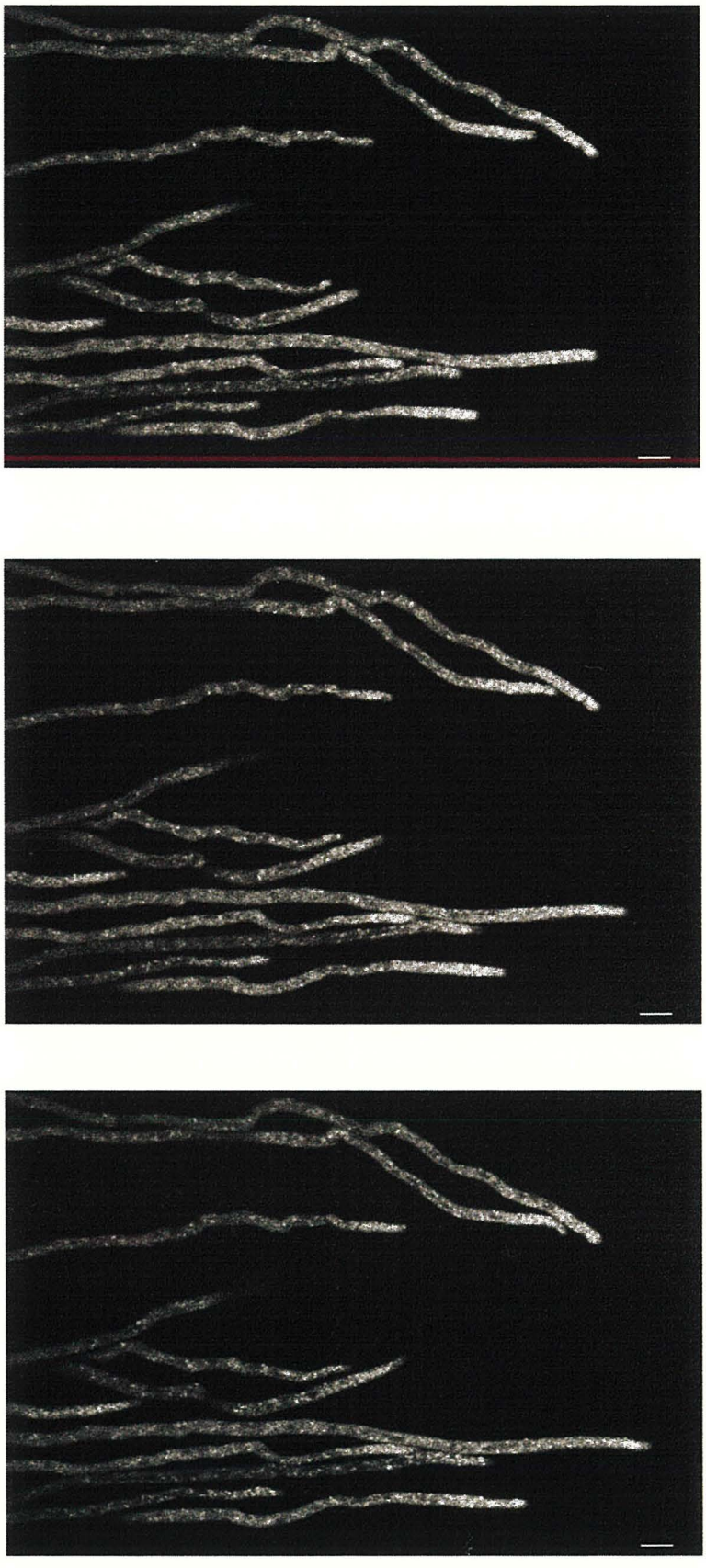

Higher powered confocal images showed that the $Sod^{VI}C$::GFP protein localised to distinct 'doughnut' shaped and elongated structures within the cytoplasm, which are presented here as being putative *A. nidulans* Golgi equivalents. (Fig 5.11(A)) The putative Golgi are packed throughout the growing hyphal tip (Fig 5.11(A) and Track 3 on CD-ROM) and can be seen to move backwards and forwards through the cytoplasm (Track 4 on CD-ROM). Diffuse fluorescence can be seen throughout the cytoplasm presumably due to $Sod^{VI}C$::GFP within the cytoplasm which has not localised to the cisternae. The nuclei within the hyphae show no staining and can be seen as dark areas within the cytoplasm (Fig. 5.11(A) indicated by red arrow). It is interesting to note that some of the putative cisternae within the cytoplasm appear much brighter than others (Fig. 5.11(B) Red boxes), this was seen in all observations carried out on the sodGFP-24 transformant.

The panel in Fig. 5.11(C) illustrates some of the different structures seen within the hyphae. These images were taken from hyphae that had been prepared as in section 2.4.8, but instead of incubating at 30°C the slides were placed at 4°C for 3-4 hours. This slowed down the movement of the structures within the cytoplasm allowing clearer pictures to be obtained. The structures obtained from the cooled mycelia were checked against ones observed in hyphae allowed to recover at 30°C and the structures were morphologically identical. Furthermore, measurements were taken of 100 structures at 30 and 4°C to compare their diameters. At 30°C the structures had an average diameter of 1.2 ±0.02μM whereas at 4°C the average diameter was 1.4 ±0.04μM. As there is no significant difference between the sizes and morphologies of the structures seen at 4°C this technique can be used to obtain clearer images for study. It should be noted that the average diameter of structures will be a lot smaller when viewed using electron microscopy techniques as the GFP

fluorophore releases light over a diffuse area and therefore the viewed structure appears larger.

(A)

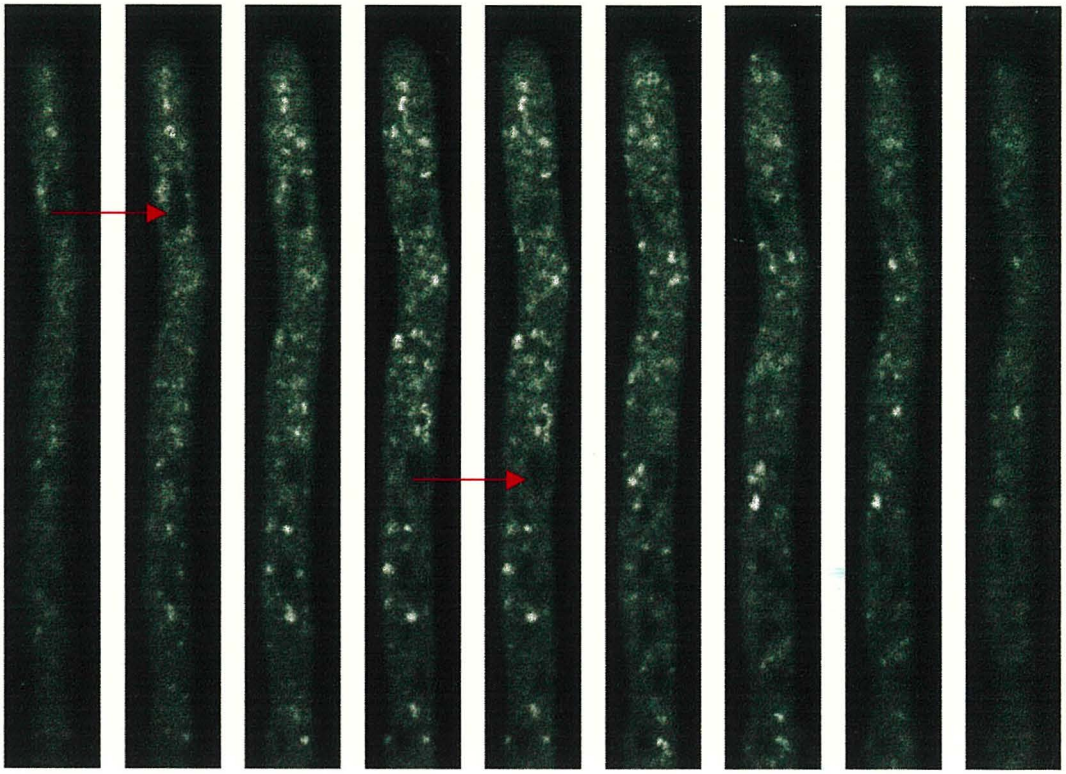

7μm

(B)

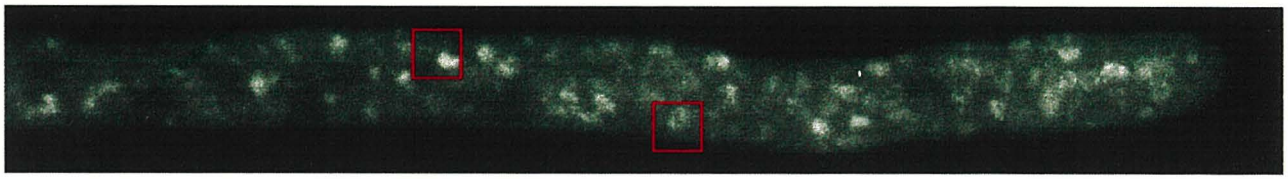

(C)

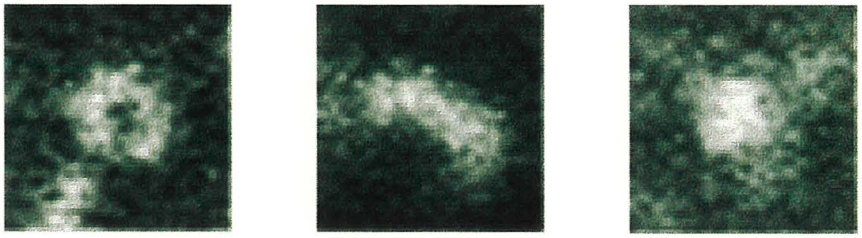

Hollow 'doughnut' Elongated Solid ball

1μM

5.5 Effect of Brefeldin A on Endomembrane Morphology

5.5.1 Quantification of BFA concentration

Work has been carried out in other organisms using BFA over a wide range of concentrations (1μg/ml-100μg/ml). As no work had been carried out with *A. nidulans*, it was necessary to first identify the correct concentration to use in this study. In order to correlate any changes in the endomembrane morphology with the action of BFA, a sub-lethal dose must be used to prevent changes in morphology due to death of the fungus. To ascertain this concentration, a simple assay was devised to determine the effects of varying amounts of BFA on germination.

Liquid CMUU media containing different amounts (0-500μg/ml) of a stock solution of BFA (10mg/ml in ethanol) was added to wells in a microtitre plate. As controls, duplicate lanes in the microtitre plate were set up with LCMUU containing equivalent volumes of ethanol without BFA in order to take account of the toxic effect of ethanol. Each well was then inoculated with $3x10^5$ spores and the plate incubated at 30°C overnight. The microtitre plates were then observed using an inverse microscope and the percentage of spores germinating for each concentration quantified visually. A dose where more than 50% germination occurred was chosen as being sub-lethal. This experiment was carried out with spores from the control strain GR5, which had been used in transformations with the GFP constructs (Table 5.1). A concentration of 150μg/ml was chosen as the optimal concentration and was used in this study. At BFA concentrations of higher than 150μg/ml loss of germination is probably due a combination of the high concentration of BFA but also the toxicity of the ethanol used in preparing the stock solution.

Table 5.1: Quantification of BFA concentration for the *sod*$^{VI}C^{+}$ strain GR5. The percentage of spores germinating in each well was scored.

BFA concentration (µg/ml)	GR5 + BFA (test)	GR5 + Ethanol (control)
0-100	98%	98%
150	75%	98%
200	75%	98%
250	25%	25%
300-500	0	0

5.5.2 Effects of Brefeldin A on ER morphology

Spores from the pMCB45 transformant ER-1 were set up on coverslips as in section 2.4.7 and incubated for 12 hours at 30°C. The media from the coverslips was carefully removed by aspiration with a thin pipette, the germlings were washed by addition of a few drops of liquid MM glycerol media to the coverslips; this was left for a few seconds and then removed by aspiration this was repeated twice. After the final wash 150µl liquid MM glycerol media containing BFA (150µg/ml) was added to the coverslips, which were then incubated at 30°C for 5 hours. Duplicate coverslips were also set up where an equal volume of liquid media containing ethanol without BFA was added to act as controls.

The coverslips were then inverted onto a fresh slide and visualised using standard fluorescence microscopy techniques for GFP (Section 2.4.7).

Figure 5.12 shows the results for the treatment of ER-1 with BFA.

Figure 5.12: Treatment of ER-1 germlings with BFA (150μg/ml).

(A) Distortion of the ER, arrows indicate swelled regions within the cytoplasm.

(B) Extreme swelling of the ER seen in a number of hyphae.

Bar = 10μM.

(A)

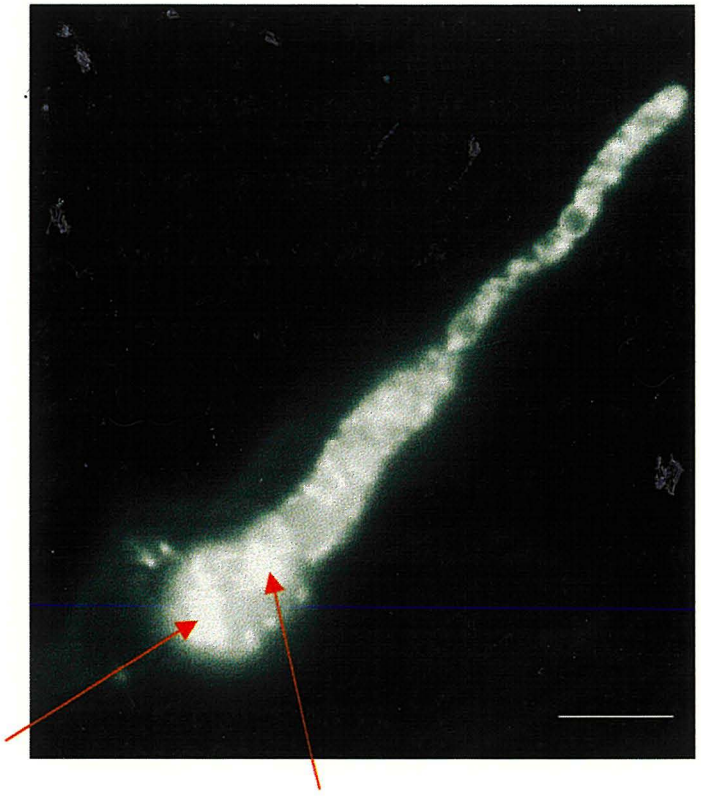

(B)

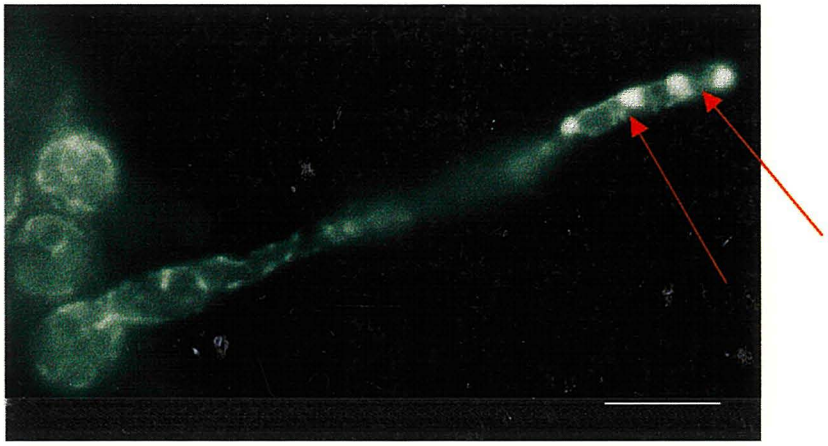

Treatment of ER-1 with BFA caused the ER morphology to change dramatically in this strain. Instead of the characteristic ribbon-like network of tubules within the cytoplasm the ER became distorted, becoming swollen and patchy in places (Fig. 5.12(A)). Some of the hyphae showed extreme swellings producing globular structures within the cytoplasm (Fig 5.12(B)). The control slides incubated with media containing ethanol appeared the same as seen for ER-1 incubated at 30°C (Fig. 5.3(A)).

5.4.3 Effects of BFA on the sodGFP-24 transformant

Spores from the sodGFP-24 transformant were set up on slides as in section 2.3.7 and treated in the same manner except that in this case MM (2%) glucose was used. The coverslips were again inverted onto fresh microscope slides and visualised using standard UV microscopy techniques. Upon incubation with BFA there was a significant change in the localisation pattern of $Sod^{VI}C$::GFP (Fig. 5.13(A) and (B)). Confocal images from untreated sodGFP-24 transformant (Fig. 5.11) show localisation of the *$sod^{VI}C$::GFP* fusion protein to a large number of distinct spherical and doughnut-shaped structures, which show the highest density at the growing hyphal tip (e.g. Fig. 5.11 (B)). In the presence of BFA localisation is seen to a few spherical bodies within the cytoplasm (Fig. 5.13(B)) some of which appeared to be swollen (Fig. 5.13(B)). Most of the GFP fluorescence was located throughout the cytoplasm, with no localisation to distinct structures.

Figure 5.13: The transformant sodGFP-24 treated with BFA.

(A) Decrease in localisation of the Sod^{VI}C::GFP fusion protein.

(B) Some hyphae showed swelled structures localised within the cytoplasm.

Bar = 10μM.

(A)

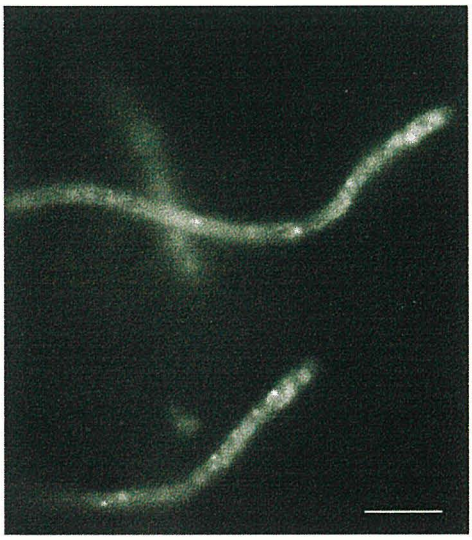

(B)

5.5 Construction of additional GFP-tagged Golgi proteins

Further studies need to be carried out in order to confirm the structure identified as the Golgi body within *A. nidulans*. Work on this was started in the form of the construction of two other GFP plasmids. The first plasmid (designated pErd2 Fig. 5.14(A)) was produced by amplification of the upstream portion of the mammalian *erd2p* gene, which encodes the Erd2 receptor found on Golgi membranes. This receptor is a cytosolically orientated membrane receptor which binds the KKXX motif on ER resident proteins targeting them for inclusion into COPI vesicles (92). This construct was a gift from P. Boevink (19) who showed that the upstream portion of the *erd2p* gene tagged with GFP localises to Golgi bodies in plants. During the amplification of the upstream portion of the gene an *Nhe*I site was introduced into the 3' end of the sequence. This *Nhe*I site was then used to attach the GFP2.5 sequence produced in the tagging of the $sod^{VI}C$ gene (Section 5.4.2). The whole construct was then ligated into the *alcA* expression vector pAL3X, transformed into *E. coli* and purified using standard techniques.

The second plasmid (designated pSat Fig. 5.14(B)) was produced in the same way as the first, the PCR template in this case was a rat sialyl transferase gene (Gift of P. Boevink (19)), which had been shown to localise to the Golgi body in plants as before. The sialyl transferase enzyme is located within Golgi cisternae and functions to add sialyl sugar units onto proteins prior to their secretion (135). Although sialyl transferases are not present in yeast and filamentous fungi, the upstream portion of the gene has been shown to be recognised as a Golgi marker and is localised to the Golgi equivalents in yeast (135).

Figure 5.14: Other GFP constructs produced to study Golgi equivalents in *A. nidulans*. (A) pSat7: Rat sialyl transferase::GFP. (B) pErd2: *erd2p*::GFP.

(A)

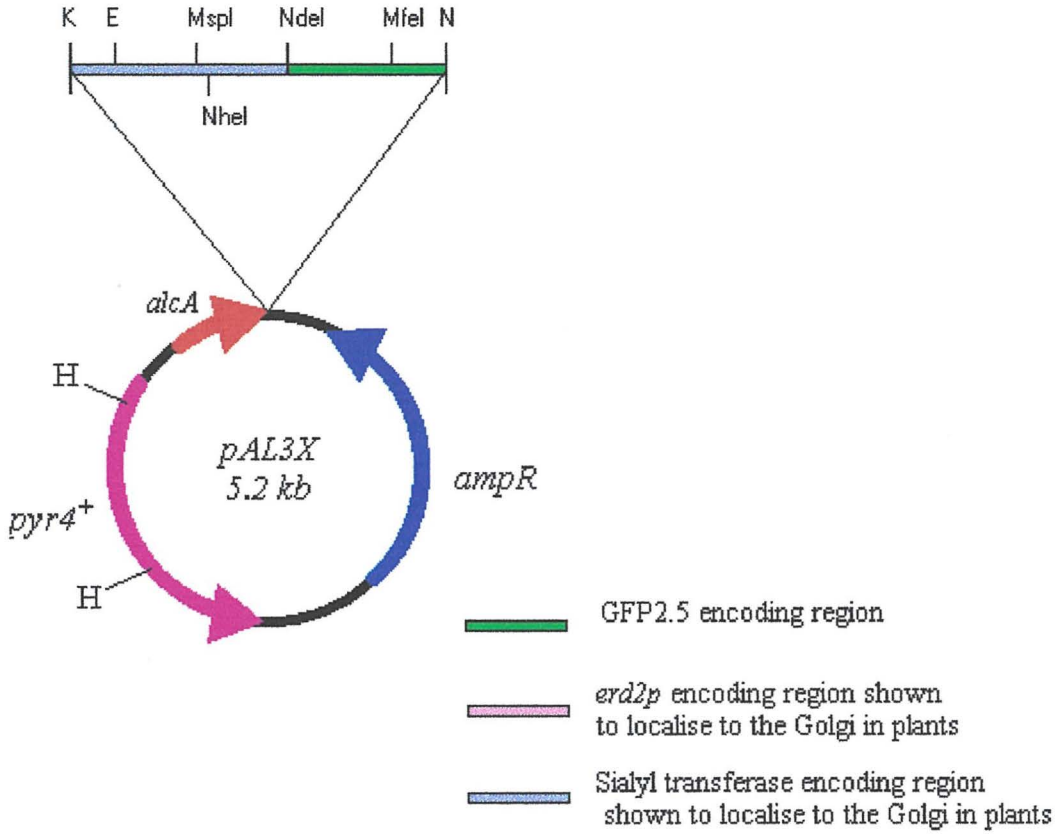

(B)

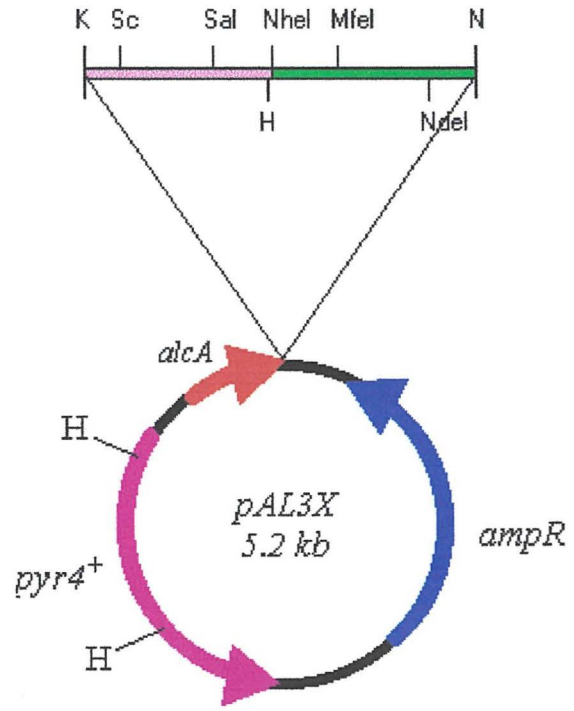

These constructs were transformed into the w.t *sod*^{VT}*C* strain GR5 and a number of transformants screened for fluorescence on glycerol inducing media, but no transformants were found to give expression of the GFP. This work was completed right at the end of this study and so additional attempts at gaining transformants were not attempted. Further optimisation of the production and screening of transformants in the future may prove more fruitful.

5.6 Discussion

5.6.1 Effects of the sod^{VI}C1 mutation on ER morphology

A *sod^{VI}C1* strain (B120) and a w.t *sod^{VI}C^{+}* strain (GR5) were transformed with the plasmid pMCB45, which contained an ER retrieval motif tagged to the *A. nidulans*-optimised GFP. The retrieval motif targets the GFP protein to the ER allowing visualisation of this organelle in living hyphae. Temperature-shift studies were carried out to look at the effects of the temperature-sensitive *sod^{VI}C1* mutation on ER morphology. The *sod^{VI}C* gene is homologous to the α-COP protein found in the protein coat complex coatomer. A mutation in this subunit may have an effect on the retrograde transport of resident ER proteins back to the ER.

If there were a decrease in the retrograde transport of ER resident proteins then we might expect to see a loss of fluorescence from the ER as ER proteins fail to be recycled from the Golgi. Labelling of the Golgi equivalents may also occur as the cisternae begin to accumulate GFP. During the up-shift experiments no distinct change in fluorescence of the ER was seen in the *sod^{VI}C1* transformant compared to the w.t *sod^{VI}C* strain. However, bright spots were seen within the cytoplasm of both the *sod^{VI}C1* and w.t strain. These spots did not look like any of the structures seen with the *sod^{VI}C::GFP* construct, which appears to localise to Golgi cisternae. The fact that the spots were observed within the control strain seems to indicate that prolonged incubation at 42°C is stressful for the fungus, resulting in intra-cellular breakdown within some hyphae.

We do not know how long the ER would remain intact with a loss, or decrease in retrograde transport. If the *sod^{VI}C1* mutation causes only a decrease in this transport then we may not expect to see an effect on this organelle within such a short time period. However, the fact that the *sod^{VI}C1* mutation causes death after 5 hours

incubation at 42°C (165) suggests something irreversible must have happened after the first few hours of up-shift. The loss of α-COP may have an effect on secretion that leads to a general mis-functioning of the secretory pathway rather than a direct effect on retrograde and anterograde transport.

A loss of recycling from the Golgi equivalents may also not be seen due to the type of protein that has been tagged. The 'artificial' ER-GFP construct may not behave in the same way as a 'normal' ER-resident protein. The ER retrieval motif allows the cell to identify proteins that are resident within the ER, aiding in retrieval when proteins are lost to the Golgi apparatus. ER resident proteins are transported from the ER when recruited incorrectly into anterograde vesicles. The main problem we have is we do not know how much of the ER-tagged GFP is lost from the ER at any time. In order to detect accumulation of the GFP within the Golgi it must be lost at a significant level from the ER.

5.6.2 Varying expression of the *sod^{VI}C* gene

The plasmid pMX4 was constructed which placed the whole of the *sod^{VI}C* coding region under the control of the inducible *alcA* promoter. This construct was used to produce transformants that were assumed to contain a w.t copy of the *sod^{VI}C* gene and at least one copy of the *sod^{VI}C* gene under the control of the *alcA* promoter. Attempts were made to quantify the number of copies of pMX4 in the transformants using Northern and Southern blotting, with little success. The assumption was made that the transformants must contain at least one extra copy of the *sod^{VI}C* gene being expressed from the alcA promoter based on transformants containing the *pyr4^{+}* marker on pMX4 plasmid.

The pMX4 transformants were grown on the two inducing alcohols glycerol (low level induction) and ethanol (high level induction). Although a slight decrease in

growth rates on both inducing media was noted, the fact that the difference was the same on both the low level (glycerol) and high level inducing (ethanol) suggests that over expression is not lethal to the hypha; a greater reduction of growth rate on ethanol would be expected if this were the case. These results can only be taken as a very preliminary look at over-expression of the *sod*^{VI}*C* gene. More work must be carried out to quantify the levels of expression within the transformants on the different inducing medias. The reason for looking at over-expression of the *sod*^{VI}*C* was because of the possibility that the *sod*^{VI}*C::GFP* construct would need to be expressed using the *alcA* promoter. The fact that the *sod*^{VI}*C::GFP* construct was successfully expressed at high enough levels from the native *sod*^{VI}*C* promoter led to more detailed studies on this work not being carried out due to time limitations.

5.6.3 GFP-Tagging of the *sod*^{VI}*C* gene

The w.t copy of the *sod*^{VI}*C* gene was C-terminally tagged with the *A. nidulans* optimised GFP (GFP2.5) (44) and cloned into the *alcA* expression vector pAL3X, giving the plasmid pSodGFP19. This plasmid was transformed into the w.t *sod*^{VI}*C* strain GR5 and a transformant containing a site-specific integration of pSodGFP19 was isolated (sodGFP-24). The site-specific integration of pSodGFP19 led to the GFP-tagged *sod*^{VI}*C* gene being expressed from the native *sod*^{VI}*C* promoter and the w.t *sod*^{VI}*C* gene being expressed from the *alcA* promoter. The site of integration of pSodGFP19 was confirmed using Southern blotting, but the Southern blot also showed a number of non-site specific integrations of pSodGFP19. All of these integrations place extra copies of the *sod*^{VI}*C* gene under the control of the *alcA* promoter; further work is underway to look at the exact number of these copies within sodGFP-24. The sodGFP-24 transformant expressed the Sod^{VI}C::GFP fusion protein

on 2% glucose medium. It was assumed that this was the result of expression of the GFP-tagged copy of the *sod*^{VI}*C* gene from the native *sod*^{VI}*C* promoter since the high concentration of glucose should repress expression from the *alcA* promoter (148), ensuring that the additional copies of the *sod*^{VI}*C* gene were not expressed. To confirm this, Northern blot analysis required comparing levels of expression of the *sod*^{VI}*C* gene in the sodGFP-24 transformant and the w.t strain GR5.

Confocal microscopy of the sodGFP-24 transformant showed that the Sod^{VI}C::GFP protein localises to distinct bodies within the cytoplasm, with the concentration of these bodies being higher at the growing hyphal tip. Higher magnification images revealed that the localised structures consisted of three distinct types. Of these structures two ('doughnut' shaped and solid ball structures Fig. 5.11(C)) are proposed to be the same structure imaged from different depths.

The structures localised by GFP-tagging of the *A. nidulans* α-COP protein are proposed to be putative Golgi equivalents from this fungus. The α-COP protein along with the 6 other COPI subunits forms the protein coat complex coatomer. Other subunits from the coatomer complex have been shown to localise to the Golgi body in yeast (98), mammalian (59) and plant cells (116). In these cells coatomer was found to be associated with Golgi membranes and to secretory vesicles directly next to the Golgi cisternae. As was stated earlier (Section 5.1) the Golgi bodies from filamentous fungi (Golgi equivalents) show marked morphological differences from those seen in mammalian and plant cells. Filamentous fungi do not contain the stacked Golgi cisternae seen in these higher eukaryotes, having instead a large number of individual cisternae within the cytoplasm (61) (75) (20) (134). These Golgi equivalents have been observed in a number of fungi as being of two types based on their cisternal diameter, these cisternae consisted of fenestrated sheets often

arranged into 3D hollow spheres or elongated cisternae (75) (20) (134) both types being found within a single hyphae. These structures were also seen within the sodGFP-24 transformant expressing the GFP-tagged *sod*^{VI}*C* gene (Fig. 5.11(C)).

In plant dyctosomes it was found that coatomer is predominantly associated with the *cis*-face and to a much lesser extent the *trans*-face of the Golgi apparatus (116). This is likely to reflect the main role of coatomer in retrograde transport and may shed some doubt as to its role in anterograde transport. Vesicles produced from the Golgi compartment by coatomer quickly lose their COPI coat upon release from the membrane (152). COPI subunits will only be associated with actively forming buds on the Golgi membranes and vesicles adjacent to the membranes which have just been released. This means that we would only expect to see localisation of the GFP-tagged Sod^{VI}C gene on and in the close vicinity of the Golgi cisternae.

As was shown in Fig. 5.11(B) many of the putative Golgi bodies from sodGFP-24 show much brighter fluorescence than others. This may represent a higher level of COPI vesicle production occurring within these cisternae, which may correspond to earlier (*cis*) Golgi compartments as seen in plants. It has been shown that individual cisternae from *S. cerevisiae* localised with different yeast Golgi markers, show distinct punctate distributions (127). This suggests that individual cisternae represent different stages along the secretory pathway of the Golgi apparatus, with secretory proteins being moved between sequential cisternae by long-range vesicle transport (127).

Growth of filamentous fungi occurs via the laying down of new cell wall materials at the hyphal tip. This represents a highly polarised secretory system; in the ascomycetes and basidomycetous fungi this polarised growth is associated with an apical body known as the Spitzenkörper (75), also known as the vesicle supply centre.

The Spitzenkörper relies on the continual delivery of newly synthesised cell wall precursors and enzymes in the form of vesicles derived from Golgi cisternae late within the secretory pathway. It is not surprising then that the localisation of the putative Golgi bodies in *A. nidulans* show such a high concentration in the hyphal tip region where they can continuously supply vesicles to the Spitzenkörper.

There are no publications to date on the visualisation of Golgi equivalents from *A. nidulans,* but unpublished electron micrographs taken by R. Roberson (124) of freeze-fractured *A. nidulans* hyphae are presented in this discussion, with thanks, for comparison (Fig. 5.15). These pictures clearly show the characteristic solid and hollow balls, and elongated cisternae (Fig. 5.15(A)) also seen in the localisation of the GFP-tagged *sod*^{VI}*C* gene, and reported for other filamentous fungi (61) (75) (20) (134). Interestingly the Golgi cisternae seem to be associated near the mitochondria in the cytoplasm (Fig. 5.15 (B)), Golgi bodies have also been seen in other filamentous fungi in association with or ensheathing whole mitochondria (20, 75) (134).

The data presented in this study strongly suggest localisation of the GFP-tagged *sod*^{VI}*C* gene is to the Golgi equivalents of *A. nidulans.* Work is currently being carried with R. Roberson (124) on localisation of the GFP in the sodGFP-24 strain using gold-labelled anti-GFP antibodies. This will allow EM comparison of the structures being localised by the GFP-tagged *sod*^{VI}*C* gene.

Figure 5.15: Electron micrographs of hyphae from *A. nidulans*
(A) Characteristic hollow ball, (i) solid ball, (ii) and elongated cisternae (iii) Bar = 30nm.
(B) The Golgi bodies (G) of *A. nidulans* are often seen in association with mitochondria (M) the association of the Golgi body with the ER can also be seen in this picture.

(A)

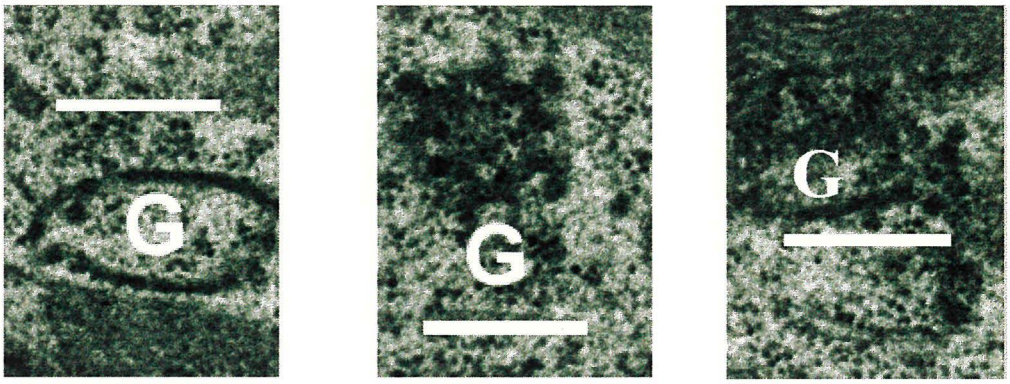

(i) (ii) (iii)

(B)

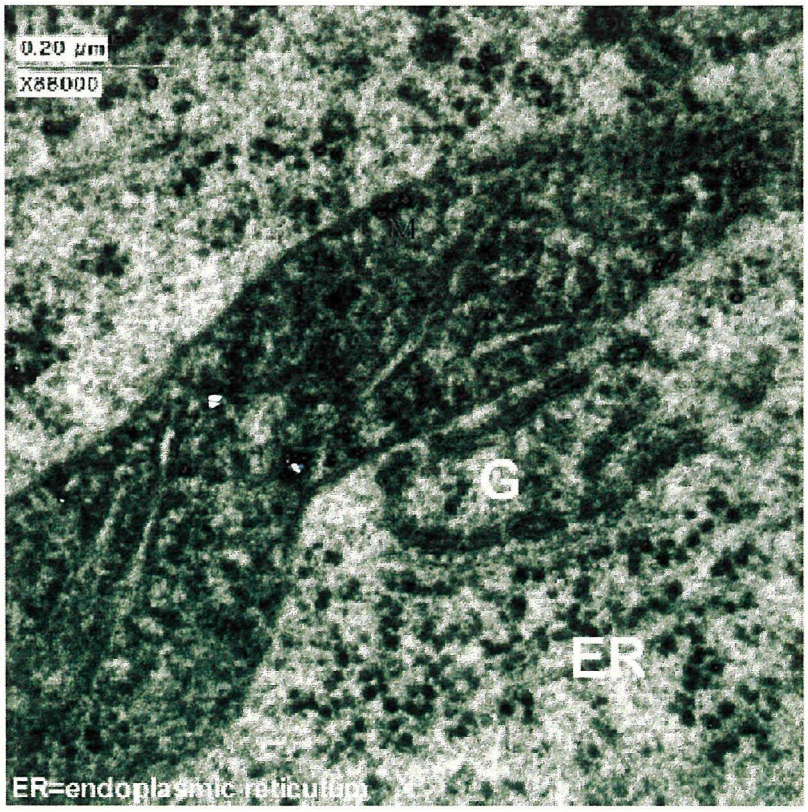

5.5.4 BFA treatment of the ER and putative Golgi bodies of *A.nidulans*

BFA studies have not been carried out on *A. nidulans* and so a sub-lethal concentration of BFA was quantified and a dosage of 150μg/ml used to carry out a preliminary study. The effect of BFA on the endomembrane system appears to vary between organisms and cell-types treated with the chemical (134). This seems to be reflected by the range of concentrations of BFA used in the literature where concentrations can range from 10-20μg/ml to 200μg/ml in some cell types (134).

The ER of *A. nidulans* when treated with BFA showed a distinct morphological change, the ER becoming swollen with the production of large fragmented portions of the ER. Treatment of the putative Golgi bodies within *A. nidulans* caused a significant loss of localisation of $Sod^{VI}C$::GFP to the Golgi cisternae. With only a few cisternae retaining fluorescence, some of these also appeared to be swollen. No hyphal tip localisation could be seen in these hyphae.

In the few fungi that have been studied using BFA very different effects have been seen. In the filamentous fungus *Magnaporthe grisea,* BFA was shown to stop apical elongation of the hyphae after 10 minutes of treatment (22) by reducing the number of apical vesicles and disrupting the organisation of the Spitzenkörper. Another group studying the filamentous fungi *Schizophyllum commune* showed again that BFA inhibits hyphal tip growth and they also reported that no re-absorption of the Golgi apparatus into the ER occurred (128) (134), although some swelling of Golgi structures within *M. grisea* was seen (22). In mammalian cells the Golgi apparatus is reabsorbed into the ER causing swelling of the ER and disappearance of the Golgi within the cytoplasm (87). It was proposed in mammalian cells that BFA causes a block in retrograde transport due to an inhibition of the ADP-ribosylation factor

(ARF1) (See Chapter 1), which prevents β-COP (and thus coatomer) being recruited to the Golgi membrane (67) (134). It has since been shown that various blocks are caused by BFA in mammalian cells (134).

In plant cells distortion of the ER occurs upon treatment with BFA, and this effect is reversible upon removal of BFA from the media (134) (18). Boevink *et al.* proposed that BFA blocks secretion from the ER causing a build up of a virally expressed GFP within the ER (18). However, a block in secretion from the Golgi apparatus could not be ruled out although a build up of fluorescence within this organelle was not observed (18), but the group reported that tobacco root Golgi bodies showed extreme sensitivity to BFA.

This paints a slightly confusing picture for what is occurring within *A. nidulans* treated with BFA. The loss of localisation of $Sod^{VI}C$::GFP from the Golgi apparatus may represent a loss of Golgi apparatus by re-absorption into the ER. However, results from other filamentous fungi do not show a loss of the Golgi equivalents upon treatment with BFA. The loss of localisation may therefore be due to a block in coatomer recruitment to the Golgi membrane as in mammalian cells, resulting in no localisation of the $Sod^{VI}C$::GFP protein. BFA may also act on a number of different sites within the secretory pathway e.g. blocking all vesicle transport. This would have the effect of blocking secretion from the ER leading to swelling of this organelle due to the build up of proteins normally secreted. Loss of vesicle transport from the Golgi apparatus would also lead to a decrease in secretory vesicles supplied to the growing hyphal tip resulting in a reduction in growth rate.

It is becoming increasingly clear that the action of BFA is far from simple. It has been proposed that the effect of BFA is dependent on concentration, with downstream events in the secretory pathway being more sensitive than upstream sites

to BFA inhibition (142). The use of different concentrations and incubation times results in different levels of effects being seen in the various organisms. Further studies need to be carried out on *A.nidulans* varying the concentrations of BFA, the time of incubation and the recovery of the cells after removal of the inhibition. It should be noted that the use of different constructs such as the Erd2 construct (Section 5.5.3) to study the Golgi apparatus when treated with BFA should be attempted as they provide different markers with which to visualise the Golgi apparatus.

Chapter Six

Discussion

The aims of this study were to:

(1) Further characterise the phenotype of the *sod*^{VI}*C1* mutation (Chapter 3).

(2) Further characterise the *sod*^{VI}*C* gene and the *sod*^{VI}*C1* mutation (Chapter 4).

(3) Study the endomembrane system of *A. nidulans* (Chapter 5).

Initial work carried out on the *sod*^{VI}*C1* mutation showed that at the sub-restrictive temperature of 37°C the *sod*^{VI}*C1* mutant formed a stable disomic. Genetic studies carried out on a constructed diploid strain showed that the chromosome VI does indeed undergo duplication at the restrictive temperature, with no segregation for other chromosome markers (e.g. spore colour). With more time, further work on this study using a multiply marked diploid strain would show decisively that no duplication of any other chromosomes occurs. Duplication events have been documented for single genes in *A. nidulans*. The *adE* gene from *A. nidulans* becomes duplicated in a gene dosage type response (100). It could therefore be proposed that the duplication of chromosome VI is a response to low levels of *sod*^{VI}*C* transcript within the cell. The fact that chromosome VI is duplicated at the semi-restrictive temperature appears to be an extreme response to the *sod*^{VI}*C1* mutation. The duplication of a whole chromosome in itself creates the additional problems with the duplication of all the genes contained on this chromosome, which may cause problems with transcript levels within the cell. If the duplication of chromosome VI is indeed a response to levels of *sod*^{VI}*C* transcript within the cell then the problems caused by duplication of a whole chromosome must be far outweighed by the benefits to growth of the *sod*^{VI}*C1* strain at the semi-restrictive temperature. It would therefore

be expected that an extra copy of chromosome VI should be able to support some growth at the restrictive temperature.

In order to look at this the cytological and morphological phenotypes of the *sod*^{VI}*C1* mutation was compared to stable disomic and trisomic strains, each possessing an extra copy of chromosome VI. If the duplication of chromosome VI does indeed have a 'gene dosage' effect, it would be expected that some sort of growth advantage be conferred at the restrictive temperature. Cytological results from this section showed that an extra copy of chromosome VI was able to partially overcome the *sod*^{VI}*C1* mutations effect at 42°C. However, this gene dosage effect was not reflected at the colony morphology level. Incubations at 42°C for 2-5 days still resulted in the characteristic lack of growth seen with the *sod*^{VI}*C1* haploid strain at this temperature, although the growth observed at 42°C with the stable disomic and trisomic strains was more leaky than with a haploid *sod*^{VI}*C1* strain. These results suggest that although an extra copy of the mutant gene is able to alleviate problems in early stages of germination and growth, the extra mutant copy is unable to sustain growth at the restrictive temperature. This may be due to the *sod*^{VI}*C1* mutation causing multiple problems in both early and late stages of the secretory pathway. This would be expected for the α-COP protein encoded by the *sod*^{VI}*C* gene, as COPI appears to have a number of diverse roles within the secretory pathway and a mis-functioning of such a key complex is reflected by the *sod*^{VI}*C1* mutants growth. Another possibility for the chromosome duplication event is if there are actually two mutations present within the *sod*^{VI}*C1* strain with the *sod*^{VI}*C1* mutation being a suppressor mutation.

The fact that the *sod*^{VI}*C1* mutation may be a suppressor mutation meant that it was important to verify that the cloned gene was indeed the *bona fide sod*^{VI}*C* gene.

The plasmid pSW2 was used to generate strains containing site-specific integrations of the plasmid. This produces two copies of the *sod*^{VI}*C* gene flanking the *pyr4*$^{+}$ sequence, one copy being from the mutant strain, and therefore containing the *sod*^{VI}*C1* mutation, and the second being from the w.t. *EcoR*I fragment. Curing of the pSW2 plasmid by growth on medium containing FOA results in the loss of the plasmid containing the *pyr4*$^{+}$ gene. This can occur by homologous recombination between either the mutant or w.t. sequence. If the cloned gene is indeed *sod*^{VI}*C* then curing of the plasmid will result in the production of ts^{+} and ts^{-} sectors. Two transformants were identified as being producing both ts^{+} and ts^{-} sectors, and the site of integration confirmed by Southern blotting. This work confirmed that the cloned gene was indeed *sod*^{VI}*C*, which means that the chromosome duplication event is caused by this mutation alone.

Work was carried out to address the nature of the *sod*^{VI}*C1* mutation. As well as identifying the site and type of the mutation it is also important to know what effects the mutation has on the protein product. A mutation in the *sod*^{VI}*C* gene could cause an effective null-phenotype; this would be the case if the *sod*^{VI}*C* gene were essential. The loss of growth seen with the *sod*^{VI}*C1* mutant would suggest that this is the case, but the same effect may be seen if the *sod*^{VI}*C1* mutation resulted in the production of a toxic protein. In order to distinguish between these possibilities a gene-knockout was carried out. In this strategy the *sod*^{VI}*C*$^{+}$ strain GR5, was transformed with the plasmid pSW4. This contained a small internal portion of the *sod*^{VI}*C* gene along with the *pyr4*$^{+}$ gene from *N. crassa*. A site-specific integration of this plasmid produced 3'- and 5'-truncated copies of the *sod*^{VI}*C* gene, flanking the *pyr4*$^{+}$ gene. Suspected site-specific transformants were confirmed with Southern blotting and PCR analysis. Growth tests on a site-specific pSW4 transformant resulted in the same null-phenotype seen with

the *sod*^{VI}*C1* mutant strain incubated at 42°C, confirming that the *sod*^{VI}*C* gene is indeed essential. The same has been shown for all of the COPI subunits with the exception of ε-COP (41). The fact that most of the subunits from COPI are essential reflects the key roles that this complex plays within the secretory pathway of eukaryotes. With increasing light being shed on the multiple roles of COPI within the cell, the loss of any of the key subunits is likely to greatly impair the ability of COPI to carry out such tasks. Interestingly results from this study suggest that the upstream and downstream portions of the Sod^{VI}C protein are partially functional, being able to sustain some growth at the permissive temperature of 30°C. Incubation at the higher temperature of 37°C (standard culture temperature for GR5) eliminated this leaky growth. Recent work published has also shown that the *S. cerevisiae* α-COP homologue contains partially functional N- and C-termini (41).

Now that we know the *sod*^{VI}*C* gene is essential and that the *sod*^{VI}*C1* mutation is not a multi-copy suppressor the question of the nature of the *sod*^{VI}*C1* mutation could be addressed. A number of sub-clones from the w.t. 9.1kb *Pst*I-*Hin*dIII fragment were generated by restriction digestion. These were then transformed as linear fragments into the *sod*^{VI}*C1* strain B120 along with the co-transforming vector pAB. Transformants were selected on MM lacking uridine and uracil and by incubating at the restrictive temperature of 42°C. Transformants that grew well at this temperature were then purified and retested at 42°C to check for complementation. A number of fragments were found to be capable of complementing the *sod*^{VI}*C1* mutation, when aligned a 1.2kb region of the *Pst*I-*Hin*dIII fragment was identified as being capable of complementing the *sod*^{VI}*C1* mutation. This region was then used to design primers to amplify fragments small enough to be sequenced easily.

The primers designed from the complementation study were used to amplify the selected regions from w.t. and mutant genomic DNA and then sequenced using the MWG-Biotech® sequencing service. A single insertion in the non-coding region of DNA just upstream from the ATG start codon was found to be present in the mutant DNA sequence and not in the GR5 genomic sequence, or in the *Pst*I-*Hin*dIII fragment sequenced previously by Whittaker *et al* (165). A single base change within the non-coding region of the *sod*^{VI}*C* gene seems an unlikely candidate for a temperature sensitive mutation. It is difficult to imagine how at the restrictive temperature a single point insertion could lead to the drastic change seen within the *sod*^{VI}*C1* strain. If the mutation was in a regulatory region the change may be sufficient for a regulatory protein to be able to bind, but a more significant change such as a short/long deletion or a short/long insertion would seem a more likely candidate for this. The insertion may cause a change in the structure of the DNA upon upshift to 42°C, which may interfere with nucleosome positioning. Some preliminary analysis into the content of the non-coding region was attempted by sequence comparison with other known *A. nidulans* regulated genes. This showed a number of possible CCAAT binding motifs, a 3'-polyadenlyation site and a number of putative transcription initiation sites. The start ATG codon for the *sod*^{VI}*C* gene was identified by computer analysis of reading frames, and by comparison with the *S. cerevisiae* α-COP homologue. The actual start of transcription has not been shown experimentally, this is a vital experiment to carry out in the future in order to rule out the possibility that the initial ATG codon is further upstream than proposed. If this were the case then it may put the *sod*^{VI}*C1* mutation within the coding region of the *sod*^{VI}*C* gene, making the temperature sensitive phenotype easier to explain. Having said this the gene dosage effect proposed for the *sod*^{VI}*C1* chromosome duplication would be more likely to be

supported by a mutation within a regulatory region causing the down regulation of the *sod*^{VI}*C* promoter. With more time Northern blot analysis of transcript levels would allow the quantification of mRNA at the different temperatures. Although some attempts were made to do this problems with isolation of good quality mRNA proved time consuming. Confirmation of the *sod*^{VI}*C* promoter region is also required, with more time studies to look at the transcription initiation site, DNA-binding assays carried out on putative CCAAT motifs, and truncations of the promoter region would be carried out. This would allow the proper identification of these upstream elements as well as giving some clues as to positions of upstream regulatory elements.

As well as trying to address the genetic and phenotypic characteristics of the *sod*^{VI}*C1* mutation work was also carried out to look at the wider effects this type of mutation may cause. The *sod*^{VI}*C* gene encodes the *A. nidulans* α-COP homologue, which functions in retrograde (and anterograde?) transport within the cell. A mutation affecting such a protein may be expected to have a secretory phenotype. Attempts were made to look at the effects of the *sod*^{VI}*C1* mutation on secretion of amylase and protease enzymes into the extracellular media. Colonies were grown on medium containing starch, skimmed milk or bovine serum albumin, and their growth rates at 37°C (semi-restrictive temperature) measured. No difference between the control strain and the *sod*^{VI}*C1* mutant was observed on starch or BSA medium. However, the *sod*^{VI}*C1* strain showed a significant decrease in growth rate on the skimmed milk media. With hindsight it is easy to see that the choice of skimmed milk as a growth medium was not very useful. Skimmed milk contains a number of nutrients besides casein, most importantly that of the milk sugar lactose. The difference between the various carbon sources used in this study may reflect a difference in the processing and/or transport of the proteins within the secretory

pathway. Or it may be a reflection of lactose intolerance in the B339 strain; although it is unlikely, this strain was generated by sexual crosses, this means that an untested mutation within the *lac* gene of *A. nidulans* could have been incorporated into this strain. The other possibility is that the decrease in growth on skimmed milk medium may be a result of effects on invertase secretion. Assays on lactose medium and re-genotyping of strains would need to be carried out to clarify this.

Other attempts to look at secretion in liquid culture and secretion of a plasmid-encoded protease were unsuccessful. This may be due in part to the low level of secretion seen with *A. nidulans*, even with native proteins, making it difficult to accurately detect small changes in secretion. Future work on this section would benefit in the use of a better range of secretory assays, looking at both intra- and extra-cellular levels of proteins. The use of GFP-tagged *A. nidulans* enzymes would make a study of this kind easier, enabling both the visualisation of protein amounts and the quantitative measuring of both internal and external levels. However, it should be noted that a number of different classes of enzymes should be studied to look at the differential processing of proteins indicated by this study.

The secretory pathway is extremely complex, comprising a number of distinct organelles and transport steps. Clearly, to improve the production of heterologous proteins more work needs to be carried out to understand at each level the key steps that regulate protein secretion. Protein folding in the ER is likely to be a rate-limiting factor in the secretory pathway. Recently the foldase enzyme protein disulphide isomerase A (PDIA) from *A. niger* has been characterised (101). As was discussed earlier this protein is a key enzyme in the ER with roles in correct folding of proteins and in the detection of mis-folded enzymes. Better understanding of key enzymes such as PDI from filamentous fungi will greatly aid the study of this pathway,

although in this case over-expression of the *pdiA* gene from *A. niger* did not increase yields of secreted HEWL (101). The advent of genome sequencing heralds a new era for work on filamentous fungi, with the *A. niger* and *A. nidulans* genomes both having been sequenced. The search for yeast homologues within these databases will allow the direct comparison of the pathways between these closely related species.

As well as looking at the secretory phenotype of the *sod*^{VI}*C1* mutation attempts were made to look its cytological effect. It was proposed that a defect within the COPI complex caused by the *sod*^{VI}*C1* mutation may have a visible effect on the morphology of the ER. *sod*^{VI}*C*$^{+}$ and *sod*^{VI}*C1* strains were transformed with the plasmid pMCB45 (44) containing the *A. nidulans* optimised GFP attached to an ER retention signal. Expression of this construct in *A. nidulans* allowed the visualisation of a large filamentous network running throughout the hyphae, which comprises the ER. Control and mutant transformant strains were incubated at permissive temperature and then up-shifted to 42°C for 1 to 5 hours. The colonies were then visualised using standard UV and confocal microscope techniques. With prolonged incubations of the *sod*^{VI}*C1* strain at 42°C punctate fluorescence was visualised within the ER network, with these structures not being seen in equivalent incubations at 30°C. However, these structures were also observed within the control strain, although they appeared to be more prevalent in the *sod*^{VI}*C1* strain.

Previous work on the *sod*^{VI}*C1* mutation showed that germlings incubated at 42°C for longer than four hours were unable to recover growth when down-shifted to permissive temperatures (165). This makes it very difficult to separate real effects from those generated by death of the strain. The fact that the punctate structures were observed in the *sod*^{VI}*C*$^{+}$ strain suggests that these structures are result of stress caused

by incubation at high temperatures. The *sod*^{VI}*C1* strain may contain more of these structures due to a combination of the stress of growth at 42°C and the *sod*^{VI}*C1* mutation causing death of the strain. It is more likely that the *sod*^{VI}*C1* mutation causes problems within the secretory pathway before any large scale morphological change can be visualised. It may be more productive to look at recycling defects on a smaller scale by studying the localisation and concentration of specific ER resident proteins (e.g. foldases such as PDI homologues) and molecular chaperones (such as BiP homologues) within the ER and Golgi apparatus. An accumulation of these proteins within the Golgi apparatus may occur far earlier than large-scale changes to ER membranes.

The α-COP protein of *A. nidulans* forms part of the multi-subunit coat complex coatomer. As was discussed in the literature review (Chapter 1), this complex is involved in transport within the Golgi complex. Previous studies using antibodies raised against COPI subunits have shown that coatomer is closely associated with Golgi membranes. No work on the structure of the Golgi equivalents in *A. nidulans* have yet been published, the GFP-tagging of the *sodVIC* gene gives us a unique opportunity to study its localisation and possibly allow the visualisation of the *A. nidulans* Golgi apparatus. The *A. nidulans* modified GFP (GFP 2.5) was attached to the 3' end of the *sod*^{VI}*C* gene by the introduction of a novel restriction enzyme site to both the *sod*^{VI}*C* sequence and GFP2.5 sequence. The GFP-tagged *sod*^{VI}*C* gene was then cloned into a vector containing the *alcA* promoter and the selectable marker *pyr4*$^{+}$, this was then transformed into a *sod*^{VI}*C*$^{+}$ strain. Integration at the *sod*^{VI}*C* locus allows the expression of the *sod*^{VI}*C::GFP* construct from the native *sod*^{VI}*C* promoter. This occurs due to crossover between the genomic *sod*^{VI}*C* gene and the plasmid encoded *sod*^{VI}*C* gene. Transformants were screened for expression of the

sod^{N71}*C::GFP* construct on 2% glucose media, which represses expression from the *alcA* promoter. The transformant psodGFP-24 was chosen as being a site-specific integrant and Southern blot analysis to confirm the site of integration was carried out. The results from the Southern blot showed that in fact a number of plasmids had been integrated into the genome. However, the appearance of a 6kb hybridising band predicted that a site-specific integration of the *sod*^{N71}*C::GFP* had also occurred alongside a number of non-site specific transformants. This is confirmed by the high level of GFP expression seen with psodGFP-24 grown on 2% glucose. With more time further analysis of the number of plasmid integrations into psodGFP-24 would be carried out, along with the generation of single copy site- and non-site specific transformants.

The *sod*^{N71}*C::GFP* construct was seen to localise to distinct 'doughnut' and spherical structures within the cytoplasm. These structures were seen to move backwards and forwards within the cytoplasm and were found at much higher concentrations towards the growing hyphal tip. Some of the structures within the cytoplasm showed much brighter fluorescence than others. These observations led to the proposal that the structures within the cytoplasm are in fact the putative Golgi equivalents from *A. nidulans*. Comparisons between the structures localised by the *sod*^{N71}*C::GFP* construct and unpublished electron microscope images of *A. nidulans* Golgi apparatus hyphae support these findings. Collaboration with a group in Arizona University is currently underway to look at the immunolocalisation and electron microscopy of the *sod*^{N71}*C::GFP* using gold-labelled anti-GFP antibodies. Future work looking at the localisation of other GFP-tagged Golgi proteins would help to confirm that what is being seen is indeed the Golgi bodies of *A. nidulans*. Some work was carried out to look at this using the Golgi resident enzyme sialyl transferase and the

Golgi receptor protein erd2p, tagged with the *A. nidulans* modified GFP. These were constructed towards the end of this study so optimisation of the transformation and selection of transformants was not completed within the time scale of this study.

The use of constructs such as these and the advent of a number of modified GFPs with different excitation and emission spectrums allowing co-localisation of different proteins will aid in the study of this organelle. Studies using chemicals such as nocodazole (actin inhibitor) and cytochalasin A (microtubules inhibitor) would allow the identification of the motor proteins responsible for the movement of the Golgi equivalents within *A. nidulans*. Further investigations using BFA at different concentrations and incubation times may help in the dissection of the secretory pathway within filamentous fungi.

Alongside the work on the GFP-tagging of the *sod*^{VI}*C* gene over-expression studies were carried out. Many of the plasmids used in GFP constructs require expression of the GFP-tagged gene from the *A. nidulans alcA* promoter. Although we hoped to generate a site-specific integration of the *sod*^{VI}*C::GFP* construct, the native *sod*^{VI}*C* promoter may not have provided sufficient expression to allow proper visualisation of the GFP localisation. With this in mind the plasmid pMX4 was constructed containing the full *sod*^{VI}*C*-coding region being expressed from the *alcA* promoter. Transformants of a *sod*^{VI}*C*$^{+}$ strain were obtained containing integrations of pMX4 and Northern and Southern blots of these transformants were attempted to look at transcript levels and plasmid copy numbers, with little success. Work proceeded on the over-expression studies on the assumption that at least one copy of the plasmid had been integrated. This was assumed due to the complementation of the *pyrG89* mutation by the *pyr4*$^{+}$ gene carried on the plasmid in the transformants. No significant differences in growth rates between the transformants and an untransformed control

strain were observed. This suggested over-expression on these types of media was unlikely to affect the results obtained with the GFP-tagged *sod*^{VI}*C* gene. Time constraints and the fact that the *sod*^{VI}*C::GFP* construct had been successfully expressed from its native promoter led to more work on this being left. With more time more attempts at the Northern and Southern blots would be attempted in order to verify copy number and transcript levels within the transformants.

The work presented in this thesis has shown that the studying such a complex system as the secretory pathway is not easy. This work has made some headway into understanding more about the *sod*^{VI}*C* gene and how it may function within the cell, but it has also raised a number of questions, which require further work to verify. It is difficult to understand how a simple base insertion in the supposed non-coding region of DNA is able to exert its affect as a temperature sensitive mutation. Also the complexity of COPI within the cell makes understanding and events on the cytological level more difficult, with more and more functions for COPI being proposed it may in time become easier to explain the chromosome duplication event as something other than a gene dosage effect. The work in this thesis does not make huge in roads into our understanding of the secretory system in *A. nidulans,* but it does serve to highlight how much more there is to learn.

1. **Aleksenko, A., and A. J. Clutterbuck** 1997. Autonomous plasmid and replication in *Aspergillus nidulans* : AMA1 and MATE elements. Fungal Genetics and Biology. **21:**373-387.

2. **Altschul, S. F., W. Gish, E. W. Myers, and D. J. Lipman** 1990. Basic local alignment search tool. Journal of Molecular Biology. **215:**403-410.

3. **Andreeva, A. V., M. A. Kutuzov, D. E. Evans, and C. R. Hawes** 1998. Proteins involved in membrane transport between the ER and Golgi apparatus: 21 putative plant homologues revealed by dBEST searching. Cell Biology International. **22:**145-160.

4. **Aoe, T., E. Cukierman, A. Lee, D. Cassel, P. J. Peters, and V. W. Hsu** 1997. The KDEL receptor, ERD2, regulates intracellular traffic by recruiting a GTPase-activating protein for ARF1. EMBO Journal. **16:**7305-7316.

5. **Archer, D. B.** 2000. Filamentous fungi as microbial cell factories for food use. Current Opinion in Biotechnology. **11:**478-483.

6. **Archer, D. B., D. D. Jeenes, and D. A. MacKenzie** 1994. Strategies for improving heterologous protein production from filamentous fungi. Antonie van Leeuwenhoek. **63:**245-250.

7. **Aridor, M., and W. E. Balch** 1996. Principles of selective transport: coat complexes hold the key. trends in CELL BIOLOGY. **6:**315-320.

8. **Assinder, S. J., and A. Upshall** 1982. Mitotic aneuploidy induced by deoxycholate in Aspergillus-Nidulans. Mutation Research. **93:**101-108.

9. **Balch, W. E., W. G. Dunphy, W. A. Braell, and J. E. Rothman** 1984. Reconstitution of the Transport of Protein between Successive Compartments of the Golgi Measured by the Coupled Incorporation of N-Acetylglucosamine. Cell. **39:**405-416.

10. **Ballance, D. J., F. P. Buxton, and G. Turner** 1983. Transformation of *Aspergillus nidulans* by the orotidine-5'-phosphate decarboxylase gene of *Neurospora crassa*. Biochemical and Biophysical Research Communications. **112:**284-289.

11. **Ballance, D. J., and G. Turner** 1985. Development of a high-frequency transforming vector for *Aspergillus nidulans.* Gene. **36:**321-331.

12. **Bannykh, S., I., and W. E. Balch** 1997. Membrane Dynamics at the Endoplasmic Reticulum-Golgi Interface. Journal of Cell Biology. **138:**1-4.

13. **Barlowe, C., L. Orci, T. Yeung, M. Hosobuchi, S. Hamamoto, N. Salama, M. F. Rexach, M. Ravazzola, M. Amherdt, and R. Schekman** 1994. COPII: a membrane coat formed by Sec proteins that drive vesicle budding from the endoplasmic reticulum. Cell. **77:**895-908.

14. **Barlowe, C., and R. Schekman** 1993. Purification and characterisation of Sar1p, a small GTP-binding protein required for transport vesicle formation from the Endoplasmic reticulum. Cell. **77:**895-907.

15. **Bar-Peled, M., D. C. Bassham, and N. V. Raikhel** 1996. Transport of proteins in eukaryotic cells: more questions ahead. Plant Molecular Biology. **32:**223-249.

16. **Birnboim, H. C., and J. Doly** 1979. A rapid alkaline extraction procedure for screening recombinant plasmid DNA. Nucleic Acids Research. **7:**1513-1523.

17. **Boeke, J. D., F. Lacroute, and G. R. Fink** 1984. A positive selection for mutants lacking orotidine 5'-phosphate decarboxylase activity in yeast -5-fluoro-orotic acid resistance. Molecular and General Genetics. **197:**345-346.

18. **Boevink, P., B. Martin, K. Oparka, S. S. Cruz, and C. Hawes** 1999. Transport of virally expressed green fluorescent protein through the secretory pathway in tobacco leaves is inhibited by cold shock and brefeldin A. Planta. **208:**392-400.

19. **Boevink, P., K. Oparka, S. S. Cruz, B. Martin, A. Betterridge, and C. Hawes** 1998. Stacks on tracks: the plant Golgi apparatus traffics on an actin/ER network. The Plant Journal. **15:**441-447.

20. **Bourett, T., and R. J. Howard** 1994. Enhanced labelling of concanavalin A binding sites in fungal endomembrane using a double sided, indirect method. Mycological Research. **98:**769-775.

21. **Bourett, T. M., and R. J. Howard** 1995. Brefeldin A-induced structural changes in the endomembrane system of a filamentous fungi, *Magnaporthe grisea*. Protoplasma. **190:**151-163.

22. **Bourett, T. M., and R. J. Howard** 1996. Brefeldin A-induced structural changes in the endomembrane system of a filamentous fungus, *Magnaporthe grisea*. Protoplasma. **190:**151-163.

23. **Brody, H., J. Griffith, A. J. Cuticchia, J. Arnold, and W. E. Timberlake** 1991. Chromosome-specific recombinant DNA libraries from the fungus *Aspergillus nidulans.* Nucleic Acids Research. **19:**3105-3109.

24. **Bullock, W. D., J. M. Fernandez, and J. M. Short** 1987. XL1-Blue - A high frequency plasmid transforming *reca Escherichia coli* strain with beta-galactosidase selection. Biotechniques. **5:**376.

25. **Carr, C. M., E. Grote, M. Munson, F. M. Hughson, and P. J. Novick** 1999. Sec1p Binds to SNARE Complexes and Concentrates at Sites of Secretion Journal of Cell Biology. **146:**333-344.

26. **Chalfie, M., Y. Tu, W. W. Ward, and D. C. Prasher** 1994. Green fluorescent protein a a marker for gene expression. Science. **263:**802-805.

27. **Chow, V. T. K., and H. H. Quek** 1996. *HEP-COP*, a novel human gene whose product is highly homologous to the α-subunit of the yeast coatomer protein complex. Gene. **169:**223-227.

28. **Christensen, T., H. Woeldike, E. Boel, S. B. Mortensen, K. Hjortshoej, L. Thim, and M. T. Hansen** 1988. High level expression of recombinant genes in *A. oryzae*. Biotechnology. **6:**1419-1422.

29. **Clutterbuck, A. J.** 1996. Parasexual recombination in fungi. Journal of Genetics. **75:**281-286.

30. **Clutterbuck, A. J.** 1997. The validity of the *Aspergillus nidulans* linkage map. Fungal Genetics and Biology. **21:**267-277.

31. **Cosson, P., C. Demolliere, S. Hennecke, R. Duden, and F. Letourneur** 1996. δ– and ζ-COP, two coatomer subunits homologous to clathrin-associated proteins, are involved in ER retrieval. EMBO Journal. **15:**1792-1798.

32. **d'Enfert, C., Wuestehube, L.J., Lila, T., Schekman, R.** 1991. Sec12p-Dependent Membrane-Binding of the Small GTP-binding protein Sar1p promotes formation of transport vesicles from the ER. Journal of Cell Biology. **144:**663-670.

33. **Donaldson, J. G., and J. Lippincott-Schwartz** 2000. Sorting and Signaling at the Golgi Complex. Cell. **101:**693-696.

34. **Doonan, J. H.** 1994. Control of Cell Growth, p. 455-478, 50 years of *Aspergillus.*, vol. 29. Elsevier Science.

35. **Doonan, J. H., and N. R. Morris** 1989. The bimG gene of Aspergillus nidulans, required for completion of anaphase, encodes a homolog of mammalian phosphoprotein phosphatase I. Cell. **57:**987-996.

36. **Duden, R., L. Kajikawa, L. Wuestehube, and R. Schekman** 1998. epsilon-COP is a structural component of coatomer that functions to stabilize alpha-COP. EMBO Journal. **17:**11.

37. **Eckardt, N. A.** 2000. Green Light for Traffic in the Early Secretory Pathway. The Plant Cell. **12:**2009-2011.

38. **Efimov, V. P., and N. R. Morris** 2000. The LIS1-related NUDF protein in *Asgergillus nidulans* interacts with the coiled-coil domain of the NUDE/RO11 protein. Journal of Cell Biology. **150:**681-688.

39. **Elazar, Z., L. Orci, J. Ostermann, M. Amherdt, G. Tanigawa, and J. E. Rothman** 1994. ADP-Ribosylation Factor and Coatomer Couple Fusion to Vesicle Budding. Journal of Cell Biology. **124:**415-424.

40. **Emr, S. D., and V. Malhotra** 1997. Membranes and sorting Current Opinion in Cell Biology. **9:**475-476.

41. **Eugester, A., G. Frigerio, M. Dale, and R. Duden** 2000. COPI domains required for coatomer integrity, and novel interactions with ARF and ARF-Gap. EMBO Journal. **19:**3905-3917.

42. **Faulstich, D., S. Auerbach, L. Orci, M. Ravazzola, S. Wegehingel, F. Lottspeich, G. Stenbeck, C. Harter, F. T. Wieland, and H. Tschochnoer** 1996. Architecture of coatomer: molecular characterisation of δ-COP and protein interactions within the complex. Journal of Cell Biology. **135:**53-61.

43. **Featherstone, C.** 1998. Coming to Grips With the Golgi. Science. **282:**2172-2174.

44. **Fernandez-Abalos, J. M., H. Fox, C. Pitt, B. Wells, and J. H. Doonan** 1998. Plant-adapted green fluorescent protein is a versatile vital reporter for gene expression, protein localization and mitosis in the filamentous fungus, Aspergillus nidulans. Molecular Microbiology. **27:**121-130.

45. **Fiedler, K., M. Veit, M. A. Stamnes, and J. E. Rothman** 1996. Bimodal Interaction of Coatomer with the p24 family of Putative Cargo Receptors. Science. **273:**1396-1399.

46. **Fincham, J. R. S.** 1989. Transformation in fungi. Microbiological Reviews. **7:**148-170.

47. **Franco, M. e. a.** 1998. Arno3, a Sec7-domain guanine nucleotide exchange factor for ADP ribosylation factor 1, is involved in the control of Golgi structure and function. Proceedings of the National Academy of Science. USA. **95:**9926-9931.

48. **Freedman, R. B.** 1989. Protein disulfide Isomerase: Multiple Roles in the Modification of Nascent Secretory Proteins. Cell. **57:**1069-1072.

49. **Gaynor, E. C., and S. C. Emr** 1997. COPI-independent Anterograde Transport: Cargo-selective ER to Golgi Protein Transport in Yeast COPI Mutants Journal of Cell Biology. **136:**789-802.

50. **Gems, D., I. L. Johnstone, and A. J. Clutterbuck** 1991. An autonomously replicating plasmid transforms *Aspergillus nidulans* at high frequency. Gene. **98:**61-67.

51. **Gerich, B., L. Orci, H. Tschochnoer, F. Lottspeich, M. Ravazzola, M. Amherdt, F. T. Wieland, and C. Harter** 1995. Non-clathrin-coat protein α is a conserved subunit of coatomer and in *Saccharomyces cerevisiae* is essential for growth. Proceedings of the National Academy of Science. USA. **92:**3229-3233.

52. **Goldberg, J.** 2000. Decoding of sorting signals by coatomer through a GTPase switch in the COPI coat complex. Cell. **100:**671-679.

53. **Gordon, C. L., D. B. Archer, D. J. Jeenes, J. H. Doonan, B. Wells, A. P. J. Trinci, and G. D. Robson** 2000. A glucoamylase :: GFP gene fusion to study protein secretion by individual hyphae of Aspergillus niger. Journal of Microbiological Methods. **42:**39-48.

54. **Gordon, C. L., V. Khalaj, A. F. J. Ram, D. B. Archer, J. L. Brookman, A. P. J. Trinci, D. D. Jeenes, J. H. Doonan, B. Wells, P. J. Punt, C. A. M. J. J. van den Hondel, and G. D. Robson** 2000. Glucoamylase::green fluorescent protein fusions to monitor protein secretion in *Aspergillus niger*. Microbiology-UK. **146:**415-426.

55. **Gotte, M., and G. Fischer von Mollard** 1998. A new beat for the SNARE drum. trends in CELL BIOLOGY. **8:**215-218.

56. **Gouka, R. J., P. J. Punt, J. G. M. Hessing, and C. A. M. J. J. van den Hondel** 1996. Analysis of Heterologous Protein Production in Defined Recombinant *Aspergillus awamori* Strains. Applied and Environmental Microbiology. **62:**1951-1957.

57. **Gouka, R. J., P. J. Punt, and C. A. M. J. J. van den Hondel** 1997. Efficient production of secreted proteins by *Aspergillus:* progress, limitations and prospects. Applied Microbiological Biotechnology. **47:**1-11.

58. **Gouka, R. J., P. J. Punt, and C. A. M. J. J. van den Hondel** 1997. Glucoamylase Gene Fusions Alleviate Limitations for Protein Production in *Aspergillus awamori* at the Transcritptional and (Post) Translational Levels. Applied and Environmental Microbiology. **63:**488-497.

59. **Griffiths, G., R. Pepperkok, J. K. Locker, and T. E. Kreis** 1995. Immunocytochemical localization of β-COP to the ER-Golgi boundary and the TGN. Journal of Cell Science. **108:**2839-2858.

60. **Griffiths, G., P. Quinn, and G. Warren** 1983. Dissection of the Golgi complex: nonensin inhibits the transport of viral membrane proteins from *medial* to *trans* Golgi cisternae in baby hamster kidney cells infected with Semliki Forest virus. Journal of Cell Biology. **96:**835-850.

61. **Grove, S. N., and C. E. Bracker** 1970. Protoplasmic organization of hyphal tips among fungi: vesicles and Spitzenkörper. Journal of Bacteriology. **104:**989-1009.

62. **Gurr, S. J., S. E. Unkles, and J. R. Kinghorn** 1987. The Structure and organisation of nuclear genes of filamentous fungi., p. 99-139. *In* J. R. Kinghorn (ed.), Gene Structure in Eukaryotic Microbes. IRL Press.

63. **Harter, C., and F. T. Wieland** 1996. The secretory pathway: mechanisms of protein sorting and transport. Biochimica et Biophysica Acta. **1286:**75-93.

64. **Hastie, A. C.** 1970. Benlate-inducing instability of Aspergillus diploids. Nature. **226:**771.

65. **Hauri, H.-P., and A. Schweizer** 1992. The endoplasmic reticulum-Golgi-intermediate compartment. Current Opinion in Cell Biology. **4:**600-608.

66. **Hegde, R. S., and V. R. Lingappa** 1999. Regulation of protein biogenesis at the endoplasmic reticulum membrane. trends in CELL BIOLOGY. **9:**132-137.

67. **Helms, J. B., and J. E. Rothman** 1992. Inhibition by Brefeldin A of the Golgi membrane enzyme that catalyses exchange of guanine nucleotide bound to ARF. Nature. **360:**352-354.

68. **Hemming, F. W.** 1995. Expression and secretion of glycoproteins by hyphal fungi. Biochemical Society Transactions. **23:**180-185.

69. **Herrmann, J. M., P. Malkus, and R. Schekman** 1999. Out of the ER-outfitters, escorts and guides. trends in CELL BIOLOGY. **9:**5-7.

70. **Hicke, L., and R. Schekman** 1989. Yeast Sec23p acts in the cytoplasm to promote protein transport from the endoplasmic reticulum to the Golgi complex *in vivo* and *in vitro*. EMBO Journal. **8:**1677-1684.

71. **Hicke, L., T. Yoshihisa, and R. Schekman** 1992. Sec23p and a novel 105kDa protein function as a multimeric complex to promote vesicle budding and protein transport from the ER. Molecular Biology of the Cell. **3:**667-676.

72. **High, S., and B. Dobberstein** 1997. Mechanisms that determine the transmembrane disposition of proteins Current Opinion in Cell Biology. **4:**581-586.

73. **Holmes, D. S., and H. Quigley** 1981. A rapid boiling method for the preparation of bacterial plasmids. Analytical Biochemistry. **114:**193-197.

74. **Hong, E., A. R. Davidson, and C. A. Kaiser** 1996. A Pathway for Targeting Soluble Misfolded Proteins to the Yeast Vacuole. Journal of Cell Biology. **135:**623-633.

75. **Howard, R. J.** 1981. Ultrastructural analysis of hyphal tip cell growth in fungi: Spitzenkörper, cytoskeleton and endomembranes after freeze-substitution. Journal of Cell Science. **48:**89-103.

76. **Hsu, S., C. D. Hazuka, D. L. Foletti, and R. H. Scheller** 1999. Targeting vesicles to specific sites on the plasma membrane: the role of the sec6/8 complex. trends in CELL BIOLOGY. **9:**150-153.

77. **Hughes, M., A. Arundhati, P. Lunness, P. J. Shaw, and J. H. Doonan** 1996. A temperature-sensitive splicing mutation in the *bimG* gene of *Aspergillus* produces an N-terminal fragment which interferes with type 1 protein phosphatase function. EMBO Journal. **15:**4574-4583.

78. **Hughes, M. A., D. A. Barnett, Z. Mohd-Noor, S. L. Whittaker, J. H. Doonan, and S. J. Assinder** 2000. The *Aspergillus nidulans hfa* mutations affect genomic stability and cause diverse defects in cell cycle progression and cellular morphogenesis. Mycological Research. **104:**1439-1448.

79. **Käfer, E., and A. Upshall** 1973. The phenotypes of the eight disomics and trisomics of *Aspergillus nidulans*. Journal of Heredity. **64:**35-38.

80. **Kimata, Y., H. Higashio, and K. Kohno** 2000. Impaired Proteasome Function Rescues Thermosensitivity of Yeast Cells Lacking the Coatomer Subunit ε-COP. Journal of Biological Chemistry. **275:**10655-10660.

81. **Kirchhausen, T.** 2000. Three ways to make a vesicle. Nature reviews: molecular cell biology. **1:**187-197.

82. **Klausner, R. D., J. G. Donaldson, and J. Lippincott-Schwartz** 1992. Brefeldin A: insights into the control of membrane traffic and organelle structure. Journal of Cell Biology. **116:**1071-1080.

83. **Lavoie, C., J. Paiement, M. Dominguez, L. Roy, S. Dahan, J. N. Gushue, and J. J. M. Bergeron** 1999. Roles for α_2p24 and COPI in Endoplamic Reticulum Cargo Exit Site Formation. Journal of Cell Biology. **146:**285-299.

84. **Letourneur, F., E. C. Gaynor, S. Hennecke, C. Demolliere, R. Duden, S. C. Emr, H. Riezman, and P. Cosson** 1994. Coatomer is essential for retrieval of dilysine-tagged proteins to the endoplasmic reticulum. Cell. **79:**119-1207.

85. **Lewis, M. J., and H. R. B. Pelham** 1996. SNARE-Mediated Retrograde Traffic from the Golgi Complex to the Endoplasmic Reticulum. Cell. **85:**205-215.

86. **Lippincott-Schwartz, J., T. H. Roberts, and K. Hirschberg** 2000. Secretory Protein Trafficking And Organelle Dynamics In Living Cells. Annual Reviews.

87. **Lippincott-Schwartz, J., L. Yuan, J. Bonifacino, and R. D. Klausner** 1989. Rapid redistribution of Golgi proteins into the ER in cells treated with brefeldin A: evidence for membrane cycling from Golgi to ER. Cell. **56:**801-813.

88. **Lopez-Franco, R., and C. E. Bracker** 1996. Diversity and dynamics of the Spitzenkorper in growing hyphal tips of higher fungi. Protoplasma. **195:**90-111.

89. **Lopez-Franco, R., R. J. Howard, and C. E. Bracker** 1995. Satellite Spitzenkorper in growing hyphal tips. Protoplasma. **188:**85-103.

90. **Lotti, L. V., M. Giovanna, M. R. Torris, and S. Bonatti** 1999. A Different Intracellular Distribution of a Single Reporter Protein Is Determined at Steady State by KK*XX* or KDEL Retrieval Signals. Journal of Biological Chemistry. **274:**10413-10420.

91. **Love, H. D., C. C. Lin, C. S. Short, and J. Ostermann** 1998. Isolation of functional Golgi-derived vesicles with a possible role in retrograde transport. Journal of Cell Biology. **140:**541-551.

92. **Majoul, I., K. Sohn, F. T. Wieland, R. Pepperkok, M. Pizza, J. Hilleman, and H. Soling** 1998. KDEL Receptor (Erd2p)-mediated Retrograde Transport of the Cholera Toxin A Subunit from the Golgi involves COPI, p23, and the COOH Terminus of Erd2p. Journal of Cell Biology. **143:**601-612.

93. **Martinelli.S.D.** 1994. *Aspergillus nidulans* as an Experimental Organism, p. 33-57. *In* Martinelli.S.D., and J. R. Kinghorn (eds), 50 years of *Aspergillus*, vol. 29. Elsevier Science.

94. **Martinez-Menarguez, J. A., H. J. Geuze, J. W. Slot, and J. Klumperman** 1999. Vesicular Tubular Clusters between the ER and Golgi Mediate Concentration of Soluble Secretory Proteins by Exclusion from COPI-Coated Vesicles. Cell. **98:**81-90.

95. **McNew, J. A., M. Sogaard, N. M. Lampen, S. Machida, Y. Ruby, L. Lacomis, P. Tempst, J. E. Rothman, and T. H. Sollner** 1997. Ykt6p, a Prenylated SNARE Essential for Endoplasmic Reticulum-Golgi Transport. Journal of Biological Chemistry. **272:**17776-17783.

96. **Meldolesi, J., and T. Pozzan** 1998. The endoplasmic reticulum Ca^{2+} store: a view from the lumen. trends in Biological Sciences. **23:**10-14.

97. **Mirabito, P. M., T. H. Adams, and W. E. Timberlake** 1989. Interactions of three sequentially expressed genes control temporal and spatial specificity in *Aspergillus* development. Cell. **57:**859-868.

98. **Morin-Ganet, M. N., A. Rambourg, S. B. Deitz, A. Franzusoff, and F. Képès** 2000. Morphogenesis and Dynamics of the Yeast Golgi Apparatus. Traffic. **1:**56-68.

99. **Nakano, A., Brada, D., Schekman, R.** 1988. A membrane glycoprotein, Sec12p, required for protein transport from the Endoplasmic reticulum to the Golgi apparatus in yeast. Journal of Cell Biology. **107:**851-863.

100. **Nga, B. H., and J. A. Roper** 1968. Quantitative intrachromosomal changes arising at mitois in *Aspergillus nidulans*. Genetics. **58:**193-209.

101. **Ngiam, C., D. J. Jeenes, P. J. Punt, C. Van den Hondel, and D. B. Archer** 2000. Characterization of a foldase, protein disulfide isomerase A, in the protein secretory pathway of *Aspergillus niger*. Applied and Environmental Microbiology. **66:**775-782.

102. **Nickel, W., and B. Brugger** 1999. COP I-mediated protein and lipid sorting in the early secretory pathway. Protoplasma. **207:**115-124.

103. **O'Connell, M. J., A. H. Osmani, N. R. Morris, and S. A. Osmani** 1992. An Extra Copy of Nimecyclinb Elevates Pre-Mpf Levels and Partially Suppresses Mutation of Nimtcdc25 in *Aspergillus nidulans*. EMBO Journal. **11:**2139-2149.

104. **Odorizzi, G., C. R. Cowles, and S. D. Emr** 1998. The AP-3 complex: a coat of many colours. trends in CELL BIOLOGY. **8:**282-288.

105. **Orci, L., M. Amherdt, M. Ravazzola, A. Perrelet, and J. E. Rothman** 2000. Exclusion of Golgi Residents from Transport Vesicles budding from Golgi Cisternae in Intact Cells. Cell. **150:**1263-1269.

106. **Orci, L., M. A. Stamnes, M. Ravazzola, M. Amherdt, A. Perrelet, T. H. Sollner, and J. E. Rothman** 1997. Bidirectional Transport by Distinct Populations of COPI-Coated Vesicles. Cell. **90:**335-349.

107. **Osmani, S. A., D. B. Engle, J. H. Doonan, and N. R. Morris** 1988. Spindle formation and chromatin condensation in cells blocked at interphase by a mutation of a negative cell cycle control gene. Cell. **52:**241-251.

108. **Osmani, S. A., G. S. May, and N. R. Morris** 1987. Regulation of the mRNA levels of *nimA*, a gene required for the G2-M Transition in *Aspergillus nidulans*. Journal of Cell Biology. **104:**1495-1504.

109. **Ostergaard, S., E. Olsson, and J. Nielson** 2000. Metabolic Engineering of *Saccharomyces cerevisiae.* Microbiology and Molecular Biology Reviews. **64:**24-50.

110. **Ostermann, J., L. Orci, K. Tani, M. Amherdt, M. Ravazzola, Z. Elazar, and J. E. Rothman** 1993. Stepwise assembly of functionally active-transport vesicles. Cell. **75:**1015-1025.

111. **Palade, G. E.** 1975. Intracellular aspects of the process of protein transport. Science. **272:**227-234.

112. **Pelham, H. R. B.** 1997. Membrane-transport - green light for Golgi traffic. Nature. **389:**17.

113. **Pelham, H. R. B.** 1991. Recycling of proteins between the endoplasmic reticulum and the Golgi complex. Current Opinion in Cell Biology. **3:**585-591.

114. **Pelham, H. R. B.** 1995. Sorting and Retrieval between the Endoplasmic-Reticulum and Golgi-Apparatus. Current Opinion in Cell Biology. **7:**530-535.

115. **Peterson, M. R., S. Hsu, and R. H. Scheller** 1996. A mammalian homologue of *SLY1*, a yeast gene required for transport from endoplasmic reticulum to Golgi. Gene. **169:**293-294.

116. **Pimpl, P., A. Movafeghi, S. Coughlan, J. Denecke, S. Hillmer, and D. G. Robinson** 2000. *In Situ* Localization and *in Vitro* Induction of Plant COPI-Coated Vesicles. Plant Cell. **12:**2219-2235.

117. **Pontecorvo, G., J. A. Roper, L. M. Hemmons, K. D. MacDonald, and A. W. J. Bufton** 1953. The Genetics of *Aspergillus nidulans.* Advances in Genetics. **5:**141-253.

118. **Prasher, C., V. K. Eckenrode, W. W. Ward, F. G. Prendergast, and M. J. Cormier** 1992. Primary strucure of the *Aequorea victoria* green-fluorescent protein. Gene. **111:**229-233.

119. **Presley, J. F., N. B. Cole, T. A. Schroer, K. Hirschberg, K. Zaal, and J. Lippincott-Schwartz** 1997. ER to Golgi traffic visualized in living cells. Nature. **389:**81-85.

120. **Pryer, N. K., N. R. Salama, R. Schekman, and W. E. Balch** 1992. Cytosolic Sec13p complex is required for vesicle formation from the Endoplasmic reticulum. Journal of Cell Biology. **120:**865-875.

121. **Rapaport, T. A., B. Jungnickel, and U. Kutay** 1996. Protein transport across the eukaryotic endoplasmic reticulum and bacterial inner membrane. Annual Review of Biochemistry. **63:**271-303.

122. **Read, N. D., and P. C. Hickey** 2001. The vesicle trafficking network and tip growth in fungal hyphae Journal of Microscopy. **Awaiting publication**.

123. **Reinhard, C., C. Harter, M. Bremser, B. Brugger, K. Sohn, J. B. Helms, and F. T. Wieland** 1999. Receptor-induced polymerization of coatomer. Proceedings of the National Academy of Science. USA. **96:**1224-1228.

124. **Roberson, R.** 2001. Electron microscopy pictures of *A. nidulans* hyphae showing Golgi equivalents. **Unpublished data**.

125. **Roberts, T. H., A. T. Hammond, B. S. Glick, and J. Lippincott-Schwartz** 1999. Membrane sorting and recycling in the early secretory pathway Molecular Biology of the Cell. **10:**1229.

126. **Robinson, M. S.** 1997. Coats and Vesicle budding. trends in CELL BIOLOGY. **7:**99-102.

127. **Rossanese, O. W., J. Soderholm, B. J. Bevis, I. B. Sears, J. O'Connor, E. K. Williamson, and B. S. Glick** 1999. Golgi Structure Correlates with Transitional Endoplamic Reticulum Organization in *Pichia pastoris* and *Saccharomyces cerevisiae.* Journal of Cell Biology. **145:**69-81.

128. **Rupes, I., W. Z. Mao, H. Astrom, and M. Raudaskoski** 1995. Effects of nocodazole and brefeldin A on microtubule cytoskeleton and membrane organization in the homobasidiomycete *Schizophyllum commune*. Protoplasma. **185:**212-221.

129. **Salama, N. R., T. Yeung, and R. W. Schekman** 1994. The Sec13p complex and reconstitution of vesicle budding from the ER with purified cytosolic proteins. EMBO Journal. **12:**4073-4082.

130. **Salmon, E. D., T. Inoue, A. Desai, and M.A.W.** 1994. High resolution multimode digital imaging system for mitosis studies *in vivo* and *in vitro*. Biological Bulletins. **187:**231-232.

131. **Sambrook, J., E. F. Frisch, and T. Maniatis** 1989. Molecular Cloning: A Laboratory Manual. Cold Spring Harbor Laboratory Press, Cold Spring Harbor, NY.

132. **Saraste, J., and E. Kuismanen** 1992. Pathways of protein sorting and membrane traffic between the rough endoplasmic reticulum and the Golgi complex. Cell. **38:**535-549.

133. **Satiat-Jeunemaitre, B., P. Boevink, and C. Hawes** 1999. Membrane trafficking in higher plant cells: GFP and antibodies, partners for probing the secretory pathway. Biochimie. **81:**597-605.

134. **Satiat-Jeunemaitre, B., L. Cole, T. Bourett, R. Howard, and C. Hawes** 1996. Brefeldin A effects in plant and fungal cells: something new about vesicle trafficking? Journal of Microscopy. **181:**162-177.

135. **Schweintek, T., C. Lorenz, and J. F. Ernst** 1995. Golgi localization in yeast is mediated by the membrane anchor region of rat-liver sialyl transferase. Journal of Biochemistry. **270:**7.

136. **Sheff, D., M. Lowe, T. E. Kreis, and I. Mellman** 1996. Biochemical Heterogeneity and Phosphorylation of Coatomer Subunits. Journal of Biological Chemistry. **271:**7230-7236.

137. **Singh, M., and U. Sinha** 1976. Chloral hydrate induced haploidization of *Aspergillus nidulans.* Experientia. **32:**1144-1145.

138. **Singleton, V. L., N. Bohonos, and A. J. Ullstrup** 1958. Decumbin, a new compound from a species of *Penicillium*. Nature. **181:**1072-1073.

139. **Som, T., and V. S. R. Kolaparthi** 1994. Developmental Decisions in *Aspergillus nidulans* Are Modulated by Ras Activity. Molecular and Cellular Biology. **14:**5333-5348.

140. **Spencer, A. J., D. D. Jeenes, D. A. Mackenzie, D. T. Haynie, and D. B. Archer** 1998. Determinants of the fidelity of processing glucoamylase-lysozyme fusions by *Aspergillus niger*. Journal of Biochemistry. **258:**107-112.

141. **Springer, S., E. Chen, R. Duden, M. Marzioch, A. Rowley, S. Hamamoto, S. Merchant, and R. Schekman** 2000. The p24 proteins are not essential for vesicular transport in *Saccharomyces cerevisiae*. Proceedings of the National Academy of Science. USA. **97:**4034-4039.

142. **Staehelin, L. A., and A. Driouich** 1997. Brefeldin A Effects in Plants. Plant Physiology. **114:**401-403.

143. **Stephens, D. J., N. Lin-Marq, A. Pagano, R. Pepperkok, and J. P. Paccaud** 2000. COPI-coated ER-to-Golgi transport complexes segregate from COPII in close proximity to ER exit sites. Journal of Cell Science. **113:**2177-2185.

144. **Stirling, C. J.** 1999. Protein targeting to the endoplasmic reticulum in yeast. Microbiology. **145:**991-998.

145. **Teasdale, R. D., and M. R. Jackson** 1996. Signal-mediated sorting of membrane proteins between the endoplasmic reticulum and the Golgi apparatus. Annual Review of Cell and Developmental Biology. **12:**27-54.

146. **Tilburn, J., C. Scazzocchio, G. G. Taylor, J. H. Zabicky-Zissman, R. A. Lockington, and R. W. Davies** 1983. Transformation by integration in *Aspergillus nidulans*. Gene. **26:**205-221.

147. **Trilla, J. A., A. Duran, and C. Roncero** 1999. Chs7p, a New Protein Involved in the Control of Protein Export from the Endoplasmic Reticulum that Is Specifically Engaged in the Regulation of Chitin Synthesis in *Saccharomyces cerevisiae*. Journal of Cell Biology. **145:**1153-1163.

148. **Turner, G. Personal Communication.**

149. **Upshall, A., B. Giddings, and J. D. mortimore** 1977. The use of benlate for distinguishing between haploid and diploid strains of *Aspergillus nidulans* and *Aspergillus terreus*. Journal of General Microbiology. **100:**413-418.

150. **Upshall, A., and I. D. Mortimore** 1984. Isolation of Aneuploid-Generating Mutants of *Aspergillus nidulans*, One of Which Is Defective In Interphase of the Cell Cycle. Genetics. **108:**107-121.

151. **Vainstein, M. H., and J. F. Peberdy** 1991. Location of invertase in *Aspergillus nidulans*: release during hyphal wall digestion and secretion by protoplasts. Mycological Research. **95:**1270-1274.

152. **Valderrama, F., A. Luna, T. Babia, J. A. Martinez-Menarguez, J. Ballesta, H. Barth, C. Chaponnier, J. Renau-Piqueras, and G. Egea** 2000. The Golgi-associated COPI-coated buds and vesicles contain β/γ-actin. Proceedings of the National Academy of Science. USA. **97:**1560-1565.

153. **Van den Voorn, L., and H. L. Ploegh** 1992. The WD40 repeat. FEBS letts. **307:**131-134.

154. **van Ljzendoorn, S. C. D., and D. Hoekstra** 1999. The subapical compartment: a novel sorting centre? trends in CELL BIOLOGY. **9:**144-149.

155. **VanRheenen, S. M., X. Cao, S. K. Sapperstein, E. C. Chiang, V. V. Lupashin, C. Barlowe, and M. G. Waters** 1999. Sec34p, a Protein Required for Vesicle Tethering to the Yeast Golgi Apparatus, Is in a complex with Sec35p. Journal of Cell Biology. **147:**729-742.

156. **Vieira, J., and J. Messing** 1982. The pUC plasmids, an M13mp7-derived system for insertion mutagenesis and sequencing with synthetic universal primers. Gene. **19:**259-268.

157. **Vitale, A., and J. Denecke** 1999. The Endoplasmic reticulum-gateway of the secretory pathway. Plant Cell. **11:**615-628.

158. **Volchuk, A., M. Amherdt, M. Ravazzola, B. Brugger, V. M. Rivera, T. Clackson, A. Perrelet, T. H. Sollner, J. E. Rothman, and L. Orci** 2000. Megavesicles Implicated in the Rapid Transport of Intracisternal Aggregates across the Golgi Stack. Cell. **102:**335-348.

159. **Von Heijne, G.** 1990. The Signal peptide. Journal of Membrane Biology. **115:**195-201.

160. **Wang, S., and T. Hazelrigg** 1994. Implicaions for bcd mRNA localization from spatial ditributions of exu protein in *Drosophila* oogenesis. Nature. **369:**400-403.

161. **Waring, R. B., G. S. May, and R. N. Morris** 1989. Characterization of an inducible expression system in *Aspergillus nidulans* using *alcA* and tubulin-coding genes. Gene. **79:**119-130.

162. **Warren, G., and V. Malhotra** 1998. The organisation of the Golgi apparatus. Current Opinion in Cell Biology. **10:**493-498.

163. **Waters, M. G., T. Serafini, and J. E. Rothman** 1991. 'Coatomer': a cytosolic protein complex containing subunits of non-clathrin-coated Golgi transport vesicles. Nature. **349:**248-251.

164. **WebGene** 2001, posting date. Gene analysis software. http:\\www.itba.mi.cnr.it/webgene/. [Online.]

165. **Whittaker, S. L., P. Lunness, K. J. Milward, J. H. Doonan, and S. J. Assinder** 1999. sod^{VI}C Is an α-COP-related Gene Which Is Essential for Establishing and Maintaining Polarized Growth in *Aspergillus nidulans.* Fungal Genetics and Biology. **26:**236-252.

166. **Wieland, F. T., and C. Harter** 1999. Mechanisms of vesicle formation: insights from the COP system. Current Opinion in Cell Biology. **11:**440-446.

167. **Wiertz, E. J. H. J., D. Tortorella, M. Bogyo, J. H. Yu, W. Mothes, T. R. Jones, T. A. Rapaport, and H. L. Ploegh** 1996. Sec61p-mediated transfer of a membrane protein from the Endoplasmic reticulum to the proteasome for destruction. Nature. **384:**432-438.

168. **Wouters, F. S., P. J. Verveer, and P. I. H. Bastiaens** 2001. Imaging biochemistry inside cells. trends in CELL BIOLOGY. **11**.

169. **Yaver, D. S., M. Lamsa, R. Munds, S. H. Brown, S. Otani, L. Franssen, J. A. Johnstone, and H. Brody** 2000. Using DNA-Tagged Mutagenesis to Improve Heterologous Protein Production in *Aspergillus oryzae*. Fungal Genetics and Biology. **29:**28-37.

170. **Yoshihisa, T., C. Barlowe, and R. Schekman** 1993. Requirement for a GTPase-activating protein in vesicle budding from the Endoplasmic reticulum. Nature. **259:**1466-1468.

Appendix 1: Key to abbreviations used

ADP	Adenosine di Phosphate
ARF1	ADP-ribosylation factor
ARS	autonomously replicating sequences
BFA	Brefeldin A
CM	complete medium
CMI	Chromosome Mitotic Index
DAPI	4'6-diamidino-2-phenylidole
EDTA	Ethylenediamine tetra acetic acid
ER	Endoplasmic reticulum
ERGIC	ER-Golgi intermediate compartment
GAP	GTP-activating protein
GEF	GTP exchange factor
GFP	Green fluorescent protein
GRAS	Generally regarded as safe
GTP	Guanosine Tri Phosphate
HEWL	Hen egg with lysozyme
M	Molar
NSF	NEM-sensitive fusion protein
PCR	Polymerase chain reaction
PDI	Protein disulphide isomerase
PGC	Post-Golgi carrier
psi	Pounds per square inch
SNAP	NSF attachment protein
SNARE	NSF attachment receptor element
SRP	Signal recognition particle
tER	*trans*-ER
TGN	*trans*-Golgi network
Tris	Tris (hydroxymethyl (aminomethane))
ts	temperature sensitive
UV	Ultraviolet
VSVG	vesicular tubular virus glycoprotein
VTCs	Vesicular Tubular Clusters
w.t.	wild-type

Appendix 2: Key to abbreviations used in *E. coli* strains

endA1	Mutation in endonuclease I gene.
gyrA96	Mutation in gene encoding DNA gyrase subunit A.
lac^c(P2 lysogen)	Uncharacterised mutation in the β-D-Galactosidase gene. Mutation enhances α-complementation to give more intense blue colour on plates containing X-Gal and IPTG.
relA1	Mutation in ATP:GTP 3'-pyrophosphotransferase required for ppGpp synthesis during stringent response to amino acid starvation.
SupE44	Mutation in suppressor tRNA.
thi-1	Mutation in hydroxyethylthiazole synthesis.
Δ(mcrA)183, Δ(mcrCB-hsdsMR-mrr)173	Mutation in gene encoding 5-methylcytosine restriction enzyme.

Appendix 3: Key to gene abbreviations

Gene symbol	Linkage group	Phenotype
adE	I	adenine requiring
argB	III	arginine requiring
biA	I	biotin requiring
chaA	VIII	chartreuse coloured conidia
glc		
lacA	VI	lactose utilisation
nicC	VI	nicotinic acid requiring
pabaA	I	p-aminobenzoic acid requiring
pyroA	IV	pyridoxine requiring
riboA	I	riboflavine requiring
sbA	VI	sorbitol utilisation
$sod^{VI}C$	VI	stabilises chromosome VI disomics
tsB5	V	t.s. mutation
wA	II	white coloured conidia
yA	I	yellow coloured conidia

Appendix 4: Promega® 1kb DNA ladder

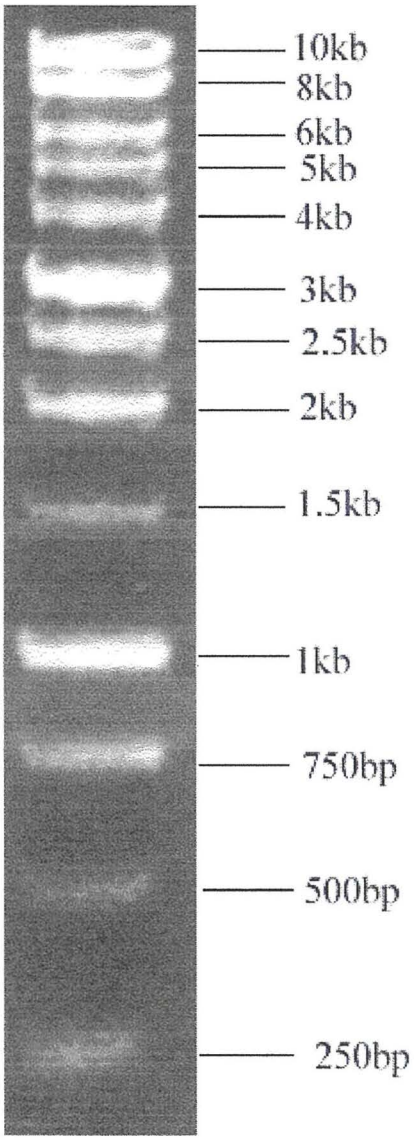

Appendix 5: Nucleotide sequence of the *sod*^{VI}*C* gene

Key: = Start Codon
= Stop Codon
= Introns

```
   1 TCTAGAGCGG CCGCCACCGC GGTGGAGCTC AAACTAGGGC TCGCATATTG TGCATCGGTT
  61 ACAAAGGCGG GCTCTCCGGA CGGGGCAGTT CGGACGGGAT TTGTGATAGT AGGCTTTCTT
 121 TTCCGGCCCC TCTTTGGACG GATTGATCCT GGATTGTCAT GATCGGAGTT GCAGTACAAC
 181 ATTTCCATCG AAGAATCAGG TCCTCCCAGT GTTTGCGCTG TCTTAGCTGC GCTGTTGACA
 241 CCTCCGTTTC GGACGTAAGT TCCTCCTCTG GCTCCTCAAT GGCATACGGT TTCACTACCT
 301 CACTTTTGAA ACCAATCCCG AATATCAGGA GGTAAGTCCT CAATGTCATA TATTTCTGGT
 361 TCGTGAGCTT TAGGGATTTC TCCGTACTGT TGATCTTGGT CGGTTCGAGG AGCAGGCGTC
 421 GGGCTGCTTC CGCCCGGATT CTTGTAAGGT TGATACAGAT CCGGGTTTTG GCCGTTTGCT
 481 CCCATAGTAC CGAGGCCCCC AATATCCACA ATAAGGGCAA TCGAGTTGTT CGGGCGAGTG
 541 CAGTTGCACT GTAGAAGAAA GAGCAAAGTT CAGCTCCTGG TAATGATTAT GGATCGGAGA
 601 TATGTCGCAT GGAAATTCCA TAATAGACCA AGTACACACT CAGCTGAGTG CGAGGACCGT
 661 CAAACATGGT TTATCATCTC GTGCTTGAAG GCAGGGGGAG ACCAGAGTGG TGGTTACGAT
 721 CAACAATGTG AGCGATGTAG CTCTTGACCG CCTTGGGCGC CATTGGCCGG CGCTACTCGC
 781 TTATTCAATA AGTCCACGTT ACCGCCATCC AAGGTGTCCT GTCCAGACCC CAGACTGTCA
 841 ATAGAGACGC TTCCAGGCTA CGTCTCTTTT TTCTTCTGCT CAATTGTCCT TGTGCAGTGG
 901 ATGAGGTGGT CGCCTTTGTG ATTCCTCTGT CTTTAGTGCG CGGAGCTTGC TTCTACTTCT
 961 ACATGGTGCG GCTTCGGCCA ACCCTTCTTC AAGATGCAAT CCTCCCCAAA CATGCTCACC
1021 AAGGTACGCC TACATCCCAT TCCAATTTGC TTGATTCTCC CACTGCTAGA CTCTAACTAG
1081 TATCTCCTGA ATAGTTTGAG TCGAAATCTT CCCGCGCAAA GGGAATTGCC TTCCACCCCA
1141 AGCGGTCAGT CGAACAGCTT ACCCCCTACT GATCGCACCG GTCTAATAAC CCCGGTACAG
1201 GCCATGGATT CTCGTCTCTT TACATTCATC GACGATCCAA CTATGGGATT ACCGTATGGG
1261 AACACTCATC GACCGATTTG AGGAGCACGA CGGCCCTGTT CGTGGCATTG ACTTTCACCC
1321 TACGCAGCCC CTCTTTGTTT CCGGAGGTGA CGACTACAAG ATCAAGGTCT GGAACTACCA
1381 GACCAGGAGA TGTCTTTTCA CATTGAATGG TCATTTGGAC TATGTGCGAA CGGTGTTCTT
1441 CCACCCCGAG CTCCCATGGA TTTTGTCTGC TTCGGACGAC CAAACAATAA GGATCTGGAA
1501 CTGGCAAAAC AGGTCATTGA GTATGTCGAA CTATAGCCGT CTGCCCTGAC TGTTACTGAA
1561 CTTTGATTTC TAGTCTGTAC CATGACCGGC CATAACCACT ACGTGATGTG CGCGCAATTC
1621 CACCCGACAG AAGACCTCAT CGCTTCCGCC TCGCTAGATC AATCCGTCCG TATCTGGGAC
1681 ATTTCGGGAC TGCGGAAGAA GCACTCGGCG CCGACCACGA TGTCGTTCGA AGATCAGATG
1741 GCCCGGGCCA ACAATGCACA GGCAGACATG TTCGGAAATA CCGATGCAGT GGTGAAGTTC
1801 GTTTTGGAAG GCCACGATCG GGGTGTCAAC TGGGTTGCCT TCCACCCGTC ATTGCCCCTG
1861 ATCGTCTCCG CGGGTGATGA CCGCCTCATA AAGCTATGGA GAATGAGCGG TATGTTGCAA
1921 ATGTGTCCAA CTCTAATGTT ATCAATGACA CTAACTCGAC TGAAGATACG AAGGCATGGG
1981 AAGTCGATAC CTGCCGTGGC CATTTTCAGA ACGCGTCCGC ATGTCTTTTC CATCCTCACC
2041 AAGACCTTAT ACTCTCCGTT GGAGAAGACA AGACGATCCG TGCCTGGGAC CTGAACAAAA
2101 GAACACCCGT CCAATCCTTC AAGCGGGATG TGGATCGGTT CTGGGTCATT GCCGCCCACC
2161 CAGAAATCAA CCTATTTGCG GCAGGTCATG ACACTGGAGT AATGGTCTTC AAGCTGGAGA
2221 GAGAGCGGCC CGCATCCGCT GTGTACCAGA ACCAGTTGTT CTACATCACC AAAGAGAAGC
2281 ACGTAAAGTC GTTCGACTTT GCGAAGAACG TTGAGTCGCC GTCCATGCTG TCATTGCGCA
2341 AACTGGGATC GCCCTGGGTG CCTCCTCGCA CGCTATCTTA CAATCCGGCC GAGCGTGCCG
2401 TACTTGTAAC ATCCCCGGCA GATGGGGGTG TGTATGAATT GATCAACCTC CCTCGAGATG
2461 CTACAGGCGC CATCGAACCC ACAGACGTCA AGCGCGGCCA GGCGTCCTCG GCTGTTTTTG
2521 TCGCGCGTAA CAGATTCGCT GTCTTCAGCC AGGCCAACCA GCAGGTGGAT ATCAAAGACT
2581 TGAGCAATTC TACGACCAAG TCCATTAAGC CTCCGGCTGG AACCACTGAT ATCTACTTTG
2641 GCGGAACTGG CAGCCTTCTC TTCATCACAC CTACCTCTGT CGTGCTGTTT GATATCCAGC
2701 AGAAGAAGCA ACTAGCGGAA TTGGCTGTGA GCGGCGTCAA GTACGTTGTA TGGTCAAACG
2761 ATGGGCTCTA TGCAGCATTG CTCAGCAAGC ACAACGTCAC CATTGTCACA AAGACTTTGG
2821 AGCAAGTGAG CAGTTTACAC GAGACTATCC GTATTAAAAG CGCGGCTTGG GATGACGCTG
2881 GCGTCCTTCT TTACTCCACC TTGAACCACG TGAAGTACTC TCTTTTGAAC GGGTAAGCCT
2941 CCTTACTAGT GCTTCTAAAA AGCTACAGAT TGAGCTAACT CTACCGTAGT GACAATGGTA
3001 TCATCCGGAC TTTGGATCAG ACAGTTTATC TGGTCAAGGT CAAAGGCCGA AGCGTCTATT
```

3061 GCCTGGATCG GAATGCTAAA CCAAGAACCT TGGAAATTGA TCCCACCGAA TACCGCTTTA
3121 AGCTCGCCCT TGTTAAGAGG AACTACGATG AGATGCTGCA AATCATAAAG ACATCCAGCT
3181 TGGTCGGTCA GAGTATCATC TCCTATTTGC AGAAGAAGGG CTATCCGGAA ATTGCTCTCC
3241 AGTTCGTCCA AGACCCTCAG ACACGTTTCG AGCTTGCGTT GGAGTGCGGT AACCTGGACG
3301 TCGCAATCGA GATGGCTAGA GAGCTGGACC GTCCCAACCT GTGGAACCGG CTTGGTATCG
3361 AGGCACTGGC ACATGGAAAC CATCAGATCG TGGAAATGGC TTACCAGAAA CAACGAAACT
3421 TTGATAAGCT GTCGTTCCTT TACCTGTCTA TTGGTGATCA GGAGAAGCTG TCAAGGATGG
3481 CGAAGATCGC GGAGCACCGC GGGGACTTCA CCTCCCGCTT CCAGAATGCC ATTTACCGGG
3541 GCGATGTTGA GGATAGGATT CAGATGTTCA AAGAGGTGGA TCTCTGTAAG TTGAAACTTG
3601 TTCTAACCTA TACAAAGTGG AGCTCTTCTA ACCACATTCA GACCCCCTTG CATACCTCAC
3661 TGCCAAGGCT CATGGATTGA CTGAGGAAGC CGAATCCATC CTCGAGGTGG TTGGTCTAAG
3721 TGAAGACCAA GTCTCCCTCC CGACTATTGA AGCTCCTCCA CAGATACCGC AACCTATTGT
3781 TGCCACCTAC AAGGCAAGCT GGCCCGTCAA GGCTGCTGCA CACTCATCGT TTGAGAAAGC
3841 CTTGCTTGGG GAAGTTAGCG CAGGCGATGA AGAAGCCGCT GAACTGGGCT TCGAGCCTGA
3901 AGAAGAAGGC GCTGTTACTG CGGGTGAAGC TCTAGAAGAT GAGGATGAAG ACGCTGCTGG
3961 TTGGGATATG GGCGACGAAA TTAACGTCGA GGAAGACGTT GACTTTGTCA ATGTTGACAG
4021 CGCCGAAGCA GGAGCTGGCA GCGTTGAAGC CGATCTCTGG GCTCGTAACT CTCCTTTGGC
4081 AGCCGATCAT GTTGCTGCTG GTTCTTTCGA TACCGCGATG CAGCTTCTCA ACCGCCAAGT
4141 TGGAGCTGTT CACTTTGCTC CTCTCAAGCC TAGGTTCCTC GAAATTTTCA AAGCCTCCAA
4201 GACCTATCTT TCTGCAACTC CCGGCCTCCC CCCGCTTGTC AACTATGTTC GACGAACTGT
4261 TGACGAAACT GACAGCCGGA AAGTGCTGCC CGCCATCCCC AGGGACCTTG AAACTATTGC
4321 TAGTGTCGAC TTGCAAGAGG GTTACGCCGC CATGAGAGCT AACAAGTTGG AGGACGGTGT
4381 TAAGATCTTC AAGAACATCC TCTACTCGGT TCTTGTAAAC GTTGTTTCGT CCGAGGCGGA
4441 GGTTGAGCAA GCAAAGAAGA TCATTGCAAC TTCTCGAGAA TATATCCTTG CAATGACTAT
4501 TGAGTTAGAA CGCCGAGCTC TTTCAACAGA TACGCCCGAG GGACTCAAGC GAAGCCTTGA
4561 GCTTTCTGCC TACTTCACTA TTCCCAAGCT GGATGTTGCC CACAGGCAAC TGGCTCTCAT
4621 GGCAGCAATG AAACTTGCGT TTACTCACAA GAACTACTCG TCTGCCCTCA GCTTCGCCAA
4681 CCGCATGCTG GCCAATGGTG GTTCTGCTAA GCTCTTGGAT CAGGTTAGTT TTTTTATTCT
4741 ATCATTTGGG TTTTGGTTTG TCTGAATTAG GTTCTAACTT TTTATTGCAG GCTAAGAAGG
4801 TCAAGGCTCA ATGCGAGCGT AACCCTCAGG ATAGTATTGA GATTGAATTC GACCAGTTTG
4861 CGGAGTTCGA CATTTGCGCG GCGTCCCATA CGCCTATCTA TAGCGGATCC CCCAGCGTCT
4921 CAGATCCGTT CACCGGTGCC AAATATCATG AACAATATAA GGGTAGCGTC GATCGGATAT
4981 CTGAAGTGAC TGAAATTGGC GCGCCGGCGA GTGGACTGCG GTTGTATGTC CCTAGCCAAC
5041 TCTAATCCCC TGACGACGTG TGATGGGTTA TGCTTAAAGA TAGAAAAGTG GACTTCTATC
5101 TTCTTATGGA CTTAATCATG GTCCTAAGGT CTGTTACATA GATATATGGA TCTGTTGCCT
5161 GTCTTCTATA ATTCTTGAGC GTTGTAATTA AATAGTTTTT CATGCGAATG CAATGCATGT
5221 AAGCAAGGAT TGGG

Appendix 6: The amino acid sequence of the *sod*^{VI}*C* gene.

Key: ■ = WD-40 repeats

```
1    MLTKFESKSS RAKGIAFHPK RPWILVSLHS STIQLWDYRM GTLIDRFEEH DGPVRGIDFH
61   PTQPLFVSGG DDYKIKVWNY QTRRCLFTLN GHLDYVRTVF FHPELPWILS ASDDQTIRIW
121  NWQNRSLICT MTGHNHYVMC AQFHPTEDLI ASASLDQSVR IWDISGLRKK HSAPTTMSFE
181  DQMARANNAQ ADMFGNTDAV VKFVLEGHDR GVNWVAFHPS LPLIVSAGDD RLIKLWRMSD
241  TKAWEVDTCR GHFQNASACL FHPHQDLILS VGEDKTIRAW DLNKRTPVQS FKRDVDRFWV
301  IAAHPEINLF AAGHDTGVMV FKLERERPAS AVYQNQLFYI TKEKHVKSFD FAKNVESPSM
361  LSLRKLGSPW VPPRTLSYNP AERAVLVTSP ADGGVYELIN LPRDATGAIE PTDVKRGQAS
421  SAVFVARNRF AVFSQANQQV DIKDLSNSTT KSIKPPAGTT DIYFGGTGSL LFITPTSVVL
481  FDIQQKKQLA ELAVSGVKYV VWSNDGLYAA LLSKHNVTIV TKTLEQVSSL HETIRIKSAA
541  WDDAGVLLYS TLNHVKYSLL NGDNGIIRTL DQTVYLVKVK GRSVYCLDRN AKPRTLEIDP
601  TEYRFKLALV KRNYDEMLQI IKTSSLVGQS IISYLQKKGY PEIALQFVQD PQTRFELALE
661  CGNLDVAIEM ARELDRPNLW NRLGIEALAH GNHQIVEMAY QKQRNFDKLS FLYLSIGDQE
721  KLSRMAKIAE HRGDFTSRFQ NAIYRGDVED RIQMFKEVDL YPLAYLTAKA HGLTEEAESI
781  LEVVGLSEDQ VSLPTIEAPP QIPQPIVATY KASWPVKAAA HSSFEKALLG EVSAGDEEAA
841  ELGFEPEEEG AVTAGEALED EDEDAAGWDM GDEINVEEDV DFVNVDSAEA GAGSVEADLW
901  ARNSPLAADH VAAGSFDTAM QLLNRQVGAV HFAPLKPRFL EIFKASKTYL SATPGLPPLV
961  NYVRRTVDET DSRKVLPAIP RDLETIASVD LQEGYAAMRA NKLEDGVKIF KNILYSVLVN
1021 VVSSEAEVEQ AKKIIATSRE YILAMTIELE RRALSTDTPE GLKRSLELSA YFTIPKLDVA
1081 HRQLALMAAM KLAFTHKNYS SALSFANRML ANGGSAKLLD QAKKVKAQCE RNPQDSIEIE
1141 FDQFAEFDIC AASHTPIYSG SPSVSDPFTG AKYHEQYKGS VDRISEVTEI GAPASGLRLY
1201 VPSQL*
```

The GenBank accession number for the DNA sequence is AFO53883.

Appendix 7: Sequences of primers used in this study

P1for	5' GCT GAA CTG GGC TTC GAG 3'
P1rev	5' TTA GAG TTG GCT AGC GAC ATA CAA 3'
P2for	5' GTA TCG ATC GCT AGC AAA GGA GAA 3'
P2rev	5' TCT AGA GGA GCG GCC GCG ACA CAT 3'
P3for	5' GTC GTT CGA AGA TCA GAT 3'
P3rev	5' GCA GTG AGG TAT GCA AGG 3'
M1	5' TCG CAT ATT GTG CAT CGG TTA 3'
M2	5' ATG TAG GCG TAC CTT GGT GAG 3'
M13uni	5' GTA AAA CGA CGG CCA GT 3'
M13rev	5' GGA AAC AGC TAT GAC CAT G 3'

Appendix 8: Sequencing of the GFP2.5 and X-B PCR products generated for the construction of the pSodGFP19 plasmid.

(A) Sequencing of X-B PCR product.

Key: = Incorporated *Nhe*I site
= Stop codon
= *Xba*I site

```
   1 GCTGAACTGG GCTTCGAGCC TGAAGAAGAA GGCGCTGTTA CTGCGGGTGA AGCTCTAGAA
  61 GATGAGGATG AAGACGCTGC TGGTTGGGAT ATGGGCGACG AAATTAACGT CGAGGAAGAC
 121 GTTGACTTTG TCAATGTTGA CAGCGCCGAA GCAGGAGCTG GCAGCGTTGA AGCCGATCTC
 181 TGGGCTCGTA ACTCTCCTTT GGCAGCCGAT CATGTTGCTG CTGGTTCTTT CGATACCGCG
 241 ATGCAGCTTC TCAACCGCCA AGTTGGAGCT GTTCACTTTG CTCCTCTCAA GCCTAGGTTC
 301 CTCGAAATTT TCAAAGCCTC CAAGACCTAT CTTTCTGCAA CTCCCGGCCT CCCCCCGCTT
 361 GTCAACTATG TTCGACGAAC TGTTGACGAA ACTGACAGCC GGAAAGTGCT GCCCGCCATC
 421 CCCAGGGACC TTGAAACTAT TGCTAGTGTC GACTTGCAAG AGGGTTACGC CGCCATGAGA
 481 GCTAACAAGT TGGAGGACGG TGTTAAGATC TTCAAGAACA TCCTCTACTC GGTTCTTGTA
 541 AACGTTGTTT CGTCCGAGGC GGAGGTTGAG CAAGCAAAGA AGATCATTGC AACTTCTCGA
 601 GAATATATCC TTGCAATGAC TATTGAGTTA GAACGCCGAG CTCTTTCAAC AGATACGCCC
 661 GAGGGACTCA AGCGAAGCCT TGAGCTTTCT GCCTACTTCA CTATTCCCAA GCTGGATGTT
 721 GCCCACAGGC AACTGGCTCT CATGGCAGCA ATGAAACTTG CGTTTACTCA CAAGAACTAC
 881 TCGTCTGCCC TCAGCTTCGC CAACCGCATG CTGGCCAATG GTGGTTCTGC TAAGCTCTTG
 941 GATCAGGTTA GTTTTTTTAT TCTATCATTT GGGTTTTGGT TTGTCTGAAT TAGGTTCTAA
1001 CTTTTTATTG CAGGCTAAGA AGGTCAAGGC TCAATGCGAG CGTAACCCTC AGGATAGTAT
1060 TGAGATTGAA TTCGACCAGT TTGCGGAGTT CGACATTTGC GCGGCGTCCC ATACGCCTAT
1021 CTATAGCGGA TCCCCCAGCG TCTCAGATCC GTTCACCGGT GCCAAATATC ATGAACAATA
1081 TAAGGGTAGC GTCGATCGGA TATCTGAAGT GACTGAAATT GGCGCGCCGG CGAGTGGACT
1141 GCGGTTGTAT GTCGCTAGCC AACTCTAA
```

(B) Sequence of modified GFP2.5.

Key: = Incorporated *Nhe*I site
= Stop codon

```
   1 GCTAGCAAAG GAGAAGAACT TTTCACTGGA GTTGTCCCAA TTCTTGTTGA ATTAGATGGT
  61 GATGTTAATG GGCACAAATT TTCTGTCAGT GGAGAGGGTG AAGGTGATGC AACATACGGA
 121 AAACTTACCC TTAAATTTAT TTGCACTACT GGAAAACTAC CTGTTCCATG GCCAACACTT
 181 GTCACTACTT TCACCTATGG TGTTCAATGC TTTTCAAGAT ACCCAGATCA TATGAAGCGG
 241 CACGACTTCT TCAAGAGCGC CATGCCTGAG GGATACGTGC AGGAGAGGAC CATCTTCTTC
 301 AAGGACGACG GGAACTACAA GACACGTGCT GAAGTCAAGT TTGAGGGAGA CACCCTCGTC
 361 AACAGGATCG AGCTTAAGGG AATCGATTTC AAGGAGGACG GAAACATCCT CGGCCACAAG
 421 TTGGAATACA ACTACAACTC CCACAACGTA TACATCATGG CCGACAAGCA GAAGAACGGC
 481 ATCAAAGCCA ACTTCAAGAC CCGCCACAAC ATCGAAGACG GCGGCGTGCA ACTCGCTGAT
 541 CATTATCAAC AAAATACTCC AATTGGCGAT GGCCCTGTCC TTTTACCAGA CAACCATTAC
 601 CTGTCCACAC AATCTGCCCT TTCGAAAGAT CCCAACGAAA AGAGAGACCA CATGGTCCTT
 661 CTTGAGTTTG TAACAGCTGC TGGGATTACA CATGGCATGG ATGAACTATA CAAATAA
```

Appendix 9: Maps of vectors used in study. (A) pBluescript, (B) pUC18, (C) pAB.

(A)

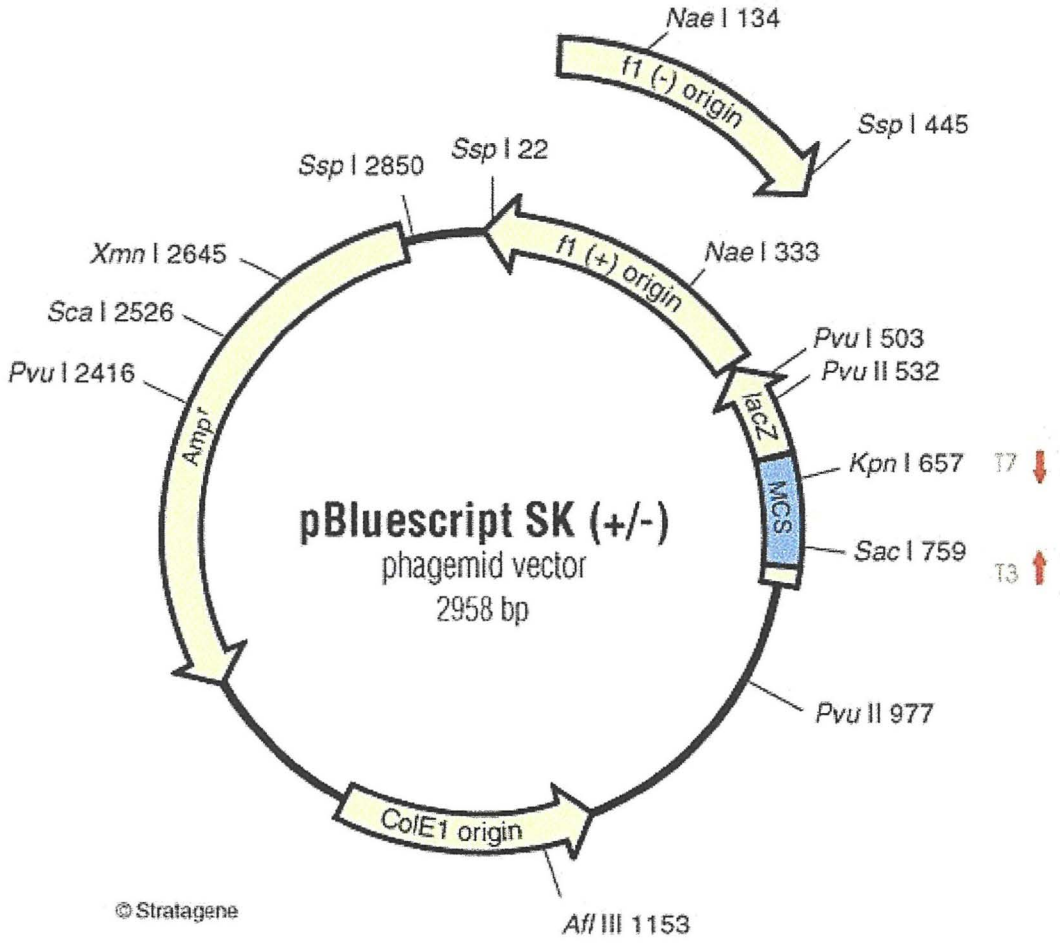

(B)

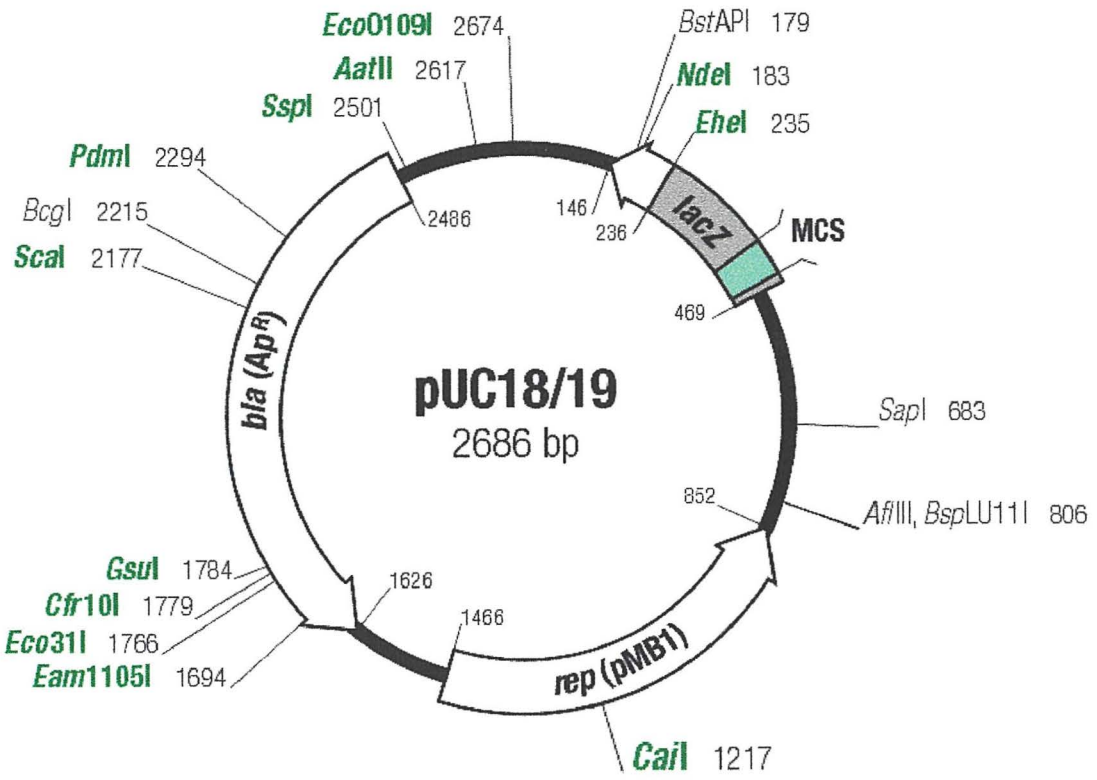
Eco0109I 2674
AatII 2617
SspI 2501
PdmI 2294
BcgI 2215
ScaI 2177
BstAPI 179
NdeI 183
EheI 235
146
236
lacZ
MCS
469
2486
pUC18/19
2686 bp
SapI 683
852
AflIII, BspLU11I 806
GsuI 1784
Cfr10I 1779
Eco31I 1766
Eam1105I 1694
1626
1466
bla (Ap^R)
rep (pMB1)
CaiI 1217

Appendix 10: Published *sod*^{VI}*C* paper.